PROCEEDINGS
THIRD WORKSHOP
GEOTHERMAL RESERVOIR ENGINEERING

December 14-15, 1977

Paul Kruger and Henry J. Ramey, Jr., Editors
Stanford Geothermal Program
Workshop Report SGP-TR-25*

*Conducted under Subcontract No. 167-3500 with Lawrence Berkeley Laboratory, University of California, sponsored by the Geothermal Division of the U.S. Department of Energy.

Library of Congress Catalog Card No.: 85-080660

TABLE OF CONTENTS

INTRODUCTION

The Third Workshop on Geothermal Reservoir Engineering convened at Stanford University on December 14, 1977, with 104 attendees from six nations. In keeping with the recommendations expressed by the participants at the Second Workshop, the format of the Workshop was retained, with three days of technical sessions devoted to reservoir physics, well and reservoir testing, field development, and mathematical modeling of geothermal reservoirs. The program presented 33 technical papers, summaries of which are included in these Proceedings.

Although the format of the Workshop has remained constant, it is clear from a perusal of the Table of Contents that considerable advances have occurred in all phases of geothermal reservoir engineering over the past three years. Greater understanding of reservoir physics and mathematical representations of vapor-dominated and liquid-dominated reservoirs are evident; new techniques for their analysis are being developed, and significant field data from a number of newer reservoirs are analyzed.

The objectives of these workshops have been to bring together researchers active in the various physical and mathematical disciplines comprising the field of geothermal reservoir engineering, to give the participants a forum for review of progress and exchange of new ideas in this rapidly developing field, and to summarize the effective state of the art of geothermal reservoir engineering in a form readily useful to the many government and private agencies involved in the development of geothermal energy. To these objectives, the Third Workshop and these Proceedings have been successfully directed.

Several important events in this field have occurred since the Second Workshop in December 1976. The first among these was the incorporation of the Energy Research and Development Administration (ERDA) into the newly formed Department of Energy (DOE) which continues as the leading Federal agency in geothermal reservoir engineering research. The Third Workshop under the Stanford Geothermal Program was supported by a grant from DOE through a subcontract with the Lawrence Berkeley Laboratory of the University of California. A second significant event was the first conference under the ERDA (DOE)-ENEL cooperative program where many of the results of well testing in both nations were discussed. The Proceedings of that conference should be an important contribution to the literature.

These Proceedings of the Third Workshop should also make an important contribution to the literature on geothermal reservoir engineering. Much of the data presented at the Workshop were given for the first time, and full technical papers on these subjects will appear in the professional journals. The results of these studies will assist markedly in developing the research programs to be supported by the Federal agencies, and in reducing the costs of research for individual developers and utilities. It is expected that future workshops of the Stanford Geothermal Program will be as successful as this third one.

Planning and execution of the Workshop was carried out with the assistance of a great many individuals. The Program Committee consisted of Robert Christiansen (USGS-Menlo Park), George Frye (Aminoil USA), Roland Horne (Stanford Geothermal Program), John Howard (Lawrence Berkeley Laboratory), Paul Kruger (Stanford Geothermal Program), Lloyd Mann (Chevron Oil Company), Stephen Lipman (Union Oil Company), Henry J. Ramey, Jr. (Stanford Geothermal Program), and Werner Schwarz (Lawrence Berkeley Laboratory).

The Program Committee recommended two novel sessions for the Third Workshop, both of which were included in the program. The first was the three overviews given at the Workshop by George Pinder (Princeton) on the Academic aspect, James Bresee (DOE-DGE) on the Government aspect, and Charles Morris (Phillips Petroleum) on the Industry aspect. These constituted the invited slate of presentations from the several sectors of the geothermal community. The Program Committee acknowledges their contributions with gratitude.

Recognition of the importance of reservoir assurance in opting for geothermal resources as an alternate energy source for electric energy generation resulted in a Panel Session on Various Definitions of Geothermal Reservoirs. Special acknowledgments are offered to Jack Howard and Werner Schwarz (LBL) and to Jack Howard as moderator; to the panelists: James Leigh (Lloyd's Bank of California), Stephen Lipman (Union Oil), Mark Mathisen (PG&E), Patrick Muffler (USGS-MP), and Mark Silverman (DOE-SAN); and to the rapporteurs: George Frye (Aminoil), Vasel Roberts (Electrical Power Research Institute), and Alexander Graf (LBL), whose valuable summaries are included in the Proceedings.

Special thanks are also due Roland Horne, Visiting Professor from New Zealand and Program Manager of the Stanford Geothermal Program, for his efforts with the Program graduate students in conducting the Workshop. Further thanks go to Marion Wachtel, who in spite of tremendous personal hardship, administered the Workshop and prepared the Proceedings in a timely and professional manner. Professor Ramey and I also express our appreciation to the Department of Energy, whose financial support of the Workshop made possible the program and these Proceedings.

Paul Kruger
Stanford University
December 31, 1977

1978 USGS GEOTHERMAL RESOURCE ASSESSMENT

L. J. Patrick Muffler
MS 18, U. S. Geological Survey
Menlo Park CA 94025

Geothermal resource assessment can be defined as the broadly based estimation of supplies of geothermal energy that might become available for use, given reasonable assumptions about technology, economics, governmental policy, and environmental constraints (Muffler and Christiansen, 1978). This assessment implies not merely the determination of how geothermal energy is distributed in the upper part of the earth's crust but also the evaluation of how much of this energy could be extracted for man's use. Thermal energy in place in the earth's crust (relative to a reference temperature) is the geothermal resource base. The accessible resource base is the thermal energy at depths shallow enough to be tapped by drilling in the foreseeable future (Muffler and Cataldi, 1978). That fraction of the accessible resource base that could be extracted economically and legally at some reasonable future time is the geothermal resource (Muffler, 1973; White and Williams, 1975; Muffler and Cataldi, 1978). This geothermal resource contains both identified and undiscovered components. Finally, the geothermal reserve is identified geothermal energy that can be extracted legally today at a cost competitive with other energy sources. The relationships between these terms can be illustrated on a McKelvey diagram for geothermal resources (figure 1).

In the United States, the U. S. Geological Survey (USGS) is the government agency responsible for assessing mineral and energy resources, including geothermal energy. The goal of the Survey's geothermal assessment is to provide a knowledge of the Nation's geothermal resource in sufficient breadth and detail to allow optimum energy planning, to encourage systematic exploration, and to support appropriate development of geothermal resources by private industry.

The first systematic effort to estimate the geothermal resources of the entire United States was carried out by the USGS in 1975 and published as USGS Circular 726 (White and Williams, 1975). This study evaluated the geothermal resource base to specified depths in several categories: (a) regional conductive environments, (b) igneous-related geothermal systems, (c) hydrothermal convection systems, and (d) geopressured systems. For each category, the USGS study then evaluated the part of the resource base that might be recovered under reasonable technological and economic assumptions.

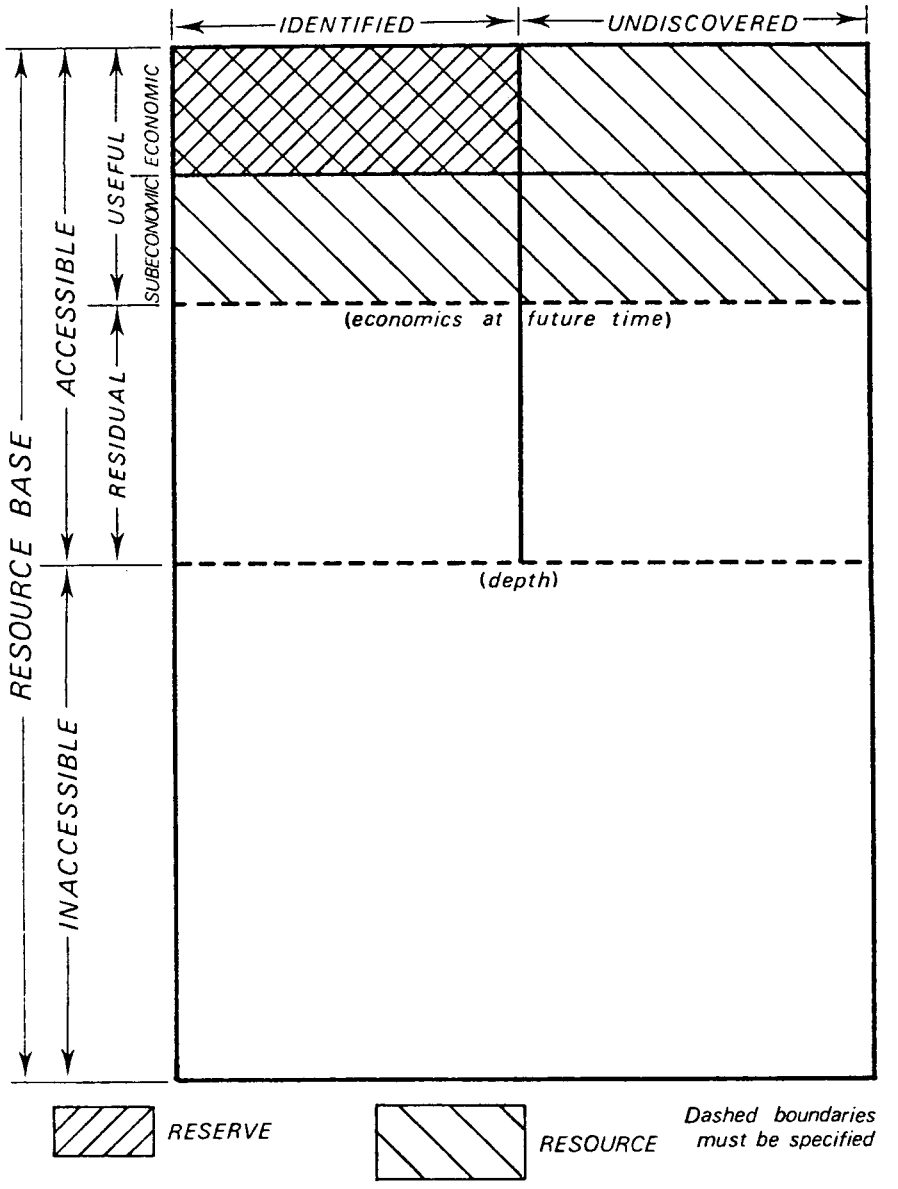

Figure 1.--McKelvey diagram for geothermal energy showing derivation of the terms resource and reserve (from Muffler and Cataldi, 1978, fig. 3). Scales are arbitrary, and thus the relative sizes of the rectangles have no necessary relation to the relative magnitudes of the categories.

Any resource assessment should be periodically updated in response to changing conditions. For geothermal energy, among these conditions are (a) increased data, resulting from expanded exploration and drilling activity, (b) development of improved and new technologies for exploration, evaluation, extraction, and utilization, (c) rapid evolution of geothermal knowledge, and (d) the increased role of geothermal energy in response to changing economic, social, political, and environmental conditions (in particular, an increasing awareness of the limits to petroleum and natural gas resources, both domestic and international).

Accordingly, the USGS plans to carry out an updated and expanded geothermal resource assessment of the United States by the end of 1978. Aspects to be given increased emphasis include the following:

a. Refinement of areas, thicknesses, and temperatures of high-temperature (>150°C) and intermediate-temperature (90-150°C) hydrothermal convection systems, in part using data acquired and compiled in the course of systematic evaluation of Known Geothermal Resource Areas (Mabey and Isherwood, 1978).

b. Improvement of methodology for estimating the fraction of energy in hydrothermal convection systems or geopressured systems that might be recoverable at the surface.

c. Interpretation of available data on low-temperature (<90°C) geothermal systems, in cooperation with the State Cooperative Direct-Heat Geothermal Program of the Division of Geothermal Energy of the Department of Energy.

d. Utilization of GEOTHERM, the new USGS system of computer-based storage and retrieval of geothermal data (Swanson, 1977).

e. Assessment of geopressured resources not inventoried in 1975 (offshore Tertiary deposits and onshore Mesozoic deposits of the Gulf Coast, and geopressured resources of other sedimentary basins).

f. Refinement of the size and age of young igneous systems and more thorough evaluation of the effects of hydrothermal convection on the cooling of plutons.

g. Evaluation and possible use of the techniques of subjective probability and Monte Carlo aggregation used in recent oil and gas resource assessments of the United States (Miller, et al., 1975).

h. Presentation of data and conclusions on a regional as well as a national basis.

This past year, the USGS has cooperated with the National Electric Agency of Italy (ENEL) in evaluating techniques for geothermal resource assessment, under the sponsorship of the U. S. Energy Research and Development Administration (ERDA), recently absorbed into the new Department of Energy. Recommendations for uniform terminology and methodology were presented at the ENEL-ERDA Larderello Workshop on Geothermal Resource Assessment and Reservoir Engineering (Muffler and Cataldi, 1978) along with a test application to central and southern Tuscany (Cataldi et al., 1978).

These joint studies identified a number of problems in geothermal resource assessment, one of which bears directly on the reservoir engineering community. This is the question of recoverability. In the petroleum and mining industries, one makes a careful distinction between the total amount of a given deposit underground prior to extraction, and that part of the deposit that might be extracted under foreseeable economics and technology. Commonly, the recoverable part is expressed as the total deposit multiplied by a recovery factor.

Extension of the term "recovery factor" to geothermal resources leads one to define geothermal recovery factor as the ratio of extracted thermal energy (measured at the wellhead) to the total thermal energy contained in a given subsurface volume of rock and water (Muffler and Cataldi, 1978). Implicit in this definition is the necessity that recovery take place in an industrial time frame (10 to 100 years) rather than in a geologic time frame ($>10^3$ years).

Recovery factors for hydrothermal convection systems were discussed in detail by Muffler and Cataldi (1978), and the test of geothermal assessment methodology in central and southern Tuscany (Cataldi et al., 1978) used the following formulations: (1) for systems producing by intergranular vaporization, the formulations of Bodvarsson (1974) and of Nathenson (1975) were modified for a 2.5 bar final pressure limitation (figure 2), and (2) for systems producing by intergranular flow, the analysis of Nathenson (1975) was extended to give a geothermal recovery factor scaled linearly from 50% at an effective porosity of 20% to 0% at an effective porosity of 0 (figure 3).

The first formulation is fairly rigorous, with the major assumption being whether the reservoir initially is filled with water or is vapor-dominated (White et al., 1971). The second formulation, however, is little more than a guess. A better basis for estimating the geothermal recovery factor is needed for geothermal resource assessment,

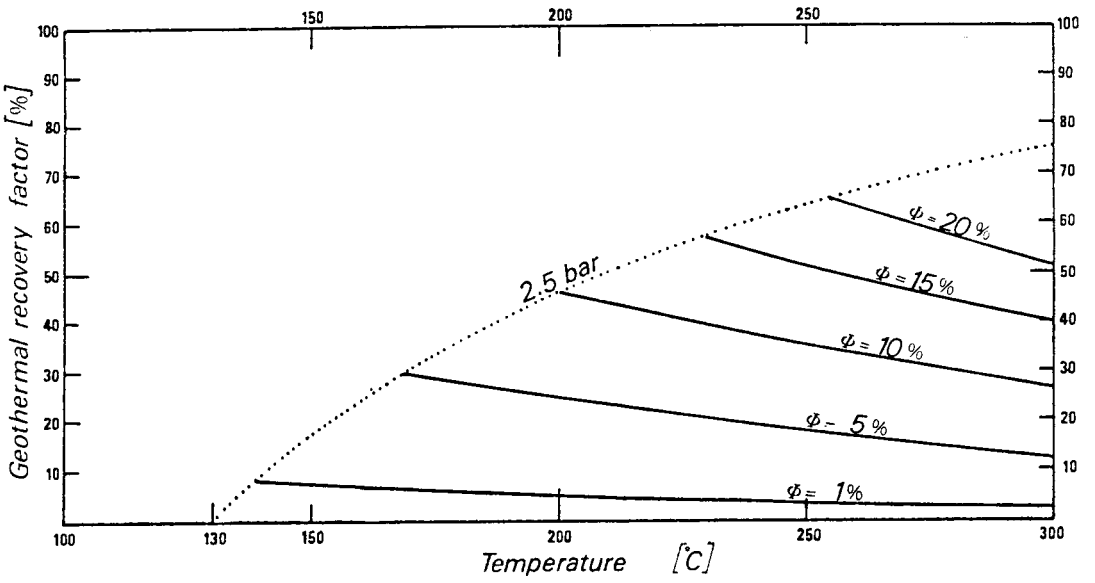

Figure 2.--Graph showing geothermal resource recovery factor (Rg) as a function of reservoir temperature and effective porosity (ϕ_e) for reservoirs produced by intergranular vaporization. From Muffler and Cataldi (1978, fig. 7), adapted from Nathenson (1975, fig. 4).

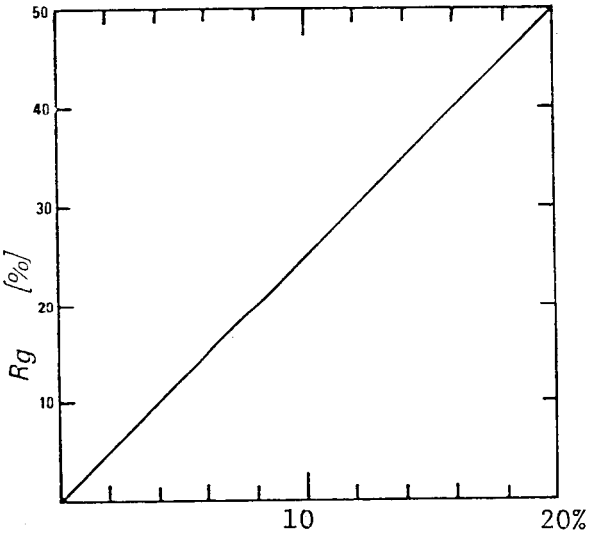

Figure 3.--Graph showing possible variation of geothermal resource recovery factor (Rg) as a function of effective porosity (ϕ_e) for reservoirs produced by intergranular flow. Rg is taken to be 50% for an ideally permeable reservoir in which total porosity = effective porosity = 20%. From Cataldi et al. (1978, fig. 9).

and I solicit the help of the reservoir engineering community in developing improved ways of estimating geothermal resources from hydrothermal convection systems produced by means of intergranular flow.

Acknowledgments

This contribution draws heavily on manuscripts prepared for the Geothermal Symposium at the IASPEI/IAVCEI Assembly of August 1977 (Muffler and Christiansen, 1978) and the Larderello Workshop on Geothermal Resource Assessment and Reservoir Engineering of September 1977 (Muffler and Cataldi, 1978; Cataldi et al., 1978).

References

Bodvarsson, G., 1974, Geothermal resource energetics: Geothermics, v. 3, p. 83-92.

Cataldi, R., Lazzarotto, A., Muffler, P., Squarci, P., and Stefani, G. C., 1978, Assessment of geothermal potential of central and southern Tuscany: Geothermics (in press).

Mabey, D. R., and Isherwood, W. F., 1978, Evaluation of Known Geothermal Resource Areas in the western United States: Geothermics (in press).

Miller, B. M., Thomsen, H. L., Dolton, G. L., Coury, A. B., Hendricks, T. A., Lennartz, F. E., Powers, R. B., Sable, E. G., and Varnes, K. L., 1975, Geological estimates of undiscovered recoverable oil and gas resources in the United States: U. S. Geol. Survey Circ. 725, 78 p.

Muffler, L. J. P., 1973, Geothermal resources: U. S. Geol. Survey Prof. Paper 820, p. 251-261.

Muffler, L. J. P., and Cataldi, R., 1978, Methods for regional assessment of geothermal resources: Geothermics (in press).

Muffler, L. J. P., and Christiansen, R. L., 1978, Geothermal resource assessment of the United States: Pure Applied Geophys., (in press).

Nathenson, M., 1975, Physical factors determining the fraction of stored energy recoverable from hydrothermal convection systems and conduction-dominated areas: U. S. Geol. Survey Open-File Rept. 75-525, 38 p.

Swanson, J. R., 1977, GEOTHERM user guide: U. S. Geol. Survey Open-File Rept. 77-504, 55 p.

White, D. E., Muffler, L. J. P., and Truesdell, A. H., 1971, Vapor-dominated hydrothermal systems compared with hot-water systems: Econ. Geol., v. 66, p. 75-97.

White, D. E., and Williams, D. L., eds., 1975, Assessment of geothermal resources of the United States -- 1975: U. S. Geol. Survey Circ. 726, 155 p.

RESERVOIR ENGINEERING MANAGEMENT PROGRAM

J. H. Howard and W. J. Schwarz
Lawrence Berkeley Laboratory
Berkeley, CA 94720

The Reservoir Engineering Management Program being conducted at Lawrence Berkeley Laboratory includes two major tasks: 1) the continuation of support to geothermal reservoir engineering related work, started under the NSF-RANN program and transferred to ERDA at the time of its formation; 2) the development and subsequent implementation of a broad plan for support of research in topics related to the exploitation of geothermal reservoirs. This plan is now known as the GREMP plan.

The continuation of support of research to NSF-RANN contract recipients has been reasonably straightforward. All these groups were conducting research that could be related to an improved capability to exploit geothermal resources and, accordingly, all contracts were continued and are in force at this time. Included here are the contracts at institutions shown in Figure 1, which also indicates briefly the scope of work being done.

In FY '77, $515 K was spent in support of these programs. It is estimated that $400 K will be spent on these contracts in FY '78.

The "GREMP" Plan

The acronym GREMP stands for "Geothermal Reservoir Engineering Management Plan" and is a misnomer. The plan addresses more than reservoir engineering and, in fact, touches on almost all technical areas involved in the exploitation of geothermal resources. The plan was deliberately made as broad as possible for several reasons: 1) in order to provide some written plan in areas for which no plan existed; 2) in order to perceive the interrelationship that exists among these technical areas, for instance physical properties of rocks and interpretive borehole geophysics; and 3) therefore, and in view of the total program and the interrelationships of the technical areas, to provide insight into how to implement the plan, e.g., what priorities should be assigned to the various tasks and what might the total cost of the program be.

Elements of GREMP

As conceived, there are 13 elements or technical areas to GREMP. These are shown in Figure 2. The elements can be grouped into seven super groups if one would want to simplify the program: 1) work related to measurement methods of use in the exploitation of geothermal resources; 2) studies of properties of materials of interest in the exploitation of geothermal resources; 3) work related to the definition, in the sense of

TITLE	CONTRACTOR
Data Compilation and Analysis From Italian Geothermal Field	Stanford-Italian
Modeling, Tracer, and Analytical Studies of Geothermal Resources	Stanford Ramey-Kruger
Wairakai Geothermal Reservoir Model	S^3
Mass and Heat Transport - Fractured Systems in Geothermal Reservoirs	Princeton
Modeling of East Mesa Geothermal Field	University of Colorado
Cerro Prieto Geothermal Modeling	UC/Riverside

Figure 1. Current NSF/RANN Legacies Contracts

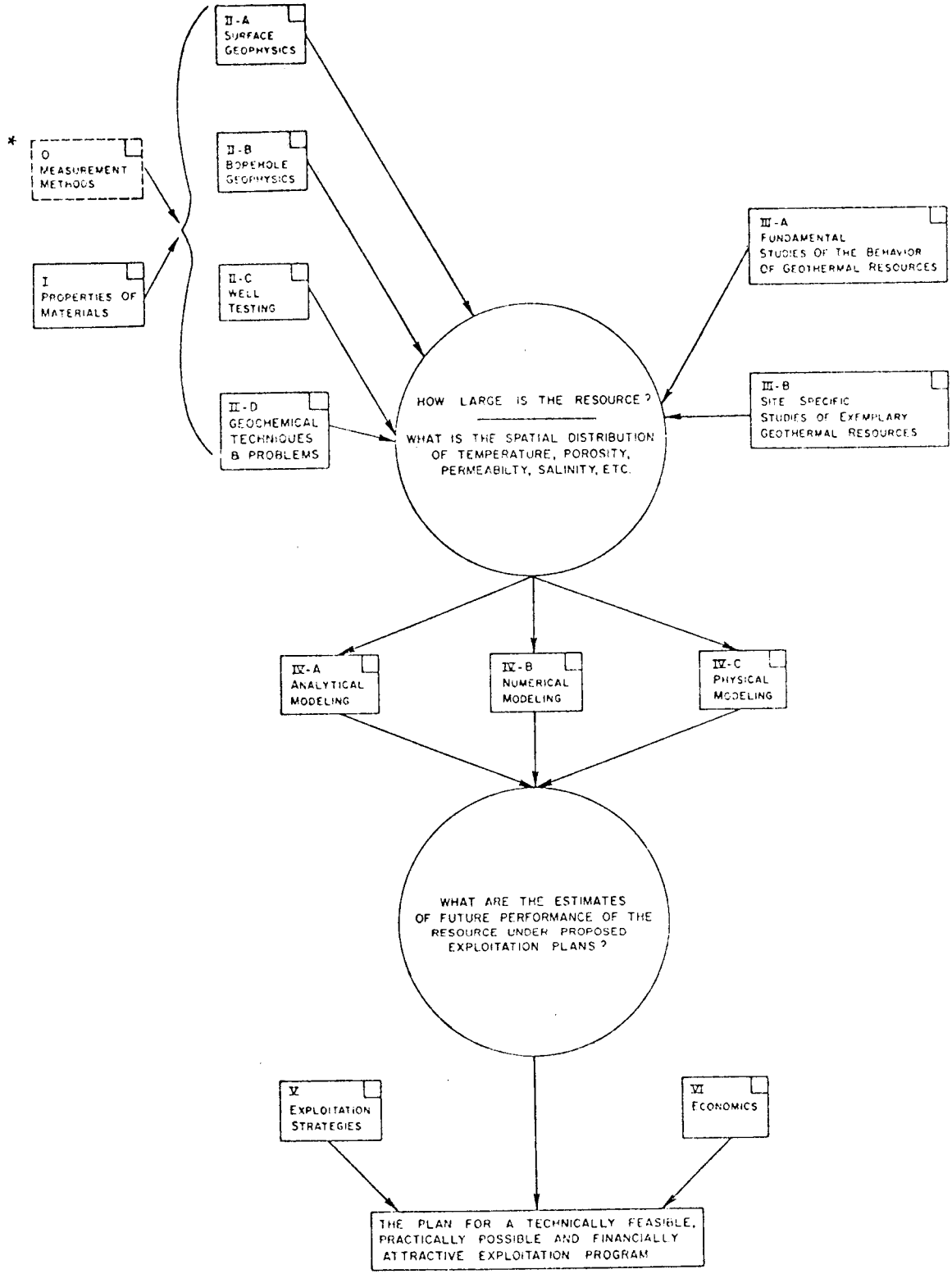

*The element "Measurement Methods" is being handled outside GREMP at this time.

Figure 2. Overview of the Geothermal Reservoir Engineering Program.

describing, of reservoir characteristics; 4) studies of specific, generalized, and hypotherical geothermal resources; 5) modeling the behavior of geothermal systems; 6) exploitation strategies; and 7) economics. Details of what each of these elements involves can be found in the report entitled "Geothermal Reservoir Engineering Management Program Plan (GREMP Plan)," issued by the Lawrence Berkeley Laboratory (LBL-7000, UC-66a, TID-4500-R66, Oct. 1977). Detailing any element of the program is a difficult task, and, if described in excessive detail, one might as well have done the research. However, there is a need for some level of detail in explaining what sorts of things should be done within each element. To illustrate the detail sought for the GREMP document the element "Well Testing" will be used as an example. As shown in Figure 3, we were able to break out research projects as a subset of the elements and research tasks as a subset of the projects. Note, for example, the recognition of the need for new operational procedures to define mass flow and energy flow (i.e., power) characteristics of a reservoir and also the desire to support work in crude estimating of the capability of a well.

Another point is illustrated by Figure 2, namely that LBL and in fact DOE/DGE does not exist alone. The well testing work involving instruments will be coordinated with the programs at Sandia because of their ongoing program in instrument development and because of the innate strength of their staff in instrument development.

Interrelationship of the Elements of GREMP

Figure 2 also shows the interrelationships of the elements of GREMP and illustrates the questions that these capabilities seek to help answer. The purpose of the entire GREMP program is to establish a higher level of technical capability to exploit geothermal resources than now exist. The "bottom line" is to produce better plans than are now possible for technically feasible, practically possible, and financially attractive exploitation programs.

Of fundamental importance are the questions: How large is the resource? and, What is the spatial distribution of temperature porosity, permeability, and salinity? With answers to these questions one should be in a position to determine if the resource contains enough energy to support a power plant of given size, if the energy can be moved out to the surface of the earth where it can be converted to electricity, and if there are any special problems to anticipate. For instance, are dissolved silica and trace elements present in such amounts that scaling of surface equipment will be a problem? The elements borehole geophysics, well testing, site specific studies (as a guide to completing a picture), all contribute to the answer to these questions.

Once the "static" situation regarding a geothermal reservoir is known, emphasis changes to the question of how the reservoir will perform when produced. Various forms of modeling can be used to predict future performance. However, the exploiter of a geothermal reservoir still does not have the plan he needs inasmuch as he must also consider the economics of the exploitation venture and the various strategies for its development. Accordingly the GREMP plan calls for some support in these areas of work.

"Well Testing" - Categories, Projects and Tasks

RESEARCH CATEGORY	RESEARCH PROJECT*	RESEARCH TASK
Well Testing	1. Assess conditions in geothermal reservoirs that affect tool and analysis requirements.	
	2. Improved data gathering systems.	a. Develop improved pressure tool capable of 650°F, 0-5000 psi pressure, 0.0. accuracy, one second minimum readout interval.
		b. Develop improved temperature tool capable of 650°F, accuracy of 1°F, continuous operating up to 90 days.
		c. Develop reliable downhole flow meter for geothermal applications.
		d. Develop automated multi-well data gathering system.
		e. Develop improved calorimetry systems.
		f. Develop improved mass flow rate measuring systems, particularly for two-phase flow.
		g. Develop packing and isolation apparatus for downhole applications such as drill stem testing.
	3. Develop new testing techniques and procedures.	a. Techniques for simultaneous analysis of mass and heat movement.
		b. New techniques for crude estimates of well capability (cf. James Method).
	4. Development of interpretation and analysis methods for hydraulic well testing and for temporary completion testing.	a. Improve and extend the analytical capability for pressure and temperature analysis for uninvestigated initial, boundary, and internal conditions of the reservoir.
		b. Perfect the use of well head values instead of sand face values in analyses.
	5. Development of methods of analysis of data from passive reservoir response.	a. Analysis of earth tides.
		b. Analysis of response to microseisms.
		c. Decline curve analysis.

*All projects and tasks involving tool, hardware and material development will be coordinated with the Geothermal Logging Development Program at Sandia Laboratories, Albuquerque, NM.

Figure 3

Use of GREMP

The GREMP program was reviewed twice by members of a so-called Review Task Force consisting of members of industry, government and the academic community. This group assigned priorities to the elements of the program. These priorities are shown in Figure 4. Highest priority was assigned to well testing, then to interpretive borehole geophysics, then to geochemical techniques and problems, and so on. The responsibility to develop a plan for geothermal log interpretation has been transferred to Los Alamos Scientific Laboratory. The balance of the program is currently being implemented by LBL; however, various considerations may possibly lead to parts of the program being revised and implemented elsewhere.

In any event, implementation of the program calls for the procedure outlined in Figure 5. The key developments are: 1) writing of a request for proposal to conduct research in the subject area, and 2) receipt and review of proposals and award of contracts in such a way as to achieve greater technical capability for the geothermal community in a particular technical area.

At the present time elements 1, 3, and 4, namely well testing, geochemical techniques and problems, and properties of materials, have been announced in the Commerce Business Daily. Over 80 requests for each category have been received to date. The RFP package for well testing is being mailed to requestors this week.

Anticipated Expenditures for GREMP in FY '78

The total currently authorized budget for supporting both the continuation of the NSF-RANN research and the initiation of new projects as a consequence of GREMP is $1 M. Of this amount, an estimated $400 K will be spent on the former NSF-RANN contractors. The balance of $600 K will be spent on new projects. At one time in development of the GREMP plan we estimated if all things we thought should be done were done, the cost would run over $2 M annually, not including the NSF-RANN contractees. Based on our experience to date with groups such as the NSF-RANN contractors, in view of expressions of interest to date, and in view of what in principle we would like to achieve, we anticipate that we can effectively spend $1.5 M in FY '78. This support would go to continuation of support to NSF-RANN contractors and to support work in well testing, geochemical techniques and problems, properties of materials, numerical modeling, analytical modeling, site specific studies, and socalled fundamental studies. Probably we will not be able to initiate any work from the GREMP program in physical modeling exploitation strategy and economics this fiscal year.

Looking at the Output of the GREMP Program

A question that can be fairly asked of those responsible for a research program is "What good have you done?" In order to have a measure of the results of a research program, one must have an objective toward

TABLE OF PRIORITIES

RESERVOIR ENGINEERING MANAGEMENT PROGRAM

Priority Number		Element/Category	Priority Scale *
1	II.C.	Well testing	9.9
2	II.B.	Interpretive borehole geophysics	8.8
3	II.D.	Geochemical techniques and problems	7.6
3	I.	Properties of materials	7.6
4	IV.B.	Numerical modeling	7.4
5	III.B.	Site specific studies	6.3
6	II.A.	Fundamental studies	5.9
7	IV.A.	Analytical modeling	5.4
8	II.A.	Surface geophysics	3.9
9	IV.C.	Physical modeling	3.4
10	VI.	Economics	1.6
11	V.	Exploitation strategy	1.5

* On a scale of 0 - 10.

Figure 4.

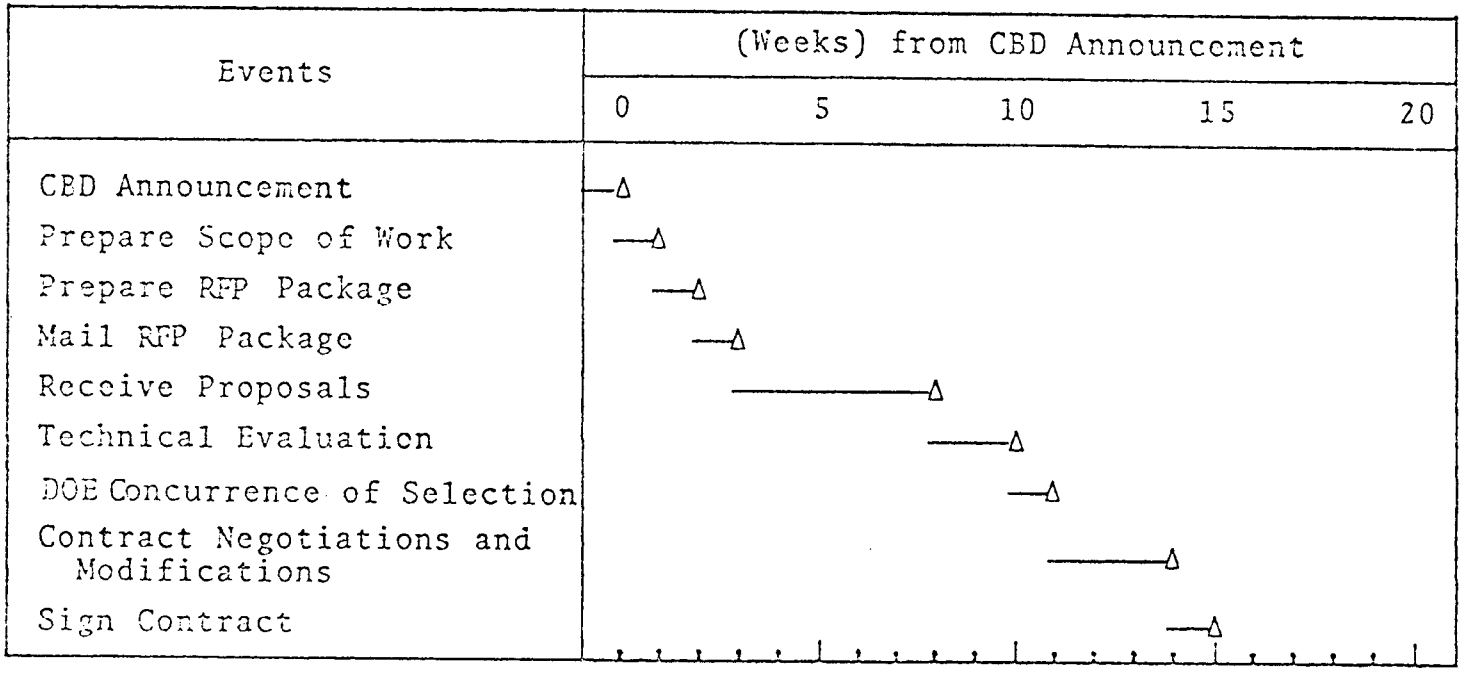

Figure 5. The competitive procurement planning schedule for GREMP.

which the research contributes. DOE/DGE has such an objective. The primary objective is to accelerate the commercial development of the nation's accessible geothermal resources.

Accordingly, research projects undertaking to solve or successfully solving or contributing to the solution of technical problems in acceleration of near-term commercialization of geothermal reservoirs should be favored. For example, work to solve the problem of successful reinjection of spent brine at a specific site should be favored through such a policy. On the other hand, many kinds of "research" are being carried out within the geothermal program; many do not meet the clearcut criteria of solving a technical impediment tomorrow. However, it is not valid to conclude that therefore this work is of no use. Research that is potentially applicable and clearly relating to the successful exploitation of geothermal resources needs to be supported, even if it is not directed at today's crisis. There are several reasons for this view. First, research done in conjunction with persons in training (usually students) broadens the education of these persons in respect to existing knowledge. In this way they are better trained to work in the geothermal industry. Second, support of basic or fundamental research invariably leads to the strengthening of the scientific basis from which technology arises. The establishment of such a scientific basis does not guarantee the development of an applicable technology but, in the hands of a practice-oriented person, can lead to the solutions needed for acceleration of commercial development. Persons with such expertise therefore turn out to be critical. Third, support for basic research usually attracts people who can generate an atmosphere of vitality and enthusiasm that is a healthy positive force for attack on both technological and scientific problems. The entropy they create is valuable and again, the use of their associated energy is focused by these alert, practice-oriented persons. Such people are critical to the success of a geothermal industry.

Conclusion and Summary

Both the NSF-RANN legacies and GREMP are in direct support of the DOE/DGE mission in general and the goals of the Resource and Technology/ Resource Exploitation and Assessment Branch in particular.

These goals are to determine the magnitude and distribution of geothermal resources and reduce risk in their exploitation through improved understanding of generically different reservoir types. These goals are to be accomplished by: 1) the creation of a large data base about geothermal reservoirs, 2) improved tools and methods for gathering data on geothermal reservoirs, and 3) modeling of reservoirs and utilization options.

The NSF legacies are more research and training oriented, and the GREMP is geared primarily to the practical development of the geothermal reservoirs.

GEOTHERMAL RESERVOIR INTERPRETATION FROM CHANGE IN GRAVITY

William Isherwood
U.S. Geological Survey
Menlo Park, California 94025

Precision gravity methods provide new information regarding geothermal reservoir mechanisms and depletion. This paper discusses the principles of present interpretations and early conclusions from two producing geothermal fields, Wairakei, in New Zealand, and The Geysers, California.

The acceleration of gravity at any point on the earth's surface is a function of numerous factors including the mass distribution beneath the point and its absolute elevation. A change in the observed gravity at a fixed location in a geothermal field therefore can be interpreted in terms of change in elevation and fluid movement in nearby reservoir rocks, other factors being either corrected for or held constant. Modern gravity meters have sensitivities sufficient to reliably measure differences in gravitational acceleration of between 5 and 10 μgal (10^{-8} m/sec/sec), although changes in gravity measured to date, because they are dependent on baselines established with older equipment, are probably accurate to only about 30 μgal. A 5-10 μgal change can be caused either by several centimeters of elevation change or by the draining of liquid water from a layer about 1 meter thick from an infinite aquifer with 20 percent porosity. Careful repeat measurements of gravity provide the potential for detecting mass loss (depletion) from geothermal reservoirs, which can be used for determining the percentage recharge occurring, for detecting areas of drainage, and to test various reservoir models, provided that elevation change is measured independently and corrected for and production data are available. In practice this requires coordination with a first-order leveling program.

Despite theoretical expectations, it must be demonstrated that changes in gravity observed are in fact related to removal of geothermal fluid--especially when so many other effects could contribute to any one measurement. Trevor Hunt of New Zealand established the first practical test of precision gravimetry in geothermal studies at the Wairakei field (Hunt, 1970, 1977). After correcting for elevation changes and showing that other effects such as changes in local topography and differential changes in ground-water level could be neglected, Hunt's demonstration of the method came largely from the observations of gravity decreases correlating spatially with the limits of the exploited field. The resultant pattern was one of maximum gravity decrease centered on the main production borefield and tapering smoothly toward zero changes at several kilometers distance. This same part of the field showed moderate subsidence, a further suggestion of net loss of fluid from the system.

A program patterned on the New Zealand study was set up at The Geysers, California (Isherwood, 1977). But the situation is, for various reasons, much more complicated. Landsliding and active tectonics could be producing vertical ground motions unrelated to fluid withdrawal. As an underpressured, "vapor-dominated" system, The Geysers may have only slight subsidence potential because internal pore pressure is apparently not contributing much support to the rock matrix. Also, if the reservoir contained only vapor in the pore space (including, of course, fractures), then the mass loss conceivably is distributed over a large volume or is occurring at some distance from the well bores. Finally, California's present severe drought could change local ground-water levels. Despite these complications, areas of gravity decreases (with respect to a reference station outside the field) closely match areas of production (fig. 1). Thirty-six of the gravity stations coincide with remeasured elevation points. Figure 2 shows the correlation between subsidence and gravity decrease. The resultant correlation of +0.72 is particularly significant, inasmuch as changes of gravity caused by landslides or block tectonic elevation changes would produce a correlation coefficient of -1.

Both Wairakei and The Geysers clearly show a net mass loss in the reservoir region. Determining the actual mechanism of loss is prerequisite to understanding the reservoir dynamics. For both reservoirs, the most likely mechanism is the replacement of hot liquid water (ρ water @240°C=0.8 g/cm^3) in the pore space by water vapor (ρ steam @240°C=0.02 g/cm^3) and removal of excess fluid. Where this flashing takes place can be further constrained (as will be explained later). Alternate mechanisms of mass loss seem unlikely or inadequate to explain observed changes. For example, evacuating steam of density 0.02 g/cm^3 from the pores of a vapor-dominated system could cause only about 0.001 g/cm^3 bulk density change (using the 5 percent porosity suggested for vapor-dominated systems); to change gravity by the amounts observed at The Geysers in just 2 1/2 years would require depletion to a depth of at least 9 km for a 40 km^2 field. Changes in density of the liquid or rock, though possible, would presumably be toward greater density, due to reservoir cooling. Similarly, any change in porosity (presumably due to subsidence) would tend to increase bulk density and consequently not contribute to a gravity decrease.

If gravity measurements are made with sufficient coverage and precision to permit accurately contouring the change in gravity over an area, then Gauss' potential theorem can be used to determine the total change of mass (in this case the net fluid loss) without assuming a shape or depth of the source. Hunt used this approach in studying mass loss from the Wairakei field over a 16-year period. Comparison of the mass loss calculated from gravity with the measured mass of produced fluid showed as much as 90 percent net loss during the early years of exploitation but an apparent increase in natural recharge percentage with prolonged production. If a true steady-state situation is eventually attained, the initial unfavorable

trends in lowered pressure, flow rate, etc., may be temporary, at least for some hot water systems. Continued monitoring will be required to confirm whether an equilibrium recharge rate has indeed been reached at Wairakei.

Preliminary calculations of the mass balance at The Geysers by Gauss' theorem show the mass loss to be essentially the same as the calculated mass of produced steam during the same time. Because of the limited areal coverage and duration of the study, this estimate of 0 percent recharge could be in error by as much as 20 percent. This uncertainty should be reduced in a few years as instrumentation is upgraded and the net is expanded to more gravity stations and more than 150 km additional first-order leveling lines. Still unresolved are (1) whether lack of recharge is related to the drought, and (2) barring eventual recharge, how large a volume can be tapped by the present wells.

Interpretations regarding the distribution of mass loss are not unique, although the "forward calculations" are. That is, if we know the net mass removed and its distribution (shape and depth) the gravity effect at all surface points can be calculated. Through such calculations more substantial conclusions about The Geysers geothermal reservoir have been made. The work at The Geysers typifies the additional information that can be derived. Certain assumptions are useful in simplifying computations. Recognizing that the distribution of mass loss may be complicated in detail, the first assumption is that we may treat the loss as a body or small number of bodies with some uniform density change. Due to the normally smooth character of the gravity field and distance from source to observation, this bulk characterization is considered reasonable. That the bulk density change is not exactly known scarcely affects the results. Representative parameters are established using reservoir properties considered reasonable on the basis of geologic and reservoir engineering studies.

For convenience of calculation, the shape of the mass loss is assumed to be that of a cylinder with its axis vertical (fig. 3). Using the mass of the net produced fluid (estimated at 7.5×10^{10} kg over 2 1/2 years) as a maximum loss, the gravity effect at the surface can be calculated for various combinations of cylinder radius and depth. Figure 4 shows such a matrix for a bulk density change of 0.04 g/cm^3. (This density change would result from the flashing of hot water of density 0.82 g/cm^3 to steam of density 0.02 g/cm^3 if the liquid initially saturated a uniform 5 percent porosity or filled half the pore volume at 10 percent porosity.) For instance, a cylinder of 1 km radius, which would have a thickness of about 600 m (density contrast and mass given), would have a gravity effect directly above it of 129 μgal if the top were 1500 m deep and bottom about 2100 m deep and an effect of only 84 μgal if the top were 2000 m deep and bottom at about 2600 m. Because a change in the radius changes the thickness, an optimum radius produces the maximum effect--in all cases decreasing with depth. The shaded zone on figure 4 represents the observations at The Geysers, where a

maximum observed change is about 120±30 μgal. Within this shading, the observed changes could be accounted for by this set of parameters and zero recharge. If the true parameters fall to the left (shallower) side of the shading where the calculated effect is too large, the observed change could have been caused by less mass loss--indicating partial recharge. To the right of the shaded zone the calculated effect is less than observed, showing (1) that there is additional mass loss by some unknown mechanism or (2) that such a shape-depth combination would be impossible. A change in the density contrast by a factor of 2 changes the depth to the center of the cylinder only a few percent at the depth range of interest, although the top and bottom will vary more to accommodate the appropriate change in cylinder thickness. Similarly, the maximum depth to the mass loss can not be increased greatly by considerations of shape (e.g. sphere versus cylinder) and it actually decreases if the regions around individual production sites are considered separately. Consequently, if we assume no additional mass loss beyond what has been produced, we can rule out the possibility of steam boiling solely off a water table deeper than about 2500 m. Some contribution from this depth is not precluded, but the major loss must be shallower, probably near the 1-2 km depth of most well completions. This supports the model of Truesdell and White (1973) which proposes liquid water throughout the reservoir, such water flashing to steam as a direct result of pressure decrease caused by exploitation.

Regions of drainage may be recognized by comparing a map of elevation-corrected changes in gravity to areas of known production. Asymmetry to the pattern of gravity change at Wairakei (Hunt, 1977) suggests greatest depletion to the west of the main production borefield. At The Geysers, some of the critical stations surrounding the present field have not yet been releveled to provide elevation correction. Consequently, although measurements from the stations to the southwest (around power plant 15, fig. 1) are suspect because of their apparent large decreases in gravity, we must await the leveling data for interpretation.

Projections of reservoir longevity at The Geysers and elsewhere will be reliable only when we have a longer period of observation and our interpretation techniques are refined. Gravity changes reflect what has happened between measurements, and, in conjunction with other reservoir data, can eventually allow for projections which will lead to informed management of reservoirs.

REFERENCES

Hunt, T. M., 1970, Gravity Changes at Wairakei Geothermal Field, New Zealand: Geol. Soc. America Bull. v. 81, p. 529-536.

Hunt, T. M., 1977, Recharge of Water in Wairakei Geothermal Field Determined from Repeat Gravity Measurements: New Zealand Jour. Geology and Geophysics, v. 20, p. 303-317.

Isherwood, W. F., 1977, Reservoir Depletion at The Geysers, California: Geothermal Resources Council, Transactions, v. 1, p. 149 (summary).

Truesdell, A. H. and White, D. E., 1973, Production of Superheated Steam from Vapor-Dominated Geothermal Reservoirs: Geothermics, v. 2, p. 154-173.

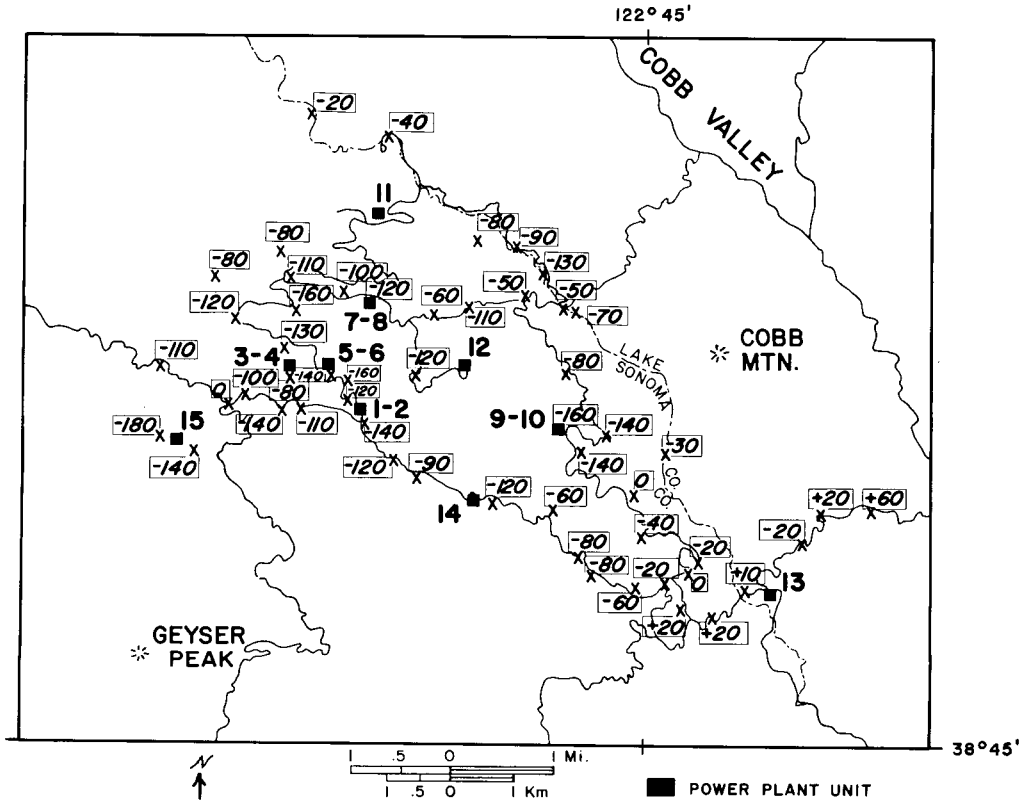

Figure 1. **GRAVITY CHANGES, IN μGAL, BETWEEN JULY 1974 AND FEB. 1977, THE GEYSERS GEOTHERMAL AREA, CALIFORNIA.**

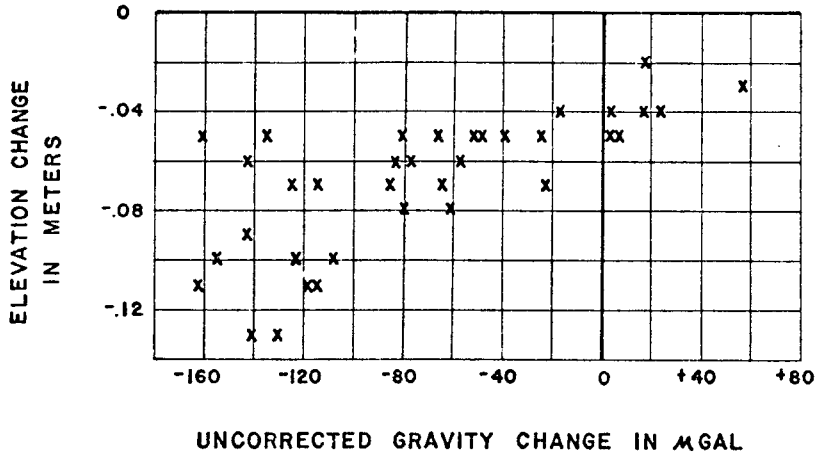

Figure 2. Relation between gravity change (July 1974 to Feb. 1977) and elevation change (late 1973 to late 1975), at The Geysers, California.

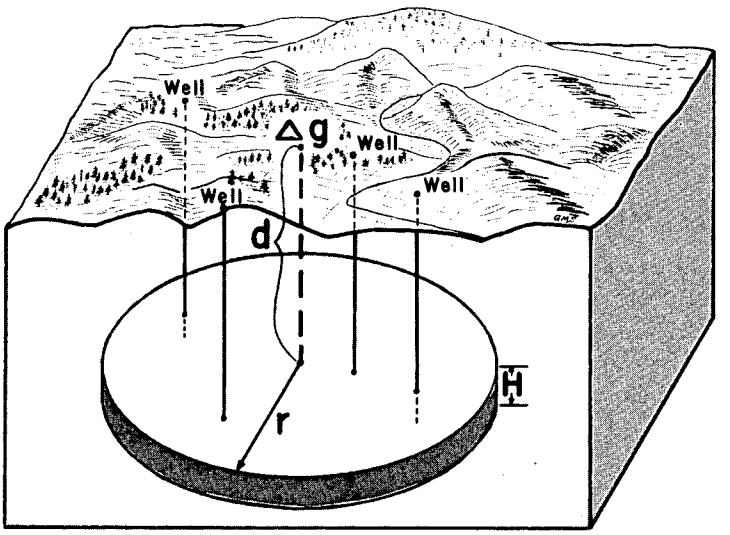

Figure 3. **CYLINDRICAL APPROXIMATION TO MASS LOSS**

$$\Delta g \text{ (in } \mu\text{gal)} = 41.85 \quad \rho \left[H - \left(\sqrt{(d+H)^2 + r^2} - \sqrt{d^2 + r^2} \right) \right]$$
(in meters)

Radius (km)	Depth to top (meters)						
	0	500	1000	1500	2000	2500	3000
.1---	167	16	8	5	4	3	3
.5---	750	275	136	82	55	40	31
1.0---	726	387	213	129	84	59	43
1.5---	405	272	177	117	81	58	44
2.0---	242	182	132	96	70	53	41
2.5---	156	125	98	75	58	46	36
3.0---	110	91	75	60	49	39	32
3.5---	81	69	59	49	41	34	28
4.0---	62	55	47	40	34	29	25

Figure 4. GRAVITY EFFECT OF CYLINDER WITH $\Delta\rho$ = 0.04 g/cm^3 (in μgal) FOR MASS OF TOTAL PRODUCING FIELD

PERMEABILITY OF KAYENTA SANDSTONE TO HYPERSALINE BRINE AT 10.3 MPa CONFINING PRESSURE AND TEMPERATURES TO 90°C*

A. J. Piwinskii and R. Netherton

University of California, Lawrence Livermore Laboratory
Livermore, California 94550

The ability to inject "spent" geothermal brine may be a critical and perhaps limited factor in the development of fluid-dominated geothermal resources. In order to understand and evaluate changes in formation permeability and porosity at depth as a result of injection of brine effluents, experiments were carried out (70°-90°C at 10.3 MPa confining pressure) in conjunction with the ongoing brine chemistry and materials evaluation effort at the Lawrence Livermore Laboratory Field Test Station located in the Salton Sea Geothermal Field, Imperial Valley, California.

SAMPLES, APPARATUS, AND EXPERIMENTAL METHOD

The sedimentary rock investigated was the Kayenta sandstone (Chan, 1977; Piwinskii and Netherton, 1977). Core samples (10.2 cm long, 2.5 cm diameter) were dried at approximately 80°C for 48 to 72 hours at a pressure of 10 kPa. After cooling, specimens were saturated with 1 M NaCl solution and stored under this solution in a desiccator. Core samples were jacketed with tygon and pressurized to 10.3 MPa (Piwinskii and Netherton, 1977). When the specimen attained thermal equilibrium, geothermal brine was admitted to the core and flow rates were measured at a series of differential pressures in order to establish that data were being collected in a laminar flow régime. Permeability was evaluated from $k = \eta QL/A[P_2 - P_1]$ (Wycoff et al., 1934; Muskat, 1937). P_2 and P_1, upstream and downstream pressure, respectively, were measured via Bourdon tube gauges, and Q, flow rate, was determined by noting the time of brine flow into a burette using a stop watch. Length (L) and Area (A) of the samples were measured and brine viscosity (η) was determined using a Brookfield LV viscometer with UL adapter (Piwinskii et al., 1977; Piwinskii and Netherton, 1977).

---

*Work performed under the auspices of the U.S. Dept. of Energy under contract No. W-7405-Eng-48.

EXPERIMENTAL RESULTS

Magmamax No. 1 brine, acidified in some cases upstream of the core sample, was the fluid used in the investigation. The experiments were conducted in three basic modes:

1) no filters operational upstream of the core,
2) one 10 μm cartridge filter operational upstream of the core,
3) one 10 μm cartridge filter and one 10 μm depth-type filter operational upstream of the core.

When the experiments were conducted with one filter or no filter in operation, the permeability calculated is a composite of the rock and a 2 to 3 mm thick filter cake composed of amorphous silica and iron which is formed on the top face of the core sample. The thickness of the filter cake is not fixed but is a function of time of sample exposure to the brine. All samples run in modes 1 and 2 show this type of cake buildup. As a result, it is very difficult to assess the intrinsic permeability of the sandstone, or the permeability of the sludge layer on the core face.

Data provided in Figure 1 indicate that the permeability of K-4 when conducted in mode 1 (no filters operational) decreased from 50 md to 1 md after 5.2 hours of flow of acidified brine (see Table 1 for inlet pH). Sample K-10 was run initially with two filters operational (mode 3). After approximately 1.6 hours of flow, the permeability decreased to 60 md. After removal of the disc filter, the permeability of sample K-10 decreased sharply from 60 md to 15 md after two hours flow of untreated brine (mode 2). When both 10 μm filters were inserted upstream of the core (mode 3), the permeability of sample K-A decreased from 700 md to 65 md after 1.5 hours of flow of brine which had been acidified to pH = 3.58 (see Table 1). It is interesting to note that after approximately 1.5 hours flow of filtered brine (see samples K-10 and K-A in Figure 1), 1360 pore volumes of pH = 3.58 brine flowed through K-A while only 421 pore volumes of pH = 5.8 (untreated) brine permeated sample K-10.

DISCUSSION

Unmodified Magmamax brine contained about 140 ppm suspended silica solids. In acidified brine, however, silica suspended solids concentrations were ≤15 ppm. Depending on pH, acidified brine effluents have long-term (20-200 hours) stability with respect to silica precipitation. In unmodified brine, suspended solids levels reach 300-400 ppm within two hours at 90°C. Rapid permeability decline occurred when *untreated and unfiltered* brine

permeated sample K-4, and when *acidified and filtered* brine passed through samples K-10 and K-A (see Figure 1). The permeability loss exhibited by K-A deserves further comment. Data given in Table 1 reveal that the pH of brine leaving K-A is much higher than the incoming brine pH. This suggests that the rock's matrix calcite cement is being dissolved by the hot, permeating acid brine, thereby yielding a carbonated exit brine of high pH. Furthermore, the SiO_2 content of brine exiting the core sample is much lower than that of the entering brine (see Table 1). This suggests that precipitation of amorphous silica occurred in the sandstone, presumably decreasing the size of pore throats and causing permeability loss.

Some evidence exists that small calcite particles resulting from the dissolution of the matrix cement and/or colloidal silica deposits are plugging pore throats. Grens (1977) measured the particle size distribution in the Magmamax No. 1 brine as it exited Kayenta sample K-4 by means of a laser light-scattering particle analyzer. He found that there was a tremendous increase in particles in the 2 to 5 μm size range in brine which had flowed through Kayenta sandstone after 0.83 hours. This suggests that small calcite particles were being generated in large quantities and/or colloidal silica particles were precipitating from the permeating brine. The combined effect on permeability is clearly observed in Figure 1.

In summary, the data portrayed in Figure 1 indicate that large permeability losses occurred in Kayenta sandstone (porosity, 20.7 ± 1.66%) when *unfiltered, untreated* Magmamax brine and *filtered, acidified* Magmamax brine were the permeating fluids. In the former case, permeability decline was due to the accumulation of a thick filter cake on the top face of the core sample which was composed of amorphous silica and iron. In the latter situation, loss of permeability was caused by the precipitation of amorphous silica and generation of large quantities of calcite particles from the dissolution of the matrix cement. The experimental results thus show that if the Salton Sea Geothermal Field were composed of porous sedimentary formations similar to Kayenta sandstone, long-term injection of unmodified Magmamax brine is not feasible. In the case of acidified brine, most of the permeability decline may result from the mobilization of calcite. Additional experiments will be carried out in the future at lower flow rates to test the possibility of long-term injection of filtered, acidified geothermal brine.

ACKNOWLEDGMENTS

We thank A. Duba, P. Gunning, G. Kelly, F. Locke, L. Owen, and R. Quong for assistance in the field, F. Dishong, R. Garrison, J. Harrar, D. McCright, C. Otto, F. Schifflin, and T. Woerhle for analytical help, N. Carlin and R. McClain for field support, A. Duba, J. Grens, F. Locke, L. Owen, and R. Quong for discussion, A. Duba and L. Owen for reviewing the manuscript, and B. Hornady for typing the manuscript.

REFERENCES

Chan, M., Personal communication (1977).

Grens, J. Z., On Particulate Materials in Geothermal Brines, Lawrence Livermore Laboratory, Livermore, Rept. UCID, in preparation (1977).

Muskat, M., The Flow of Homogeneous Fluids Through Porous Media (McGraw-Hill, New York, 1937).

Piwinskii, A. J., and Netherton, R., An Experimental Investigation of the Permeability of Kayenta and St. Peter Sandstones to Magmamax No. 1 Brine at 10.3 MPa Confining Pressure and Temperatures to 90°C, Lawrence Livermore Laboratory, Livermore, Rept. UCRL, in preparation (1977).

Piwinskii, A. J., Netherton, R., and Chan, M., Viscosity of Brines from the Salton Sea Geothermal Field, Imperial Valley, California, Lawrence Livermore Laboratory, Livermore, Rept. UCRL-52344 (1977).

Wycoff, R., Botset, H., Muskat, M., and Reed, D., "The Measurement of the Permeability of Porous Media for Homogeneous Fluids," Rev. Sci. Instrum. 4, 394-405 (1934).

Table 1. Data on pH and SiO_2 Composition of Brine

	Kayenta Sandstone		
	K-4	K-10	K-A
Mean inlet pH	5.00±0.20	5.80±0.08	3.58±0.60
Mean outlet pH	5.95±0.35	5.65±0.09	4.78±0.24
Inlet SiO_2 composition of brine (ppm)	445	425	477
Outlet SiO_2 composition of brine after 0.38 hr flow (ppm)	---	267	---
Outlet SiO_2 composition of brine after 0.90 hr flow (ppm)	---	---	400
Outlet SiO_2 composition of brine after 3.55 hr flow (ppm)	---	172	---
Outlet SiO_2 composition of brine after 5.33 hr flow (ppm)	---	---	353
Outlet SiO_2 composition of brine after 15.75 hr flow (ppm)	181	---	---

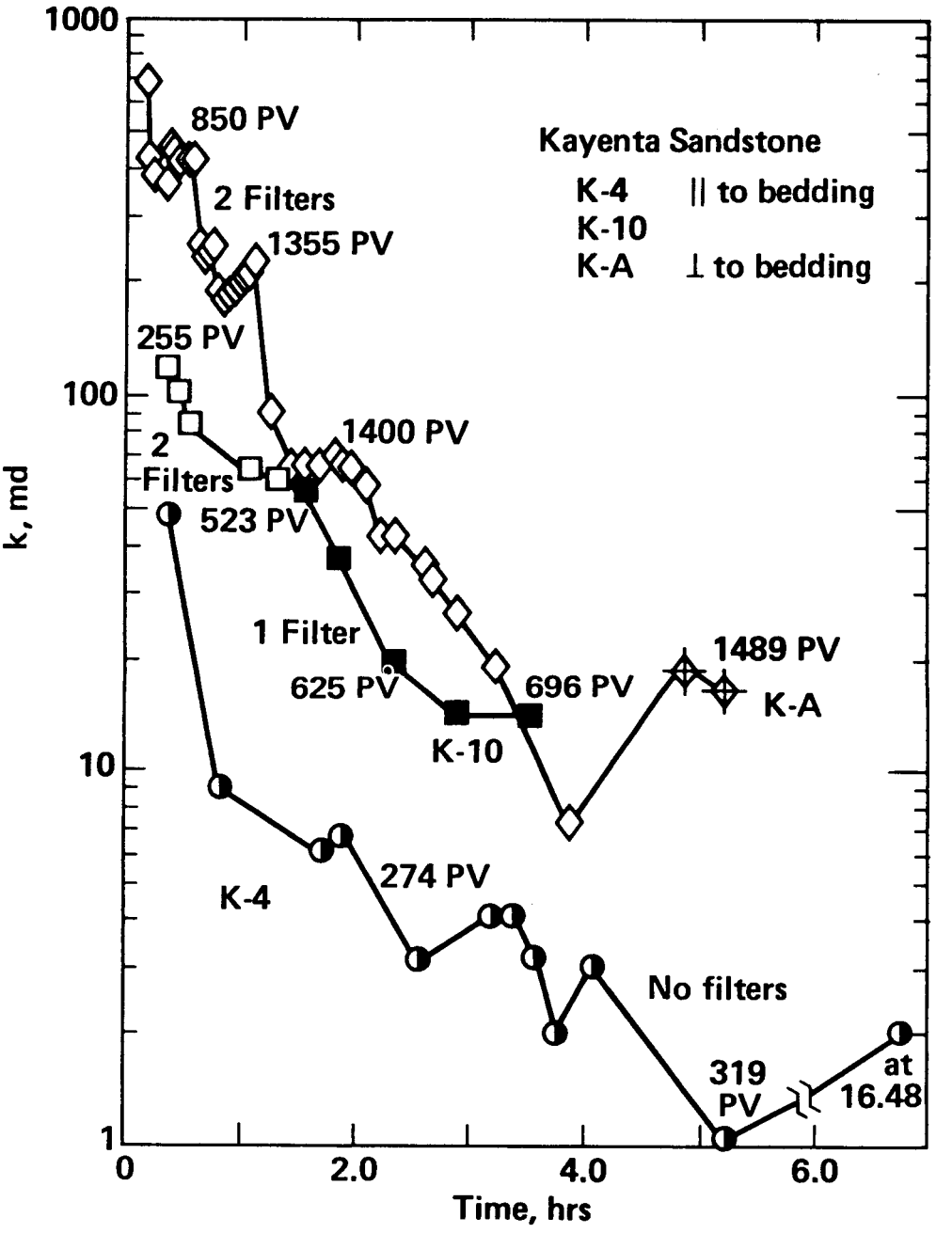

FIGURE LEGEND

Figure 1. Permeability of Kayenta sandstones, K-4 and K-10, parallel to the bedding, and K-A, perpendicular to the bedding, as a function of the total time of flow of brine through the core. Also plotted are the number of pore volumes (PV) of brine which passed through the core samples at the time indicated. Data on the mean pH and SiO_2 content of brine entering and leaving each core are given in Table 1.

THE REAL GAS PSEUDO

PRESSURE FOR GEOTHERMAL STEAM -- SUMMARY REPORT

L. S. Mannon
Atlantic Richfield Co.
1860 Lincoln Suite 501
Denver, Colorado 80295

and

P. G. Atkinson
Union Oil Co.
P. O. Box 6854
2099 Range Ave.
Santa Rosa, California 95406

INTRODUCTION

The producing characteristics of vapor-dominated geothermal steam reservoirs bear some strong resemblances to those observed in hydrocarbon natural gas reservoirs. Consequently, many geothermal steam well tests are commonly analyzed using flow theory developed for the isothermal flow of hydrocarbon natural gases. Such analysis is most often made using the idealization of perfect gas fluid flow behavior in the reservoir.

This study investigated the real gas flow characteristics of geothermal steam over the ranges of pressure, temperature, and noncondensable gas content commonly found in vapor dominated geothermal systems. Details of this study are available elsewhere (Mannon, 1977).

THEORY

The transient flow of a real gas in an incompressible porous medium is described by a highly nonlinear partial differential equation. For the case of an ideal gas, this equation, while still nonlinear is similar in form to the classical diffusivity equation which describes transient liquid flow in porous media. Aronofsky and Jenkins (1953) provided numerical solutions to this equation which demonstrated that transient ideal gas flow could be analyzed using some of the techniques developed for transient liquid flow.

Al-Hussainy et al. (1966) proposed an integral transformation which converts the form of the nonlinear flow equation for a real gas into one, which, while still nonlinear, is also similar in form to the diffusivity equation. Thus, there exists the possibility that real gas transient fluid flow can be analyzed in terms of the transformed pressure variable using techniques developed for transient liquid flow. This possibility was verified for hydrocarbon natural gases in radial flow systems by Al-Hussainy and Ramey (1966) and Wattenbarger and Ramey (1968).

RESULTS

The integral transformation proposed by Al-Hussainy et al. has been called the "real gas pseudo pressure" and is:

$$m(p) = \int_{p_o}^{p} \frac{p\, dp}{\mu(p)\, z(p)} \quad ;$$

where; m = real gas pseudo pressure
p = pressure
p_o = arbitrary base pressure
μ = viscosity of the gas
z = compressibility factor for the gas

In this study, the real gas pseudo-pressure, m(p), was evaluated for geothermal steams over the range 20 to 1000 psia (2-75 bars), temperature range 300 to 600°F (150-325°C) and various noncondensable gas contents. Other physical properties relevant to single-phase isothermal gas flow in porous media were also evaluated and compiled.

The m(p) function was found to be linear in p^2 for low pressures (up to approximately 150 psia or 10 bars). This is depicted in Fig. 1. This behavior is described by a relationship of the form:

$$m(p) = a_1 p^2 + b_1 \qquad (1)$$

At higher pressures a graph of log m(p) vs. log p produced straight lines of the form:

$$m(p) = a_2 p^{b_2} \qquad (2)$$

where b_2 varied between 2.045 and 2.099 (Fig. 2). High accuracy curve fits of Figs. 1 and 2 are presented in Tables 1 (Engineering Units) and 2 (International Units). Varying the mole fraction of carbon dioxide in the gas up to a mole fraction of 60% did not change the basic shape of the curves in Figs. 1 and 2, and tended to increase the value of m(p) by a factor of less than 2.

DISCUSSION

These results will allow the reservoir engineer to more accurately analyze transient flow of superheated geothermal steams. Geothermal steam wells have traditionally been analyzed using the ideal gas flow model, described by Eq. 1, without quantitative justification. The results of this study will allow for quantitative justification of the ideal gas flow assumption, where possible. Alternatively, they will facilitate use of the more correct pseudo-pressure function when analyzing geothermal steam wells.

REFERENCES

Al-Hussainy, R., and Ramey, H.J., Jr.: "Application of Real Gas Flow Theory to Well Testing and Deliverability Forecasting," Jour. Petroleum Technology, May 1966, 637

Al-Hussainy, R., Ramey, H.J., Jr., and Crawford, P.B.: "The Flow of Real Gases Through Porous Media." Jour. Petroleum Technology, May 1966, 624

Aronofsky, J., and Jenkins, R.: "Unsteady Radial Flow of Gas Through Porous Media," Jour. Applied Mechanics, Vol. 20, 1953, 210

Mannon, L.S.: "The Real Gas Pseudo Pressure for Geothermal Steam," M.Sc. Report, Department of Petroleum Engineering, Stanford University, September 1977; to be issued as a Stanford Geothermal Program Technical Report.

Wattenbarger, R.A., and Ramey, H.J., Jr.: "Gas Well Testing with Turbulence, Damage, and Wellbore Storage," Jour. Petroleum Technology, May 1966, 637.

TABLE 1

ANALYTICAL EQUATIONS FOR APPROXIMATING

THE REAL GAS PSEUDO-PRESSURE

(Engineering Units)

Temperature	Limits	Curve Fit Equation
300°F	$p \leq 60$ psia	$m(p) = 36.88p^2 - 8396$
350°F	$p \leq 70$ psia*	$m(p) = 33.93p^2 - 7819$
	$p \geq 70$ psia	$m(p) = 21.60p^{2.095}$
400°F	$p \leq 80$ psia	$m(p) = 31.41p^2 - 7248$
	$p \geq 80$ psia	$m(p) = 21.33p^{2.080}$
450°F	$p \leq 100$ psia	$m(p) = 29.25p^2 - 6769$
	$p \geq 100$ psia	$m(p) = 19.94p^{2.078}$
500°F	$p \leq 140$ psia	$m(p) = 27.36p^2 - 6336$
	$p \geq 140$ psia	$m(p) = 18.65p^{2.075}$
550°F	$p \leq 160$ psia	$m(p) = 25.71p^2 - 5946$
	$p \geq 160$ psia	$m(p) = 18.02p^{2.068}$
600°F	$p \leq 190$ psia	$m(p) = 24.31p^2 - 5916$
	$p \geq 190$ psia	$m(p) = 18.25p^{2.053}$

* At the meeting point, the upper and lower equations agree to 3 or more significant figures.

TABLE 2

ANALYTICAL EQUATIONS FOR APPROXIMATING

THE REAL GAS PSEUDO-PRESSURE

(International Units)

Temperature	Limits	Curve Fit Equation
150°C	$p \leq 4$ bars	$m(p) = 36.80p^2 - 40.65$
175°C	$p \leq 5$ bars *	$m(p) = 34.20p^2 - 38.60$
	$p \geq 5$ bars	$m(p) = 27.89p^{2.099}$
200°C	$p \leq 6$ bars	$m(p) = 31.93p^2 - 36.74$
	$p \geq 6$ bars	$m(p) = 26.78p^{2.081}$
225°C	$p \leq 7$ bars	$m(p) = 29.93p^2 - 34.94$
	$p \geq 7$ bars	$m(p) = 24.96p^{2.079}$
250°C	$p \leq 10$ bars	$m(p) = 28.31p^2 - 37.04$
	$p \geq 10$ bars	$m(p) = 23.35p^{2.076}$
275°C	$p \leq 10$ bars	$m(p) = 26.62p^2 - 33.09$
	$p \geq 10$ bars	$m(p) = 22.25p^{2.069}$
300°C	$p \leq 12$ bars	$m(p) = 25.23p^2 - 32.74$
	$p \geq 12$ bars	$m(p) = 21.66p^{2.056}$
325°C	$p \leq 13$ bars	$m(p) = 23.93p^2 - 30.66$
	$p \geq 13$ bars	$m(p) = 21.11p^{2.045}$

* At the meeting point, the upper and lower equations agree to 3 or more significant figures.

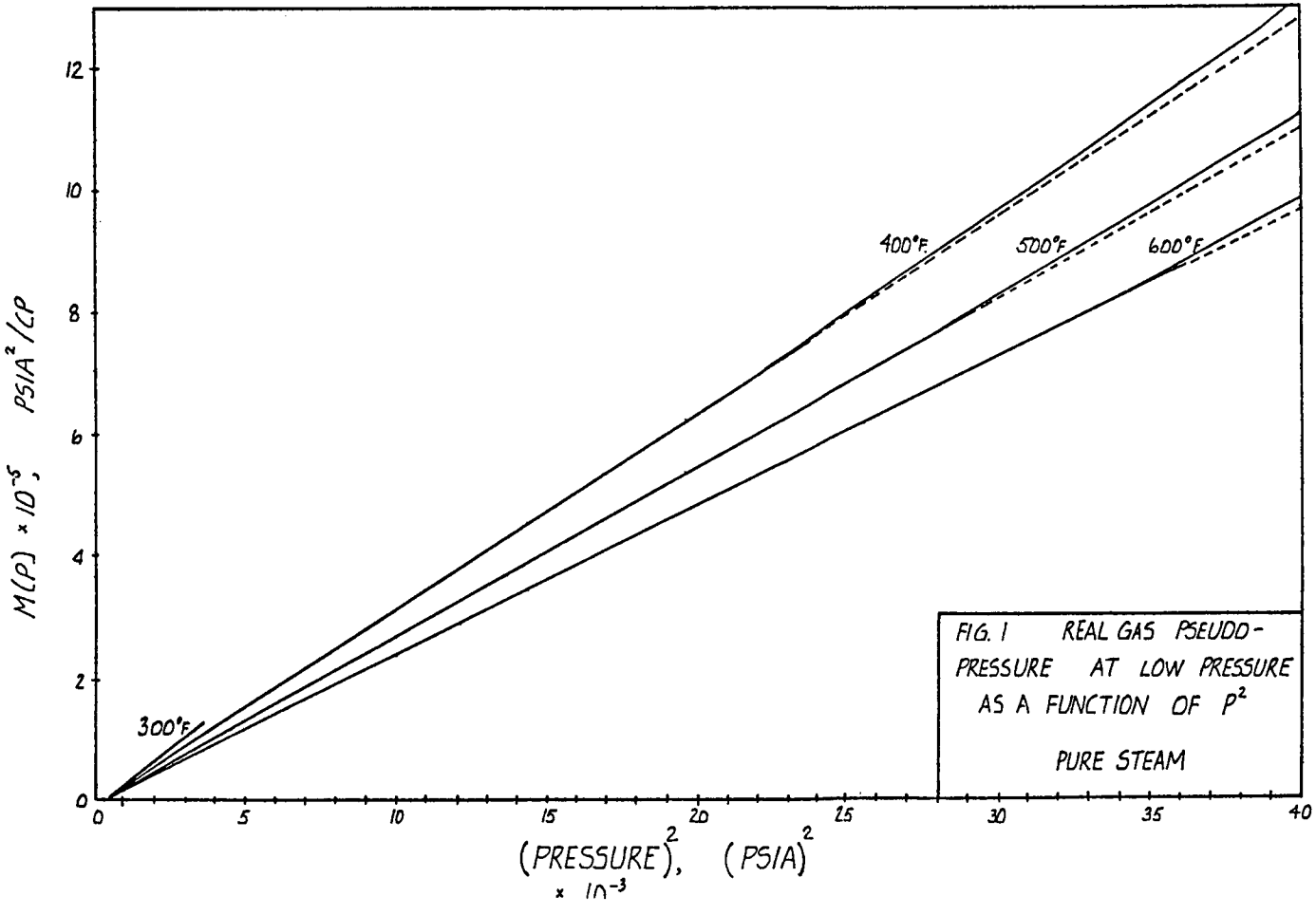

FIG. 1 REAL GAS PSEUDO-PRESSURE AT LOW PRESSURE AS A FUNCTION OF P^2

PURE STEAM

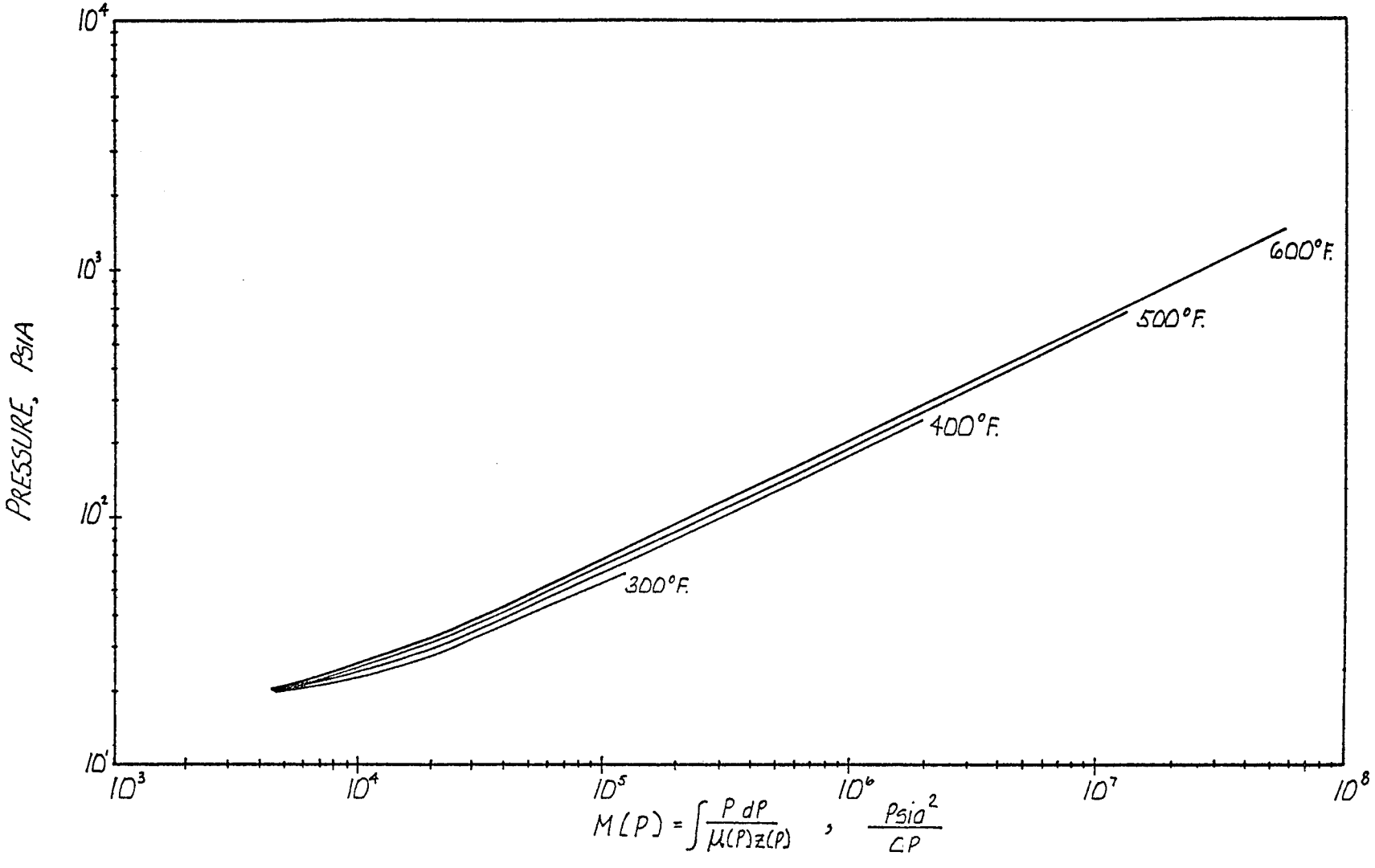

FIG. 2 REAL GAS PSEUDO-PRESSURE M(P) FOR PURE STEAM

HYDRAULIC FRACTURE INITIATION SITES IN OPEN BOREHOLES IDENTIFIED BY GEOPHYSICAL LOGS

Robert M. Potter
University of California
Los Alamos Scientific Laboratory
P. O. Box 1663
Los Alamos, NM 87545

Smith et al (1975) have proposed the creation of man-made geothermal energy reservoirs by drilling into relatively impermeable rock to a depth where the temperature is high enough to be useful; creating a reservoir by hydraulic fracturing; and then completing the circulation loop by drilling a second hole to intersect the hydraulically fractured region.

The initiation of hydraulically created fluid reservoirs in highly impermeable hot dry rock must by definition take place in a wellbore. The nature of these initiation sites will provide the initial resistance to flow into the reservoir and therefore will strongly influence the rate of energy withdrawal. The nature of the interception site in a second wellbore which has been directed to intersect the reservoir will have a similar effect.

The program to create and study such artificial geothermal reservoirs in hot dry rock is being pursued by the Los Alamos Scientific Laboratory and has been presented to these workshops by Murphy (1975) and Murphy et al (1976). In parallel with the drilling of the two boreholes rather complete suites of wellbore geophysical logs were run followed by further diagnostic logging both during and after fracturing operations. This paper discusses some aspects of what has been learned about the entrances and exits of some of the hydraulic fractures created in both the GT-2 and EE-1 wellbores. Table 1 gives the location of the more important fractures and the types of logs used to both identify the location of these fractures and to measure some of their properties.

The Caliper Log

This important and quite dependable logging technique has proved to be the most useful method for detecting both potential sites for fracturing and the actual fractures. Pressure-volume records taken during the fracturing process show that the great majority of fracture initiations show no breakdown; this observation is consistent with the opening of incompletely cemented natural fractures occurring along the open borehole. Also the cemented zone in these natural fractures appears to have widths great enough after erosion by the drilling process for the caliper arm to register. Figure 1 is a 4-arm caliper log taken in EE-1 at the end

of the drilling and prior to fracturing. The strong response of one set of arms is consistent with a set of highly vertical slots. This region was subsequently determined by means of temperature and tracer logs to be the entrance to the main EE-1 fracture. This fracture has a very low impedance and exhibits the desirable property of self-propping. The caliper log has revealed other regions in the two boreholes with similar caliper signatures that may be other cemented fractures with desirable features. A series of such fractures when hydraulically stimulated may provide the nucleus of a three-dimensional geothermal reservoir.

The Spinner Log

The measurement of the flow of fluid into a fracture opening provides the most conclusive proof of fracture location. Figure 2 shows the response of the spinner tool during a flow of ∿170 gpm into two open hole fractures. By averaging the results from 8 spinner runs a detailed analysis of the locations of the two fractures was made. This analysis was later confirmed by televiewer pictures. The relative flow fraction and the flow distribution into each fracture can be derived from this log. This log would have been used more often but its temperature capability to date has limited its use to upper regions of the boreholes.

The Borehole Televiewer

The conditions existing in the two boreholes are ideal for the use of this logging technique except for high temperature. Scott Keyes of the United States Geologic Survey in cooperation with G. C. Summers* has recently developed a high temperature televiewer which has been used successfully in EE-1 at a depth of 10,000 ft and a temperature of 205°C. Figure 3 is a televiewer composite of the region in GT-2 that was shown in Figure 2. A fracture with a dip of 87° relative to the borehole and a strike of N4°E is identified between 6526 and 6540 ft. The vertical range of the fracture is identical with that derived from the spinner surveys.

The Spontaneous Potential Log

Significant changes in the potential field measured in an open wellbore are caused by hydraulic fracturing and the subsequent flow of fluid into the fracture. Figure 4 shows both the reversible and irreversible changes accompanying such fracturing. A background log from casing to TD in the open borehole is followed by a second log taken after fracturing. Two permanent large anomalies mark accurately the position of two fractures. Later SP logs taken both during pumping and venting show that the widest anomaly accepts most of the flow and is therefore designated the main fracture. SP logs taken under both static and dynamic conditions are proving to be extremely valuable in understanding the total fracture process in open boreholes.

---

* Simplec Manufacturing Co., Inc., Dallas, TX.

The Impression Packer

The impression packer has been used to record the nature and orientation of fractures created from open wellbores. Figure 5 shows a tracing of the outer surface of an impression packer taken in GT-2 over the region covered both by the spinner log and the televiewer. Table 2 gives the parameters of the two fractures obtained from the various logs. As with some of the other logging techniques, higher temperatures have prevented its further use.

Oriented Cores

Numerous oriented cores have been obtained during the drilling of both GT-2 and EE-1 and the geologic information that they contain has aided greatly in the understanding of the total system. Figure 6 shows a map of a core taken under rather unique circumstances. Recent redrilling of the GT-2 wellbore was directed towards the interception of the main EE-1 fracture (origin at ∿9060 ft) which was kept pressurized. The drilling of GT-2 was halted at the time when a major drop in pressure in EE-1 was noticed. The core taken at this point shows the bottom portion (marked A in the Figure) of the intercepted pressurized fracture. The initial success of this operation suggests that further attempts may produce cores that will contain extremely valuable samples of actual fracture surfaces.

The Tracer Log

This type of log can yield important information concerning the flow of fluid through the borehole system and its subsequent movement into any accompanying fracture or porosity. Figure 7 shows the history of a released I^{131} sample as it was pumped down the EE-1 casing and then returned up behind the casing through an uncemented annulus to a hydraulically created fracture centered at 9060 ft. Almost 80% of the injected flow appears to be following this flow path. This fracture opening would have been difficult to detect and accurately locate with any other logging technique.

This powerful method will be used extensively in the analysis of complex flow systems that will arise from multiple fracturing from open wellbores.

The Temperature Log

This standard wellbore logging technique has proved invaluable in locating both fracture origins and zones of porous rock. Temperature logs have been taken during the pumping of fluid into the fracture system, subsequent venting and the following temperature recovery phase. Figure 8 shows the temperature history measured in the EE-1 wellbore. The numbered positions have generally been related to various features noted in other wellbore logging surveys. This logging technique will have great value in understanding the heat removal process especially if they can be run throughout the long-term heat extraction experiments.

REFERENCES

1. Murphy, H. D., Dec. 15-17, 1975; "Hydraulic-Fracture Geothermal Reservoir Engineering," First Workshop on Geothermal Reservoir Engineering and Well Stimulation, Stanford University, Stanford, CA (sponsored by NSF).

2. Murphy, H. D., Lawton, R. G., Tester, J. W., Potter, R. M., Brown, D. W., and Aamodt, R. L, Dec. 1-3, 1976; "Preliminary Assessment of a Hot Dry Rock Geothermal Energy Reservoir Formed By Hydraulic Fracturing," Second Workshop on Geothermal Reservoir Engineering, Stanford University, Stanford, CA.

3. Smith, M. C., Aamodt, R. L., Potter, R. M., and Brown, D. W., May 19-29, 1975; "Man-Made Geothermal Reservoirs," Second United Nations Geothermal Energy Symposium, San Francisco, CA.

TABLE 1

Logging Techniques Used to Define Fracture Positions

Log	Fracture (Borehole, Approx. Depth (ft)) GT-2, 6530; 6560	GT-2B, 8740;	EE-1, 6420;	EE-1, 9060;	EE-1, 9670
Caliper (4-arm)	x	x	x	x	x
Spinner	x	-	-	-	-
Televiewer	x	-	-	-	x
Spontaneous Potential	-	x	x	-	-
Impression Packer	x	-	-	-	-
Oriented Core	-	x	-	-	-
Tracer	-	-	-	x	x
Temperature	-	x	-	x	x

TABLE 2

Fracture Measurements in GT-2 at 6525-6570 ft.

Log	Upper Fracture Orientation	Upper Fracture Vertical Range (ft)	Lower Fracture Orientation	Lower Fracture Vertical Range (ft)
Spinner	--	6526-40	--	6554-6568
Televiewer	N3°E	6526-40	N12°E	6555-6569
Impression Packer	N25°E	--	N25°E	--

FIGURE 1

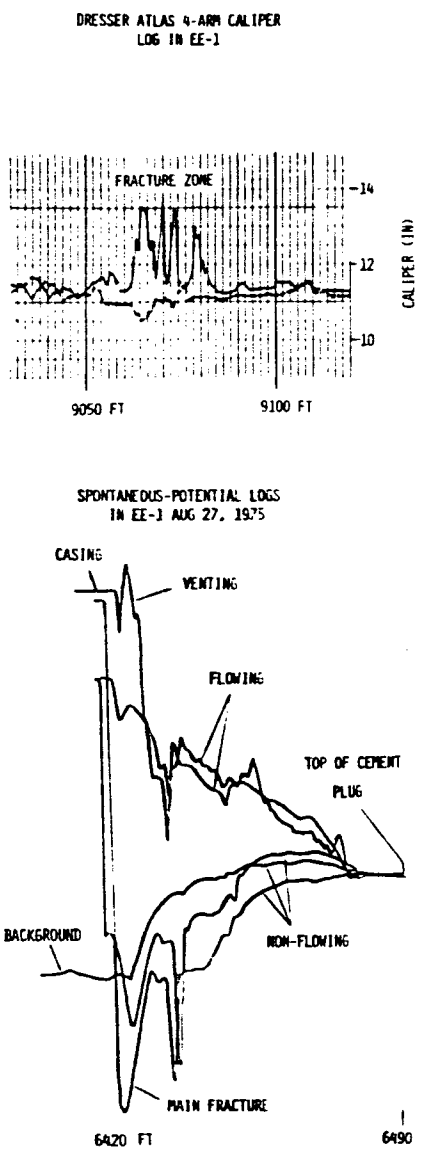

FIGURE 2

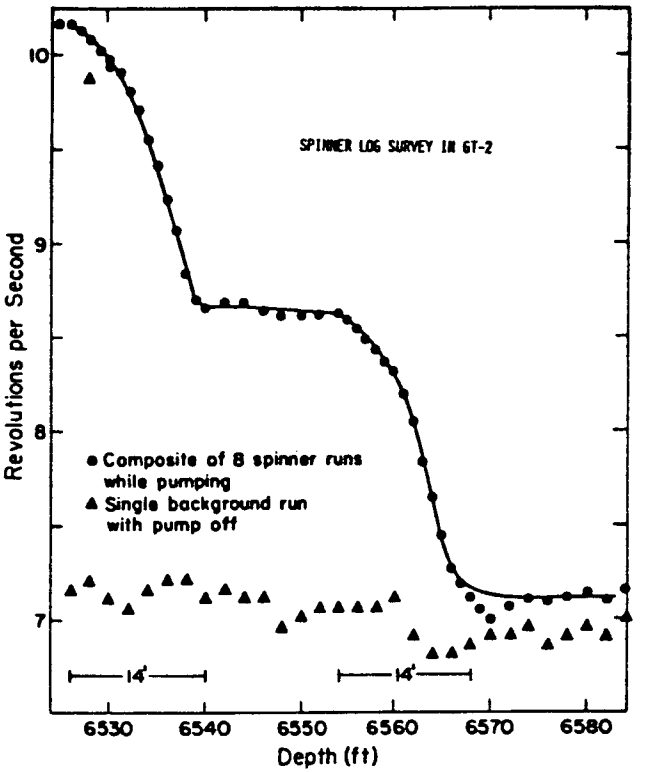

FIGURE 3

FIGURE 4

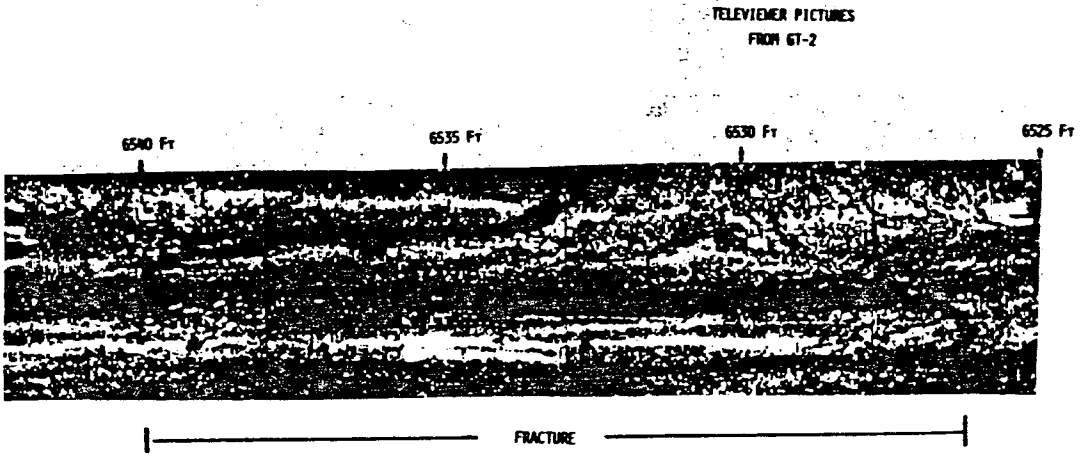

FIGURE 5

TRACING OF IMPRESSION FROM
UPPER PACKER IN GT-2

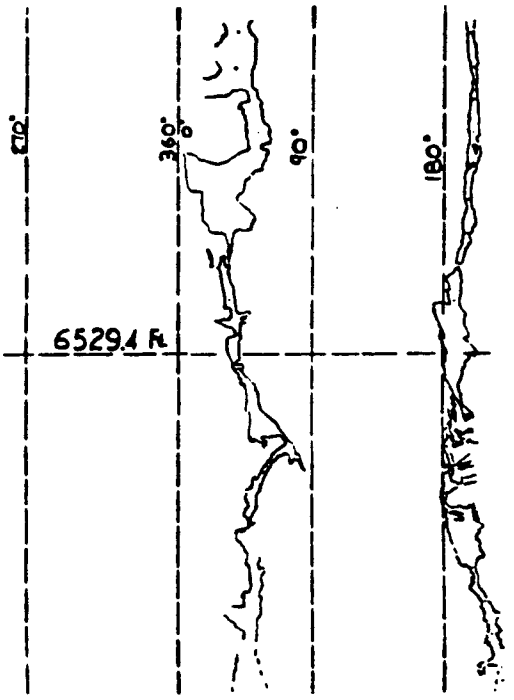

FIGURE 6

MAP OF CORE TAKEN IN
GT-2B AT 8742 FT

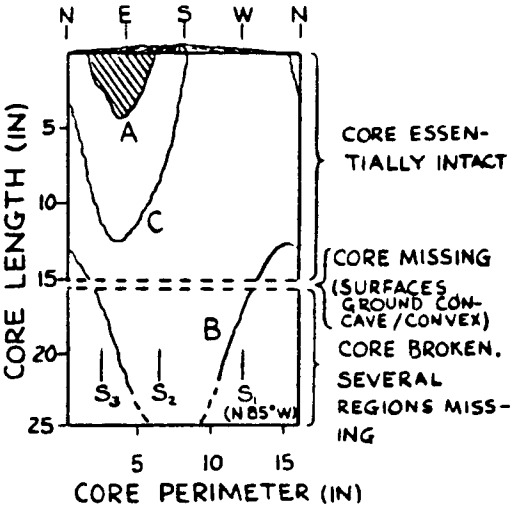

FIGURE 7

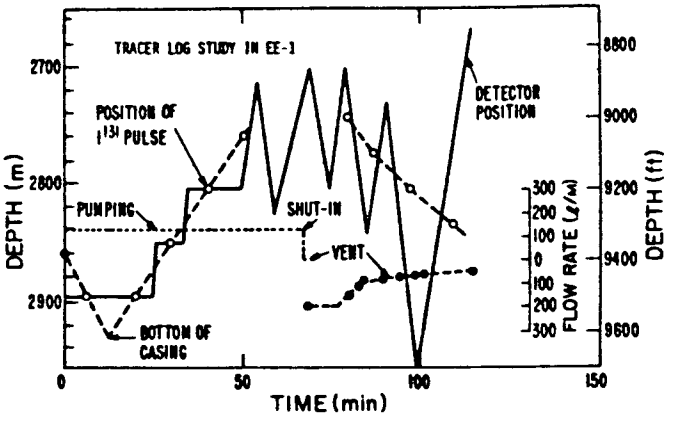

FIGURE 8

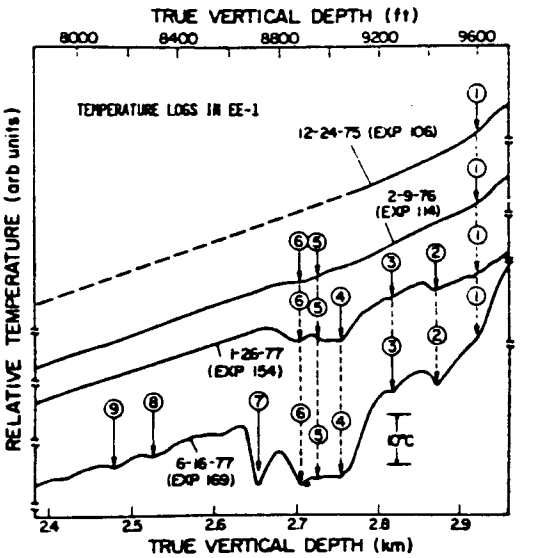

THE "HEAT-PIPE" EFFECT IN VAPOR-DOMINATED GEOTHERMAL SYSTEMS

W. N. Herkelrath
U.S. Geological Survey
Water Resources Division
Menlo Park, CA 94025

Introduction

White, Muffler, and Truesdell (1971) and Truesdell and White (1973) developed a conceptual model of transport in vapor-dominated geothermal zones. The main theme of the model is that coexisting liquid and vapor phases form a counterflowing convection system similar to that observed in a heat pipe (Dunn and Reay, 1976). It is hypothesized that water evaporates from a deep water table, passes upward through the formation, and condenses at an impermeable cap rock, effectively transferring the latent heat of boiling through the formation. The liquid water then percolates downward, completing the cycle. The physics involved in the flow system is illustrated in the following analysis of an idealized one-dimensional, homogeneous, 2 km deep vapor-dominated zone which is bounded below by a water table which has a temperature of 236°C.

Flow of water and steam in the system is assumed to be described by Darcy's law for unsaturated porous materials:

$$\text{(water)} \quad q_\ell = \frac{-\rho_\ell K K_\ell}{\mu_\ell} \left(\frac{d\psi_\ell}{dZ} - \rho_\ell g \right) \qquad (1)$$

$$\text{(steam)} \quad q_v = \frac{-\rho_v K K_v}{\mu_v} \left(\frac{dP_v}{dZ} - \rho_v g \right). \qquad (2)$$

The liquid water potential, ψ_ℓ, defined as the Gibb's free energy per unit volume of water, is used in place of the liquid pressure in equation (1) because flow in a highly unsaturated medium is to be considered.

Static steam zone

Consider first a static, isothermal system (zero heat flow) in which the reservoir fluids have equilibrated with the deep water table. Capillary and adsorption forces are balanced against gravity, so that the liquid water potential decreases linearly with height above the water table:

$$\psi_\ell = \rho_\ell g \left(Z - Z_o \right). \qquad (3)$$

Liquid continuity is not required for equation (3) to apply because equilibration can occur through condensation of steam.

This equation implies that two kilometers above the water table the liquid water potential is -160 bars. As is shown in figure 1, at this low potential the level of liquid saturation varies greatly from one type of porous medium to another. Water retention in the fractured porous materials which form vapor-dominated systems has not been measured. However, in order to illustrate the physical principles involved in the flow system, an estimate of the drainage characteristic has been made. For simplicity it is assumed that ψ_ℓ is uniquely related to S and T through the empirical relation

$$\psi_\ell = \psi_o \quad (S^{-A}-1) \quad (B-CT) , \qquad (4)$$

in which ψ_o, A, B and C are constants.

Pressure in the steam phase increases with depth according to

$$P_v = P_{vo} \exp \left\{ \frac{(Z - Zo)\, Mg}{RT} \right\} . \qquad (5)$$

Equation (5) illustrates that liquid in a static vapor-dominated zone has a vapor pressure less than the saturated value. Figure 2 indicates the distribution of liquid water potential, vapor pressure, and liquid saturation in a system composed of the hypothetical material described by equation (4).

Isothermal, steady-state flow

A solution to equation (1) which is relevant to this discussion is the case of steady infiltration at the top of the steam zone. Assuming that the system is isothermal and that the water table is stationary, one can show (Childs, 1969) that the saturation decreases rapidly above the water table, but eventually assumes a constant value at which

$$KK_\ell = \frac{q_\ell \mu_\ell}{\rho_\ell^{\,2}\, g} . \qquad (6)$$

Simply stated, constant infiltration into the top of the steam zone increases the liquid saturation until the liquid permeability rises enough for the water to drain away at the same rate. Assuming an infiltration rate of 2.35×10^{-8} g/cm^2 sec, figure 3 illustrates the dependence of ψ_ℓ, P_v, and S upon depth for the hypothetical fractured material, which is assumed to have relative permeabilities given by

$$K_\ell = S^3 \qquad (7)$$

$$K_v = (1 - S) . \qquad (8)$$

Nonisothermal steady-state flow

When variations in temperature are considered, the equations describing the flow can be written as

$$q_\ell = \frac{-\rho_\ell K K_\ell}{\mu_\ell} \left(\frac{\partial \psi_\ell}{\partial S} \frac{dS}{dZ} + \frac{\partial \psi_\ell}{\partial T} \frac{dT}{dZ} - \rho_\ell g \right) \quad (9)$$

$$q_v = \frac{-\rho_v K K_v}{\mu_v} \left(\frac{\partial P_v}{\partial S} \frac{dS}{dZ} + \frac{\partial P_v}{\partial T} \frac{dT}{dZ} - \rho_v g \right) . \quad (10)$$

Assuming the system is closed and neglecting heat conduction

$$q_\ell = -q_v = \frac{-q_H}{L} . \quad (11)$$

equation (9), (10), and (11) may be solved to yield dT/dZ and dS/dZ as functions of temperature, saturation, the heat flow, and the properties of the medium. The distribution of T, S, ψ_ℓ, and P_v in the system can be obtained by numerical integration.

For the small gradients in temperature usually found in steam zones (Hite and Fehlberg, 1976) the extra terms in equations (9) and (10) are small and the saturation distribution is not much different from that obtained in isothermal infiltration. Liquid water condenses at the cap rock and increases the liquid saturation until the permeability becomes

$$KK_\ell = \frac{q_H \mu_\ell}{L\rho_\ell \left(\frac{\partial \psi_\ell}{\partial T} \frac{dT}{dZ} - \rho_\ell g \right)} \quad (12)$$

Assuming a heat flow rate of 4.187×10^{-5} j/cm^2 sec (1OHFU), figure 4 illustrates the depth distribution of ψ_ℓ, P_v, and S. This heat flow results in the same condensation rate as was used in the isothermal infiltration example of figure 3.

Conclusion

Comparison of figures 2 and 4 illustrates that the liquid saturation in a two-phase convection system can be much higher than that predicted from a static pressure analysis. As a result, the "vapor pressure lowering" effect expected in a static system disappears. The decrease in P_v at the top of figure 4 is caused by temperature decrease; the relative vapor pressure in the dynamic system is above 99%.

However, the permeability used in this example is very low. At higher permeabilities the condensing steam drains out of the system much faster, and the saturation approaches the static profile.

Symbols

ℓ	-	subscript indicating liquid	q_H	-	heat flow rate
v	-	subscript indicating vapor	R	-	ideal gas constant
g	-	acceleration of gravity	S	-	volume relative saturation
K	-	permeability	T	-	absolute temperature
K_ℓ	-	relative permeability	Z	-	depth below caprock
M	-	molecular weight of water	Z_o	-	depth to water table
P_v	-	vapor pressure	ρ	-	density
P_{vo}	-	saturation vapor pressure	μ	-	viscosity
q	-	mass flow rate	ψ_ℓ	-	liquid water potential

REFERENCES

Childs, E. C., 1969. An Introduction to the Physical Basis of Soil Water Phenomena, Wiley (Interscience), New York.

Dunn, P. and Reay, D. A., 1976. Heat Pipes, Pergamon Press, New York.

Hite, J. R. and Fehlberg, E. L., 1976. Steam Zone Temperature Gradients at The Geysers, Summaries, Second Workshop, Geothermal Reservoir Engineering, December 1-3, Stanford University, Calif.

Truesdell, A. H. and White, D. E., 1973. Production of Superheated Steam from Vapor-Dominated Geothermal Reservoirs, Geothermics, v. 2, pp. 154-173.

White, D. E., Muffler, L. J. P., and Truesdell, A. H., 1971. Vapor-Dominated Hydrothermal Systems Compared with Hot-Water Systems, Economic Geology, v. 66, pp. 75-97.

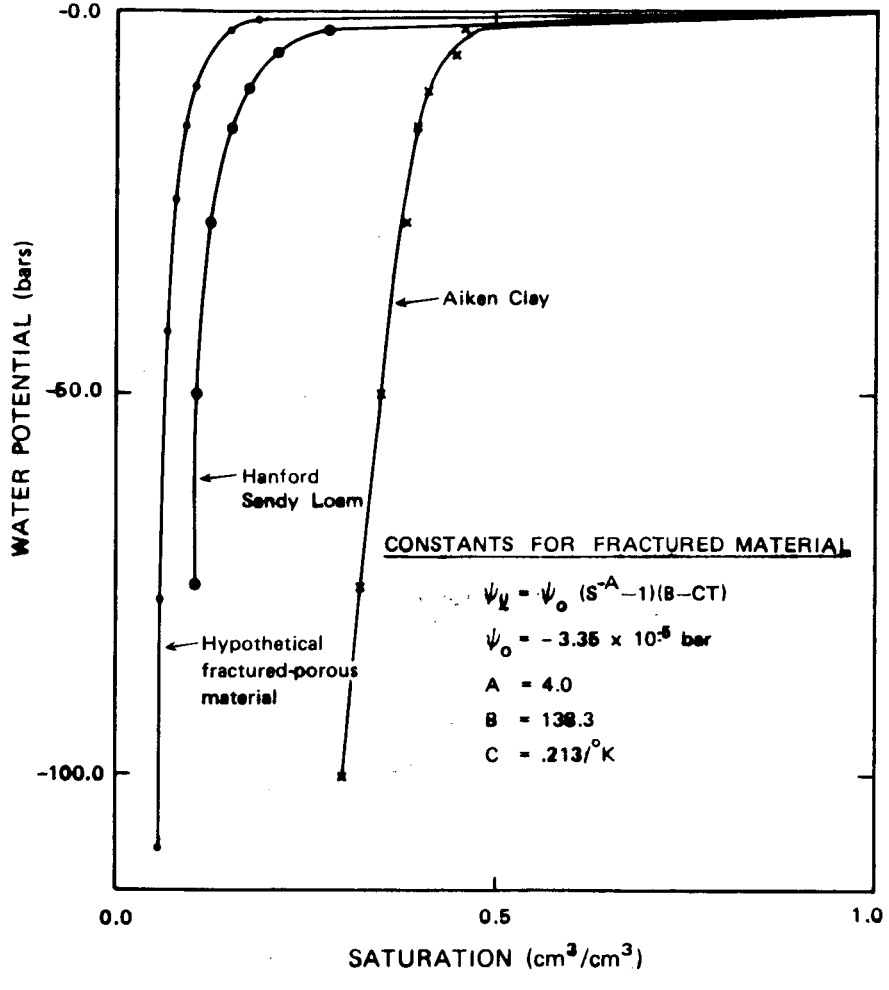

FIGURE 1. Dependence of liquid water potential upon saturation for representative porous materials.

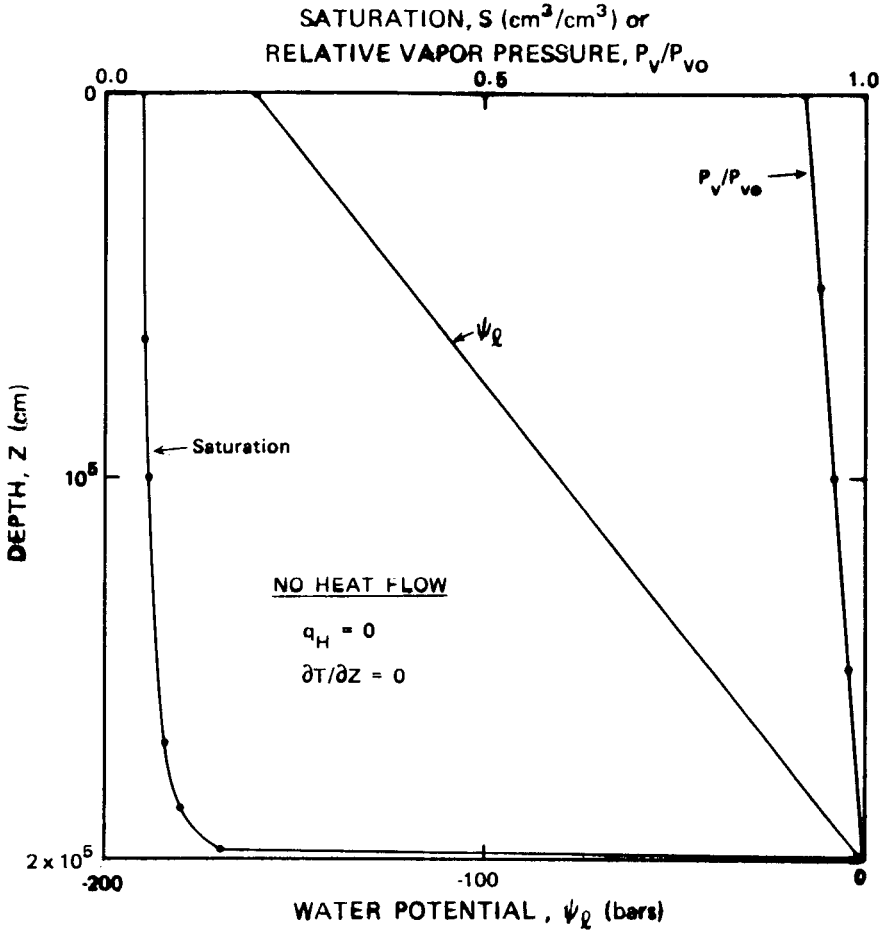

FIGURE 2. Dependence of liquid saturation, liquid water potential, and steam pressure upon depth in a static vapor-dominated zone.

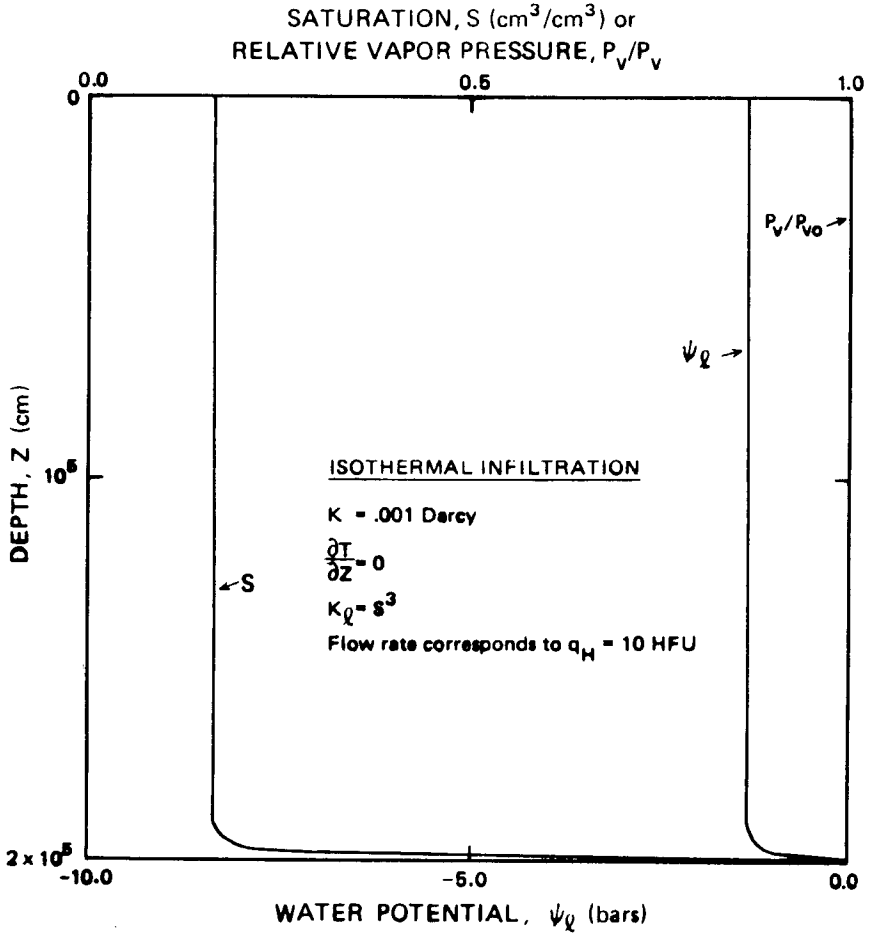

FIGURE 3. Distribution of liquid saturation, liquid water potential and steam pressure with steady isothermal infiltration of liquid at the top of a vapor-dominated zone.

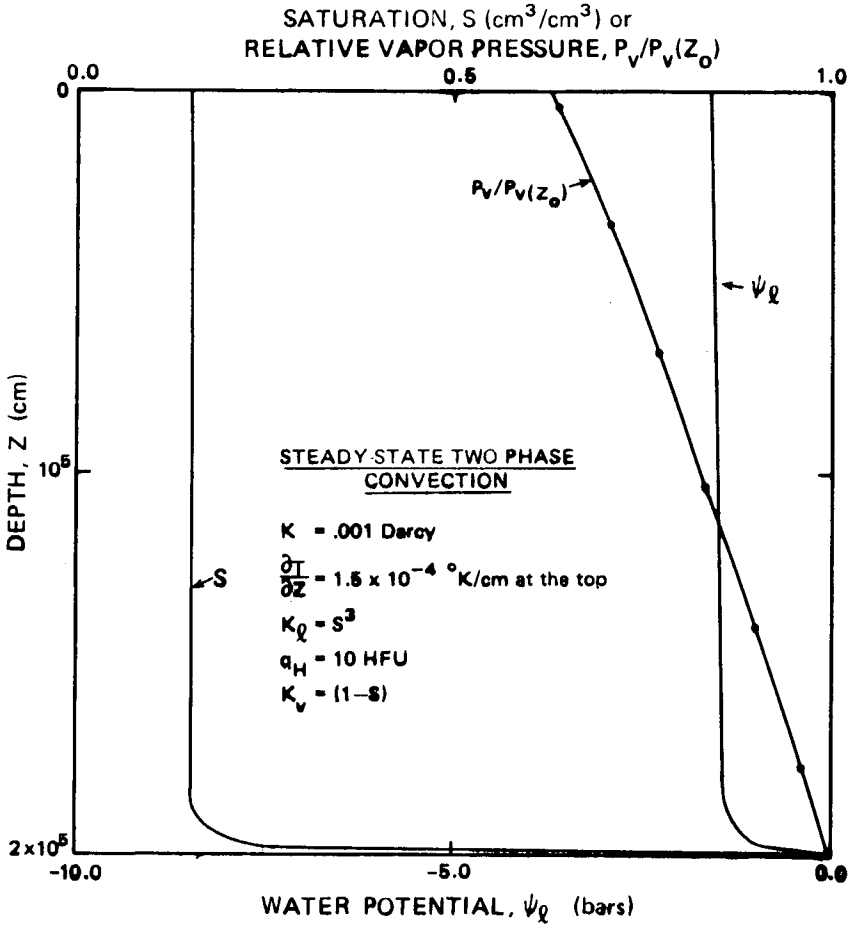

FIGURE 4. Distribution of liquid saturation, liquid water potential, and steam pressure when steam condenses at a steady rate at the top of a non-isothermal vapor-dominated zone.

ENERGY EXTRACTION EXPERIMENTS IN THE SGP RESERVOIR MODEL

A. Hunsbedt, A. L. London, R. Iregui, P. Kruger, and H. J. Ramey, Jr.
Stanford University, Stanford, CA 94305

Much of the immense quantity of geothermal energy stored in the earth's crust is widely dispersed and occurs as hot igneous rock with permeabilities that are too low for adequate fluid circulation. Fracture-stimulation of such systems is needed to improve fluid circulation and expose new heat transfer surface in the hot rock. Hydrothermal resources which may need fracture stimulation are those with inadequate fluid content for heat removal flow rates or those in which the transit time of reinjected fluids is too rapid for adequate reheating. Fracture-stimulation techniques proposed to enhance the energy recovery include hydraulic or explosive fracturing and thermal stress cracking. Experimental methods needed to evaluate the thermal extraction effectiveness of such stimulation practices and of hydrothermal reservoirs in general are a part of the Stanford Geothermal Program (SGP).

Experiments are being conducted in the SGP large geothermal reservoir model utilizing rock systems with several characteristics resembling high permeability, fracture-stimulated systems. The broad objective of these experiments is to evaluate nonisothermal fluid production and heat transfer processes and to analytically model these for such rock systems. Three nonisothermal energy extraction and production processes, referred to here as in-place boiling, sweep, and steam-drive, were considered during the early phases of this study. The general production, injection, and reservoir conditions maintained during the three different experiments are listed in Table 1.

Table 1. Types of Energy Extraction Experiments

Experiment Type	Description
In-Place Boiling	Pressure reduction and boiling in formation. Production of steam from a top producing zone with or without fluid recharge at the bottom.
Sweep	Injection of cold water at bottom. Hot water produced from a top producing zone. Compressed liquid reservoir.
Steam-Drive	Production of hot water from the bottom and no recharge. Steam and noncondensable gases above liquid/steam interface providing "steam-drive." Slightly subcooled reservoir conditions.

This work has been reported in previous reports and papers [References 1 through 3]. The results showed that all three processes are feasible in the experimental systems considered. However, the effectiveness of the processes, as illustrated in Table 2, varied widely.

Table 2. Results of Energy Extraction Experiments

Experiment Type	Specific Energy Extraction (Btu/lb_m)	Energy Extraction Fraction (dimensionless)
In-Place Boiling	> 36	> 0.75
Sweep	> 62	> 0.80*
Steam-Drive	> 9	> 0.22

*Based on the steady-state water injection temperature as the lower reference. The others are based on the saturation temperature corresponding to the end pressure.

The specific energy extraction (energy extracted per pound of rock) was greatest for the sweep process and smallest for the steam-drive process. The fraction of thermal energy stored in the rock between the initial temperature and reference lower temperature that was actually extracted is also seen to vary widely. The question of which of these energy extraction processes is practical in large-scale field development will depend on the particular conditions that prevail at the site.

The simple analytic models developed for the model reservoir and for the heat transfer from the rock successfully predicted the experimental results as long as the assumptions inherent in the models were not seriously violated. However, it was recognized that more detailed experimental and analytic studies of the heat transfer aspects were required, and such studies have since been performed by Iregui [Reference 4]. The final report of these results is in preparation and the highlights are given below.

Rock Heat Transfer Studies

Prediction of heat transfer from a collection of irregularly shaped rocks is complicated because the rocks vary in size and shape. The effect of rock shape was investigated by Kuo [Reference 5]. The results showed that a rock with an irregular shape can be treated analytically as a sphere with equivalent radii used in the Fourier and Biot numbers determined by a single parameter referred to as the sphericity of the rock. The sphericity is defined as the ratio of the surface area of the equivalent spherical rock having the same volume to the actual surface area of the rock. Additional work was performed utilizing this concept to predict the thermal behavior of a collection of rocks with given size distribution and shape for arbitrary boundary or cooldown conditions.

The basis for the rock temperature transient prediction for a single rock was the one lump, spherical solution presented in Reference 1

for constant cooldown conditions. This solution was modified to variable cooldown conditions by superposing constant cooldown rate solutions, a procedure frequently used in heat transfer analyses. The validity of this model was verified by comparing the predicted rock temperature to the measured rock temperature. An illustration of such a comparison is given in Figure 1 where the predicted and measured temperatures for instrumented Rock No. 1, located at the bottom of the reservoir model, are shown as functions of time. Another illustration is given in Figure 2 for Rock No. 2 located near the center. Two in-place boiling experiments and one sweep experiment were conducted to provide the data for the comparisons. The rock used in these experiments (third rock loading) consisted of granitic rock fragments with a mean equivalent diameter of 1.62 inches. It was obtained from the piledriver chimney produced by a nuclear explosion at the Nevada Test Site.

The results of the temperature transient comparisons, similar to those illustrated in Figures 1 and 2, showed that the one-lump thermal model utilizing the equivalent radii defined by Kuo predicts the rock temperature transients satisfactorily over a wide range of conditions and is preferred over exact solutions because of its relative simplicity. The transient model for a single rock was subsequently used to formulate an energy extraction model for a collection of rocks with a given size distribution. This model was applied to the laboratory system with known size distribution and average rock shape. The predicted energy extraction was compared to the measured energy extraction for one experiment. The results showed that the prediction was of the same order as the measured, but the model verification was not conclusive because of relatively large uncertainties in the measured energy extraction. Further work is needed to assess the uncertainties in the measurements.

The energy extraction model was used to determine the sensitivity of parameters such as mean rock size, average sphericity, cooldown history, rock size distribution, and the dispersion about the mean for hypothetical large-scale systems. These parameters will generally not be known precisely for such systems, and in many cases will have to be assumed. The effect of rock size distribution and the sphericity are given in Figures 3 and 4, respectively, where the rock energy extraction fraction is plotted as a function of total time to deplete the reservoir. The energy extraction fraction is defined as the ratio of thermal energy extracted to the theoretical maximum, i.e., the energy stored between the initial temperature and the instantaneous fluid temperature surrounding the rock. These results show that the fraction of energy that can be extracted from the rock decreases when the reservoir is produced over a shorter time period. The energy extraction also decreases when the proportion of large rocks increases. This is the case when the dispersion about their mean increases or the shape of distribution changes (e.g., from exponential to normal). Further details of these studies are presented in Reference 4.

Current and Future Experiments

The experiments performed in the SGP reservoir model have utilized rock systems with porosities between 35 and 44 percent and essentially

infinite horizontal and vertical permeabilities. Thus, these systems are not very representative of naturally or artificially fractured geothermal reservoirs where a typical porosity may be in the range of ≤5 to 20 percent and the permeabilities in the range of 5 to 500 md. Experiments with a more representative rock system have, therefore, been initiated. This fourth rock system consists of the granitic rock utilized in the third rock system (piledriver rock), but the void spaces are filled with 80 to 100 mesh sand. The porosity of this system has been determined to be about 21 percent, and the vertical permeability is being measured. Several energy extraction experiments of the in-place and sweep type will be conducted with this rock system in the near future.

In the longer term, experiments to study the characteristics of thermal stress cracking in granite are being evaluated. Efforts to assess the usefulness and feasibility of such experiments have been initiated. The ability to detect small cracks created by thermally induced stresses is of particular concern. It is anticipated that preliminary experiments will be conducted in a small bench-scale model to determine major parameters for use in analytic modeling of proposed experiments in the SGP large geothermal reservoir model.

References

1. Hunsbedt, A., Kruger, P., and London, A. L., "Laboratory Studies of Stimulated Geothermal Reservoirs," SGP-TR-11, Advanced Technology Dept., RANN, National Science Foundation, Grant No. NSF-AER-72-03490, December 1975.
2. Hunsbedt, A., Kruger, P., and London, A. L., "Recovery of Energy from Fracture-Stimulated Geothermal Reservoirs," Paper No. SPE 5875, 46th Annual California Regional Meeting, SPE of AIME, Ventura, California, April 2-4, 1976. (Accepted for publication in Journal of Petroleum Technology, August 1977.)
3. Hunsbedt, A., Kruger, P., and London, A. L., "Laboratory Studies of Fluid Production from Artificially Fractured Geothermal Reservoirs," Paper No. SPE 6553, 47th Annual California Regional Meeting, SPE of AIME, Bakersfield, California, April 13-15, 1977. (Accepted for publication in Journal of Petroleum Technology.)
4. Iregui, R., "Heat Transfer in Fractured Rock Media," Engineer's degree dissertation, Stanford University, 1978.
5. Kuo, M.C.T., Kruger, P., and Brigham, W. E., "Shape Factor Correlations for Transient Heat Conduction from Irregular-Shaped Rock Fragments to Surrounding Fluid," SGP-TR-16, Advanced Technology Dept., RANN, National Science Foundation, Grant No. NSF-AER-72-03490, August 1976.

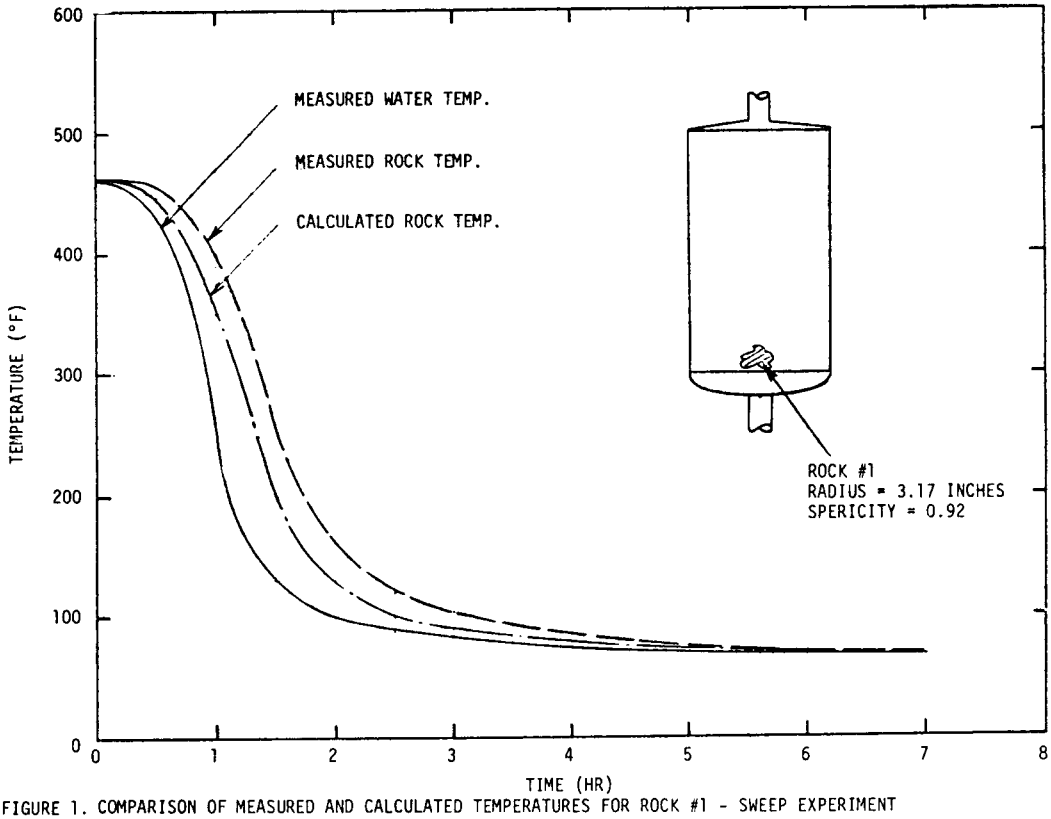

FIGURE 1. COMPARISON OF MEASURED AND CALCULATED TEMPERATURES FOR ROCK #1 - SWEEP EXPERIMENT

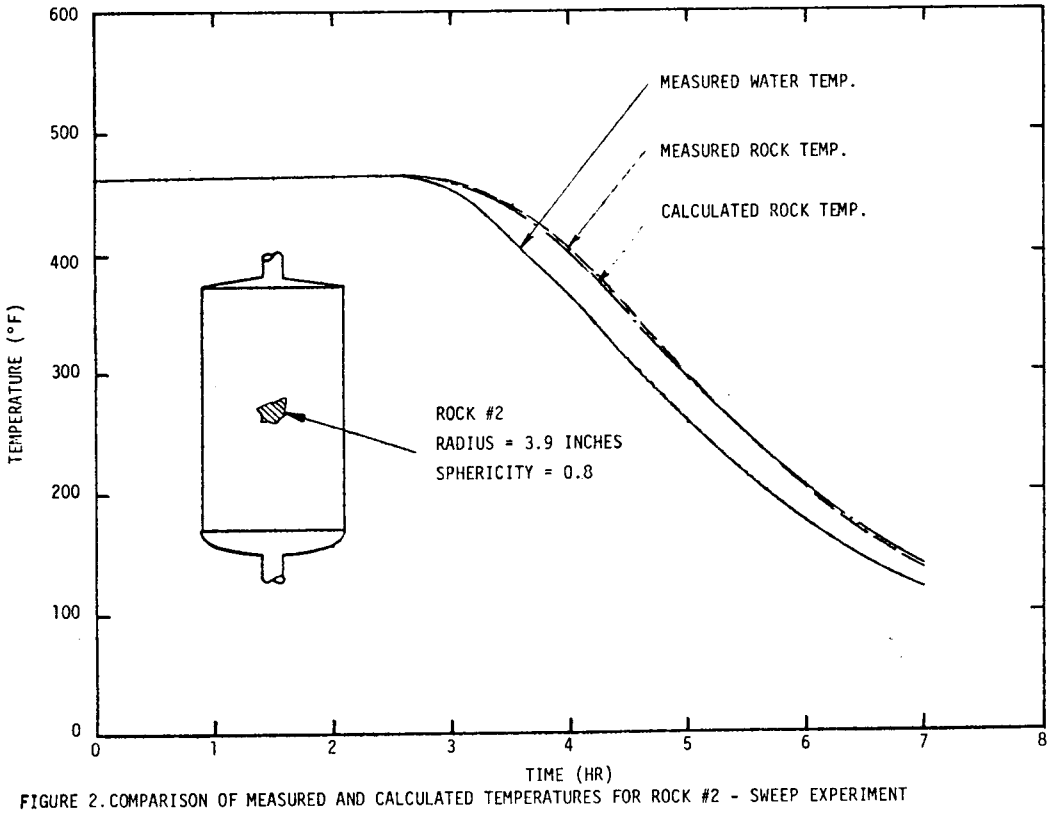

FIGURE 2. COMPARISON OF MEASURED AND CALCULATED TEMPERATURES FOR ROCK #2 - SWEEP EXPERIMENT

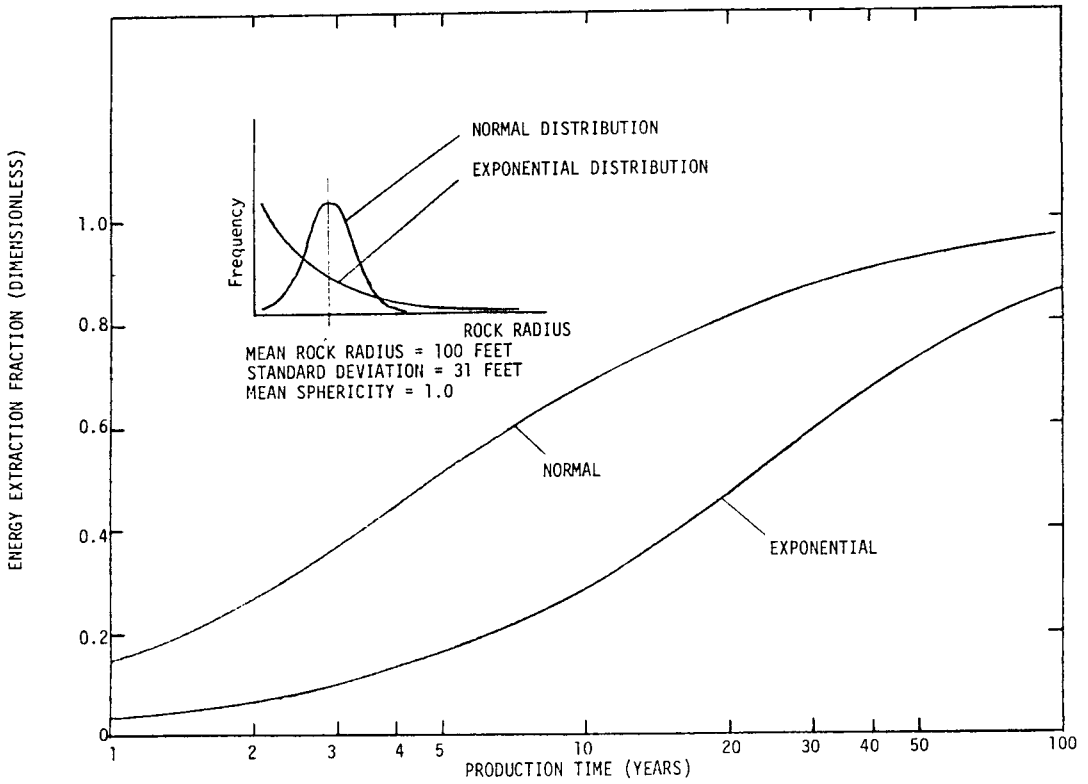

FIGURE 3. ENERGY EXTRACTION FRACTION AS A FUNCTION OF TOTAL PRODUCTION TIME FOR TWO DIFFERENT ROCK SIZE DISTRIBUTIONS.

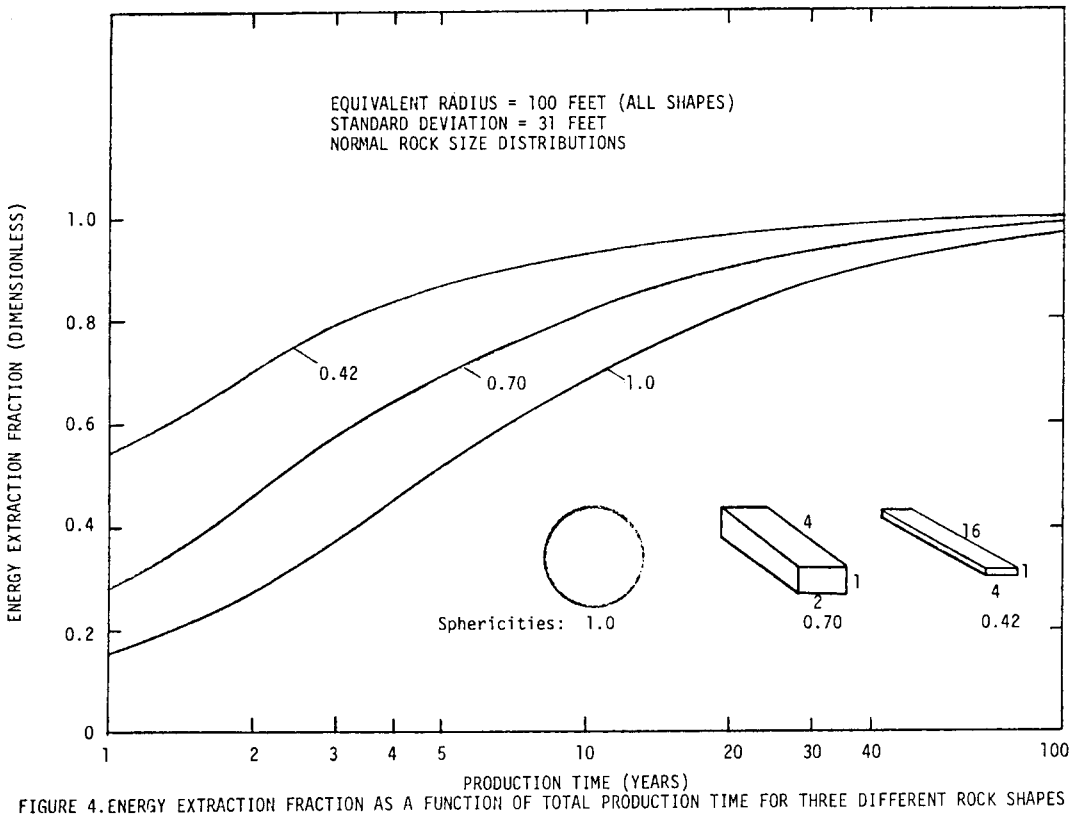

FIGURE 4. ENERGY EXTRACTION FRACTION AS A FUNCTION OF TOTAL PRODUCTION TIME FOR THREE DIFFERENT ROCK SHAPES

THE USE OF NOBLE GASES AND STABLE ISOTOPES TO INDICATE TEMPERATURES AND MECHANISMS OF SUBSURFACE BOILING AND (LESS CERTAINLY) RESERVOIR DEPLETION IN GEOTHERMAL SYSTEMS

Robert W. Potter, II, Alfred H. Truesdell, and Emanuel Mazor*
U.S. Geological Survey
Menlo Park, California 94025

Salts are essentially insoluble in the low pressure steam produced from vapor-dominated systems. Hence, the normal chemical constituents used in studying hot-water geothermal systems prove ineffective in the study of subsurface conditions of vapor dominated systems. However, noble gases and stable isotopes of water may be used to fill this gap and may, in addition, provide a means of estimating the degree of reservoir depletion.

Although steam alone is produced from wells and natural vents in vapor-dominated systems, it is generally accepted that liquid water exists at depth. During exploitation this water boils in response to pressure decrease to produce steam which feeds the wells (Truesdell and White, 1973). As the liquid boils, gases and isotopes of hydrogen and oxygen fractionate between steam and remaining liquid. Oxygen-18 is fractionated preferentially into the liquid phase at all temperatures below the critical point of water while deuterium is preferentially fractionated into liquid water below 221°C. Above 221°C deuterium is preferentially fractionated into the vapor with a maximum fractionation occurring at 280°C. There is no fractionation of deuterium at 221°C and fractionation of both oxygen-18 and deuterium is zero at the critical point where the distinction between liquid and vapor disappears (Truesdell, et al., 1977).

Gases also exhibit temperature-sensitive fractionation between liquid and vapor, and their contents may be used to interpret subsurface boiling processes. The contents of the major gases of geothermal systems (CO_2, H_2S, H_2, etc.) are, however, also affected by chemical reactions and cannot be simply interpreted in terms of subsurface boiling. This limitation does not apply to the atmospheric noble gases (Ne, Kr, Xe, and most Ar) which are not reactive and originate only from solution of air in recharge waters (Mazor, 1976).

The solubilities of the noble gases, He, Ne, Ar, Kr, and Xe, have recently been determined up to the critical point of water (Potter and Clynne, 1977). The solubility in the liquid phase decreases steadily at temperatures greater than 0°C, then

* on leave from the Weizmann Institute, Rehovoth, Israel.

passes through a minimum (He = 25°C, Ne = 70°C, Ar = 100°C, Kr and Xe = 125°C) and finally increases steadily up to the critical point. The solubilities of the noble gases and nitrogen (which is also inert in most systems) are shown in figure 1 as Henry's law constants equal to the ratio of the partial pressure of the gas to its mole fraction in the liquid. Larger Henry's law constants indicate relatively liquid-insoluble gases, smaller constants relatively soluble gases.

The initial noble gas compositions of the recharge water can be estimated from the mean temperature of the recharge area, the noble gas composition of air and the experimental solubilities. Since the intake compositions can be estimated, it is possible to calculate the temperature of boiling from the noble gas contents of the steam. The assumptions involved in this calculation are that (1) the liquid water at depth has the same noble gas contents as the recharge water, (2) that the quantity of steam boiled off is small compared to the quantity of water remaining, and (3) that the water at depth is well mixed.

Instead of using absolute concentrations of the noble gases, it proves more reliable to use ratios of the various gases. Since He has a major non-atmospheric source we cannot use it in estimating boiling temperatures. The other noble gases are essentially all atmospheric and their original concentrations in the liquid phase can be estimated. Neon is the least soluble of the noble gases (Fig. 1) and ratios of neon with other gases are most useful in indicating boiling processes. Unfortunately, the Xe/Ne ratio changes little with temperatures above 80°C and therefore large uncertainties in the calculated boiling temperature result from analytical errors. The Ar/Ne versus T curve also has difficulties in that it goes through a maximum at about 230°C to 250°C and then decreases. The Kr/Ne curve is, however, a smoothly increasing function of temperature with a moderate slope and is satisfactory for boiling temperature estimation. In figures 2 and 3 these ratios are shown for steam samples from a geochemical section across the Larderello geothermal field (Table 1 and Mazor, 1977) with boiling temperatures calculated using an estimated recharge temperature of 10°C. The noble gas ratios appear to indicate slightly higher temperatures than those measured at the wellhead during flow. This is not unexpected as temperature decreases occur in the well due to adiabatic expansion.

The differences may however result from depletion of liquid water in the reservoir. It is reasonable to assume that the production of steam from a well may be modelled as a Rayleigh distillation process. Figure 4 is a Kr/Ne versus T plot on which contours for various fractions of water removed from the reservoir

by conversion to steam have been plotted. Data from the Pineta well did not plot near the established ratio curves in figures 2 and 3; however, figure 4 suggests that this is due to a high degree of depletion of the recharge fluid. This observation is in agreement with Pineta's history as well as its lower production temperature. In Figure 4 it can be noted that the ratio for Columbaia lies on the zero depletion curve. This observation agrees with the observation that it is the only well of this group which contains tritium, hence indicating active recharge of the system.

If samples of both the liquid and steam phase are available, the fractionation patterns of the stable isotopes will allow the temperature of boiling to be calculated. The isotopic data may also be used to set constraints on possible models of steam separation. Combined with noble gas data, models for subsurface steam separation in a geothermal system can be established. These models can be improved and more complete knowledge obtained of boiling mechanisms and of the volume and situation of liquid and vapor in steam-producing geothermal systems through long-term monitoring of stable isotopes and noble gases.

References

Mazor, Emanuel, 1976, Atmospheric and radiogenic noble gases in thermal waters: their potential application to prospecting and steam production studies: Proc. 2nd U.N. Symp. on Geothermal Energy, San Francisco, 1975, p. 793-802.

Mazor, Emanuel, 1977, Noble gases in a section across the vapor dominated geothermal field of Larderello, Italy: Pure Appl. Geophy. (in press)

Potter, R. W., II, and Clynne, M., 1977, The solubility of the noble gases, He, Ne, Ar, Kr and Xe in water up to the critical point: Jour. Solution Chem. (in press)

Truesdell, A. H., and White, D. E., 1973, Production of superheated steam from vapor-dominated geothermal reservoirs: Geothermics, v. 2, nos. 3-4, p. 154-173.

Truesdell, A. H., Nathenson, Manuel, and Rye, R. O., 1977, The effects of subsurface boiling and dilution on the isotopic compositions of Yellowstone thermal waters: Jour. Geophys. Res., v. 82, p. 3694-3704.

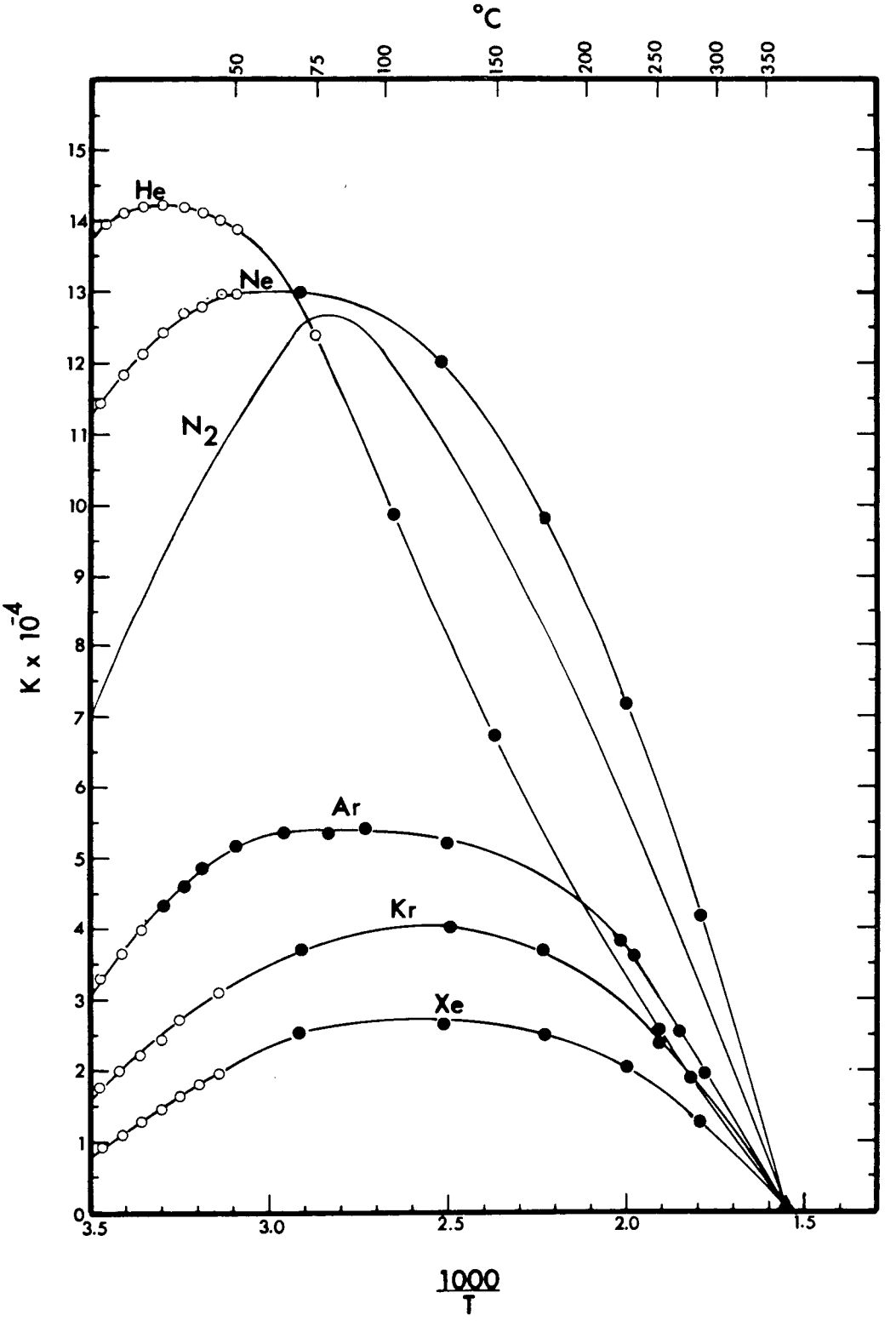

Figure 1. Solubilities of the noble gases He, Ne, Ar, Kr, and Xe and of nitrogen from 0 to 374°C expressed as Henry's law constants equal to the partial pressure of the gas in atmospheres divided by its mole fraction in the solution.

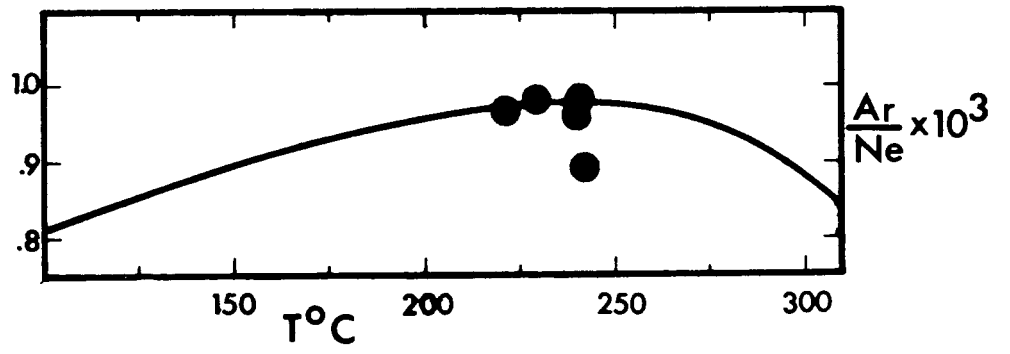

Figure 2. The ratios of Ar/Ne in steam samples from Larderello wells compared with calculated ratios for the first steam separated at various temperatures from a large well mixed body of water originally equilibrated with air at 10°C.

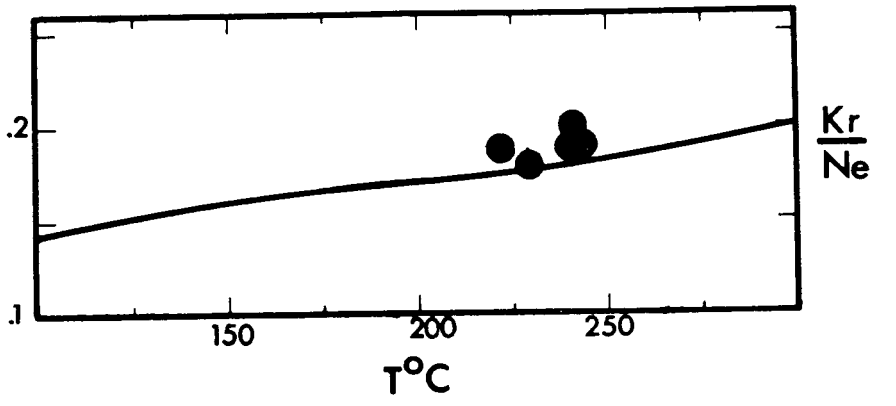

Figure 3. The Kr/Ne ratios calculated as in figure 2 compared with observed Larderello steam values.

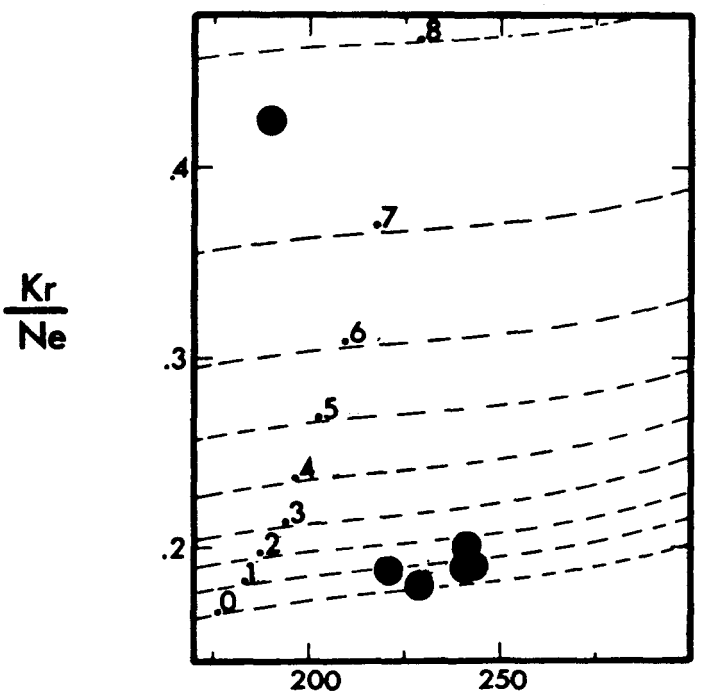

Figure 4. The ratios of Kr/Ne calculated for various temperatures and amounts of boiling (expressed as the fraction of steam boiled off) of a well mixed water body and the observed ratios of the Larderello steam samples.

Table 1. Characteristics of wells sampled.

Well	Date drilled	Depth m.	Production t./hr.	In August 1975 WHT* °C	WHP* kg/cm^2	Gas/steam l./kg STP
Columbaia	?	470	9.1	229	2.4	3.25
La Pineta	1942	316	11.1	200	4.3	17.5
Lard.57	∿1951	486	10.7	241	4.3	46.1
Lard.155	∿1961	844	15.3	222	4.9	33.9
Gabbro 6	1964	771	52.2	242	7.7	69.3
Gabbro 1	1962	853	44	240	7.4	54.2

*Well head temperature and pressure during flow

A GEOPHYSICAL APPROACH TO RESERVOIR DELINEATION IN THE GEYSERS

Iain M. Jamieson
GeothermEx, Inc.
901 Mendocino Avenue
Berkeley, California 94707

Recent syntheses of geophysical work at The Geysers (Chapman 1975, Isherwood 1975) have provided useful insights into regional structure in this complex and chaotic area. Regional studies of this type, however, are of limited value to reservoir investigations and it may be that the more detailed temperature gradient/heat flow studies (Frye 1976) can supply more useful information.

The survey discussed here was carried out on the Rorabaugh lease in the southwest sector of The Geysers geothermal field in an area of known production, good drilling records and closely spaced data points. Initial drilling on this lease was carried out by Geothermal Resources International and the area was subsequently developed for a 55 mW power plant by Pacific Energy Corporation and their successor, Thermogenics, Inc. The study included data from several producing wells, three deep suspended wells and four shallow (250'-500') temperature gradient holes.

The raw data were corrected for terrain (Jamieson 1976) and isotherms plotted from 25°C to 240°C (Fig. 1). Gradients in Big Sulphur Creek Valley were as high as 7.2°C/100 ft. and required terrain corrections of minus 20 per cent. Gradients on the ridge above the creek were as low as 1.88°C/100 ft. and required terrain correction of almost 100 per cent.

The 240°C isotherm plotted from these data lies just above steam shows in the producing area. This suggests that the terrain corrections were of the correct order of magnitude, that the thermal conductivity of the formation is reasonably uniform and that there is good conductive coupling between the reservoir and the surface (Urban, et al 1975).

The rapid down turn of the 240°C isotherm outside the producing area suggests a sharp field boundary, a postulate supported by the absence of steam in Rorabaugh A8. It further suggests a very high angle field boundary, which is in accord with the high angle fractures encountered during drilling and with the high angle structural features which appear in

geological mapping. The nature of the boundary is undefined, and it may correspond to faulting, changes in fracture intensity, changes in metamorphic grade or changes in silica content. The position of the boundary, however, is fairly precisely defined, and this should be of considerable interest when interpreting well test data from this field.

The success of this survey in a comparatively simple situation suggests that it may be developed to handle more complex areas with shallow hot water zones, variable lithology and variable microclimates. If this can be done, it may provide a useful link between geothermal exploration and reservoir engineering.

References

Chapman, R. H., 1975, Geophysical study of the Clear Lake region, California: Calif. Div. Mines & Geol., Spec. Rept. 116, 37 p.

Frye, G. A., 1976. Investigation of a fluid boundary: Second Workshop, Geothermal Reservoir Engineering, Stanford Geothermal Program, pp. 30-33.

Isherwood, W. H., 1975, Gravity and Magnetic Studies of The Geysers--Clear Lake Geothermal Region, California, U.S.A. Proceedings of Second United Nations Symposium on the Development and Use of Geothermal Resources, V. 2, pp.1065-1073.

Jamieson, I. M., 1976, Heat Flow in a Geothermally Active Area: The Geysers, California: Ph.D. Dissertation, University of California, Riverside.

Urban, T. C., Diment, W. H., Sass, J. H. and Jamieson, I. M., 1975, Heat Flow at The Geysers, California, USA: Proceedings of Second United Nations Symposium on the Development and Use of Geothermal Resources, V. 2, pp. 1241-1245.

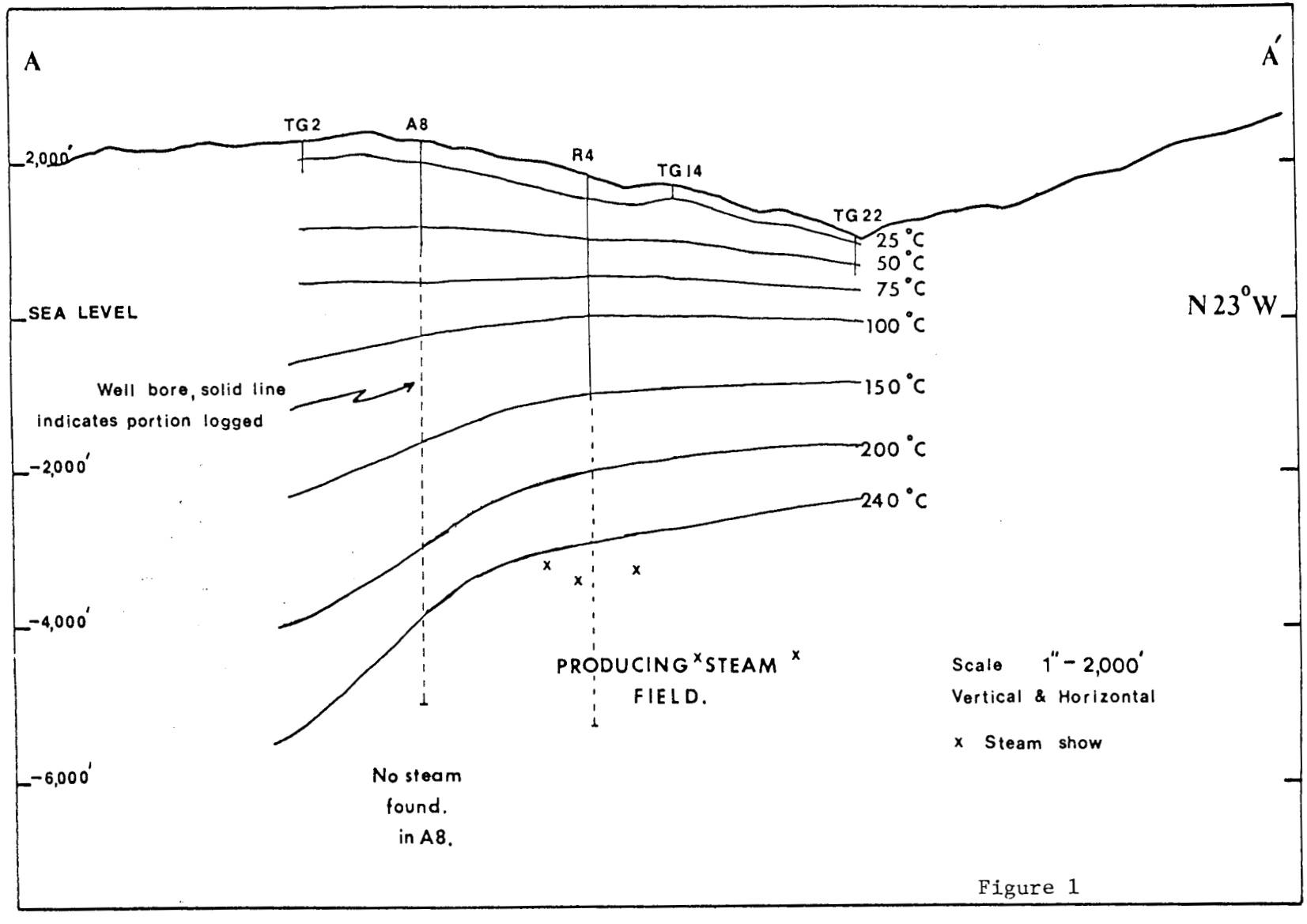

Fig. 1. Isotherms along the profile AA' showing temperature gradient holes, wells and steam shows. Portions of the well bores for which temperature data were obtained are shown as solid lines and portions for which no temperature data are available are shown as broken lines.

TRANSIENT PRESSURE ANALYSIS IN GEOTHERMAL STEAM RESERVOIRS WITH AN IMMOBILE VAPORIZING LIQUID PHASE -- SUMMARY REPORT

A. F. Moench
U.S. Geological Survey
Water Resources Division
345 Middlefield Road
Menlo Park, CA 94025

and

P. G. Atkinson
Union Oil Company
P.O. Box 6854
2099 Range Ave.
Santa Rosa, CA 95406

Introduction

The application of transient pressure analysis methods to vapor-dominated geothermal systems has generally been done using methods developed for noncondensable gas reservoirs. These methods have been satisfactory in many cases; however, because they neglect effects of vaporization and condensation, the results may be misleading. The study presented here was motivated by a perceived potential need to incorporated phase changes into the analysis of pressure drawdown and recovery data. It is hoped that this will allow for an increased understanding of the processes occurring in geothermal systems where steam and liquid water are thought to coexist.

A finite-difference model for the horizontal, radial flow of steam in the presence of an immobile vaporizing or condensing liquid phase was adapted from the model of Moench (1976). Results were generated for real physical parameters, and are presented in terms of standard dimensionless pressure (actually pressure-squared) and time groupings. The analysis assumes an initial constant temperature and pressure in the aquifer and an initial uniform liquid-water distribution which partially fills the void space. It is also assumed that the steam and liquid water in the reservoir are in local thermal equilibrium with the reservoir rocks and that temperature changes occur only in response to phase changes. In the examples which follow permeability, porosity, and well discharge are constant.

Results

The computed pressure drawdown plotted in figure 1 (P_D vs. log t_D) shows the comparison of dry steam (S=0.0) with three examples having different quantities of initial liquid-water saturation (S=0.05, S=0.10, S=0.20). The latter results are displaced, as a group, from the response for dry steam by an amount which depends upon the heat capacity per unit volume of the reservoir rock. The slope of the straight line obtained for dry steam is that predicted by the line-source solution to the diffusivity equation.

Figure 2 shows interference pressure drawdown data (log P_D vs. log t_D/r_D^2) compared with the line-source solution. The slight displacement of the results for dry-steam to the left of the line-source solution at early time is due to the spatial increments used in the finite-difference model.

Figure 3 shows Horner buildup graphs (P_D vs. $(t_o + \Delta t)/\Delta t$) for three different values of initial liquid-water saturation. Production time is the same for each case and is approximately 9 hours in duration. Initially (small Δt) the pressure rises rapidly because the steam is superheated in the vicinity of the production well. This is followed by a period during which the pressure is nearly constant owing to the onset of condensation. Continued rise in pressure as time goes on (large Δt) is due to heating by condensation. The location of the plateau in figure 3 depends upon the heat capacity per unit volume of the reservoir rock and upon the amount of liquid which was available for vaporization per unit volume during the period of production.

Discussion

Drawdown data generated with the two-phase simulation model for radial flow to a discharging well shows that the existence of a vaporizing liquid-water phase is manifested on plots of dimensionless time only by a shift in the horizontal direction from the dry steam case. This can be explained as an apparent increase in compressibility of the system. Assuming the validity of the assumptions of this analysis, this result suggests that the presence of a vaporizing liquid will not complicate evaluation of the reservoir permeability-thickness product from drawdown data when the usual methods of gas reservoir engineering are applied. However, this also implies that such a test cannot distinguish between the presence or absence of liquid in the pore space.

Simulated pressure buildup data, on the other hand, show characteristics which are markedly different from that expected for noncondensable gas. Condensation holds the pressure at saturated-vapor pressure and is responsible for the zone of nearly constant pressure seen in the pressure buildup graphs. If phase change plays an important role in pressure transient well testing, it should be manifested in pressure buildup tests.

Details of this analysis will become available in a forthcoming paper by the authors. Further studies are underway that will change some of the assumptions made herein.

Notation and Definition of Dimensionless Groups

P_D	dimensionless pressure squared $= \frac{\mu k h M_w}{q \mu Z_i R T} (P_i^2 - P^2)$	t_D	dimensionless time $= \frac{k P_i t}{\phi \mu r_w^2}$
r_D	dimensionless distance $= \frac{r}{r_w}$	S	liquid-water saturation (percent of void space)
r	radial distance	t	time
r_w	well radius	t_o	production time
q	production rate	Δt	time since shut-in
P	pressure	μ	steam viscosity
P_i	initial pressure	Z_i	initial compressibility factor
k	permeability	R	gas constant
h	reservoir thickness	T	temperature
M_w	molecular weight water	ϕ	porosity

Values of Parameters Used

P_i	30×10^6 dynes/cm^2	M_w	18 g/Mole
k	7×10^{-8} cm^2	μ	1.8×10^{-4} dyne-sec/cm^2
h	714 cm	Z_i	0.9
q	4.16×10^4 g/s	R	8.3×10^7 dyne-cm/(°C Mole)
ϕ	0.10	r_w	15 cm
T	507 °K	t_o	3.22×10^4 s

Reference

Moench, A.F., 1976, Simulation of steam transport in vapor-dominated geothermal reservoirs, U.S. Geol. Survey Open-File Report 76-607, 43 p.

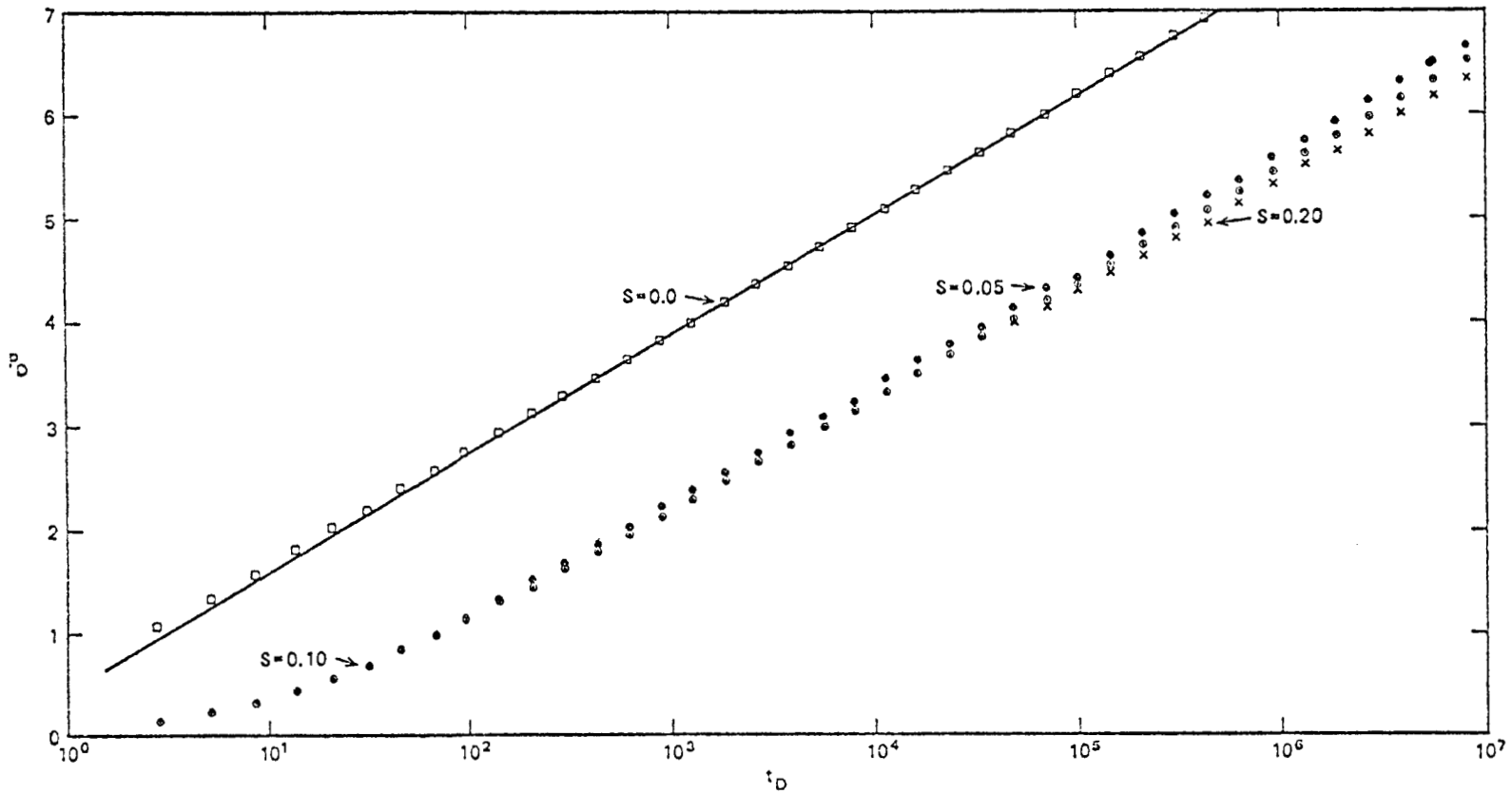

FIGURE 1. Dimensionless pressure drawdown versus log dimensionless time for dry steam (S=0.0) and various values of initial liquid-water saturation.

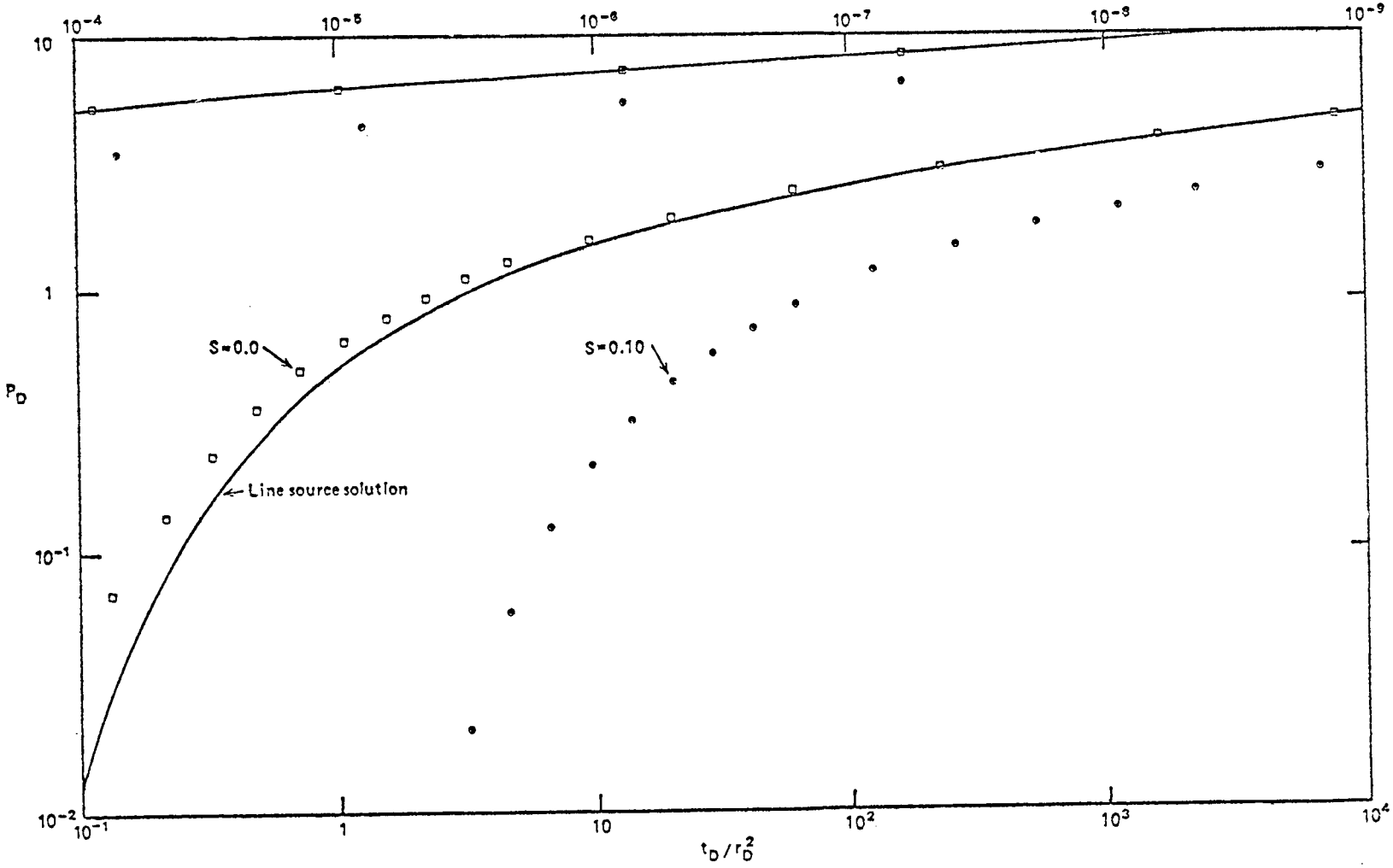

FIGURE 2. Log dimensionless pressure drawdown versus log dimensionless time for dry steam (S=0.0) and one value of initial liquid-water saturation compared with the line-source solution.

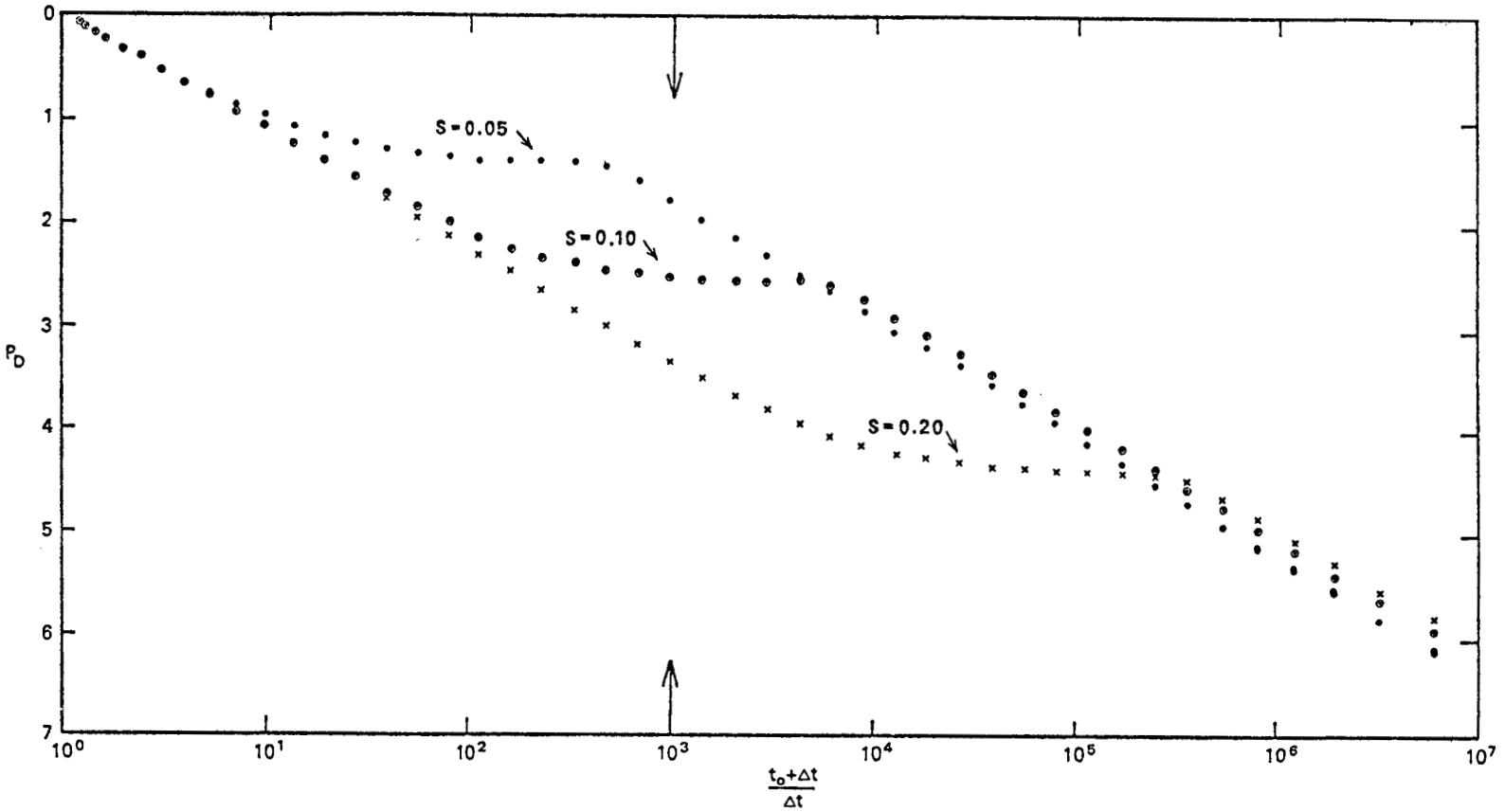

FIGURE 3. Dimensionless pressure buildup vs. Horner time group for various values of initial liquid-water saturation. Arrow on abscissa refers to a real recovery time of 32 s.

JAPANESE PRIMARY ENERGY SUPPLY AND GEOPHYSICAL WELL LOGGING

Seiichi Hirakawa
The University of Tokyo
Department of Mineral Development Engineering
Faculty of Engineering
7-3-1 Hongo, Bunkyo-ku, Tokyo 113, Japan

Japan is scarce in domestic natural resources. In fact, the degree of dependence on imports of basic raw materials is quite high. This paper describes primary energy supply as a background to the status of geothermal energy developments, and geophysical well logging in geothermal wells.

Primary Energy Supply of Japan

Although Japan made a high level of economic growth from 1960 until the oil crisis in 1973, the oil crisis has had such a considerable effect on the Japanese economy as to shake its foundation. As the base of Japan's energy policy, "The Long Range Prospects for Energy Supply and Policies" was issued in 1975 by the Energy Council. In Table 1, which is its long term energy supply program, the degree of dependence on imported oil will decrease from 77 percent in 1973 to 63 percent in 1985. On the other hand, in order to attain the target of reducing dependence on imported oil, acceleration of the development of domestic energy and the large-scale introduction of LNG will be necessary.

The Japanese government has decided to make a new energy plan by next year, paying due regard to the growing sense of energy crisis. The new energy policy will be founded on the following principles: (1) to decrease dependence on crude oil, (2) to secure the stable supply of hydrocarbon energy, (3) to realize that the present target for nuclear energy is doubtful, (4) to develop various sorts of energy resources and their technologies, (5) to promote energy saving, (6) to establish friendship trade with overseas countries through international cooperation.

The advisory committee of Energy Council announced its revised plan (Table 2) in June this year, though it is not yet final. The former government plan has been variously criticized ever since it was reported. In particular there were lively arguments about the feasibility of achieving the targets of the plan, mainly: (1) in the areas of nuclear energy and LNG, realization of the plan's target is doubtful; (2) the assurance of available funds should have been made clear, in order to carry through the plan; (3) the level of oil imports would not be so easy to achieve. Each of these points was an important indication for the necessity of revising the energy plan.

Table 1. Actual Results and Forecast of Primary Energy Supply

Sources		1			2
Primary Energy \ Year		FY 1973	FY 1975	FY 1985	FY 1985
Domestic Supply	Hydro-Power, 10^6KW	21.20	25.43	28.30	27.00
	Geothermal Energy, 10^6KW	0.03	0.05	2.10	0.50
	Oil & Natural Gas, 10^6KL	3.70	3.53	14.00	8.20
	Coal 10^6ton	21.68	18.60	20.00	20.00
	Nuclear Power, 10^6KW	2.30	5.95	49.00	27.00
Imported Supply	LNG, 10^6ton	2.37	5.06	42.00	27.00
	Coal, 10^6ton	58.00	62.34	102.40	(S) 88.60 (L) 81.48
	Crude oil & LPG, 10^6KL	318.00	285.27	485.00	(S)499.46 (L)440.63
	Total 10^{13}KCal	383.	366.	710.	(S)658. (L)597.

Notes:

a) Sources of Information

Source 1) Energy Council (Aug. 1975)

Source 2) The Institute of Energy Economics(Dec. 1976)

b) For Institute of Energy Economics,

(S) indicates standard case

(L) indicates low growth case

c) Conversion rates of petroleum to heat

1 liter of petroleum 9,400 KCal

Table 2. Japan's Energy Plan

Primary Energy \ Year		FY 1975 (Actual data)	FY 1985	
			Government Plan (1975. Aug.)	Revised Plan (1977. June)
Domestic Supply	Geothermal Energy, 10^6KW	0.05	2.10	1.0
	Oil & Natural Gas, 10^6KL	3.50	14.00	11.0
	Coal, 10^6ton	18.60	20.00	20.0
	Nuclear Power, 10^6KW	6.62	49.00	33.0
Imported Supply	LNG, 10^6ton	5.06	42.00	30.0
	Coal, 10^6ton	62.34	102.40	102.0
	Crude Oil & LPG, 10^6KL	286.00	485.00	432.0
	New Energy, 10^6KL	-	-	2.3

Table 3. Geothermal Power Plants in Operation and under Construction in Japan (1977, July)

	Name of Company	Name of Station	Location (Pref.)	Capacity (KW)	Starting Operation
In Operation	Japan Metals and Chemicals Co.	Matsukawa	Iwate	22,000	1966, Oct.
	Kyushu Electric Power Co.	Otake	Ōita	11,000	1967, Oct.
	Mitsubishi Metal Mining Co.	Ōnuma	Akita	10,000 (7,500)	1974, June
	Electric Power Development Co.	Onikobe	Miyagi	25,000 (12,500)	1975, Mar.
	Kyushu Electric Power Co.	Hatchobaru	Ōita	50,000 (23,000)	1977, June
	Sub-total			118,000 (76,000)*	*(actual data)
Under Construction	Japan Metals and Chemicals Co. / Tōhoku Electric Power Co.	Katsukonda (Takinoue)	Iwate	50,000	1977, Dec.
	Dohnan Geothermal Energy Co.	Mori (Nigorikawa)	Hokkaido	50,000	1979, Mar.
	Sub-total			100,000	

Geothermal Resources and Development in Japan

At present, five geothermal power stations are being operated, and another two stations are under construction, as shown in Table 3. An organized basic investigation for geothermal resources was started in the fiscal year of 1973 by the Geological Survey of Japan.

Japan is set on parts of a volcanic belt; that is, the volcanic ranges of Chishima, Nasu, Chokai, Fuji, Norikura, Hakusan, Kirishima and so on. Hot springs occurring in the vicinity of these volcanoes have been used for bathing. According to a report (1975) by the Geological Survey of Japan, there are 111 sites of steam fumaroles, boiling springs and hot springs having temperatures more than 90°C, although in total there are about 1,500 hot spring resorts in Japan. Prospective sites for geothermal energy development usually lie around the hot spring zones of volcanoes. As part of the long-term new energy research and development program named "Sunshine Project", the Geological Survey of Japan picked up the thirty high potentiality geothermal fields (Fig. 1) characterized by conspicuous geothermal anomalies, particularly fumaroles and hot springs of temperature above 90°C.

Geophysical Well Logging in Geothermal Wells

The purpose of geothermal well logging differs from that of oil or gas wells in some respects. Geothermal wells are usually drilled in hotter and harder formations, which often are fractured. This combination of high temperatures and hard formations (igneous or metamorphic, not sedimentary formations) causes some problems in geothermal well logging.

In Japanese geothermal energy development companies such as the Japan Metals & Chemicals Co., Ltd., geologists and reservoir engineers have mainly conducted research into the evaluation of fractures and geothermal reservoirs by electric logging (S.P., resistivity), temperature and pressure logging, caliper logging and so on.

Our governmental support for geothermal well logging may be grouped into two kinds. First, the Japan Geothermal Energy Development Center is now investigating geothermal potential and the feasibility of its development using surface surveys and boring wells (about 1,000 meters depth) under instructions from the Power generation section and the Geothermal resources development investigation committee, which belong to the Ministry of International Trade and Industry. The following geophysical measurements in these wells are available: temperature logging, electric logging (S.P., resistivity), core analysis (rock density, magnetic susceptibility, acoustic velocity, thermal conductivity) and so on.

A second kind is the Geothermal Energy Research and Development program of "Sunshine Project," planned by the Industrial Technology Agency. Included are the following four R & D groups:

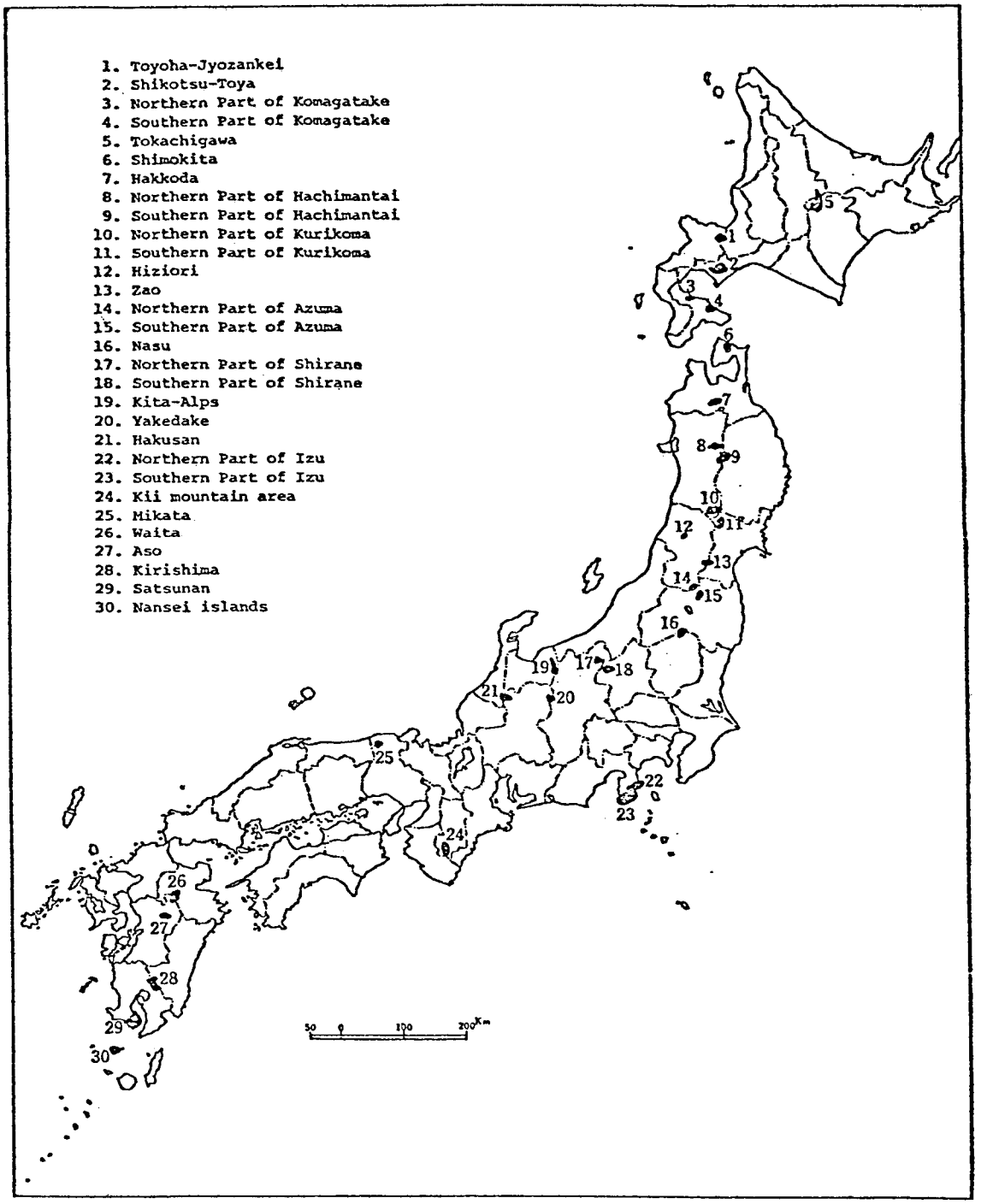

Figure 1. Locations of the 30 geothermal fields to be investigated by the Geological Survey of Japan.

(1) exploration, drilling and production, (2) geothermal power generation and plant, (3) recovery of volcanic energy, energy from dry hot rock etc., (4) environmental problems, multiple utilization of steam and hot water etc. One of them is the R & D on well logging probes and devices with a view of geothermal energy development. In 1975, the study was initiated by our Borehole Measurement (geothermal well logging) Committee which consists of members from the Geological Survey of Japan, University of Tokyo, Geothermal Energy Research and Development Co. (secretariate), Japan Metals & Chemicals Co., Teikoku Oil Co., Japan Petroleum Exploration Co. and so on.

A feasibility study and selection of well logging tools were conducted in early stages of this study. These tools are usually designed for operation in an environment of 250°C and 200 ~ 300 Kg/cm^2. The following equipment will be constructed and operated by the coming March.

(1) Testing Vessel
(2) Downhole Flowmeter for hot water (continuous recording type)
(3) Acoustic Velocity Logging device measuring the compressional wave and shear wave simultaneously
(4) Bore Hole Television Camera
(5) Temperature Logging and Pressure Logging devices.

These hot spring zones have peculiar landscapes such as volcanic valleys and have often been designated as national parks or quasi-national parks. Geothermal development within the area of a national park needs prior permission of the Director of Environment Agency. The Governor's permission would not be easily obtained. However, in view of the very high dependence of Japan's energy supply on foreign resources, the development of the domestic geothermal energy resources should be promoted as a national policy.

References

1. Seiichi Hirakawa and Shigero Kusano, "Japan's Energy Policy and Role of LNG", 5th International Conference on LNG, Session 1, (1977).

2. Junji Suyama et al., "Assessment of Geothermal Resources of Japan", Geological Survey of Japan (1975).

3. Tsutomu Inoue, "Present Status and Future Prospects of the Geothermal Energy Development in Japan", 9th WEC, Division 3 (1974).

TABLE 4.

Comparison of field data with calculated results.

Test Well	Total Mass Rate (t/hr)	Predicted Flow Regime	Pressure Drop Δp_m (kgf/cm^2)	Pressure Drop Δp_c	Percent Difference
T-205-1	32.5	F,B	39.2	38.8	- 1.0
T-205-2	39.7	F.B	36.7	37.3	1.6
T-205-3	47.3	F,B	33.0	30.8	- 6.7
T-205-4	54.9	F,B	30.5	26.9	-11.8
C-1-1	78.1	F,B	62.82	59.13	- 5.9
C-1-2	147.5	F,B	52.06	52.81	1.4
C-1-3	198.6	F,B	44.52	47.72	7.1
C-2-1	127.5	F,B	56.05	58.02	3.5
C-2-2	209.9	F,B	50.65	53.02	4.8
C-2-3	229.0	F,B	48.65	48.78	0.2

F=Froth, B=Bubble,

Percent Difference $= \frac{(\Delta p_c - \Delta p_m)}{\Delta p_m} \times 100$

TABLE 5.

Well Data from Takinoue, Japan (1975-6).

Test Well	Reference Depth (m)	Cased Depth (m)	Steam Rate (t/hr)	Water Rate (t/hr)	Wellhead Pressure (kscg)	Wellhead Quality
T-205-1	700	500	1.9	30.6	12.7	0.058
T-205-2	700	500	3.3	36.4	10.6	0.083
T-205-3	700	500	5.2	42.1	9.8	0.110
T-205-4	700	500	7.7	47.2	8.0	0.140
C-1-1	950	752	6.5	71.6	10.9	0.083
C-1-2	950	752	14.8	132.7	10.2	0.100
C-1-3	950	752	17.9	180.7	9.3	0.090
C-2-1	880	829	6.9	120.6	13.98	0.054
C-2-2	860	829	21.4	188.5	13.98	0.102
C-2-3	860	829	26.8	202.2	13.22	0.117

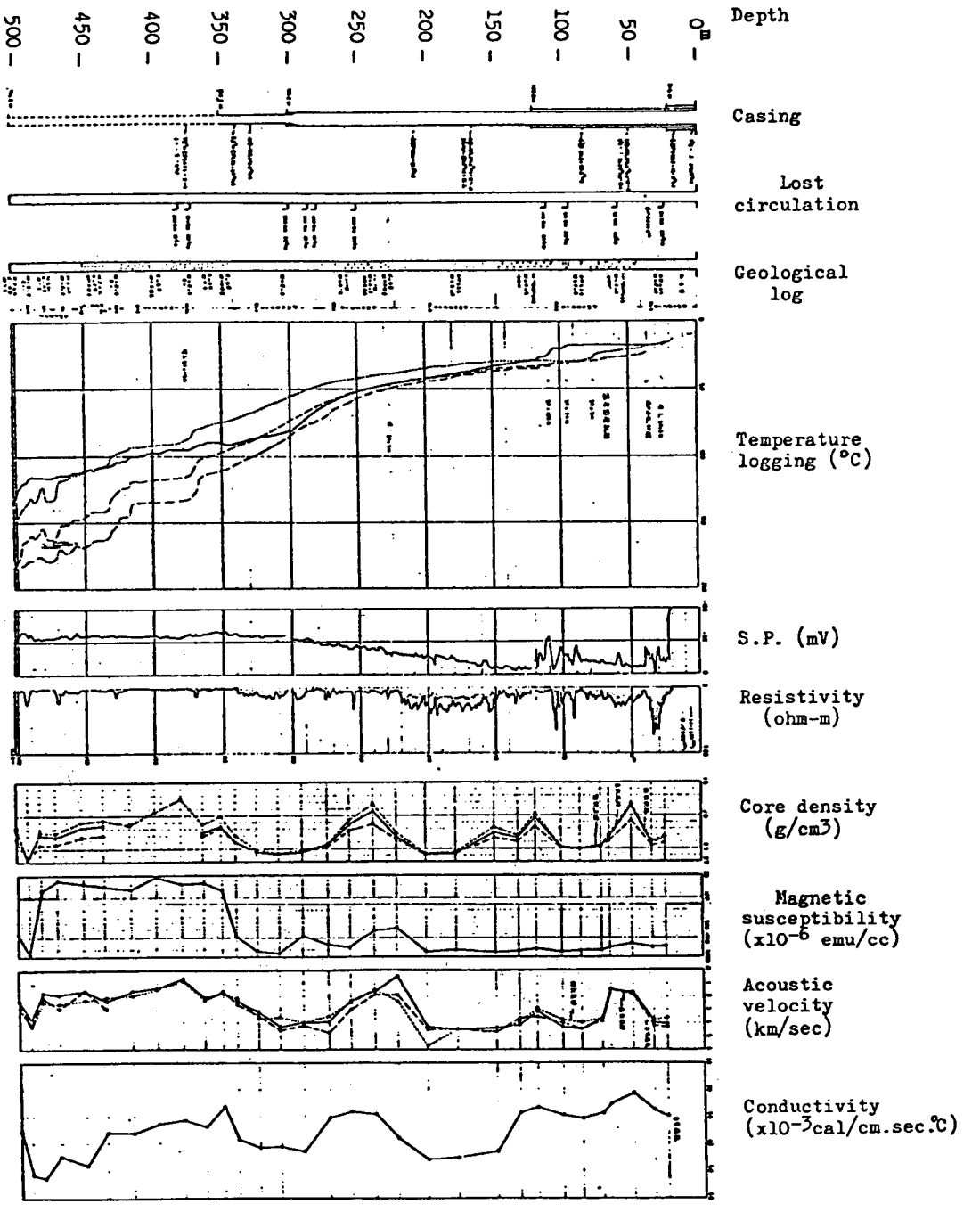
500 –
450 –
400 –
350 –
300 –
250 –
200 –
150 –
100 –
50 –
0m –
Depth
Casing
Lost circulation
Geological log
Temperature logging (°C)
S.P. (mV)
Resistivity (ohm-m)
Core density (g/cm3)
Magnetic susceptibility (x10-6 emu/cc)
Acoustic velocity (km/sec)
Conductivity (x10-3cal/cm.sec.°C)

Figure 2.

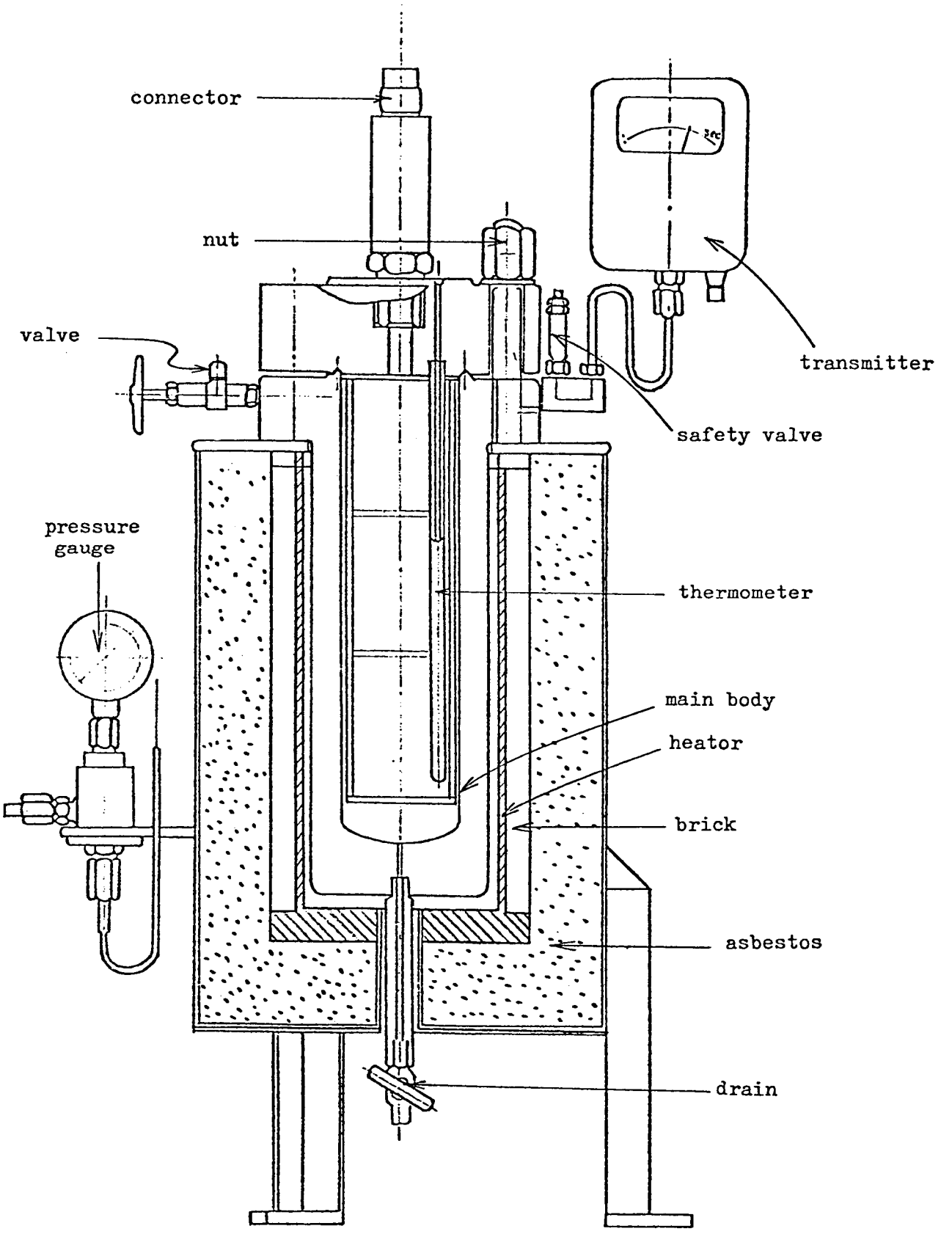

Figure 3. Testing Vessel

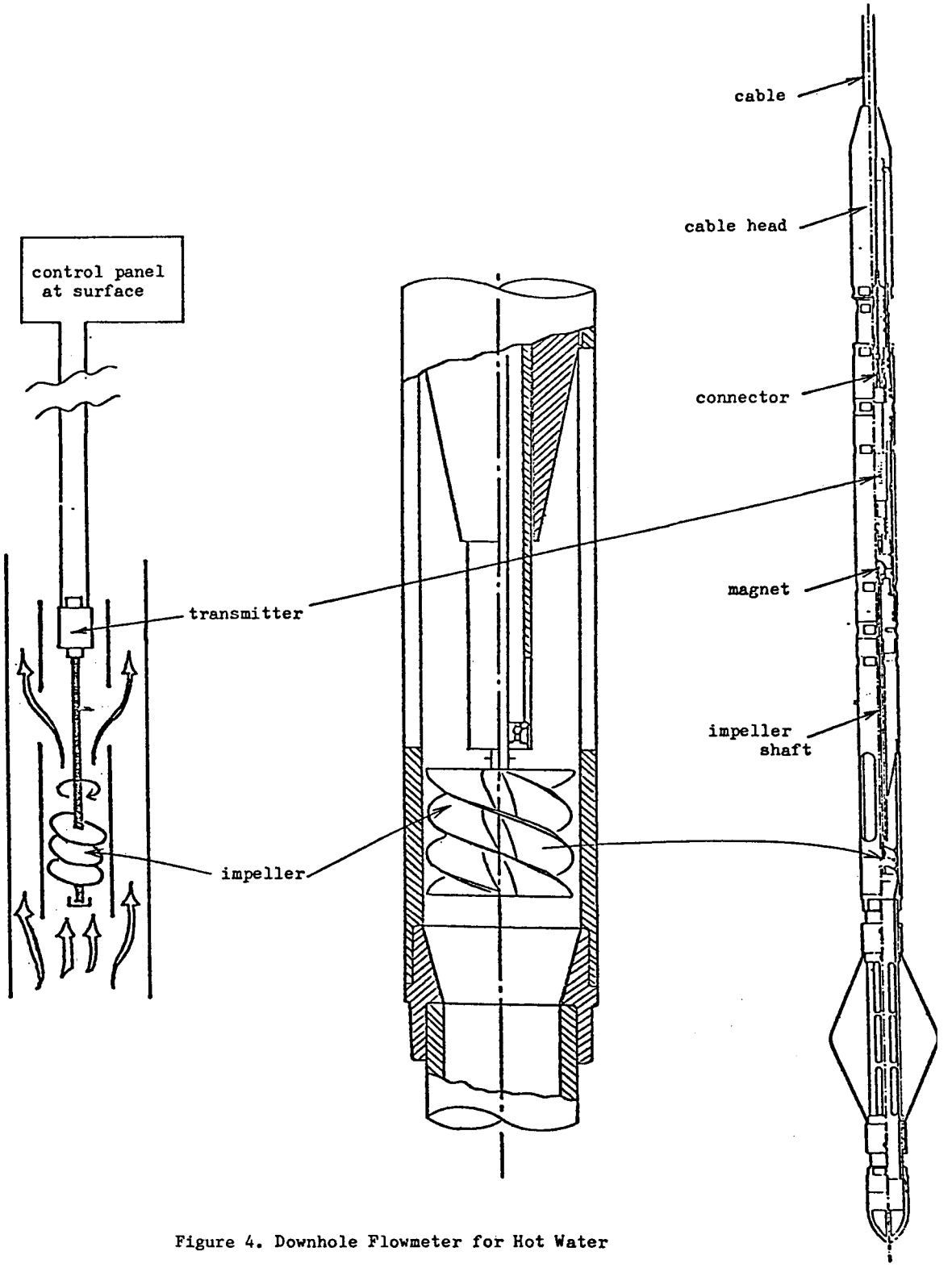

Figure 4. Downhole Flowmeter for Hot Water

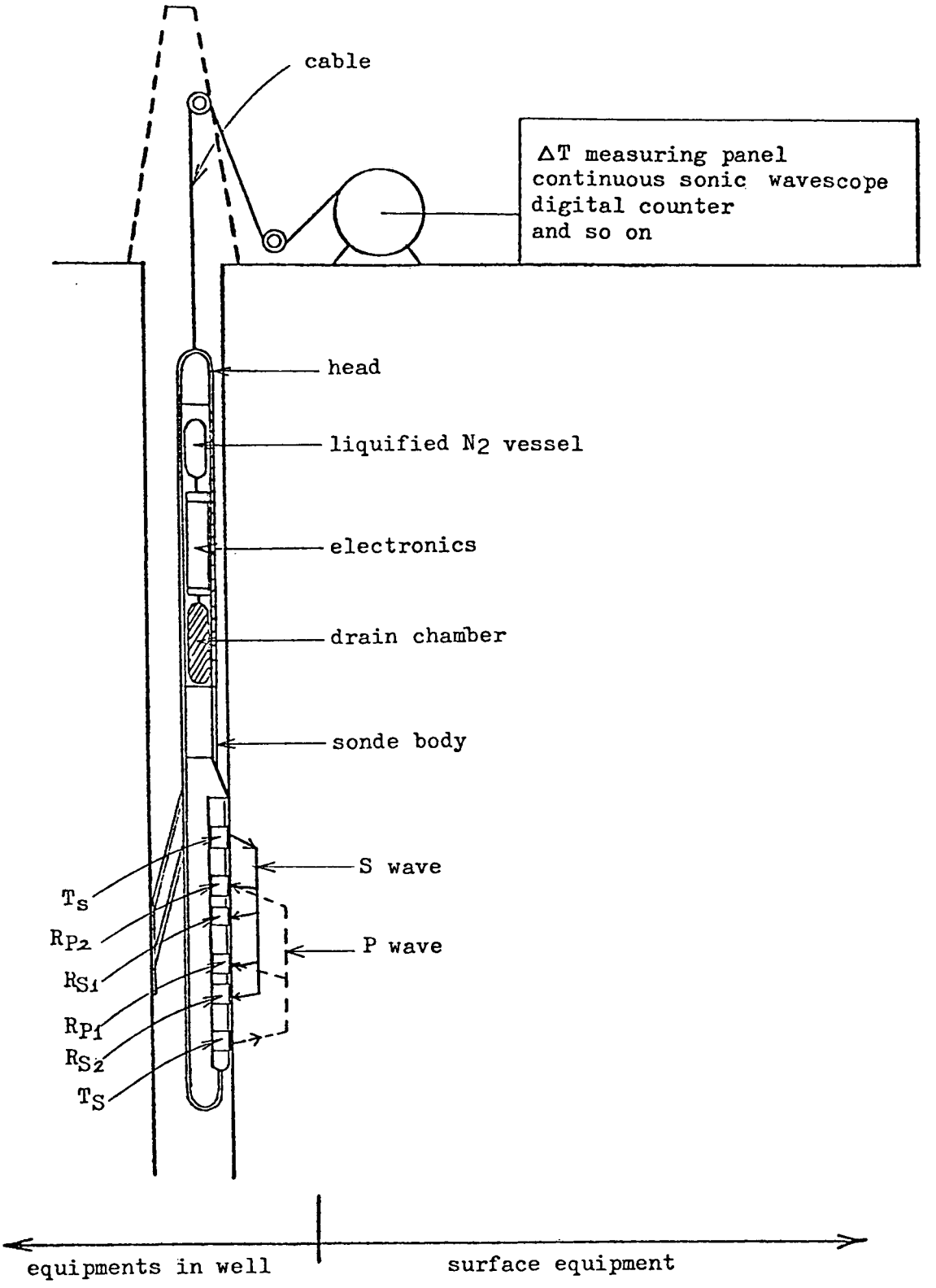
cable
ΔT measuring panel
continuous sonic wavescope
digital counter
and so on
head
liquified N2 vessel
electronics
drain chamber
sonde body
S wave
P wave
Ts
RP2
RS1
RP1
RS2
Ts
equipments in well
surface equipment

Figure 5.

ANALYSIS OF GEOTHERMAL WELL LOGS*

by

Subir K. Sanyal
Stanford University
Stanford, CA 94305

INTRODUCTION

In the petroleum industry, well logging is a well-developed discipline that has matured over a fifty-year period. Compared to this, geothermal well logging is a very new field of activity.

The current practice is to use the same logging equipment and the same log interpretation techniques for geothermal wells as had been used for petroleum wells. However, this approach has proven either inadequate or ineffective in most geothermal areas. The problems here are of two types: (1) those associated with logging equipment and operation, and (2) those connected with log interpretation techniques. Temperatures encountered in geothermal wells are normally higher (greater than 175°C or 350°F) than those in petroleum wells. In many geothermal wells, some of the standard well logs cannot be run due to the well temperatures being higher than the maximum temperature for which those logging tools are designed. Lack of financial incentive has so far discouraged large investments by logging service companies in developing new logging instrumentation or interpretation techniques for geothermal wells. U.S. Department of Energy (formerly U.S. ERDA) has established a new geothermal logging hardware development program at the Sandia Laboratories in New Mexico. The U.S. Geological Survey also has a similar program of hardware development for geothermal logging. These programs have progressed well and there is a strong hope that most of the hardware-related problems of logging geothermal wells will be resolved over the next few years. Sanyal and Meidav (1977) have discussed the differences in the objectives of well logging in the geothermal reservoirs from those in the petroleum reservoirs, and their implications on the state-of-the-art of geothermal well logging. These authors have also discussed the problems associated with the logging operation, log quality problems and log interpretation problems in the geothermal industry. This paper focuses on the log interpretation aspects only.

PROBLEMS IN ANALYSIS OF GEOTHERMAL LOGS

The existing techniques of interpretation of well logs in the geothermal industry are inadequate or ineffective in many wells. Some of the reasons are as follows:

*Summary of the paper presented at the Third Annual Stanford Geothermal Program Workshop on Geothermal Reservoir Engineering, Dec. 14-16, 1977.

(1) For an accurate formation evaluation, one needs a "suite" of well logs. Because of the temperature limitation of logging equipment, a complete suite of logs is not available from many geothermal wells.

(2) In many geothermal wells, logs are run faster than usual to avoid undue thermal strain on the equipment. This reduces the quality of the log, making interpretation less accurate. This rush sometimes causes operational problems.

(3) Many concepts and formulas used in well log interpretation have been developed over the last four decades from laboratory study of rock and fluid samples at ambient conditions. It is now known that many petrophysical properties of reservoir rocks are altered, reversibly or irreversibly, at elevated temperatures and pressures (for example, refer to Sanyal, et al., 1972; Sanyal, et al., 1974). However, sufficient experimental data are lacking. Thus, the usual approach to geothermal well log interpretation may be fraught with inaccuracies.

(4) Well logging experience in the petroleum industry has been confined to sedimentary formations, while geothermal wells may encounter any rock type (sedimentary, igneous, or metamorphic) often subjected to hydrothermal alteration. Also, lithology in a geothermal reservoir can vary drastically from layer to layer or from well to well, thus complicating log interpretation. The responses of the logging tools to such unfamiliar lithologies are not well known; calibration data for such cases are lacking. Since logging tools were originally designed for sedimentary formations, using them in igneous and metamorphic rocks tend to give poorer quality logs.

(5) The estimation of the location, orientation, and aperture of fractures is very important in planning production from many geothermal wells. Naturally fractured petroleum reservoirs are less common, hence the technology of estimating fracture location, orientation, and aperture is not well developed in the petroleum industry. Also, unlike most petroleum reservoirs, large scale natural fractures or faults may be the primary flow conduits in geothermal reservoirs. Current logging technology is inadequate to delineate such large scale fractures.

(6) Permeability is a most important property for both petroleum and geothermal reservoirs. No widely used well log exists that can measure in-situ permeability of a reservoir. In the petroleum industry, permeability is either measured from core samples of rocks taken from the well or estimated from well test data. For detailed formation evaluation, permeability is estimated from log-derived porosity values by using a suitable empirical correlation, which is developed for each petroleum

field from core analysis data. Sufficient data are not yet available to develop such empirical correlations for most geothermal fields. Moreover, presence of fractures in a geothermal reservoir can drastically increase the permeability around a well bore, while small core samples may not reflect the existence of such in-situ fractures. In any case, coring of hard, igneous and metamorphic formations is more expensive than coring of sedimentary formations. Hence, cores are usually not taken in geothermal wells.

(7) Accurate measurements of formation temperature are not critical for most petroleum wells. Hence, techniques for estimating the equilibrium temperature profile of the formation from measured temperature profiles are not well known.

(8) The composition of the formation water is a critical parameter in the geothermal industry, while in the petroleum industry it is usually not. Hence, the techniques for prediction of formation water quality from well logs are not sophisticated.

(9) Perhaps the most important log-derived parameter in the petroleum industry is the hydrocarbon saturation in the reservoir. A major part of the research and development in well log interpretation techniques has historically been devoted to detecting and estimating hydrocarbon saturation. In geothermal wells there is no hydrocarbon saturation, hence, many of the classical developments are not useful to the geothermal log analyst.

(10) Only a limited number of geothermal fields has been developed to date. A large enough data base, and consequently, useful empirical correlations of rock and fluid properties, do not exist in the geothermal industry.

(11) A geothermal reservoir is usually more complicated in geometry and flow behavior than its petroleum counterpart. For this reason, it is desirable and often imperative to correlate the well log data with surface geophysical and geochemical measurements. This aspect has not been as important in the petroleum industry.

Besides the above-mentioned problems, geothermal well logs display a myriad of log quality problems, many of which are also found in the petroleum industry and most can be rectified. This presentation includes a number of examples of these problems and their solutions, where possible.

CONCLUSIONS

Analysis of geothermal well logs is fraught with problems. However, with proper care, experience and a synergistic approach one may obtain an effective analysis of geothermal logs. However, this is not assured. There is an urgent need for further research to improve the state-of-the art of geothermal well log analysis.

REFERENCES

Baker, L. E., Campbell, A. B., and Hughen, R. L., 1975a. "Well-Logging Technology and Geothermal Applications," Sandia Laboratories, Energy Report SAND 75-0275, May 1975

Baker, L. E., Campbell, A. B., and Hughen, R. L., 1975b. "Geothermal Well Logging: Air Assessment of the Art," The Log Analyst, Vol. XVI, No.6, November-December, 1975, p.21

Sanyal, S K., Marsden, S. S., Jr., and Ramey, H. J., Jr. 1974. "Effect of Temperature on Electrical Resistivity of Porous Media," Trans. Thirteenth Annual Loggging Symp. of Soc. Prof. Well Log Analysts, Tulsa, Oklahoma, May 1972

Sanyal S. K., S. S., Marsden, Jr., H. J. Ramey, Jr., 1974."Effect of Temperature on Petrophysical Properties of Reservoir Rocks," Paper #SPE 4898 presented at the 49th Annual Fall Meeting of the Society of Petroleum Engineers, Houston, Texas, October 1974.

Sanyal, S. K., and Meidav,H. T., 1976. "Well Logging in the Geothermal Industry," Paper presented at the 17th Annual Logging Symp. of the SPWLA, Denver, Colorado, June 1976.

Sanyal, S. K., and Meidav, H. T., 1977. "Important Considerations in Geothermal Well Log Analysis," SPE paper No. 6535, presented at the 47th Annual California Regional Meeting of the SPE of AIME, Bakersfield California, April 13-15, 1977

DECLINE CURVE ANALYSIS IN GEOTHERMAL RESERVOIRS

Elliot J. Zais
Elliot Zais & Associates
320 Quarry Road
Albany OR, 97321

Decline curves are among the oldest and most commonly used tools in analyzing petroleum production. Arps's (1,2) analysis is the basis for numerous methods currently in use from hand calculations to computer studies. The successful adaptation to geothermal problems of pressure testing methods developed in the petroleum and ground water fields suggests that decline curve analysis should be looked at more closely. Rivera (12) presented a paper at the 1977 GRC conference in which he analyzed 3 wells from Cerro Prieto and found fits to Arps's hyperbolic, harmonic, and exponential models. A quick check using Gentry's (6) method confirms his observations. A test of some Wairakei data indicates exponential decline. A detailed comparison of all the available methods was severely hampered by a lack of good field data. The methods have all been thoroughly verified on oil and gas fields, but little has yet been published on their use in geothermal reservoir engineering.

Steam fields can often be treated as natural gas fields so natural gas methods can be applied. Ramey (10) in his Petroleum Engineering 269 videotape course at Stanford and Brigham and Morrow (3) discuss the use of P/z vs. cumulative production plots. Ramey (10) published such a plot for The Geysers which shows a smooth linear decline.

Most decline curve methods have been tested with oil wells and fields but Russell et al (13) suggested that "under stablized flow conditions, the production rate decline (in gas fields) is hyperbolic during the constant pressure period... The limit of application for the hyperbolic rate decline is believed to be a function of the variation of gas properties with pressure."

In 1961 Guerrero (7,8) published some easy to follow "recipes" for analytic and graphical solutions to decline curve problems. The analytic method is simple enough to program on a good hand held calculator. The Wairakei data were checked with this method and found again to be exponential. Slider (15) developed a type curve approach to hyperbolic decline curve analysis and published it in 1968. In 1969 Ramsay and Guerrero (11) reported on Ramsay's MS work and concluded that "1. There is a more frequent occurrence of the hyperbolic and harmonic types of decline curves than has been previously indicated in the literature. 2. The ideal application of decline curves should employ the hyperbolic decline curve in the full range of $0 \leq b \leq 1$ and should include the linear exponential and reciprocal rate (harmonic) decline curves as special cases at the extremities of the range of b."

The above methods work well with reasonably smooth data but might present a problem with scattered data. Then some method such as Least Squares could be used to put a best curve through the data. Locke, Schrider, and Romeo (9), Schrider and Cerullo (14), and Cerullo and Romeo (4) have developed linear and non-linear Least Squares programs in FORTRAN and have warned against the careless analysis of decline curves. If Arps's hyperbolic equation is analyzed using linear Least Squares methods, the solution minimizes the squared residuals of the <u>logarithms</u> of the production rates rather than the squared residuals of the production rates. This can lead to large residuals in production rate and large errors in reserve calculations. Scarborough's non-linear Least Squares method eliminates the problem by fitting the data directly. A good initial approximation is needed, but this can be gotten from the linear Least Squares method.

In 1972 Gentry (6) published 2 figures for solving all kinds of decline curve problems. All of the equations used to describe decline are solutions of the differential equation

$$D = Kq^n = -(dq/dt)/q.$$

Given the initial production rate q_i, rate at time t, q, and cumulative production Q at time t, the decline exponent n and the decline rate D can be

found quite easily. The Wairakei and Cerro Prieto data were checked with this method. The Wairakei data still appear to be exponential and the Cerro Prieto data are as reported by Rivera.

Fetkovich (5) recently presented a method using log-log type curve analysis in an analogous way to pressure transient methods. I was able to match some data from the central part of the Larderello field fairly well with the small type curve in the paper. The data were hand digitized from a small ungridded graph so it would be imprudent to try making any calculations from this rough a match.

Assessment of reserves is one of a reservoir engineer's main tasks, and the above methods should prove to be of great utility in the geothermal field.

References

(1) Arps, J. J., "Analysis of Decline Curves", Trans AIME (1945) 160, 228-247.

(2) Arps, J. J., "Estimation of Primary Oil Reserves", Trans AIME (1956) 207, 182-191.

(3) Brigham, W. E. and W. B. Morrow, "P/z Behavior for Geothermal Steam Reservoirs", SPE 4899 presented at 44th Annual California Regional Meeting of SPE of AIME, San Francisco CA, April 4-5, 1974.

(4) Cerullo, R. E. and M. K. Romeo, A Review of the Curve-Fitting Method of Least Squares As Applied to Petroleum Engineering, US Bureau of Mines Information Circular 8449, 1970.

(5) Fetkovich, M. J., "Decline Curve Analysis Using Type Curves", SPE 4629 presented at 48th Annual Fall Meeting of SPE of AIME, Las Vegas NV, Sept 30-Oct 3, 1973.

(6) Gentry, R. W., "Decline-Curve Analysis", JPT, XXIV, (Jan 1972), 38-41.

(7) Guerrero, E. T., "How to Determine Performance and Ultimate Recovery by Exponential Decline-Curve Analysis", Oil and Gas J., (May 22, 1961), 86.

(8) Guerrero, E. T., "How to Determine Performance and Ultimate Recovery of a Reservoir Declining Hyperbolically", Oil and Gas J., (July 17, 1961), 94.

(9) Locke, C. D., L. A. Schrider, and M. K. Romeo, "A Unique Approach to Oil Production Decline Curve Analysis with Applications", SPE 2224 presented at 43rd Annual Fall Meeting of SPE of AIME, Houston TX, Sept 29-Oct 2, 1968.

(10) Ramey, H. J., Course notes for Petroleum Engineering 269, Stanford University, 1975.

(11) Ramsay, H. J. and E. T. Guerrero, "The Ability of Rate-Time Decline Curves to Predict Production Rates", JPT, XXI, (Feb 1969), 139-141.

(12) Rivera R., J., "Decline Curve Analysis-A Useful Reservoir Engineering Tool for Predicting the Performance of Geothermal Wells", GRC Trans 1, (May 1977), 257-259.

(13) Russell, D. G., J. H. Goodrich, G. E. Perry, and J. F. Bruskotter, "Methods for Predicting Gas Well Performance", JPT, XVIII, (Jan 1966), 99-108.

(14) Schrider, L. A. and R. E. Cerullo, "A Decline Curve Pitfall Using Least-Squares Solution", JPT, XXII, (April 1970), 441-442.

(15) Slider, H. C., "A Simplified Method of Hyperbolic Decline Curve Analysis", JPT, XX, (March 1968), 235-236.

PREDICTION OF FINAL TEMPERATURE

Gary W. Crosby
Phillips Petroleum Company
P.O. Box 752
Del Mar, CA 92014

The engineering necessity of achieving maximum cooling of the borehole during drilling and logging operations on geothermal wells prohibits the determination of equilibrium temperature in the subsurface before virtual rebound from the drilling disturbance some months after operations cease. Clearly, substantial economic benefits would accrue, in many cases, if a reasonable prediction of equilibrium temperature can be made while the rig is still over the borehole. Certain flow tests are desirable when commercial temperatures are known to be present in the reservoir. The manner in which the well is to be completed depends on its anticipated uses in the future. Before the rig is released a decision must be made as to the drilling of a confirmation well.

Several methods have been worked out to predict equilibrium temperatures; all are based on (1) rebound following the physical law of logarithmic decay, and (2) rebound being by conductive processes. Perhaps the most sophisticated method is one worked out by Albright (1975); unfortunately, the amount of data required to apply the method is not generated in the course of normal drilling operations. Since temperature rebound follows the same logarithmic decay law as does pressure buildup following a reservoir flow test, a Horner plot is suggested as a graphical method of predicting equilibrium temperature, and the Horner plot is a commonly used device. Its mathematical expression in several forms is given as the Lachenbruch-Brewer equations (1959, p. 79) which are applied herein.

The purpose of this brief report is to provide an abbreviated explanation of the physical principles of temperature rebound and provide a convenient plotting method similar to the Horner plot in order to standardize temperature prediction in Geothermal Operations. It has the further purpose of outlining methods to determine an approximate thermal conductivity value for reservoir rocks and rebound times after drilling from the nature of the rebound curve.

During the drilling of geothermal wells the drilling fluids serve the additional purpose of cooling the rocks adjacent to the bore in order to prolong the life of bits and drill string, and to control potential blowouts. The temperature of the fluid changes with cooling variations of the mud on the surface and with depth as the wallrock temperature changes.

Fluids moving in or out of the borehole via fractures transfer heat by nonconductive processes; and, if such fluid movements involve large volumes at or near the depth where equilibrium temperature is to be predicted, the conductive methods treated here are not applicable. If the well tries to produce, however, a relatively short flow test makes possible an approximate determination of reservoir temperature.

Line Source Solution

The well bore closely approximates a line source heat sink during drilling operations. All subsequent temperature measurements are made on this line, usually during multiple log runs.

Assuming the rock intersected by the bore is homogeneous, heat (cooling) of strength Q, applied instantaneously along the axial line at time $t = t_o$, produces rebound according to:

$$T_f - T_n = \frac{Q}{4\pi K} \frac{1}{t_n - t_o} \qquad t_n > t_o \tag{1}$$

where T_f is final equilibrium temperature, T_n is temperature measured at some time after t_o, and K is thermal conductivity. The quantity t is time since the drill bit first reached the depth in question.

But cooling at a given depth is applied not instantaneously but over a period of time, usually irregularly. Rebound is obtained by

$$T_f - T_n = \frac{Q}{4\pi K} \int_o^s \frac{q(\Delta t)}{t_n - \Delta t} dt \qquad t > s \tag{2}$$

where q(t) is a continuous source in units of heat per unit time per unit depth and s is the time elapsed since the bit reached the depth in question to the time drilling (circulation) ceased. Ordinarily s, like t, is different for each depth.

If q(t) is a constant, or is averaged and applied during time s, that is, $q(t) = \bar{q}s$, then the solution of the integral is

$$T_f - T_n = \frac{\bar{q}s}{4\pi K} \ln \frac{t_n}{t_n - s} \qquad t > s \tag{3}$$

Graphical solution

The last equation forms the basis for the graphical solution of final temperature (Fig. 1); it was solved repeatedly to produce the graph. In practice the T_n's, T_1, T_2, T_3····, are plotted against the log term, to graphically solve for the final temperature, T_f.

After the first maximum borehole temperature, T_1 is obtained, from the first logging run, a convenient temperature value is chosen and labeled on the bottom line. This value, in general, is a multiple of ten next below T_1. After this datum value is chosen, the ordinate is labeled at the same scale as the upper part of the graph. Each temperature is plotted against $\ln t_n/t_n - s$ as it becomes available with each logging run.

The last tool to go into the hole is ordinarily a continuous temperature log. This run provides an opportunity to determine the depth of the maximum temperature, which is not always at T.D. The same maximum reading thermometers, clamped in turn onto the Schlumberger logging line, should be placed onto the wire line of the temperature sonde in order to check the correlation between the two tools. The maximum reading thermometers, usually two or three run simultaneously, should be clamped onto the Agnew and Sweet wire line 30 ft. above the bottom of the tool. This is the approximate average height of the thermometers above the base of the Schlumberger sondes.

After all the temperatures are plotted, the best fit straight line is passed through the points. When the fit is difficult, the last few data obtained should be given more weight. This is because the short term fluctuations of temperature during drilling damp out early and the later measurements better follow the average heat sink temperatures assumed in construction of the graph. The line projected through the plots, and perhaps even some of the control points may plot into the upper part of the graph. This is of no consequence.

The intersection of the line with the $\ln t_n/t_n - s = 0$ ordinate gives the predicted final temperature, T_f.

In the event tables or a calculator are not available for calculating the natural logarithms, the ratio t/s, can be worked out by longhand and plotted using the logarithmic scale across the top of the graph. Plotting with a logarithmic scale is a little less accurate, however.

The graph is designed for two further operations. With a parallel ruler the best fit line is moved into the upper part of graph to the position at which it passes through the "origin" of the family of guidelines, at the left side of the graph. The interpolated value of the guideline that coincides with the plotted line is then determined. This guideline value is the ratio, $\bar{q}s/K$, in equation (3). If either value of the quotient is known, the other can be determined. This also can be solved graphically with the small graph in the upper right corner.

Knowledge of the term $\bar{q}s$ is of no particular intrinsic value, but thermal conductivity, K, is. No convenient method for determining $\bar{q}s$ can be outlined at this time; however, the duration of the disturbance, s, is known and it is possible that $\bar{q}$ can be estimated empirically from

flow line temperatures or some other indicator, but further work to demonstrate this is required. When K can be determined, the information will aid in interpreting other temperature data on the prospect and will make possible a calculation of rebound time.

Two dashed lines pass through the larger graph, one labeled 5° and the other 1°. These lines indicate the times when the well has rebounded to within 5°C and 1°C respectively of the final equilibrium temperature. These specific rebound times can be determined by picking the ln t_n/t_n- s value where the plotted line intersects the 5° or 1° line, whichever is of interest, say the 5° line. With this ln t_n/t_n- s value, enter the graph in the lower right corner through the bottom scale and move vertically up to intersection with the appropriate s line, the duration of the temperature disturbance. Moving to the left scale gives the rebound time, t - s, in hours, and moving to the right scale gives t - s in days.

Knowledge of rebound time to temperatures within 5° and 1° of complete rebound is helpful in planning followup temperature surveys. Without this knowledge more surveys may be run than are necessary, and each cost between $1000 and $2000.

Example

Roosevelt Hot Springs #9 - 1 data from Utah are tabulated and plotted in figure 2 to illustrate the method. The drilling history indicates that the duration of circulation, s, at a depth of 1518 m., prior to taking temperature measurements, was 15 hours, distributed in drilling, coring and well conditioning. The scatter about the best fit straight line is not large, and probably reflects, in the main, small inaccuracies in time and temperature measurements.

The line projects to 186.3°C at ln t_n/t_n- s = 0. After the logging runs that produced these temperature readings, Well #9 - 1 was deepened to 2096 m., reaching this T.D. on April 8, 1975. Approximately three months later, on July 14, 1975, a continuous temperature log was run to T.D. This log shows a temperature of 192.8°C at depth 1518 m. Thus, this prediction scheme predicted a final temperature below steady state equilibrium temperature by a minimum of 6.5°C.

Moving the best fit line into the upper part of the diagram, using parallel rulers, to the position at which it passes through the "origin" of the family of curves, the interpolated value for $\bar{q}s/K$ is 508. Making use of the diagram in the upper right corner, the quantity $\bar{q}s$ is 508 when K = 1, 254 when K = 2, 169 when K = 3, and so on. The units of $\bar{q}$ are calories per unit depth per second

times 3.6×10^3. Flow line temperature during drilling and coring at this depth averaged 50°C, but they are unknown during circulation to condition the hole. A core was obtained a few feet below the point of temperature measurements; namely, in the interval 1524-1525.5m. Thermal conductivity measurements on recovered granodiorite produced a K value of 4.77. In this case, where K and s are known, $\bar{q}$ is restrained at 107. When enough data of these types are available, it may be possible to determine a reasonable value for thermal conductivity by estimating $\bar{q}$ through flow line temperatures.

It is important to know how far from complete rebound the well was on July 14, 97 days after circulation ceased, when the last temperatures were measured. The best answer can only be an approximation in this case because the well was deepened after the temperature measurements were made, and thus s changed. Using the data available to complete the example, however, the best fit line, with $\bar{q}s/K = 508$, intersects the 5° and 1° dashed lines at $\ln t_n/t_n - s = .13$, and $= .03$, respectively. Entering the graph in the lower right corner with these values the well was within 5°C of final temperature in about 5 days, and within 1° in about 22 days. Thus, the temperature on the run of July 14 was probably less than 1°C from equilibrium.

References Cited

Albright, J. N., 1975, A new and more accurate method for the direct measurement of earth temperature gradients in deep boreholes: Proc., Second U. N. Symposium on Development and Use of Geothermal Resources, San Francisco, p. 847 - 851

Lachenbruch, A. H. and Brewer, M. C., 1959, Dissipation of the temperature effect of drilling a well in Arctic Alaska: U. S. Geothermal Survey Bull. 1083 - C, p. 73 - 109.

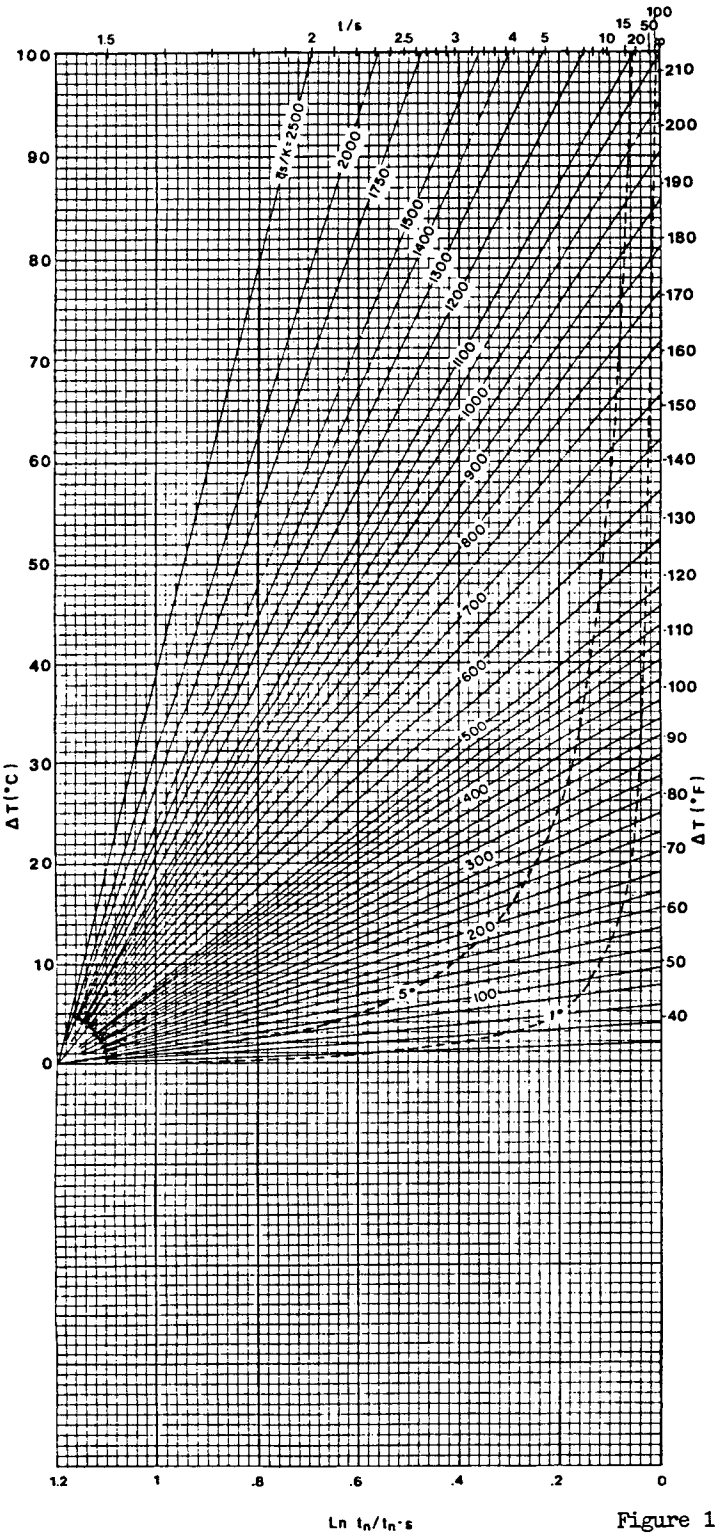

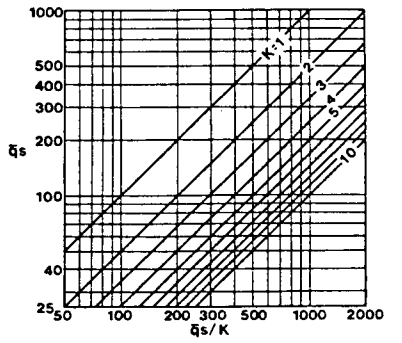

t T Ln tn/tn-s

s
t1
t2
t3
t4
t5
t6
t7

Well Field
Co. St.
Date Int.
Comments

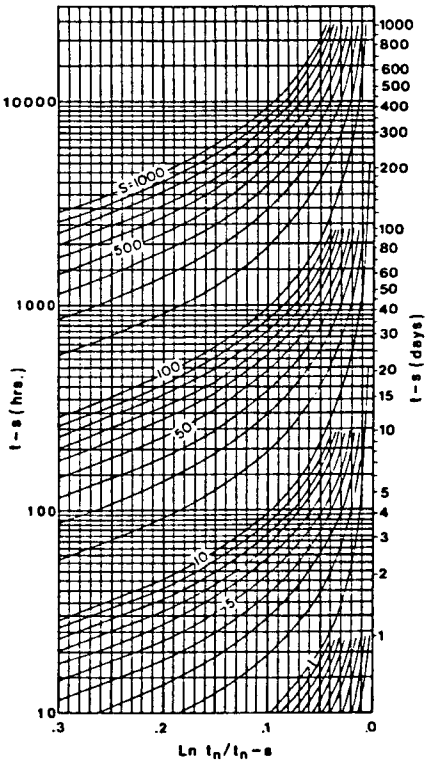

Figure 1

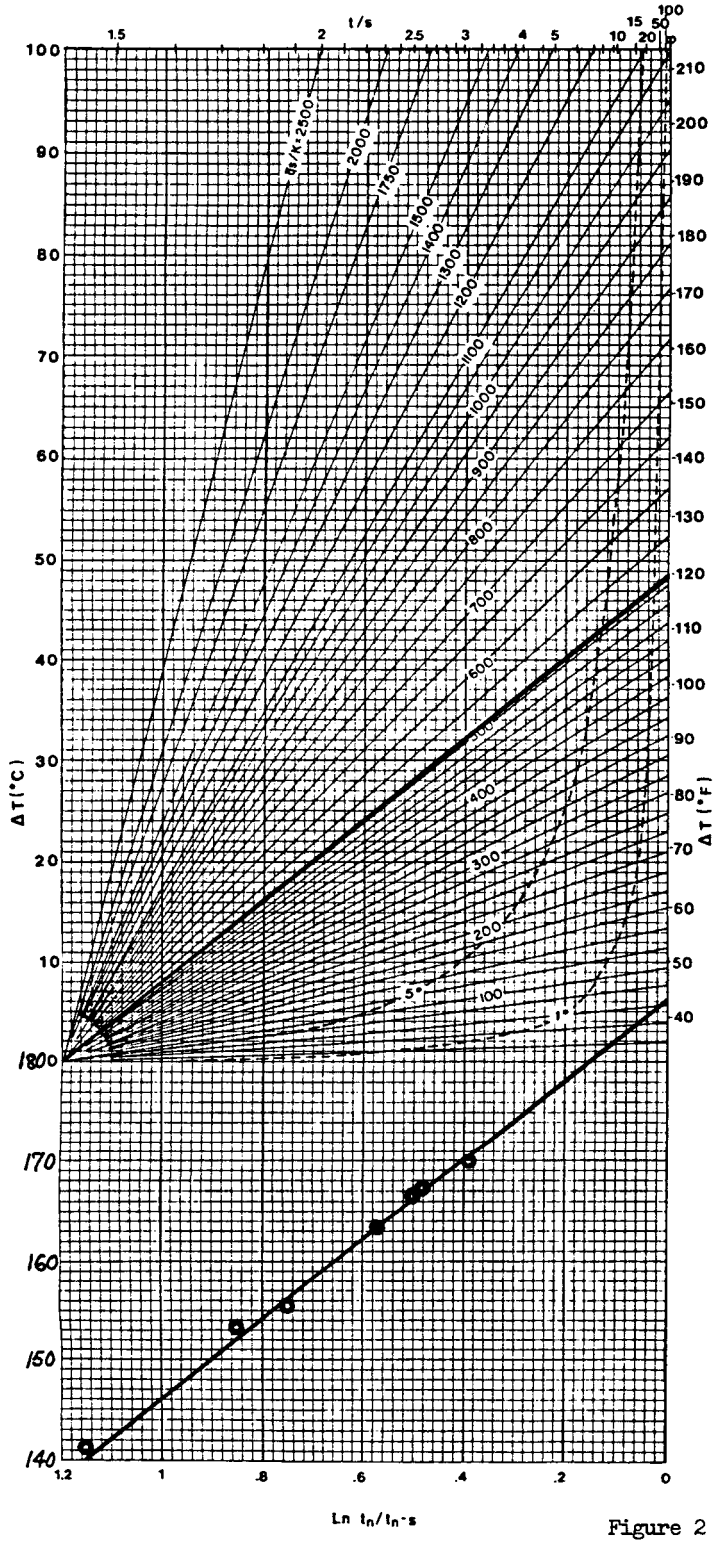

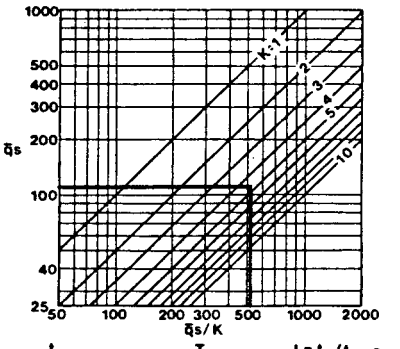

	t	T	Ln tn/tn-s
s	15.00		
t_1	22.00	141.11	1.15
t_2	26.25	153.33	.85
t_3	28.50	155.56	.75
t_4	34.50	163.33	.57
t_5	38.33	166.67	.50
t_6	39.60	167.22	.48
t_7	46.00	170.00	.39

Well #9-1 Field Roosevelt
Co. Beaver St. Utah
Date 8/25/77 Int. GWC.
Comments Depth of measurements - 1518 m. Well drilled to 2096 m TD on 4/8/75. Temp. at 1518 m on 7/14/75 was 192.8 °C.

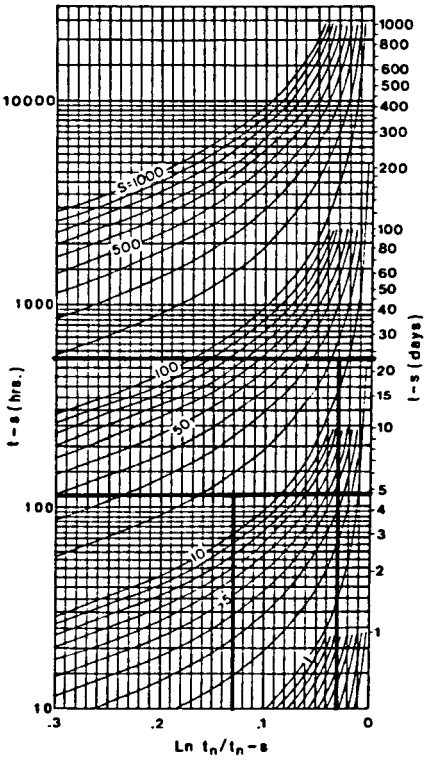

Figure 2

MOMOTOMBO GEOTHERMAL RESERVOIR

H. Dykstra* and R. H. Adams**

INTRODUCTION

Flow tests and pressure measurements were made on a group of five wells in the Momotombo geothermal reservoir, Nicaragua. The purpose of these tests was to evaluate the hot water reservoir, to determine well interference effects, to determine reservoir boundary conditions and to obtain mass flow rates and enthalpy.

Static bottom hole pressures were measured on three wells and bottom hole flowing pressures and shut-in buildup pressures were measured on one of the wells. A Hewlett-Packard quartz crystal pressure gauge was used in connection with a Sperry Sun expandable chamber hung on steel capillary tubing to measure downhole pressure.

Flow tests were made on all five wells. Four wells were flowed through a horizontal discharge pipe. One well was flowed through a vertical discharge pipe.

GEOLOGY

The dominant feature in the area is the dormant volcano, Momotombo. It is the heat source for the geothermal system. The aquifer for the system is unknown but is probably deep seated and large.

The deepest penetration in the field has been to 7,384 feet. At total depth, the formations continued to be older pyroclastics. Andesitic-basaltic pyroclastic deposits and lavas predominate throughout the column. The area of geothermal development is part of a much older volcanic structure. A north-south cross section through the field shows correlative formations which are relatively flat with minor dipping that increases with depth to the north toward the center of the volcano.

The occurrence of geothermal fluids is not associated with a structure of closure. See Figure 1. The conduits containing geothermal fluids are a series of northwest/southeast-trending faults which connect the developed area to the aquifer. These faults are believed to be numerous and to form a band, or faulted zone. The occurrence of a fault conduit is generally indicated during drilling by a partial or total loss of drilling fluid. Subsequent to completion of the well, these faulted sections can be recognized by anomalies of high-temperature.

Following the development of the field, interference tests were made which suggested some interference between certain wells, little interference between

*Petroleum Engineering Consultant, Concord, California 94520
**California Energy Company Santa Rosa, California 95402

other wells, and no interference between other wells. This suggests a series of fault planes, or conduits, with pressure and fluid connection in some instances and no connection in others. It is believed that all fluids come from the same aquifer but travel by different paths. Because of this common origin, the reservoir appears to have a common vapor-fluid interface, or flash point, recognized in MT-3 and MT-12 as being in the interval between 748 feet and 796 feet subsea.

The effects of rainfall on bottom-hole pressures are also pertinent to the geology of this area. This phenomenon was apparent following rainfall from June 1 through June 3, 1977, and suggests an "open" reservoir without structural closure. The closure for the system becomes the cooled, hydrostatic-fluid column at distance from the heat mass.

STATIC PRESSURES

Static bottom-hole pressures for MT-2 and MT-3 are shown in Figures 2 and 3 respectively. As can be seen the pressures show considerable fluctuation within any 24 hour period as well as from day to day with MT-2 showing considerably greater fluctuation than MT-3.

The reason for the difference in behavior is that the wellbore of MT-2 is filled with liquid to the surface whereas the wellbore of MT-3 contains steam to a depth that is below the pressure sensing device. Thus MT-2 can be considered a "hard" well; that is, the fluid in the wellbore has a low compressibility so that pressure pulses can be transmitted into the wellbore with a negligible quantity of fluid moving into the wellbore. On the other hand, MT-3 can be considered a "soft" well; that is, the fluid in the wellbore has a high compressibility so that a considerable amount of fluid would have to move into the wellbore in order to increase the pressure. In effect, the steam in the wellbore acts to dampen rapid pressure changes.

In order to get a better picture of pressure versus time, a daily average pressure and its standard deviation were calculated for 48 values at one-half hour intervals. A plot of the daily average pressure for MT-2, MT-3, and MT-9 prior to the time they were put on production is shown in Figure 4. The standard deviation range is plotted as a vertical line. Here the variation in standard deviation can be readily seen.

The dates that MT-9, MT-12, and MT-17 were opened is also shown. The pressure trend on MT-3 does not indicate an interference effect. The fluctuations in pressure on MT-2 are such that an interference effect cannot be determined. The distance between MT-2 and its nearest producer, MT-12, is 610 feet. The distance between MT-3 and its nearest producer, MT-9, is 1040 feet.

WELL FLOW CHARACTERISTICS

For the four wells that were flowed through horizontal discharge pipes, wellhead pressures, upstream and downstream orifice pressures, and lip pressures were measured. For the well that flowed through a vertical discharge pipe only, wellhead and lip pressures were measured. The method of James (1962, 1965) was used to calculate flow rates.

Flow characteristics of MT-2 are shown in Figure 5. The well required a little less than two weeks to stabilize after which wellhead pressure, mass flow rate, and enthalpy remained essentially constant within the accuracy of the data. The wellhead pressure stabilized at 142 psi and the mass flow rate at 520 kph. The enthalpy stabilized at an average of 545 Btu/lb. This enthalpy is greater than that of water at a maximum temperature in this well and indicates flow of steam from the steam cap into the wellbore.

The flow tests on the five wells indicate that from one to four weeks are required for the wells to stabilize. The stabilized rate averaged about one-half of the maximum flow rate exhibited in the first few hours of production. For MT-2, for example, the stabilized rate was almost exactly one-half the rate calculated from the data obtained shortly after the well was opened.

The time that MT-9 was shut in is also shown in Figure 5. Here, no effect can be seen on the wellhead pressure, for example, again indicating no interference between MT-2 and MT-9.

DRAWDOWN AND BUILDUP ON MT-9

The drawdown behavior of MT-9 is shown in Figure 6. For the first 3 days, or until MT-12 was placed on production, the pressure, except for the variations within a 24-hour period, decreased linearly with the logarithm of time. After MT-17 was placed on production, the pressure decreased linearly with time at a rate of one psi per day for the next 23 days, at which time the well was shut-in. This constant rate of pressure decrease seems to suggest that pseudo steady state behavior had been reached by this well and it is producing from a limited source. As will be shown later this conclusion is at variance with the conclusion based on other data that the Momotombo reservoir is a large resource.

The pressure buildup on MT-9 is shown in Figure 7. The initial rise in pressure was very rapid, increasing from 423 psi to 480 psi in 30 minutes. Thereafter, the pressure rose much more slowly, showing an average daily increase of about one psi per day for five days. After MT-2, MT-12 and MT-17 were shut-in, the pressure increased about two psi per day to an average of 498 psi on 28 July, the last full day of pressure measurements. Pressures measured the last day of the test program fell in the pressure range that existed prior to the start of production as shown in Figure 7. It appears highly likely that the average daily pressure would reach the 510 to 511 psi that existed prior to the start of the flow test on MT-9. This would then indicate essentially complete recharge.

Wellhead pressures were also measured on MT-3 during 16 days of production and during the subsequent shut-in. At the end of the test period, the wellhead pressure had built up to essentially the same value that existed prior to the start of production, again indicating essentially complete recharge.

In the discussion of the drawdown of MT-9, it was mentioned that the linear decline in pressure seemed to indicate pseudo steady state. A more likely explanation in the light of data showing almost complete recharge is that the production rate of MT-9 exceeded the ability of the system to supply fluid to MT-9. If so, then a lower rate or a longer time should result in the flowing pressure of MT-9 leveling off at a pressure consistent with the ability of the system to supply fluid.

REFERENCES

1. James, Russell; "Steam-Water Critical Flow Through Pipes"; Proc. Inst. Mech. Engrs. (1962) 76 No. 26, 741

2. James, Russell; "Metering of Steam-Water Two Phase Flow by Shrp Edged Orifices"; Proc. Inst. of Mech. Engrs. (1965-66) 180 Part 2, 549

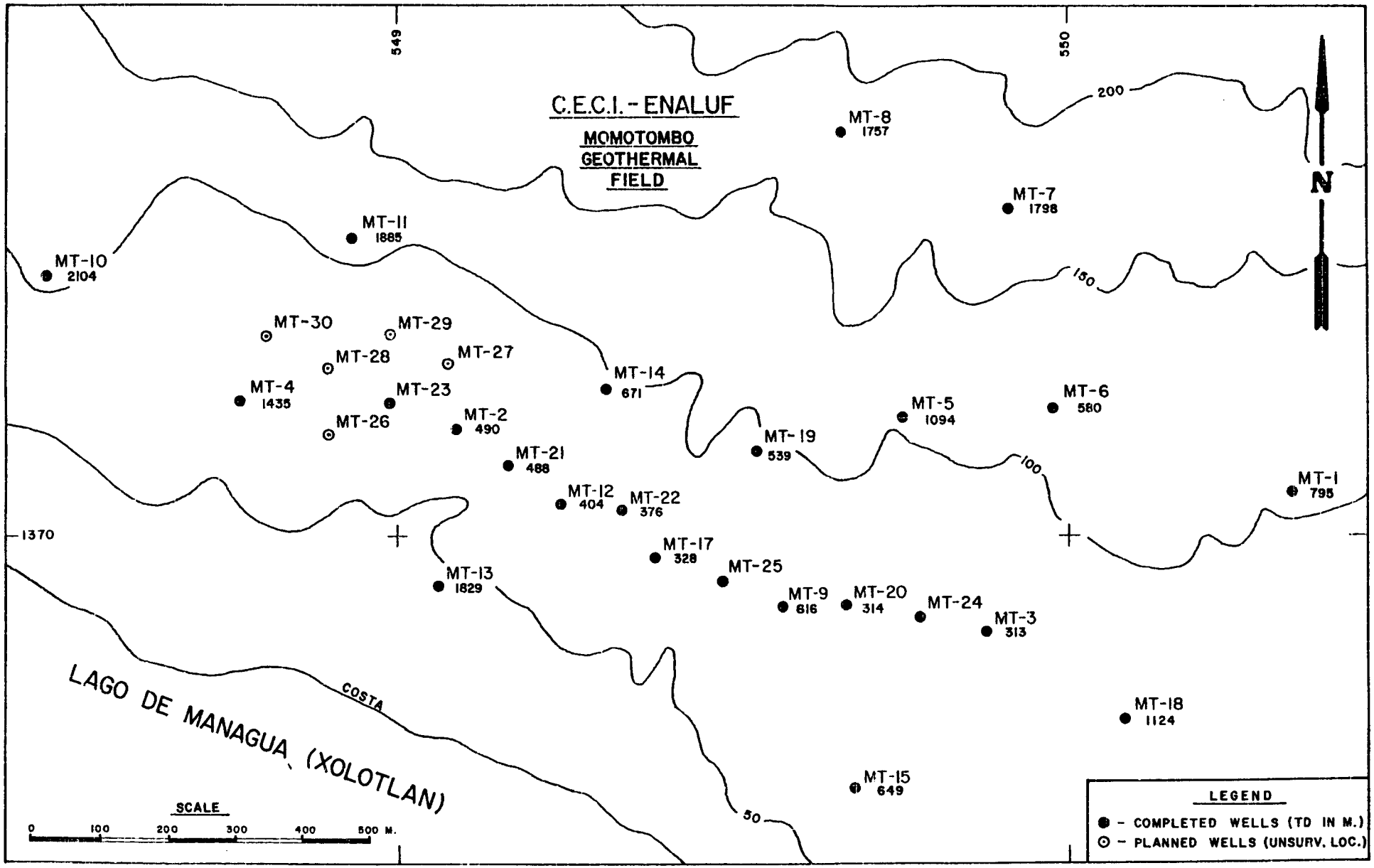
C.E.C.I. - ENALUF
MOMOTOMBO GEOTHERMAL FIELD
549
550
200
150
100
50
1370
N
MT-8 1757
MT-7 1798
MT-11 1885
MT-10 2104
MT-30
MT-29
MT-28
MT-27
MT-14 671
MT-4 1435
MT-23
MT-26
MT-2 490
MT-5 1094
MT-6 580
MT-19 539
MT-21 488
MT-12 404
MT-22 376
MT-1 795
MT-17 328
MT-25
MT-13 1829
MT-9 616
MT-20 314
MT-24
MT-3 313
MT-18 1124
MT-15 649
LAGO DE MANAGUA (XOLOTLAN)
COSTA
SCALE
0 100 200 300 400 500 M.
LEGEND
● - COMPLETED WELLS (TD IN M.)
⊙ - PLANNED WELLS (UNSURV. LOC.)

FIGURE 1

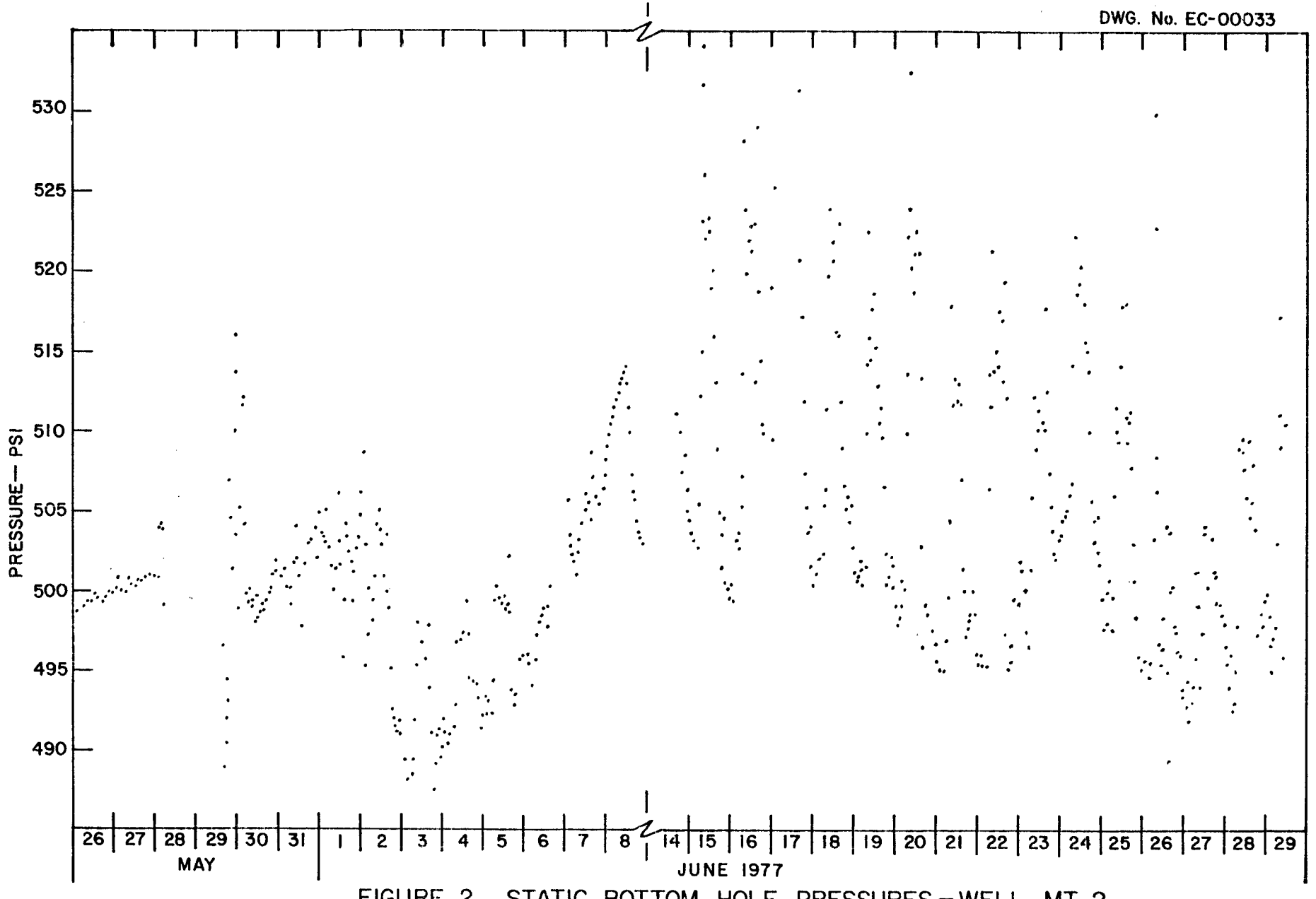

FIGURE 2. STATIC BOTTOM HOLE PRESSURES – WELL MT-2.

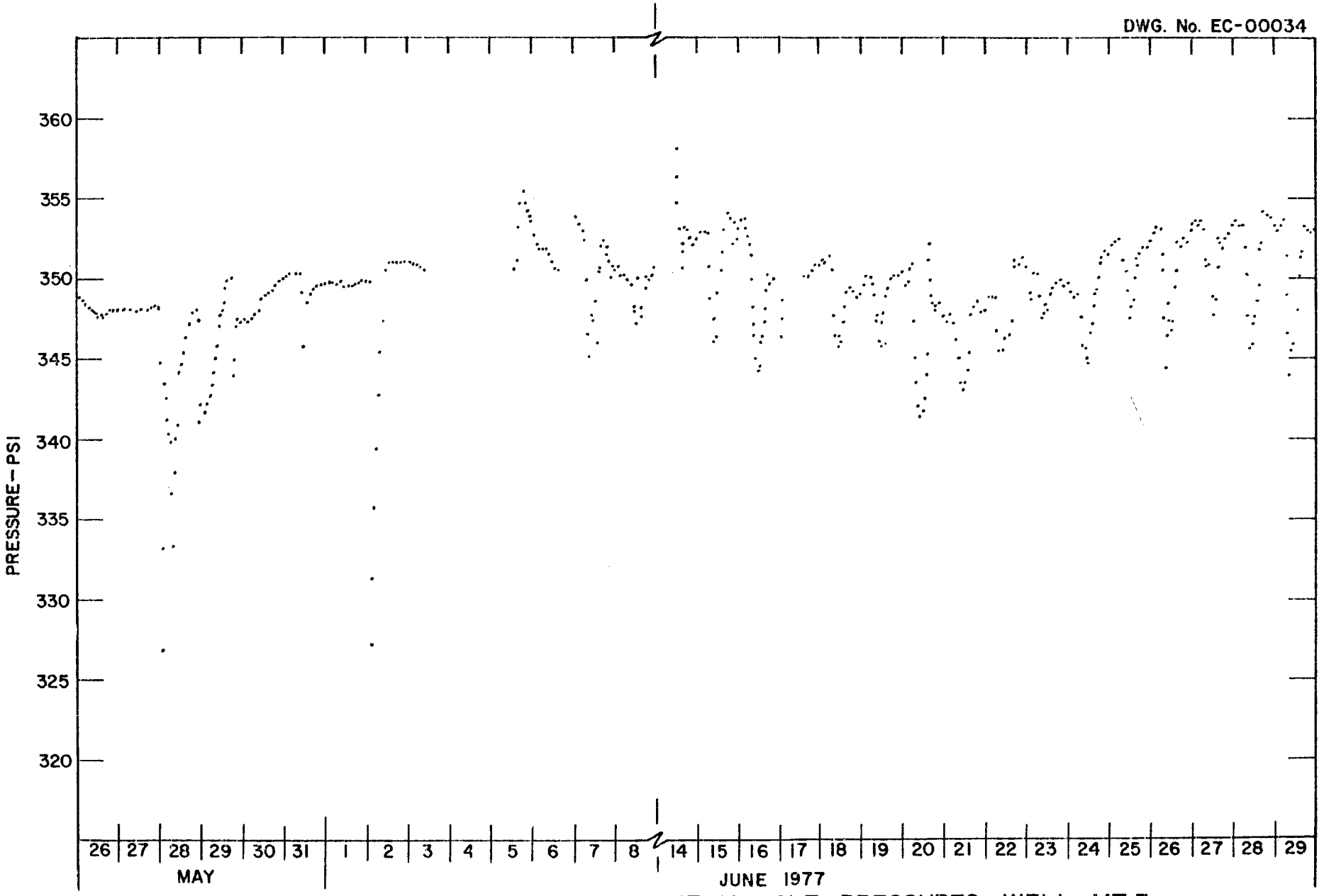

FIGURE 3. STATIC BOTTOM HOLE PRESSURES - WELL MT-3.

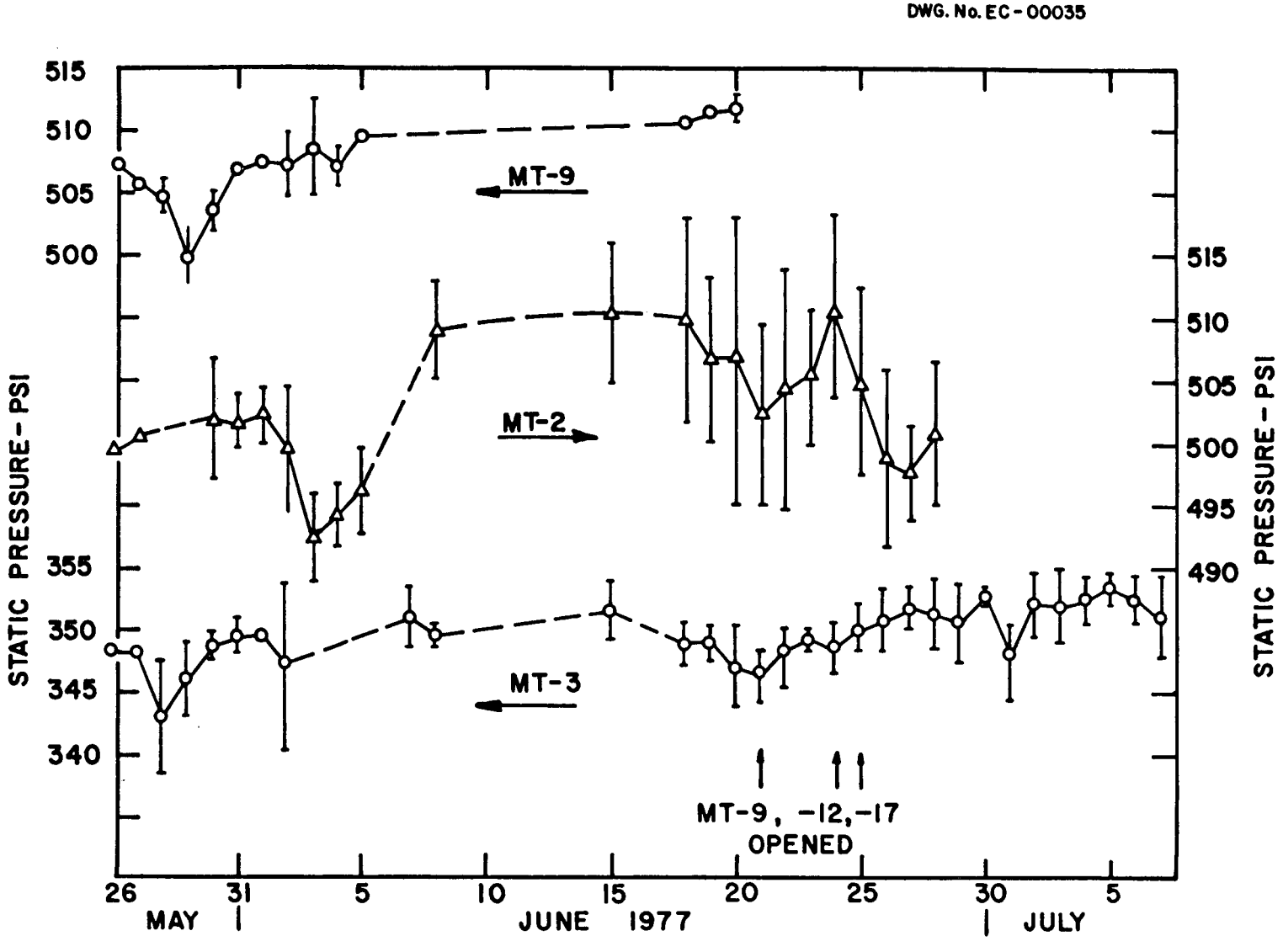

FIGURE 4. AVERAGE DAILY STATIC BOTTOM HOLE PRESSURES

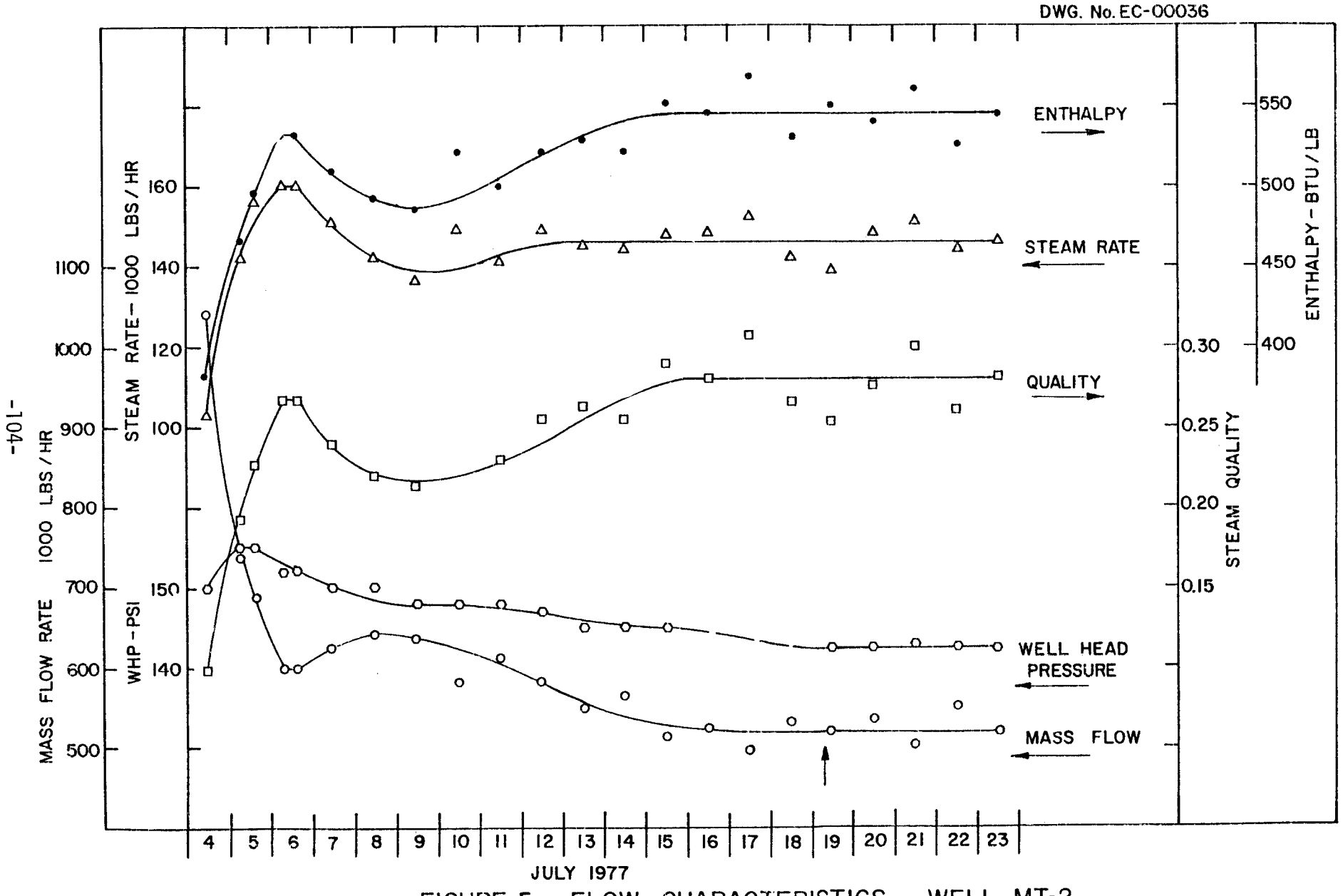

FIGURE 5. FLOW CHARACTERISTICS – WELL MT-2

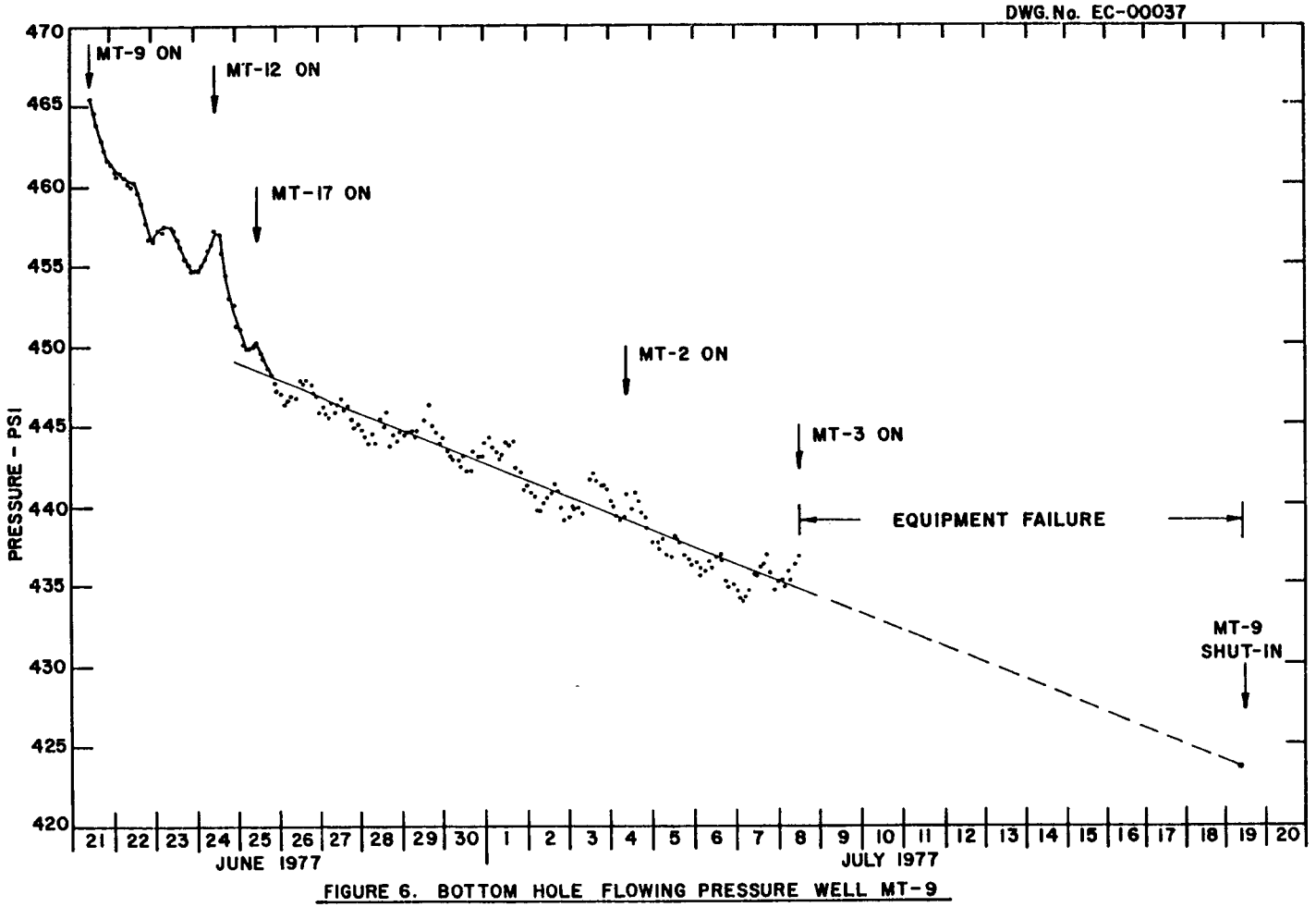

FIGURE 6. BOTTOM HOLE FLOWING PRESSURE WELL MT-9

DWG. No. EC-00038

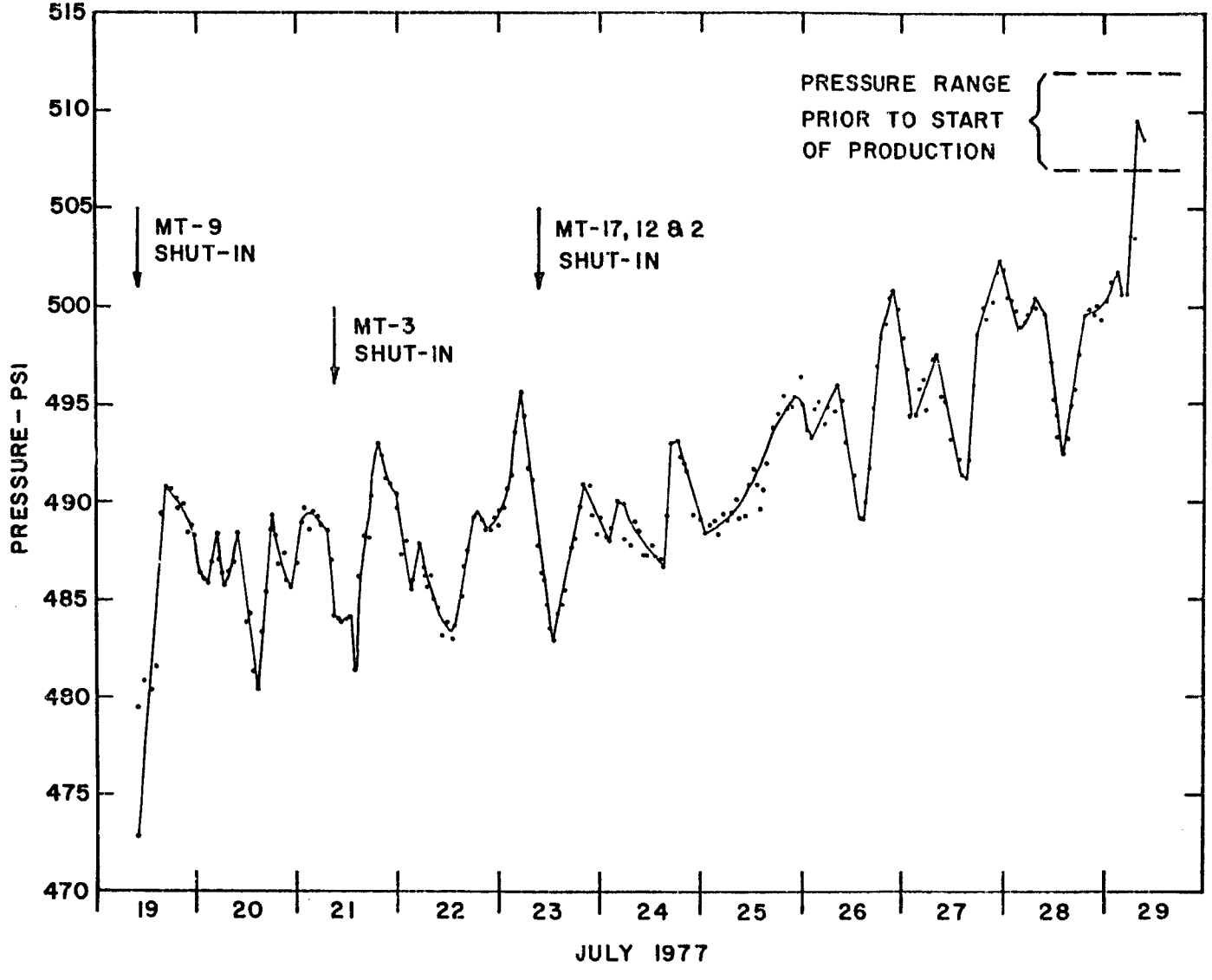

FIGURE 7. BOTTOM HOLE SHUT-IN PRESSURES WELL MT-9

MODELING THE HEBER GEOTHERMAL RESERVOIR

Erdal O. Tansev
Chevron Resources Company
P.O. Box 6854
San Francisco, CA 94119

and

Mel L. Wasserman
Chevron Oil Field Research Company
P.O. Box 446
La Habra, CA 90631

Abstract

In this paper we briefly describe the lithology, temperature, and pressure of the Heber Geothermal Reservoir. This we base on the extensive data gathered in the past few years through well drilling and testing. We then describe our three-dimensional, heterogeneous, single phase water flow simulator, including the equations solved, and the assumptions made. We present several applications of the numerical simulator, in predicting the reservoir behavior with time. Conclusions based on an analysis of simulator results are finally presented.

Introduction

The Heber Geothermal Anomaly, located in the Imperial Valley of California, could be the first commercial hot water power generation project in the United States. Chevron Resources Company will operate the proposed Heber Unit. Currently, plans are for developing a nearly circular area of 7500 acres, with each plant increment representing a pie-shaped segment. Producers will be placed at the temperature high which is at the center. The processed fluid will be reinjected at the periphery of the reservoir. Wells will be drilled from centrally located surface islands, most of them being directionally drilled. Production rates at Heber will ultimately reach several millions of barrels per day. This requires large surface facilities and large well equipment. Revenues cannot be realized until a power plant is constructed. Due to large initial investment, an accurate reservoir performance prediction becomes an important factor. The predictions in this paper are limited by the accuracy of the data collected and analyzed, and by our modeling assumptions.

Reservoir Description

The Heber Geothermal Anomaly is a circular shaped, moderate temperature, low salinity, water dominant reservoir. It is characterized by high heat flow, low electrical resistivity and high gravity. It is part of the Colorado River deltaic environment, consisting of interbedded sandstones and shales. Shales are thick and predominant from the surface to 2000 feet. Sand layers become predominant below 2000 feet, where shale layers become thinner. At 8000 to 10,000 feet sands are predominant with minor shale breaks. A few faults have been identified, others are probably present; however, any occurring in the predominantly sandy section would not be significant barriers to fluid flow. Reservoir

continuity of several sand layers have been confirmed by interference tests. Pressure drawdown and buildup tests have indicated a radius of investigation greater than 20,000 feet.

Porosity and horizontal permeability of the sand layers at Heber were determined by using available density logs and core analysis information. Good correlations were found between density log porosity and core porosity, also between core porosity and core permeability. Permeability of each sand was calculated from the latter correlation and the log derived porosity values. It was possible to correlate these permeabilities to permeabilities computed from flow test analysis. In general, sandstone layers demonstrated decreasing permeability and porosity with depth.

The Heber Geothermal Anomaly has a mushroom-shaped temperature profile. The maximum temperature at the center of the field is around 375°F. Conductive heat flow at shallow depths could be deduced from high temperature gradients and the presence of thick impermeable shales. Below this depth heat flow is naturally convective, as temperature gradients become small and sandstones dominate. To a reference temperature of 200°F, the heat in place under approximately 7500 acres, and between 2000 to 6000 feet is 5.4 quadrillion (10^{15}) BTU's. Heber could be classified as a normal pressured reservoir with measured static gradients of 0.42 psi/foot.

Reservoir Model

To predict Heber's performance under various development schemes, a three-dimensional, radial, heterogeneous, and single phase water flow simulator was used. The simulator basically solves the mass and the energy balances. The equation of continuity, expressing conservation of mass[1], is:

$$\frac{\partial (\rho_\ell \phi)}{\partial t} = - \nabla \cdot \rho_\ell \underset{\sim}{V}_\ell - Q \qquad \text{.....(1)}$$

where:

ℓ denotes liquid, ρ_ℓ is liquid density (lbm/ft^3), ϕ is porosity, t is time (days), $\nabla \cdot$ is divergence operator (1/ft), Q is mass production or injection. It is a function of position and time (lbm/day ft^3), a positive value denotes production. $\underset{\sim}{V}_\ell$ is the Darcy velocity vector of the fluid (ft/day) and expressed as:

$$\underset{\sim}{V}_\ell = - 6.328 \frac{k}{\mu} (\nabla P - \rho_\ell \underset{\sim}{g}) \qquad \text{.....(2)}$$

where:

k is permeability (Darcy), μ is viscosity (cp), P is pressure (psi), and g is gravitational vector.

The following assumptions were made:

- Porosity is not a function of time; it can, however, be a function of position.
- Viscosity is a function of temperature.
- Liquid density is a function of temperature, but is independent of pressure, making the model "partially compressible". Zero fluid compressibility is satisfactory for single phase water systems.

Next we expand the density derivatives in equation (1).

$$\phi \frac{\partial \rho_\ell}{\partial T} \frac{\partial T}{\partial t} = - \rho_\ell \nabla \cdot \underline{V}_\ell - \underline{V}_\ell \cdot \nabla \rho_\ell - Q \qquad .....(3)$$

where T is temperature. We also assume that the reservoir fluid volumes are locally in balance. Therefore:

$$\nabla \cdot \underline{V}_\ell = -\frac{1}{\rho_\ell} Q \qquad .....(4)$$

Without this assumption we could not let density vary with temperature without using a fully compressible two-phase model. The produced fluid at Heber will be initially at $\simeq 360^{o}F$, the injected water will be at $\simeq 200^{o}F$. In order to maintain a mass balance between production and injection, we assumed that the required mass came across the outer reservoir boundary at a temperature under $200^{o}F$. Thus, we avoided solving - complicated and costly - coupled mass and energy balances.

The equation for conservation of energy[1] is:

$$\frac{\partial}{\partial t} [(\rho C_v)^* T] =$$

$$\phi C_{v_\ell} \frac{\partial}{\partial t} (\rho_\ell T) + (1-\phi)\rho_s C_{v_s} \frac{\partial T}{\partial t} = \nabla \cdot (K^* \nabla T) - C_{v_\ell} \nabla \cdot (\rho_\ell T \underline{V}_\ell) - Q C_{v_\ell} T_N \qquad .....(5)$$

where:

s denotes solid, C_v is specific heat at constant volume (BTU/lbm^{o}F), K is thermal conductivity (BTU/ft day^{o}F), T_N is injection fluid temperature if $Q<0$, T_N is produced fluid temperature if $Q>0$.

The left hand side of equation (5) represents heat accumulation; the terms on the right hand side are respectively, conduction, convection and injection and/or production.

In relation to equation (5) we have defined the following volumetric averages:

$$K^* = \phi K_\ell + (1-\phi) K_s \qquad \text{.....(6)}$$

$$\rho C_v^* = \phi \rho_\ell C_{v_\ell} + (1-\phi) \rho_s C_{v_s}$$

And we made the following assumptions:

- The solid and liquid are locally in thermal equilibrium.
- The viscous dissipation energy losses are negligible.
- Specific heats are independent of pressure, temperature, and position.
- Thermal conductivities are independent of pressure and temperature.
- Rock densities are constant.

Solution - We have independently solved equations (4) and (5). Equation (4) gave us a steady-state solution for pressure, and provided the velocity terms required by the energy balance, equation (5). We conservatively used two temperature time steps per pressure solution. The need for recomputing pressures arose when: (a) the temperature dependent viscosities materially changed, (b) injection and/or production rates changed with declining reservoir temperature in order to maintain constant energy.
Time Dating of Terms - In equation (4) the latest temperatures were used to calculate liquid density and viscosity. In the finite difference form of equation (5), temperature was used implicitly in the conduction term, explicitly in the convection term. Densities were evaluated at start of time steps.
Overburden and Underburden - The first four and the last four layers of the model were used as overburden and underburden with zero fluid permeabilities.
Numerical Dispersion - In an effort to reduce smearing of the temperature profiles, a two-point-upstream approximation[2], for temperature, was used in the convection term. The illustration below shows two cell blocks.

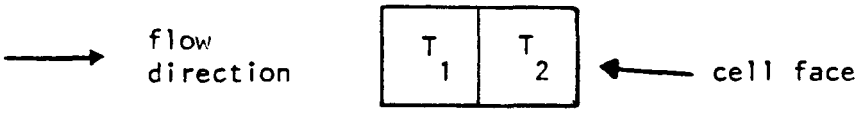

In evaluating the temperature T in the $\rho_\ell T \underset{\sim}{V}_\ell$ term at the cell face, T_1 and T_2 are linearly extrapolated to the cell face. A one-point-upstream approximation uses only T_2 and results in excessive smearing of temperatures. Averaging upstream and downstream values gave temperature oscillations and was discarded.
Flow Splitting - Flow rates for production wells were supplied and were split among the layers according to the product of productivity index and pressure drawdown - difference between current cell and well bore pressure. Injection wells used either fixed pressures or supplied flow rates.

Applications

Based on lithological correlations and production constraints, we defined two zones: zone 1, 2000 to 4000 feet: zone 2, 4000 to 6000 feet. We then subdivided zone 1 into 15 and zone 2 into 13 horizontal sand and shale layers of field-wide averaged thickness. Figure 1 shows the geometry we used. We further divided Heber into 8 areal pies, each pie having 15 rows. Therefore, 1800 cells in zone 1, 1560 cells in zone 2 represented the reservoir. We also made the following assumptions:

- The sand and shale layers themselves are continuous, homogeneous and isotropic.
- The initial temperatures are a function of radial coordinate; they do not vary with vertical coordinate in a given zone.
- The regional northerly ground water movement is small, hence negligible.
- There is no heat recharge from the underburden.

Pies initially were chosen such that their boundaries coincided with stream lines as obtained from the previous streamtube model runs. Most 3-D simulator runs were made assuming no cross flow between the pies.

Figure 2 shows bottom hole temperatures at the producers versus time for 100 megawatts (MW) constant energy production from each zone. Equivalent starting rates are 1.24×10^6 barrels per day per zone. Also shown on this figure are the previous predictions using the streamtube model. The difference in predictions can be explained as follows: the 3-D simulator has the capability of solving a rigorous heat conduction equation, given the actual thicknesses of sand and shale layers. The streamtube model assumed vertical thermal equilibrium between sand and shale in each reservoir layer. It could handle the shales as thin layers of infinite thermal conductivity. The injected fluid, upon contacting these shales, absorbed all their heat. In zone 1, the streamtube model predicted a greater temperature decline and in zone 2 it predicted about the same temperature decline as the 3-D simulator. We think the small difference in zone 2 is due to the use of slightly less shale. The difference in general was due to a better vertical lithological description and a more rigorous heat conduction equation. The 3-D model shows a $30^{\circ}F$ decline in thirty years for both zones.

Figure 3 shows the bottom hole temperature at the producers versus the cumulative water produced. This figure indicates the large volume of water required to produce 100 MW constant energy from each zone.

Figure 4 shows heat recovery from Heber versus bottom hole temperature at the producers. This plot is for two zones combined. The $200^{\circ}F$ temperature is used as a lower bound in determining the heat in place. We have tentatively decided to place the injectors near the $265^{\circ}F$ isotherm. If we use an economic temperature of $320^{\circ}F$ for the power plant, as a cut-off point, Figure 4 shows a recovery of 30% of the heat in place.

Figure 5 shows the predicted average pressure drops between injectors and producers versus time.

The following case studies showed little or no difference in our predictions:

- Combining both zones - simultaneous injection and production in both zones.
- Introducing shale breaks - making 10% of the shale volume permeable to flow.
- Introducing a few "idle pies" - by partitioning the bigger ones, with no injection and production, and allowing crossflow between all pies.

Conclusions

As a result of our modeling studies to date, we conclude the following:

- Heber has 5.4 quadrillion (10^{15}) BTU's in place to a temperature of 200°F. This heat is under approximately 7500 acres within the 265°F isotherm, and between 2000 to 6000 feet.
- 30% of this heat in place is recoverable with respect to the plant economic temperature of 320°F.
- Heber Reservoir between 2000 to 6000 feet alone can support a 250 MW development.
- At Heber, development in general will be more restricted by pressure drops than by temperature decline.
- Economics will govern the power plant type and the development potential at Heber.

References

1. Bird, R. B.; Stewart, W. E.: and Lightfoot, E. N., Transport Phenomena, Wiley, 1960.
2. Todd, M. R.; O'Dell, P. M.: and Hirasaki, G. J., Methods for Increased Accuracy in Numerical Simulators, Society of Petroleum Engineers Journal (December 1972), pp 515-530.

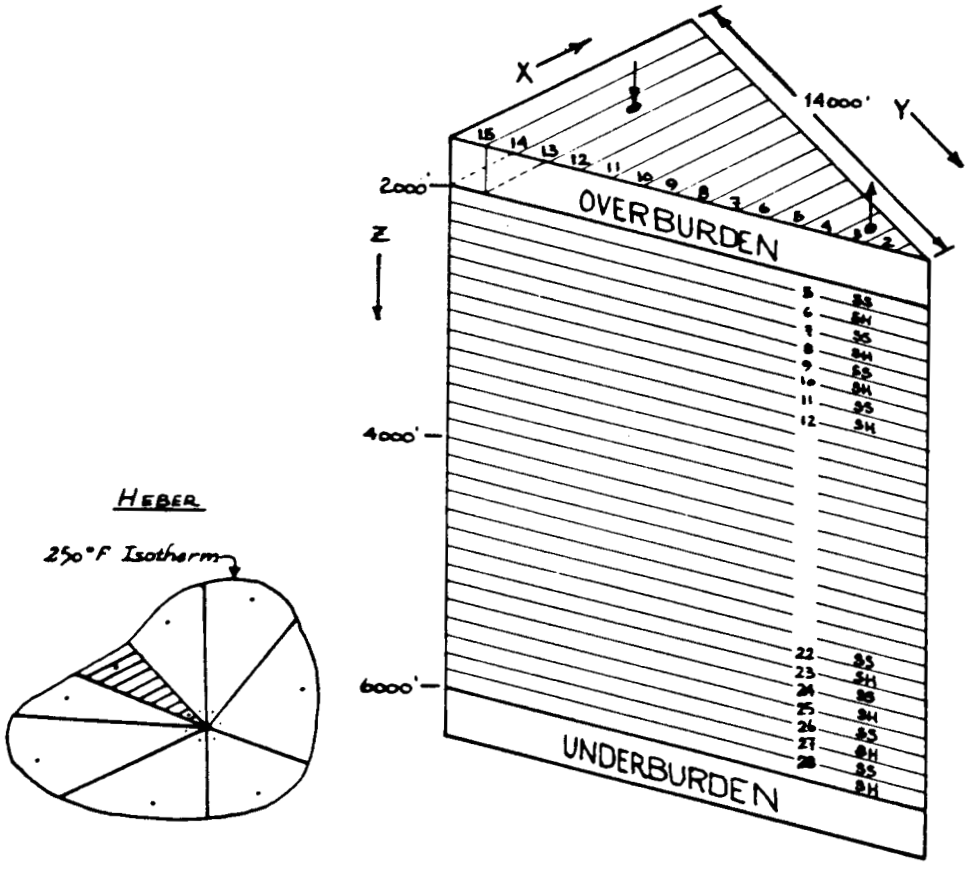

GEOMETRY OF 3-D RESERVOIR MODEL

FIGURE 1

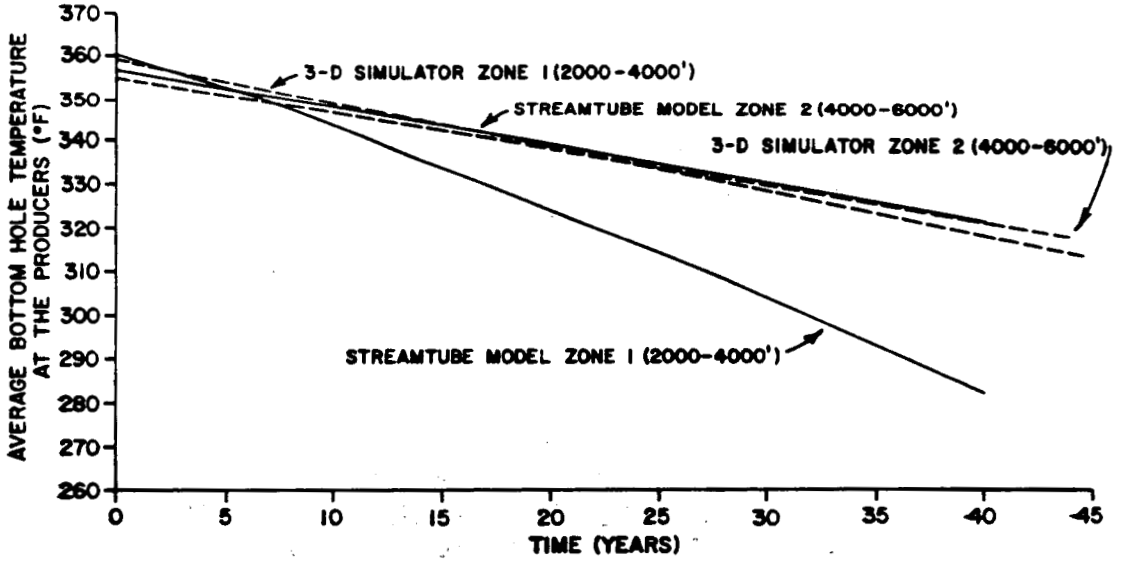

BOTTOM HOLE TEMPERATURE AT THE PRODUCERS VS. TIME FOR 100 MW CONSTANT ENERGY PRODUCTION PER ZONE

FIGURE 2

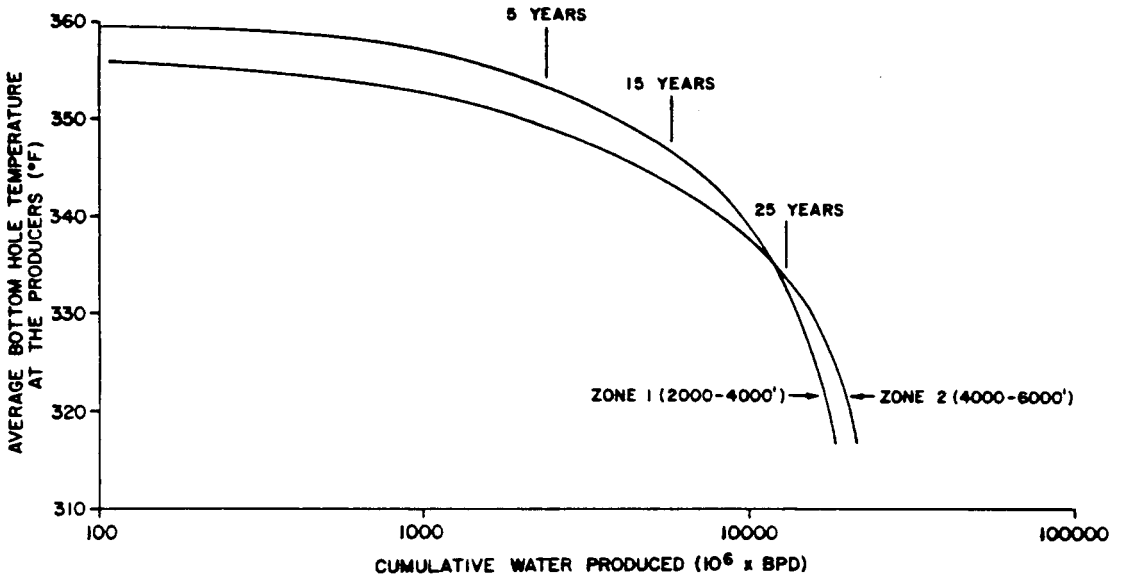

BOTTOM HOLE TEMPERATURE AT THE PRODUCERS VS.
CUMULATIVE PRODUCTION
(100 MW CONSTANT ENERGY FROM EACH ZONE)

FIGURE 3

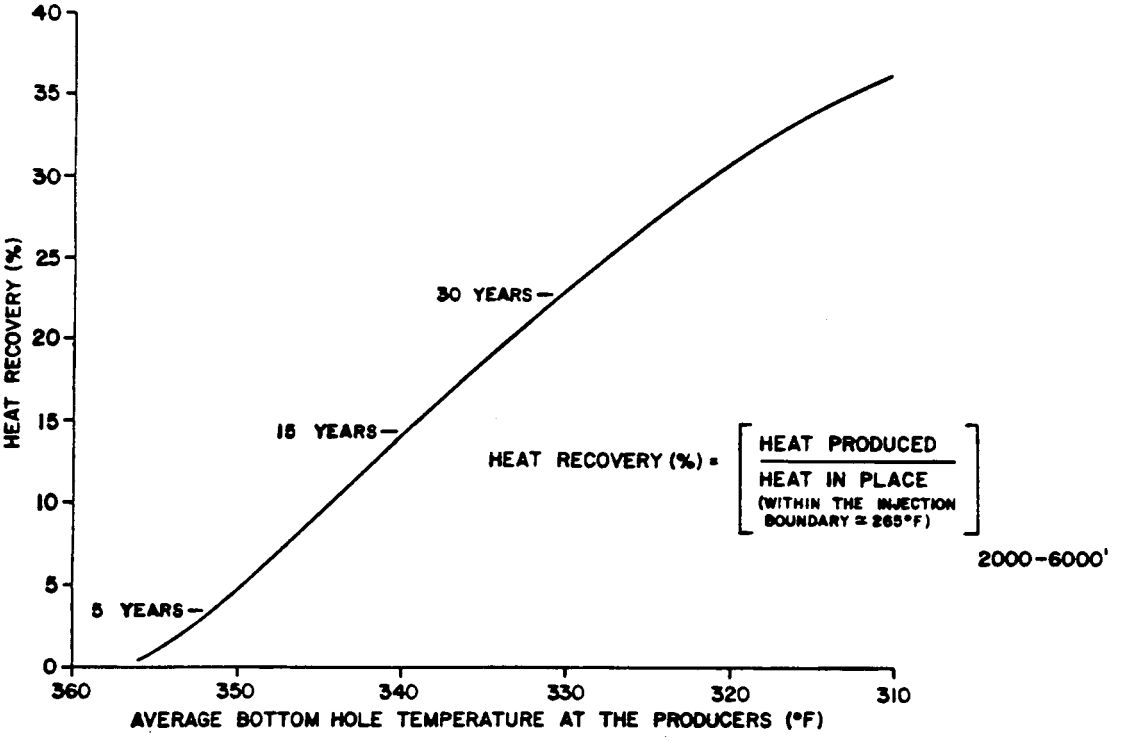

HEAT RECOVERY VS. BOTTOM HOLE TEMPERATURE AT THE PRODUCERS
(200 MW CONSTANT ENERGY FROM TWO ZONES COMBINED)

FIGURE 4

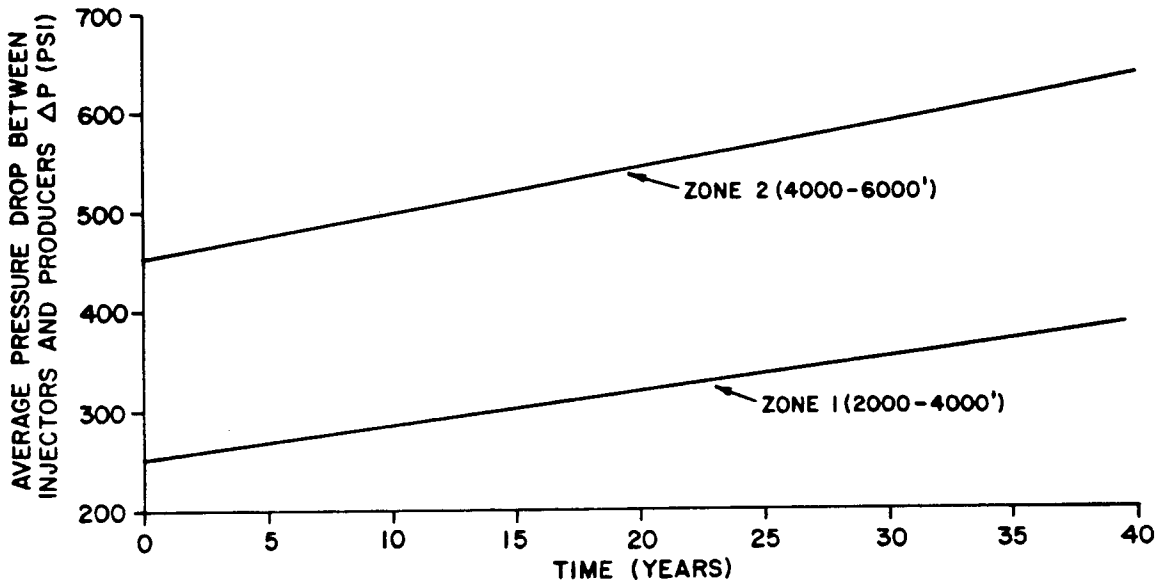

AVERAGE PRESSURE DROP
BETWEEN INJECTORS AND PRODUCERS VS. TIME
(100 MW CONSTANT ENERGY FROM EACH ZONE)

FIGURE 5

RECENT RESULTS FROM TESTS ON THE REPUBLIC GEOTHERMAL WELLS, EAST MESA, CALIFORNIA

by

T.N. Narasimhan, R.C. Schroeder, C.G. Goranson, D.G. McEdwards
Lawrence Berkeley Laboratory, University of California

and

D.A. Campbell, J.H. Barkman
Republic Geothermal Inc., Santa Fe Springs, California

Introduction

The East Mesa KGRA (Known Geothermal Resource Area) is located in the Imperial Valley of Southern California close to the Mexican border. Republic Geothermal Inc. has leased lands in the northern part of the geothermal anomaly and has so far drilled six wells, ranging in depth from 7,400 to 9,100 feet. Current plans of Republic include construction of a 50 MW power plant based on the resource. Crucial to the success of this venture is a proper understanding of the physical properties of the geothermal reservoir tapped by the wells. Towards the south, the geothermal anomaly is being explored and assessed by the U.S. Bureau of Reclamation (5 wells) and the Magma Power Co. (3 wells).

In order to achieve a proper understanding of the resource at East Mesa, Lawrence Berkeley Laboratory collaborated with Republic in conducting a series of three well tests. These included production, injection and interference tests with durations varying from a few days to several weeks and yielded valuable information on reservoir parameters as well as geometry. The purpose of this presentation is to summarize the important findings from the tests. In particular, attention will be restricted to the production-interference tests. The results of injection tests are outside the scope of this presentation.

Geology

The East Mesa resource occurs in a young (tertiary) and geologically active sedimentary basin filled with over 20,000 ft. of sandstones, siltsones and clays. Structurally, the basin appears to be considerably faulted in the East Mesa area and at least three faults varying in trend from NNW to WNW have

been identified (U.S. Bureau of Reclamation, 1974). In addition, growth faults, penecontemporaneous with deposition and trending towards northeast have also been inferred (J.L. Smith, personal communication).

Description of Test Wells

In all, seven wells were involved in the well tests; six of these belong to Republic and one to the U.S. Bureau of Reclamation. The locations of the wells are given in Fig. 1.

REPUBLIC Geothermal Wells, East Mesa, California.

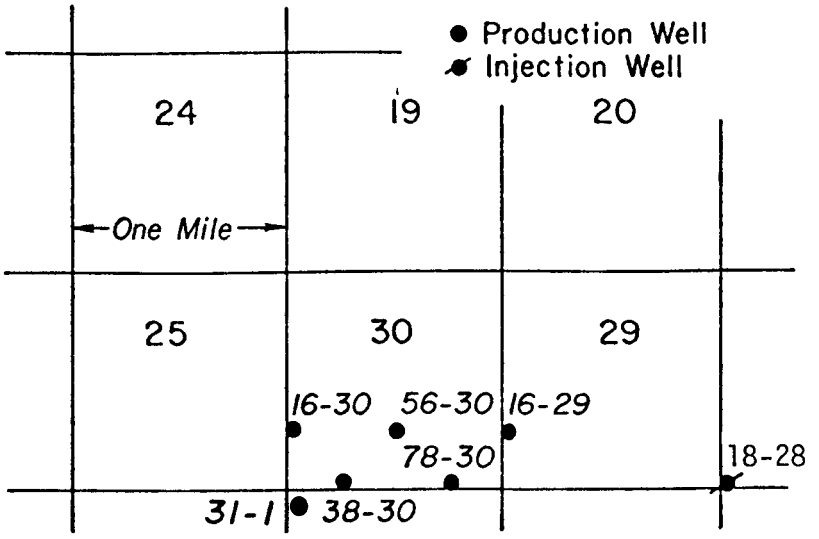

Fig. 1. Republic Geothermal Well Tests: Location Map

Two of these 38-30 and 16-29 were alternately used as production wells and one, 18-28 was used for disposal of the produced waters by reinjection. The rest of the wells were used as non-producing observation wells. A brief description of the wells is given in Table 1.

Table 1: Description of Republic Geothermal Wells, East Mesa, California

Well	Total Depth ft.	Slotted Interval Feet	Net Sand feet (in those intervals open during test)	Date Completed	Remarks
16-30	8,000	1,600 between 6,400 and 8,000 ft.	1,116	July, 1977	
56-30	7,520	2,225 between 5,300 and 7,550 ft.	1,841	June, 1977	
16-29	7,998	1,335 between 6,400 and 7,998 ft.	827	Dec., 1975	
18-28	8,001	1,840 between 5,110 and 8,000 ft.	231	Jan., 1976	No water entry between 6,400 and 8,000 ft.
78-30	7,442	1,520 between 5,900 and 7,450 ft.	1,257	Aug., 1977	
38-30	9,090	2,265 between 6,300 and 8,900 ft.	499	Oct., 1975	Filled to 7,022 ftt.
31-1	6,175	760 between 5,400 and 6,200 ft.	Not Available	June, 1974	Owned by U.S. Bureau of Reclamation

The first two of the three tests conducted were short duration (few days) production-interference tests while the last was a long-duration interference test which lasted for several weeks. The details of the tests are summarized in Table 2. All the tests involved varying flow rates. The flow rates were measured by first separating steam and water and then passing each through separate orifice meters. Pressure differentials in the observation wells (all of which are artesian) were measured with the help of sensitive quartz crystal pressure transducers. The flow data as well as the pressure data were automatically recorded as printouts or strip charts.

Table 2: Republic Geothermal Well Tests: Details of Tests

Test No.	PRODUCTION WELL	Method of Production	Flow Rate (gpm)	Pressure Measurement	Date	Observation Wells and Instruments 1	2	3	4
1	38-30	Valve* control	Step-wise variable * 500, 750, 900, 500, 225	Sperry Sun down-hole pressure monitor	July 14 to July 18, 1977	56-30	16-29	31-1	
						← Paro Scientific well-head transducer →			
2	16-29	Valve* control	Variable 200 to 700	Denver Research Institute and Sperry Sun down-hole pressure monitor	July 26 to July 30, 1977	16-30	51-30	31-1	
						← Paro Scientific well-head transducer →			
3	38-30	Downhole Pump	Variable 200 to 1,000	None	August 22 to Oct. 5, 1977	16-30	56-30	78-30	31-1
						← Paro Scientific well-head transducer →			

* Natural, well-bore flashing flow

Results and Interpretation

All the tests conducted were characterized by variable discharges. At the outset, therefore, it became impossible to use the conventional type-curve matching procedures of analysis which are generally based on fixed flow rates. Instead, a computer assisted curve-matching procedure recently developed at LBL (Tsang, et al., 1977) formed the backbone of all the interpretation.

The interference data collected during the first test from wells 56-30 (kh=26,300 md-ft; ϕch=4.5x10^{-4} ft/psi) and 31-1 (kh=35,400 md-ft; ϕch=2.07x10^{-3} ft/psi) indicated the possible presence of a barrier boundary, that could be represented by an equivalent image of well of 38-30 located 4,600 feet from 56-30 and 2,700 feet from 31-1. In addition, both test 2 and test 3 brought to light the very interesting fact that well 16-30 did not show any pressure response to the production either from 16-29 or 38-30. This is all the more remarkable because well 56-30, whose distance from 38-30 is the same as that between the latter and 16-30, experienced a drawdown of as much as 21 psi during the first test and 45 psi during the third. The three pieces of data, namely, the image well distances from 56-30 and 31-1 and the non-response of 16-30 strongly suggest the presence of a prominent, NNE trending barrier boundary as shown in Fig. 2. This boundary apparently does not conform to any of the geologically mapped faults, although its trend parallels those of inferred growth faults.

REPUBLIC Geothermal Wells, East Mesa, California.

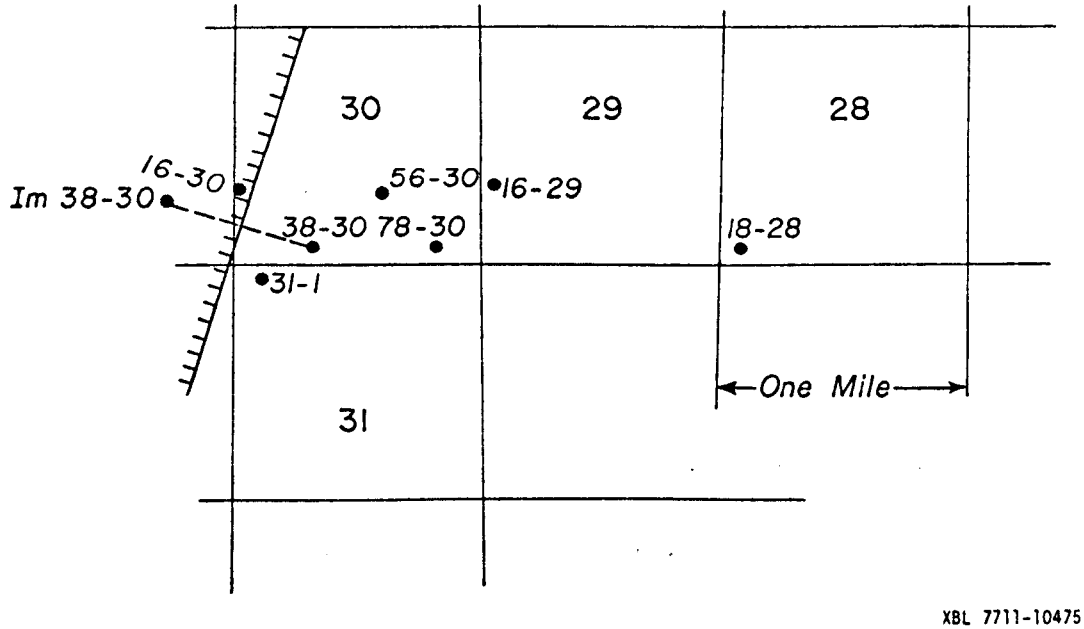

Fig. 2 Republic Geothermal Well Tests: Inferred presence of hydrologic barrier boundary

The production well data collected during test 1 suggested a kh of approximately 25,000 md-ft for the reservoir in the vicinity of 38-30. In addition, the data also indicated a negative skin for well 38-30.

Interference data collected during the third test from 31-1 yielded kh, ϕch and image well distances comparable with those obtained during test 1. However, data from 56-30 indicated somewhat lower kh and lower image well distance (see Table 3) than the first test. It may be noted here that at the start of test 3, the reservoir was still recovering from the effects of 38-30 and 16-29. The discrepancies mentioned may be attributable to the buildup effects of 16-29 which were ignored during the interpretation.

Interference data collected from 78-30 during test 3 indicated anomalously low kh values of 10,400 md-ft for the reservoir between 38-30 and 78-30. The maximum pressure drop observed in 78-30 during the test was about 3 psi while computations showed that one would have normally expected drawdowns of the order of 12 to 15 psi. The reasons for this anomalous observation are being studied. From borehole logs and cores it appears that 78-30 has sands of quality and thickness comparable to those in 38-30. It is therefore of particular interest to adequately explain the low value of kh inferred between 38-30 and 78-30.

The estimates for the reservoir parameters obtained from the three tests are summarized in Table 3. This table also contains estimates of kh values obtained from borehole logs. As can be seen, a reasonable agreement exists between the current and previous estimates. In general, the reservoir below the Republic Geothermal lease has a kh of approximately 30,000 md-ft.

Table 3: Summary of Test Results from Republic Geothermal Wells

Well	Test 1 (38-30 Producing)	Test 2 (16-29 Producing)	Test 3 (38-30 Producing)	Previous Estimates
38-30	kh=24,800 md-ft ϕchr_e^2=1.36 ft^3/psi	--	--	Borehole Logs (Intercomp) kh=44,000 md-feet Build-up Test (Intercomp) kh=31,700 md-feet Interference Test (L&L) kh=29,500 md-feet
56-30	kh=26,300 md-ft ϕch=4.5x10^{-4} ft/psi r_i=4,600 ft	To be analyzed	kh=23,600 md-ft ϕch=7.89x10^{-4} ft/psi r_i=3,500 ft	
31-1	kh=35,400 md-ft ϕch=2.07x10^{-3} ft/psi r_i=2,660 ft	To be analyzed	kh=31,700 md-ft ϕch=2.4x10^{-3} ft/psi r_i=2,450 ft	
16-29	kh=21,800 md-ft ϕch=2,36x10^{-3} ft/psi	--	--	Borehole Logs (Intercomp) kh=30,000 md-feet Build-up Test (Intercomp) kh=34,700 md-feet
78-30	--	--	kh=10,400 md-ft ϕch=6.68x10^{-3} ft/psi r_i=3,300 ft	

In conclusion, it should be pointed out that interpretations are still continuing and the results presented here are tentative and subject to revision.

Acknowledgements

We would like to thank the U.S. Bureau of Reclamation for permission to monitor pressures on well 31-1.

This work was supported by the U.S. Department of Energy.

References

1. Tsang, C.F., D.G. McEdwards, T.N. Narasimhan and P.A. Witherspoon, "Variable Flow Well-Test Analysis by a Computer-Assisted Matching Procedure", Paper No. 6547, 47th Annual Western Regional Meeting, SPE of AIME, Bakersfield, California, April 13-15, 1977.

2. U.S. Bureau of Reclamation, "Geothermal Resource Investigations, East Mesa Test Site, Imperial Valley California, Status Report-1974", November, 1974.

Table 1: Description of Republic Geothermal Wells, East Mesa, California

Well	Total Depth ft.	Slotted Interval Feet	Net Sand feet (in those intervals open during rest)	Date Completed	Remarks
16-30	8,000	1,600 between 6,400 and 8,000 ft.	1,116	July, 1977	
56-30	7,520	2,225 between 5,300 and 7,550 ft.	1,841	June, 1977	
16-29	7,998	1,335 between 6,400 and 7,998 ft.	827	Dec., 1975	
18-28	8,001	1,840 between 5,110 and 8,000 ft.	231	Jan., 1976	No water entry between 6,400 and 8,000 ft.
78-30	7,442	1,520 between 5,900 and 7,450 ft.	1,257	Aug., 1977	
38-30	9,090	2,265 between 6,300 and 8,900 ft.	499	Oct., 1975	Filled to 7,022 ftt.
31-1	6,175	760 between 5,400 and 6,200 ft.	Not Available	June, 1974	Owned by U.S. Bureau of Reclamation

Table 2: Republic Geothermal Well Tests: Details of Tests

Test No.	PRODUCTION WELL	Method of Production	Flow Rate (gpm)	Pressure Measurement	Date	Observation Wells and Instruments 1	2	3	4
1	38-30	Valve* control	Step-wise variable ≈ 500, 750, 900, 500, 225	Sperry Sun down-hole pressure monitor	July 14 to July 18, 1977	56-30	16-29	31-1	
						← Paro Scientific well-head transducer →			
2	16-29	Valve* control	Variable 200 to 700	Denver Research Institute and Sperry Sun down-hole pressure monitor	July 26 to July 30, 1977	16-30	51-30	31-1	
						← Paro Scientific well-head transducer →			
3	38-30	Downhole Pump	Variable 200 to 1,000	None	August 22 to Oct. 5, 1977	16-30	56-30	78-30	31-1
						← Paro Scientific well-head transducer →			

* Natural, well-bore flashing flow

Table 3: Summary of Test Results from Republic Geothermal Wells

Well	Test 1 (38-30 Producing)	Test 2 (16-29 Producing)	Test 3 (38-30 Producing)	Previous Estimates
38-30	kh=24,800 md-ft ϕchr_e^2=1.36 ft^3/psi	--	--	Borehole Logs (Intercomp) kh=44,000 md-feet Build-up Test (Intercomp) kh=41,700 md-feet Interference Test (LBL) kh=29,500 md-feet
56-30	kh=26,300 md-ft $\phi ch=4.5x10^{-4}$ ft/psi r_i=4,600 ft	To be analyzed	kh=23,600 md-ft $\phi ch=7.89x10^{-4}$ ft/psi r_i=3,500 ft	
31-1	kh=35,400 md-ft $\phi ch=2.07x10^{-3}$ ft/psi r_i=2,660 ft	To be analyzed	kh=31,700 md-ft $\phi ch=2.4x10^{-3}$ ft/psi r_i=2,450 ft	
16-29	kh=21,800 md-ft $\phi ch=2,36x10^{-3}$ ft/psi	--	--	Borehole Logs (Intercomp) kh=30,000 md-feet Build-up Test (Intercomp) kh=34,700 md-feet
78-30	--	--	kh=10,400 md-ft $\phi ch=6.68x10^{-3}$ ft/psi r_i=3,300 ft	

UPDATE ON THE RAFT RIVER GEOTHERMAL RESERVOIR

J. F. Kunze - EG&G Idaho, Inc.
R. C. Stoker- EG&G Idaho, Inc.
C. A. Allen - Allied Chemical Co.

Idaho National Engineering Laboratory*
Idaho Falls, Idaho 83401

ABSTRACT

Since the last conference, a fourth well has been drilled to an intermediate depth and tested as a production well, with plans to use this well in the long term for injection of fluids into the strata above the production strata. The third, triple legged well has been fully pump tested, and the recovery of the second well from an injection well back to production status has revealed very interesting data on the reservoir conditions around that well.

Both interference testing and geochemistry analysis shows that the third well is producing from a different aquifer than that supplying the No. 2 well. There is an effective barrier, yet unidentified as to structure, making pressure communication between these aquifers quite negligible. These results have led to significantly different models for the aquifer system than those previously believed to apply.

THE 4-WELL SYSTEM

The Raft River Geothermal Program now has 3 deep production wells, with producing zones between 3750 and 6000 ft. An intermediate depth well was recently drilled for injection testing into the zone between 1850 and 2500 ft. Figure 1 shows the location of the wells with respect to the major faults in the region. Figure 2 shows cross sections of each well. Additional details on these wells may be found in Reference 1 (last year's conference).

PRODUCTION TESTING

RRGE-1

This well has been used as a production well for the last 18 months, with greater than 95% capacity factor. It has been supplying fluids for a variety of heat exchanger tests, corrosion coupon tests, and water for several direct heat utilization experiments. Flow rates were deliberately throttled to supply only the fluids essential for these tests (150 to 300 gallons/minute (0 to 20 liters/sec), all using the artesian head. Pressures of 100 psig minimum have been maintained in all heat exchanger and coupon testing to prevent off-gasing and entry of air into these systems.

* This work has been performed under contract to the U.S. Department of Energy, Division of Geothermal Energy, and Idaho Operations Office.

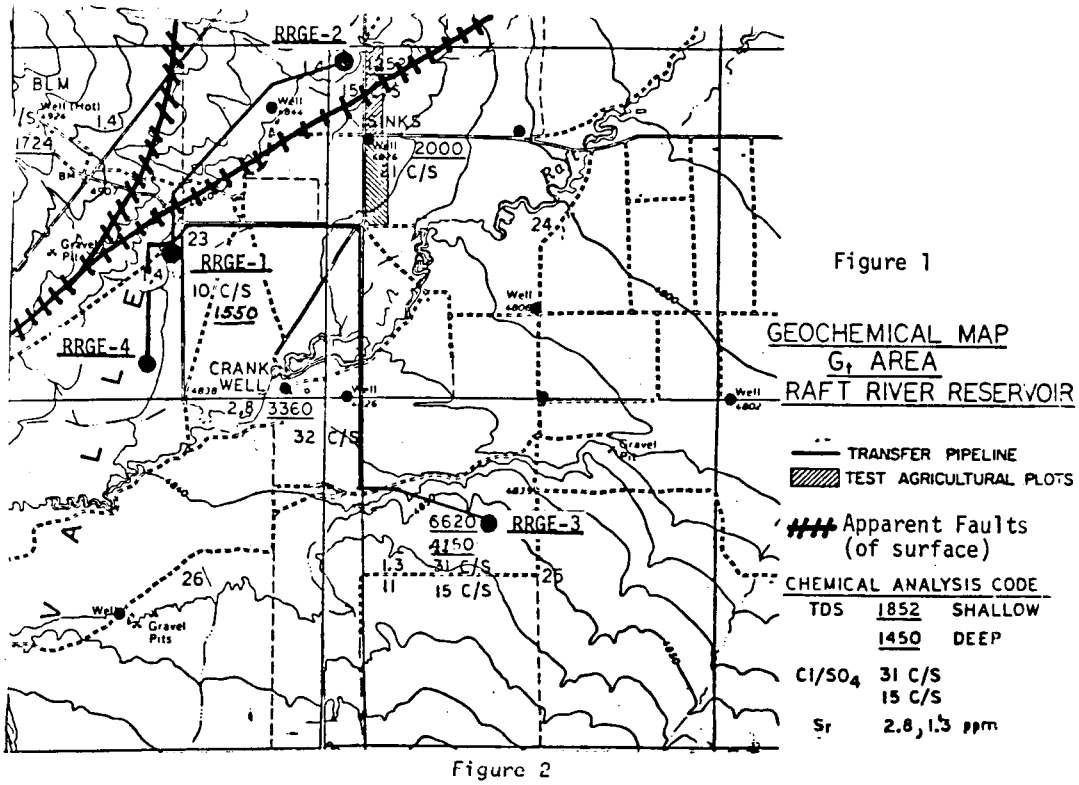

Figure 1

GEOCHEMICAL MAP
G_t AREA
RAFT RIVER RESERVOIR

Figure 2

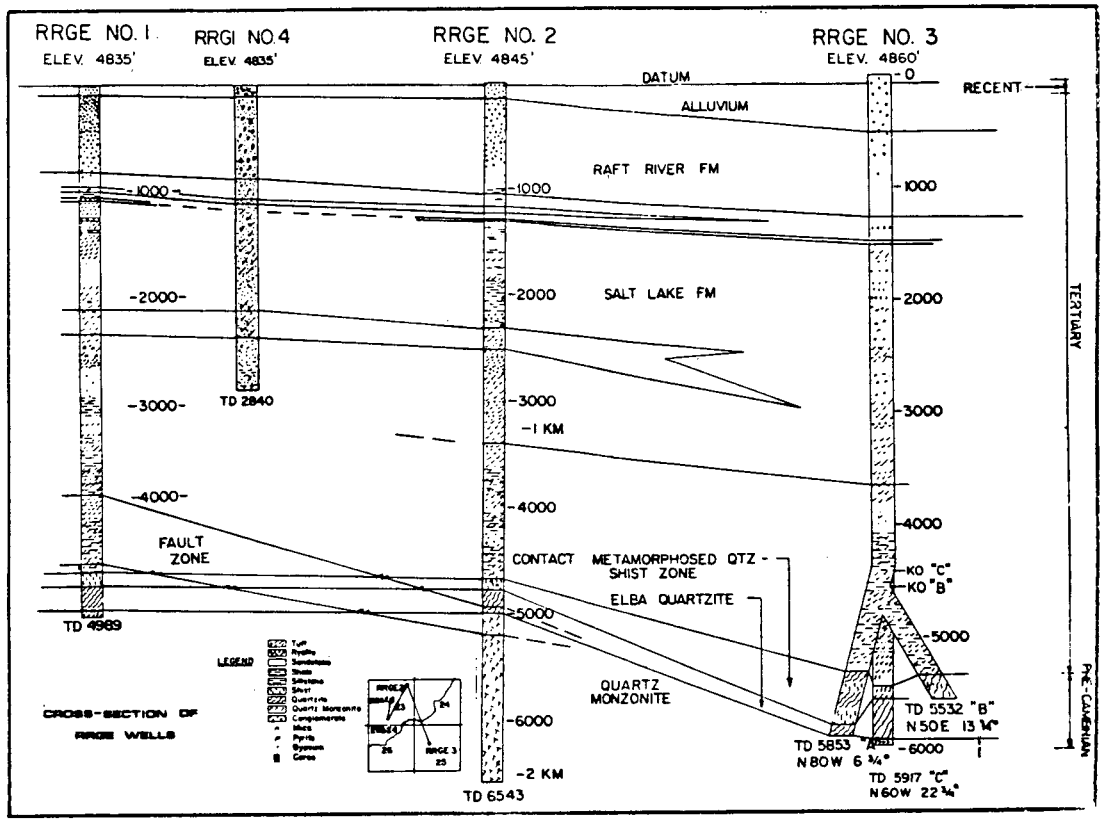

The well performance data during the 18 months has shown no decrease in productivity vs pressure, if anything a slight increase. The drawdown since the start of the long term operation is so far, on the time logarithmic scale. Short term fluctuations in flow (and hence pressure) have occurred as demanded by the variety of experiments, and are the predominant variable change.

The apparent productivity curve for this well is as shown in Figure 3. It is the most productive well in the reservoir. The chemistry of the fluids has remained essentially the same as after the first thorough flow testing, 2-1/2 years ago. Dissolved solids are 1550 ppm (mg/liter). Temperature has shown no change during this period. At these low flow rates, with the large 13-3/8 in. casing, the temperature loss in the well bore is only approximately 12°C (22°F). At the nominal design flow rate of 1200 gal/min (80 liters/sec) planned for this well with a pump in place, temperature loss should be reduced by nearly a factor of 4. Production zone temperatures have held at 147°C (296°F).

RRGE-2

No significant flow testing during the last 12 months.

RRGE-3

A submersible pump was installed in this well at the 800 ft (244 m) level. Pump testing at 500 to 600 gal/min (90 l/sec) have been conducted for periods of several weeks to a month in duration. These have been at constant flow, using the Thies asymptotic semilogarithmic approach to obtain transmissivity and permeability thickness factors. Except for some possible early time effects before encountering a nearby boundary, the Thies analysis shows excellent linearly (semilog plot), giving a T = 850 ± 100 gal/day ft and kH - 8000 ± 1000 millidarcy-ft.

Pressure communication does not appear to occur, at least unambiguously over a two week period, with RRGE-2, 7000 ft away, as measured with a quartz transducer with ±0.01 psi sensitivity. Somewhat less ambiguous indication of pressure communication has been observed with the intermediate depth RRGI-4, 5000 ft away. The chemistry of the RRGE-3 well has been generally consistent throughout 1-1/2 years of limited testing (because of difficulty in disposing of the water) at 4150 ppm (mg/liter).

RRGI-4

This well was completed in May 1977, to be used for injection testing of the feasibility of disposing of water into the intermediate depth aquifer. It has 13-3/8 in. casing to 1835 ft, and is barefoot from there to its total present depth of 2840 ft. The relatively permeable section appears to extend from the casing bottom to about 2500 ft.* Though the well accepted

* When drilling out the shoe, the lower two sections of casing (80 ft total) dropped off and are wedged between 1895 and 1975 ft, effectively blocking out the formation in this region.

injected water quite readily, the production testing (the well has a hot artesian head of about 40 psig at 250°F) gave a transmissivity of 1600 ± 200 gal/day ft. This value is not much different from RRGE-2. The well has about 2300 ppm (mg/liter) solids coming from the producing region. It has slight pressure communication with RRGE-3, quite noticeable communication with the USGS No. 3 well (1300 ft deep, 2200 ft away), and no detectable communication to date with RRGE-1 or 2.

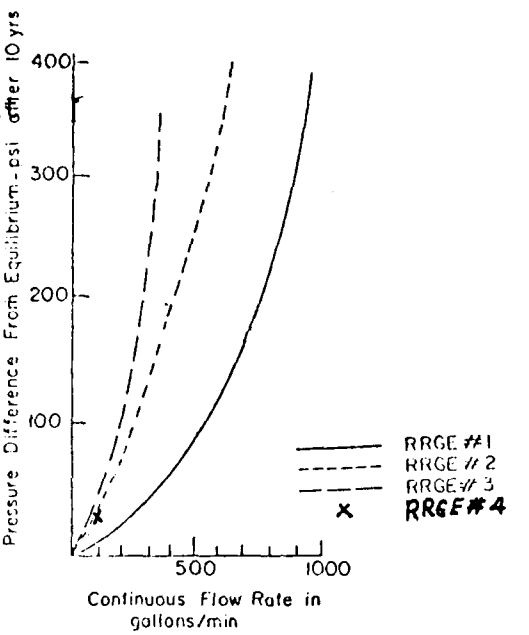

Figure 3 - Well productivity vs, drawdown after constant flow for 10 yr period. Note: Wells 1, 2, 3 have a positive (artesian) head of 150 psig when at hot"equilibrium." The 4th well has an artesian head of 40 psig.

GEOCHEMISTRY

The chemistry of the waters produced from the three deep wells and the Crank (400 ft or 122m) and BLM (500 ft or 152m) wells has shown that the chemical species in these wells seem to be originating from two quite different systems. The one has chemistry similar to RRGE-3 (4150 ppm), the other similar to RRGE-2 (1250 ppm) RRGE-1, the BLM, and the Crank wells appear to be mixtures of these two systems, as shown in Table 1. In that Table, X_m represents the fractional contribution from the system representative of RRGE-2.

It thus appears that the most chemical laden waters and those with the highest indicated reservoir temperatures are upwelling in the region of RRGE-3 and the Crank well, and leaking into the area near RRGE-1 and the BLM well. Much purer waters are apparently feeding RRGE-2 (to the northeast) and leaking into the BLM and RRGE-1 areas. RRGI-4, for the little it has flowed, also seems to be composed of both waters.

CONCLUSIONS

The long hypothesized model of the geothermal heat source being located away from the immediate area, with the hot waters being fed into the region of the wells via the "narrows" structure to the southwest, is not supported by the geochemical analysis. Instead, it would seem that another model would be that of a hot plate effect under much of the valley, with a localized somewhat hotter, poorly convective region near RRGE-3.

TABLE I

TOTAL DISSOLVED SOLIDS AND MIXING FRACTIONS
IN THE RAFT RIVER WELLS

	RRGE-2	RRGE-1	BLM	Crank	RRGE-3
TDS	1267	1560	1640	3720	4130
X_m	1	.898	.870	.143	0
Apparent Reservoir Temperature					
S_iO_2	158°C	155°C	--	--	165°C
Na/K/Ca	185°C	180°C	--	--	190°C

It does appear that a barrier of some type exists between RRGE-3 and the other two deep wells, restricting both pressure and flow communication, isolating the two systems with quite distinctly different chemistry.

Finally, the longer term test has not shown any major boundary restrictions or with significant regions of highly channelled flow (none isotropic). Based on these tentative conclusions and the information presented in Ref. 1, one can conclude the following about the known reservoir, that within a mile of the existing three wells.

Minimum area of Known reservoir $\sim$ 5 sq mi. (2)

Geothermal Aquifer Capacity - 300,000 acre-ft, with effective porosity of $\sim$ 0.15.

Near surface aquifer probably contains 12 million acre ft, and sees annual precipitation of 200,000 acre ft (2)

Geothermal aquifer heat content (known reservoir only, heat above 250°F only) = 160 MW-Centuries (about 20 MW-Centuries net electrical output with binary-isobutane conversion system.

REFERENCE

1. D. Goldman, J. F. Kunze, L. G. Miller, R. C. Stoker, "Studies on the 3-Well Reservoir System in Raft River," 2nd Workshop on Geothermal Reservoir Engineering, Stanford University 1976.

2. Geothermal R&D Project Report for October 1976 to March 1977, TREE-1134, EG&G Idaho, Inc.

3. E. H. Walker, L. C. Dutcher, S. O. Decker, and K. L. Dyer, The Raft River Basin, Water Intermountain Bulletin No. 19, State Department of Water Resources (1970).

THE BOISE, IDAHO GEOTHERMAL RESERVOIR

R. C. Stoker - EG&G Idaho, Inc.
J. F. Kunze - EG&G Idaho, Inc.
L. B. Nelson - EG&G Idaho, Inc.
D. Goldman - University of Idaho

Idaho National Engineering Laboratory (INEL)*
Idaho Falls, Idaho 83401

ABSTRACT

Geothermal district space heating has been practiced in Boise over the last 85 years. The system has used two wells drilled approximately 50 ft (15 m) apart in the early 1890s. The wells have a combined maximum reported production rate of 1800 gpm (114 l/sec) at 170°F (77°C) discharge at the wellhead. The system has served as many as 400 homes and Natatorium; presently it serves approximately 200 homes and a large state laboratory and office building.

The heating district remained at the present capacity (two wells) for 85 years primarily because of the unknown nature of the reservoir and availability of other energy sources. Not until 1974 was the question of further development given serious consideration. Rising energy costs due to expanding energy demands and higher costs for foreign oil brought about a reevaluation of the resource. The INEL, Boise State University, and the Idaho Bureau of Mines and Geology began an investigation into the nature of the resource and the economics of space heating several large buildings and homes. Two deep, approximately 1250 ft (381 m), exploratory wells were drilled and tested by the INEL to determine the nature and size of the reservoir. Drilling and reservoir engineering test results have confirmed the presence of a large reservoir that can be developed further without adversely effecting the two production wells and heating system now in operation.

EXISTING PENITENTIARY WELLS

Hot water at 170°F (77°C) was first encountered in two wells drilled in early 1891 to a depth of only 394 ft (120 m) and 404 ft (123 m). The wells were only 50 ft (15 m) apart and were drilled in a swampy area formed by hot water seepage. Eventually the system evolved into two 16-in. (41 cm) production wells about 425 ft (130 m) deep with centrifugal pumps set to 160 ft (49 m). These wells will still become artesian if pumping is stopped and the wells are allowed to recover for approximately 3 or 4 days. The original artesian head of 50 ft (15 m) in these wells is still attainable by shutting in for a longer period.

---

* This work has been performed under contract to the U.S. Department of Energy (DOE), Division of Geothermal Energy, and the DOE-Idaho Operations Office.

During the last year, these old production wells have been monitored for water level drawdown. During late January, 1977, the drawdown reached a maximum of 143 ft (44 m) below ground level (just above the pump bowls). High flow rates (up to 1600 gpm from both wells) caused by unusually cold weather and system leakage accounted for this extreme drawdown.

TWO EXPLORATORY WELLS

In the winter and early spring of 1976, the INEL drilled two exploratory wells 1000 ft (305 m) apart and approximately 1-1/2 mi (2.4 km) northwest of the penitentiary wells. Each of the exploratory wells were drilled within the immediate area of the main NW-SE trending Boise Front Fault and intersecting linears trending from the NE out of the mountains. The well locations are identified on Figure 1. The BEH-1 (BLM) well was drilled to a total depth of 1222 ft (372 m), has 7-in. (18 cm) production casing set to 610 ft (186 m) and a slotted 3-1/2 in. (9 cm) liner hung from the production casing to total depth. See Figure 2.

The BHW-1 (Beard) well was drilled to a total depth of 1283 ft (391 m), has 8-in. (20 cm) production casing set to 202 ft (62 m) and a slotted 4-1/2 in. (11 cm) liner with 100 ft (30 m) of screen hung from the production casing to total depth. See Figure 3.

The BEH-1 (BLM) well was drilled with water out of the production casing but encountered clay lenses (Montmorillonite) during drilling which necessitated cleanout of the pits three different times. BHW-1 (Beard) well was drilled with light mud in an attempt to stabilize the loosely-cemented sand beds encountered between 450 and 800 ft (137 and 245 m).

EXPLORATORY WELL TESTING

Reservoir engineering testing of the two exploratory wells has been as follows:

1. Temperature profiles of the wells were taken during drilling and after the well had stabilized. See Figure 4 for the temperature profile of BHW-1 (Beard). The profile on BEH-1 (BLM) is essentially identical.

2. Artesian wellhead pressure was monitored all during the 1976-77 heating season at BEH-1 (BLM). No correlatable pressure communication was observed as a result of the pumping conducted at the old penitentiary wells. A seasonal pressure decline of 2-1/2 psia was observed during the winter,but recovery began with the spring run off.

3. Artesian and pumped flow tests on each of the exploratory wells was conducted. A shaft driven pump set at approximately 185 ft (56 m) was employed for the pumped flow tests. Table I summarizes the Boise testing completed to date.

4. Interference testing revealed a rapid pressure communication between the two wells; 0.1 psia change within two minutes of the start of a test.

The BEH-1 well production (artesian flow) will be used for space heating of a BLM warehouse this winter and the long term drawdown will be monitored.

CONCLUSIONS

1. The 170° F geothermal reservoir boundaries have not been detected and the reservoir appears to be capable of usage rates far exceeding the present rate.

2. The reservoir is proven to extend at least 1-1/2 miles along the Fault.

3. Similar geologic conditions occur in several locations along the Boise Front Fault that apparently control the geothermal resource as now defined by the existing four wells.

4. Test results indicate that future production wells (properly located) will have high production rates in the order of 600 to 1000 gpm for 12 to 16 in. (30 to 40 cm) wells at pump setting depths of 400 feet.

5. The geothermal resource can be encountered at relatively shallow depths (<1000 ft or 305 m) and at temperatures (170°F or 77°C) adequate for large scale space heating. The wells should be located close to the intersection of NE trending linears with the Front Fault for the greatest possible production rates and highest temperatures close to the service areas.

The authors wish to thank the geology students, faculty and especially Renald N. Guillemette of Boise State University for their assistance and help during the Boise Project.

WELL LOCATIONS IN BOISE IDAHO

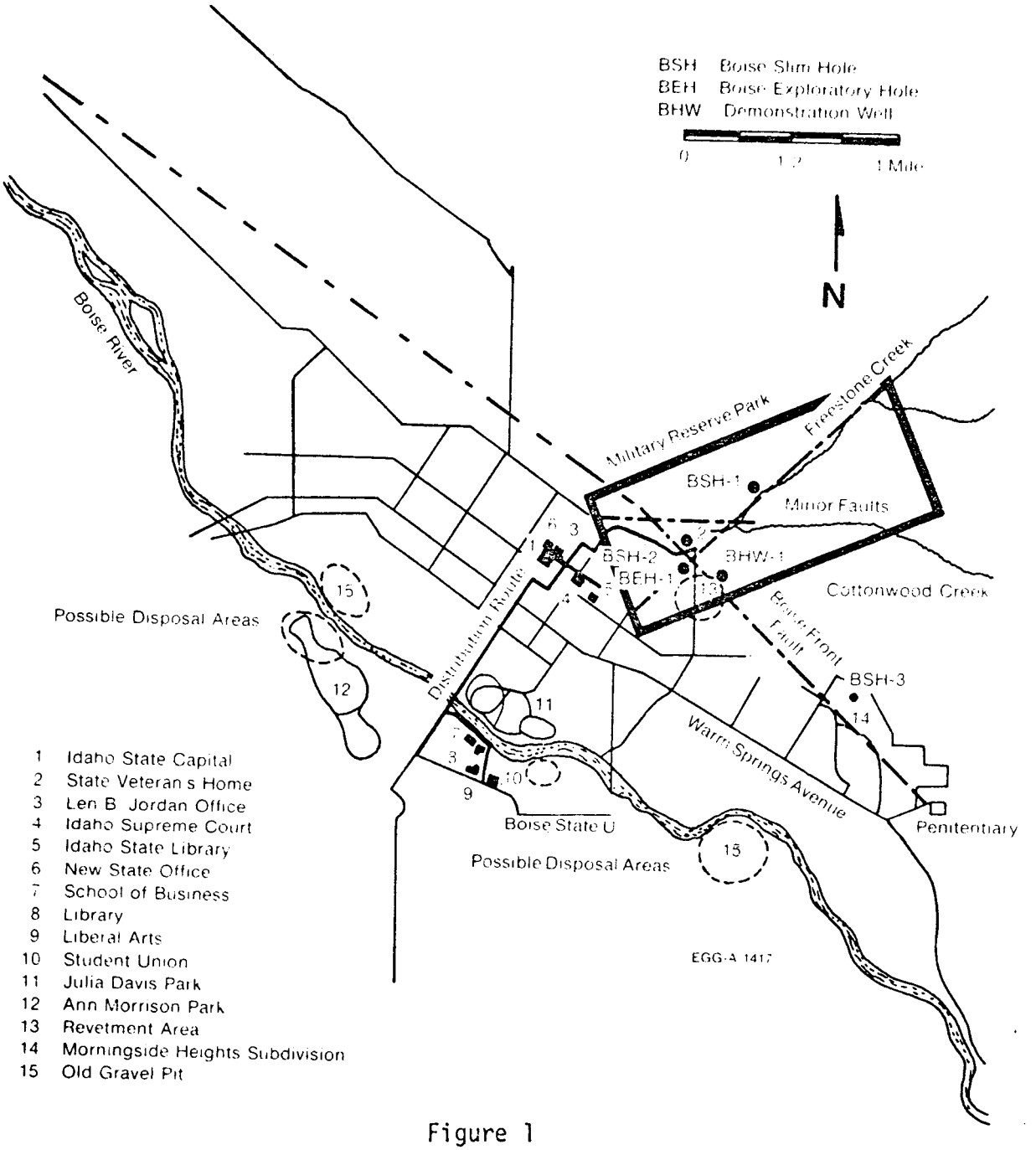

Figure 1

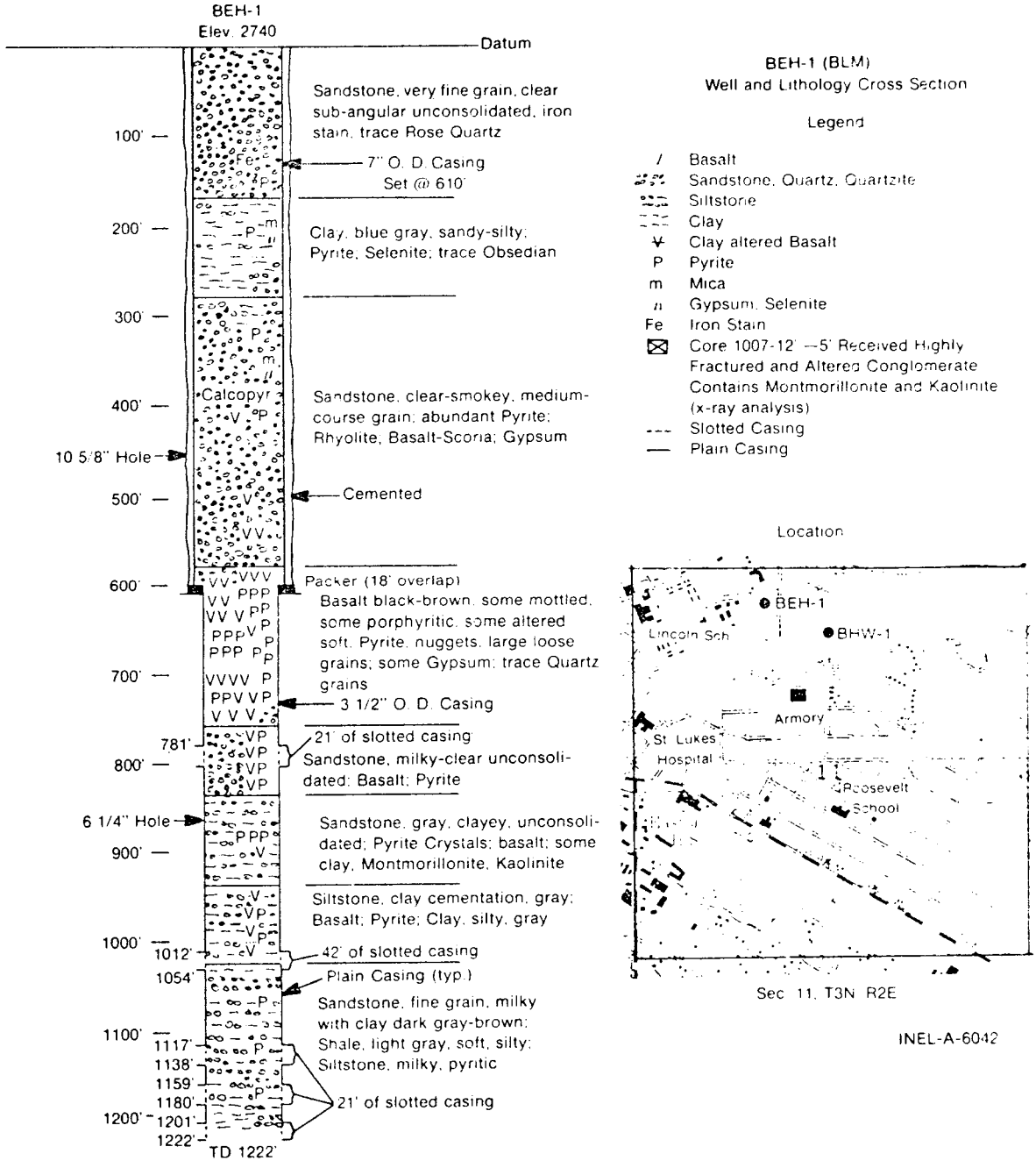
BEH-1
Elev. 2740
Datum
Sandstone, very fine grain, clear sub-angular unconsolidated, iron stain, trace Rose Quartz
7" O. D. Casing Set @ 610'
Clay, blue gray, sandy-silty; Pyrite, Selenite; trace Obsedian
Sandstone, clear-smokey, medium-course grain; abundant Pyrite; Rhyolite, Basalt-Scoria; Gypsum
10 5/8" Hole
Cemented
Packer (18' overlap)
Basalt black-brown, some mottled, some porphyritic, some altered soft, Pyrite, nuggets, large loose grains; some Gypsum; trace Quartz grains
3 1/2" O. D. Casing
21' of slotted casing
Sandstone, milky-clear unconsolidated; Basalt; Pyrite
6 1/4" Hole
Sandstone, gray, clayey, unconsolidated; Pyrite Crystals; basalt; some clay, Montmorillonite, Kaolinite
Siltstone, clay cementation, gray; Basalt; Pyrite; Clay, silty, gray
42' of slotted casing
Plain Casing (typ.)
Sandstone, fine grain, milky with clay dark gray-brown; Shale, light gray, soft, silty; Siltstone, milky, pyritic
21' of slotted casing
TD 1222'
100'
200'
300'
400'
500'
600'
700'
781'
800'
900'
1000'
1012'
1054'
1100'
1117'
1138'
1159'
1180'
1200'
1201'
1222'
BEH-1 (BLM)
Well and Lithology Cross Section
Legend
Basalt
Sandstone, Quartz, Quartzite
Siltstone
Clay
Clay altered Basalt
P Pyrite
m Mica
Gypsum, Selenite
Fe Iron Stain
Core 1007-12' —5' Received Highly Fractured and Altered Conglomerate Contains Montmorillonite and Kaolinite (x-ray analysis)
Slotted Casing
Plain Casing
Location
BEH-1
BHW-1
Lincoln Sch
Armory
St Lukes
Hospital
Roosevelt
School
Sec 11, T3N R2E
INEL-A-6042

Figure 2

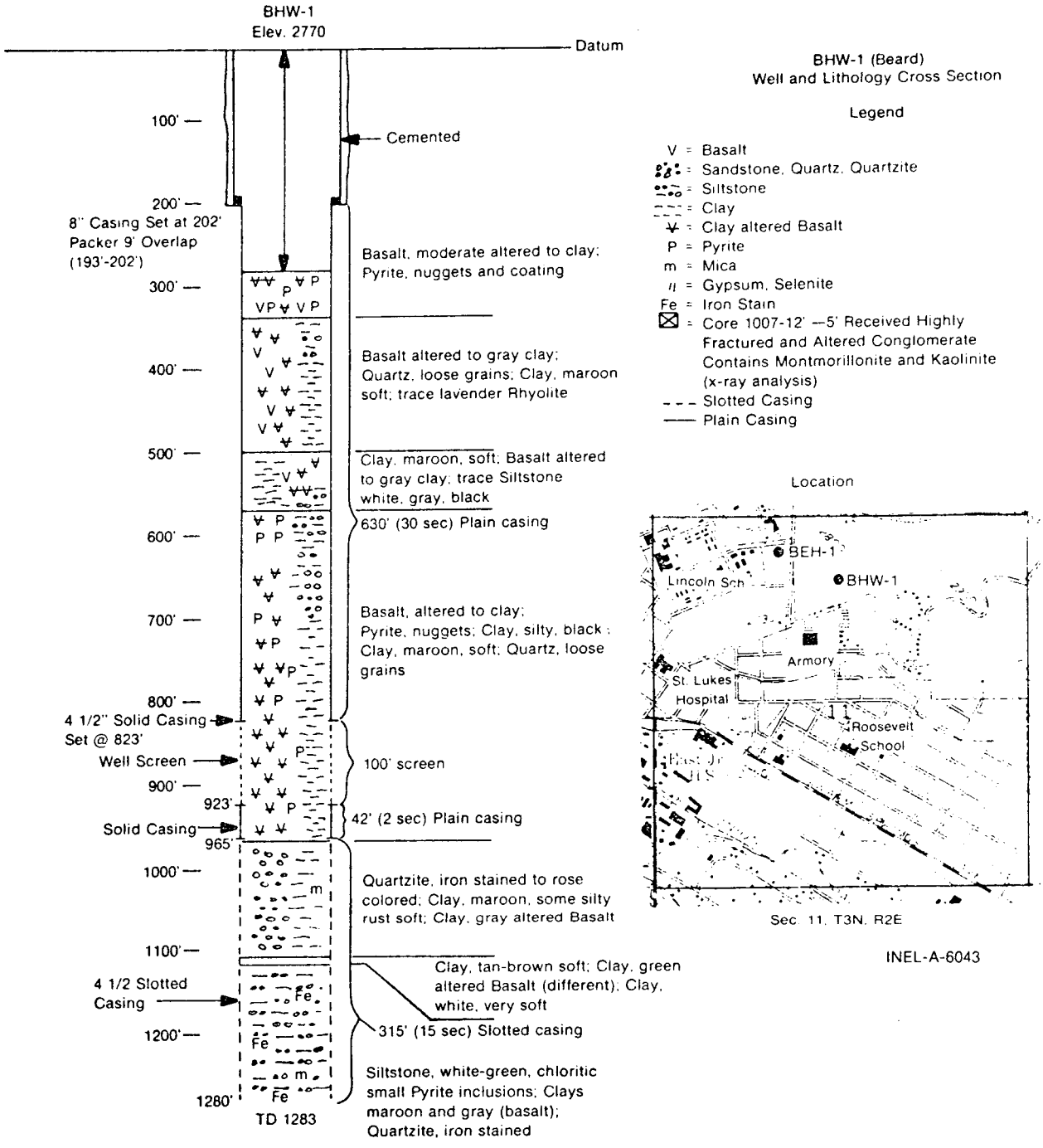
BHW-1
Elev. 2770
Datum
100'
200'
8" Casing Set at 202'
Packer 9' Overlap
(193'-202')
Cemented
300'
400'
500'
600'
700'
800'
4 1/2" Solid Casing
Set @ 823'
Well Screen
900'
923'
Solid Casing
965'
1000'
1100'
4 1/2 Slotted
Casing
1200'
1280'
TD 1283
Basalt, moderate altered to clay;
Pyrite, nuggets and coating
Basalt altered to gray clay;
Quartz, loose grains; Clay, maroon
soft; trace lavender Rhyolite
Clay, maroon, soft; Basalt altered
to gray clay; trace Siltstone
white, gray, black
630' (30 sec) Plain casing
Basalt, altered to clay;
Pyrite, nuggets; Clay, silty, black;
Clay, maroon, soft; Quartz, loose
grains
100' screen
42' (2 sec) Plain casing
Quartzite, iron stained to rose
colored; Clay, maroon, some silty
rust soft; Clay, gray altered Basalt
Clay, tan-brown soft; Clay, green
altered Basalt (different), Clay,
white, very soft
315' (15 sec) Slotted casing
Siltstone, white-green, chloritic
small Pyrite inclusions; Clays
maroon and gray (basalt);
Quartzite, iron stained
BHW-1 (Beard)
Well and Lithology Cross Section
Legend
V = Basalt
= Sandstone, Quartz, Quartzite
= Siltstone
= Clay
= Clay altered Basalt
P = Pyrite
m = Mica
= Gypsum, Selenite
Fe = Iron Stain
= Core 1007-12' —5' Received Highly
Fractured and Altered Conglomerate
Contains Montmorillonite and Kaolinite
(x-ray analysis)
Slotted Casing
Plain Casing
Location
BEH-1
BHW-1
Lincoln Sch
Armory
St. Lukes
Hospital
Rooseveit
School
Sec. 11, T3N, R2E
INEL-A-6043

Figure 3

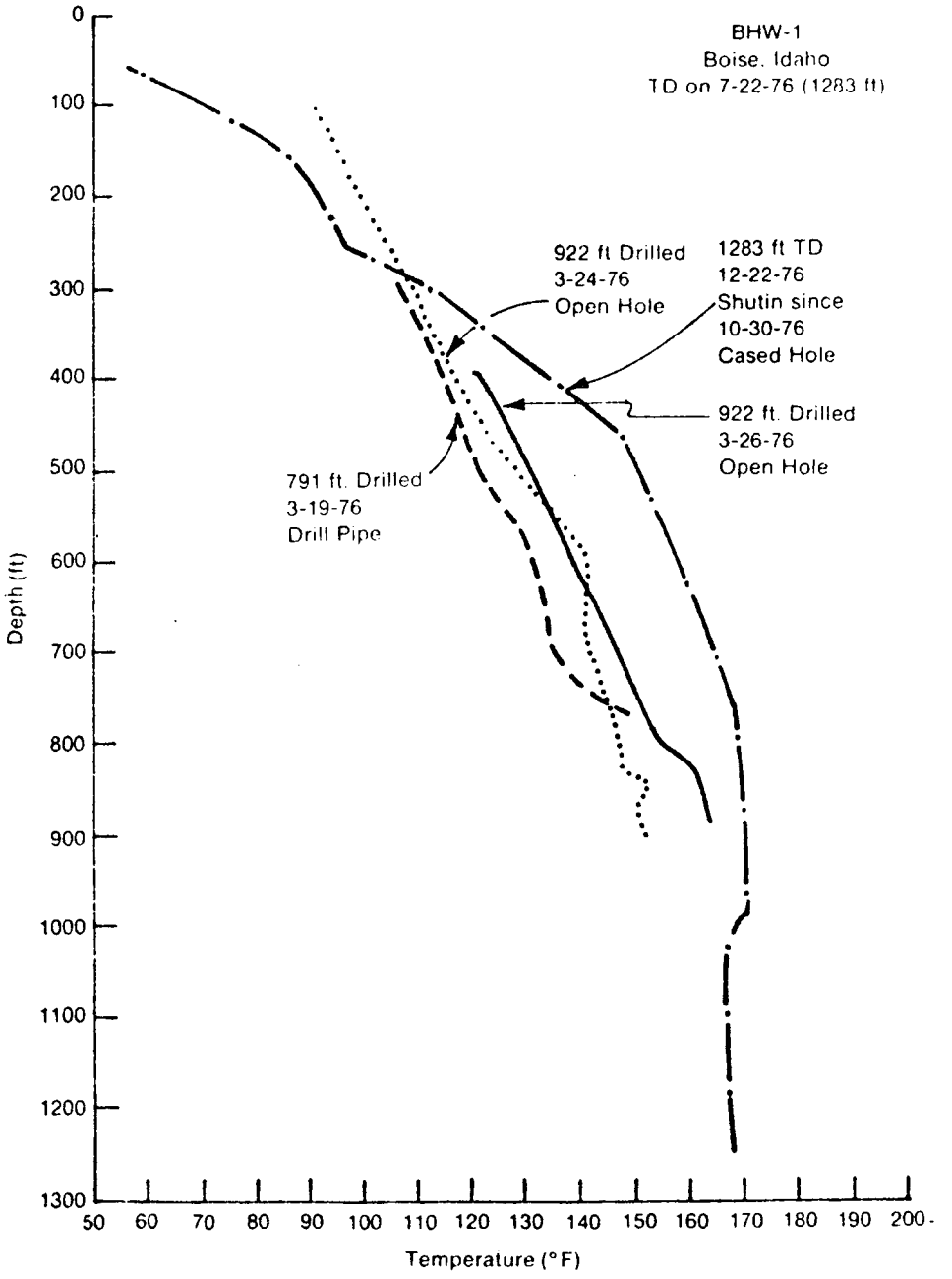
BHW-1
Boise, Idaho
TD on 7-22-76 (1283 ft)
922 ft Drilled
3-24-76
Open Hole
1283 ft TD
12-22-76
Shutin since
10-30-76
Cased Hole
922 ft. Drilled
3-26-76
Open Hole
791 ft. Drilled
3-19-76
Drill Pipe
Depth (ft)
0
100
200
300
400
500
600
700
800
900
1000
1100
1200
1300
50 60 70 80 90 100 110 120 130 140 150 160 170 180 190 200
Temperature (°F)

Figure 4

BOISE TESTING

Pumping Well	Q gpm	Date Begun	Duration	Calc. Based on Well	Kh Md. ft Drawdown	Kh Md. ft Recovery	Method	Notes
BLM	90	10-10-77	30 hrs	BLM	4.3×10^{4}	-	S/L	Questionable Poor
				Beard	1.6×10^{7}	2.2×10^{6}	S/1	Fair
				Beard	4.8×10^{6}	-	L/L	-
Beard	240	9-13-77	10 hrs	BLM	3.7×10^{6}	9.2×10^{6}	S/1	Fair
Beard	350	9-14-77	9 hrs	BLM	6.5×10^{6} 3.4×10^{6}	bef. bkpt. aft. bkpt.	S/L	R ∿ 4300' from BLM
Beard (1)	150		12 days	BLM	3.5×10^{5}	3.5×10^{6} (2)	SL	
				Beard	1.4×10^{6}	No data not fully shut in	SL	

(1) Field Plots

(2) Partial data

TABLE 1

SUMMARY OF RESULTS OF HGP-A WELL TESTING

D. Kihara, B. Chen, P. Yuen, and P. Takahashi
University of Hawaii
Honolulu, Hawaii 96822

The experimental well, HGP-A, drilled under the auspices of the Hawaii Geothermal Project, is located on the island of Hawaii near the eastern rift of Kilauea volcano. Drilling was completed to a depth of 6450 feet in April 1976. The well is cased to 2230 feet below the surface, which is 600 feet above sea level, with a slotted liner running from the end of the casing to bottomhole. Cuttings and core samples obtained during drilling indicate that the region is composed of volcanic basalt with a profile that contains a zone of open fractures (3300-4500 feet) and a zone of partially sealed fractures (4500-6450 feet) as shown in Figure 1.

The well has undergone five flash discharge tests since an initial flashing on July 2, 1976. The maximum bottomhole temperature during quiescent periods has been measured at 358°C. Test water samples were taken at various times under varying flow conditions and analyzed. The median values for the downhole samples are shown in Table 1.

TABLE 1 HGP-A Geochemical Summary

pH	Less than 5
Electrical conductivity	3100 μmho/cm
Salinity	2.3°/$_{oo}$
Chloride	925 mg/l
Silica as SiO_2	420 mg/l
Sulfide	100 mg/l
Sodium	600 mg/l
Potassium	123 mg/l
Calcium	40 mg/l
Magnesium	1 mg/l
Tritium	Less than 0.1 tritium unit or at least 12 years old

It is seen that the HGP-A discharge is a slightly saline water containing about 5% ocean water but with fairly high silica content.

Following installation of the separator-silencer, flow tests were run in November, December, January, and March. In the last three cases, pressure buildup tests were conducted after the well was shut in.

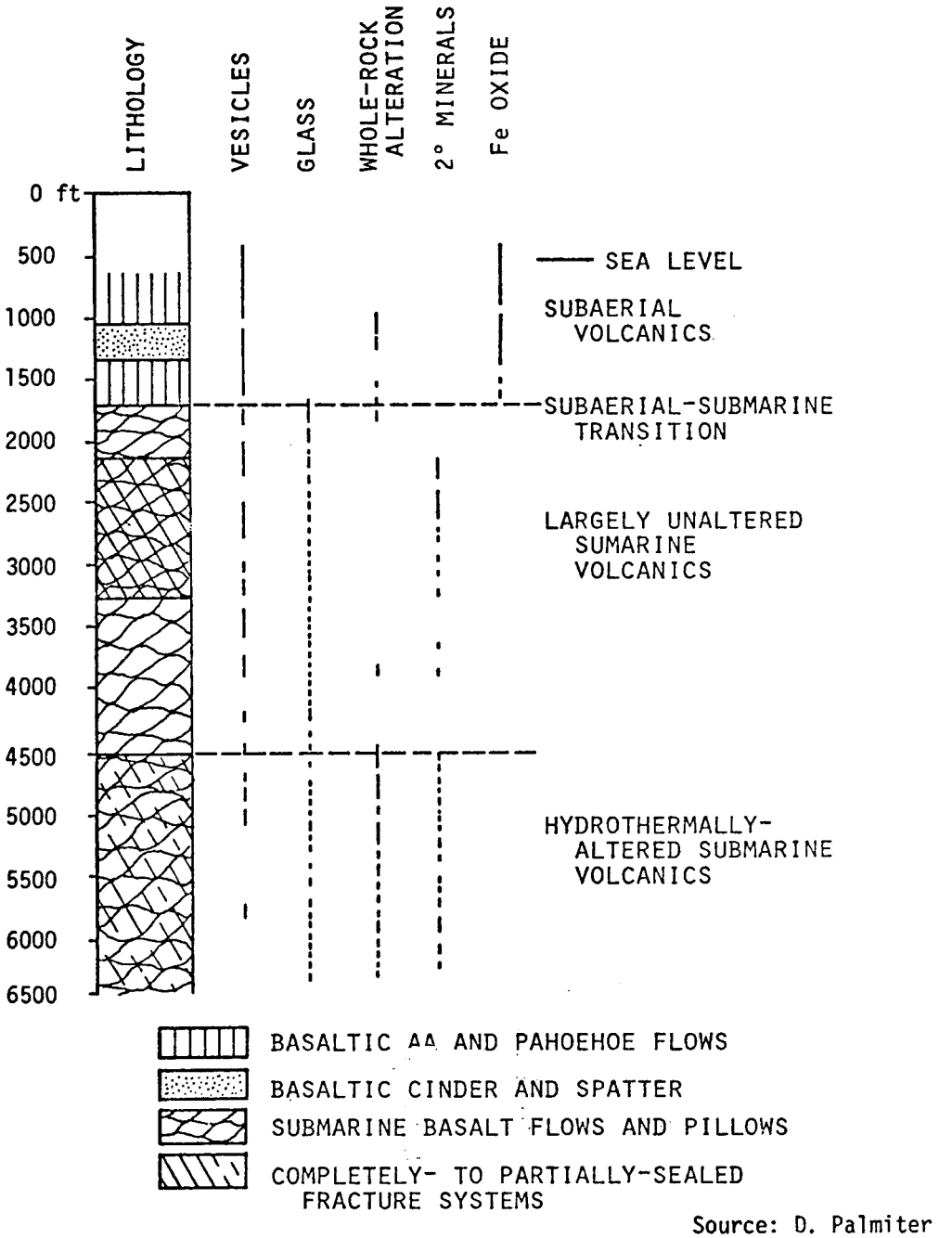

FIGURE 1. HGP-A LITHOLOGIC LOG FROM CORES AND CUTTINGS

Comparison of flow characteristics during the early stages of these four tests (Table 2) shows that with each subsequent test the flow rate has increased. A possible explanation for this improvement in well performance is that skin damage due to the use of drilling mud is being alleviated as each flow test partially cleans out embedded mud.

Table 2

COMPARISON OF DISCHARGE TESTS AT 25 HOURS AFTER INITIATION OF FLOW

	Nov.	Dec.	Jan.	Mar.
Wellhead Pressure (psig)	47	53	59	59
Wellhead Temperature (°C)	146	150	151	153
Lip Pressure (psig)	7.9	10.1	12.5	13.9
Weir Height (inches)	3-1/2	4	4-1/8	4-3/16
Mass Flow Rate (Klb/hr)	87.9	103.4	114.3	120.4
Water Flow Rate (Klb/hr)	24	34	36	38
Steam Flow Rate (Klb/hr)	63.8	70.0	78.0	82.7
Steam Quality (%)	73	68	68	69
Enthalpy (BTU/lb)	888	833	845	842
Thermal Power (Mw)	22.9	25.2	28.3	29.7

The January and March flow tests consisted of series of discharges in which the flow was throttled by placing orifice plates of various sizes in the discharge line. The results are summarized in Table 3. There is a substantial increase in wellhead pressure from 51 psig to 375 psig as the mass flow rate is reduced from 100% or 101 Klb/hr to 75% (76 Klb/hr) of wide open flow.

Table 3 PRELIMINARY THROTTLED FLOW DATA

Orifice Size (Inches)	Total Mass Flow Rate (Klb/hr)	Steam		Wellhead		Possible Electrical Power Output (MWe)
		Flow Rate (Klb/hr)	Quality (%)	Pressure (psig)	Temp. (°F)	
8	101	64	64	51	295	3.3
6	99	65	66	54	300	3.4
4	93	57	64	100	338	3.5
3	89	54	60	165	372	3.5
2-1/2	84	48	57	237	401	3.3
2	81	43	53	293	419	3.1
1-3/4	76	39	52	375	439	3.0

The electrical power output possible from these flow conditions was calculated assuming a turbine-generator efficiency of 75% as the steam expands from wellhead pressure to a back pressure of

4 inches of mercury. There is a broad power output maximum of 3.3 to 3.5 MWe over a range of wellhead pressures from 50 to 237 psig. This range will allow a wide latitude in the design of a wellhead generator system.

Pressure and temperature profiles taken during the throttled flow tests in January are shown in Figures 2 and 3. These profiles indicate that the fluid in the wellbore is at saturation conditions with a mixture of liquid and vapor flowing up to the wellhead, that is, with flashing occurring in the reservoir. Also shown in Figure 3 is the temperature profile 25 days after the well was shut in (zero flow rate). Examination of Figure 2 shows that the pressure profiles are essentially three constant slope lines meeting at the junction of the casing and slotted liner and at approximately 4300 feet. These constant pressure gradient lines indicate that the major production zones are near bottomhole and in the vicinity of 4300 feet.

Some limited information about the reservoir can be obtained by utilizing the theory for oil and gas wells. These standard petroleum engineering techniques, however, assume single phase flow, while the flow in HGP-A is definitely two-phase, so that extreme caution is required in interpreting the results of these analyses. Following the December discharge, a pressure buildup test was conducted, with bottomhole pressure being measured using two Kuster KPG pressure elements and recorders in tandem to ensure that pressure data were acquired in spite of equipment malfunction because of the high temperature. Figure 4 is a log-log type curve of the difference between bottomhole pressures during static (no flow) and flow conditions. It shows two distinct wellbore storage effects; the top of the second wellbore storage interval is indicated by the arrow A. Arrow B indicates the onset of the radial flow period, roughly 70 hours after the well is shut in. From these curves, the product of permeability and production zone thickness (kh) is calculated to be approximately 880 millidarcy-feet, with the pressure drop across the mud-damaged skin of the well being 560 psi.

Bottomhole pressure measurements made after HGP-A was shut in following the January test produced data and plots similar to those for the December test. However, close examination of the data shows that two consecutive straight-line approximations may be made to the Horner plot (Figure 5). Interpretation of this occurrence is that there are at least two different production layers in the wellbore with different kh values. The same effect is also present in the December data, but until it was reproduced in the January test, little credence was given to it. The results of these analyses are summarized in Table 4.

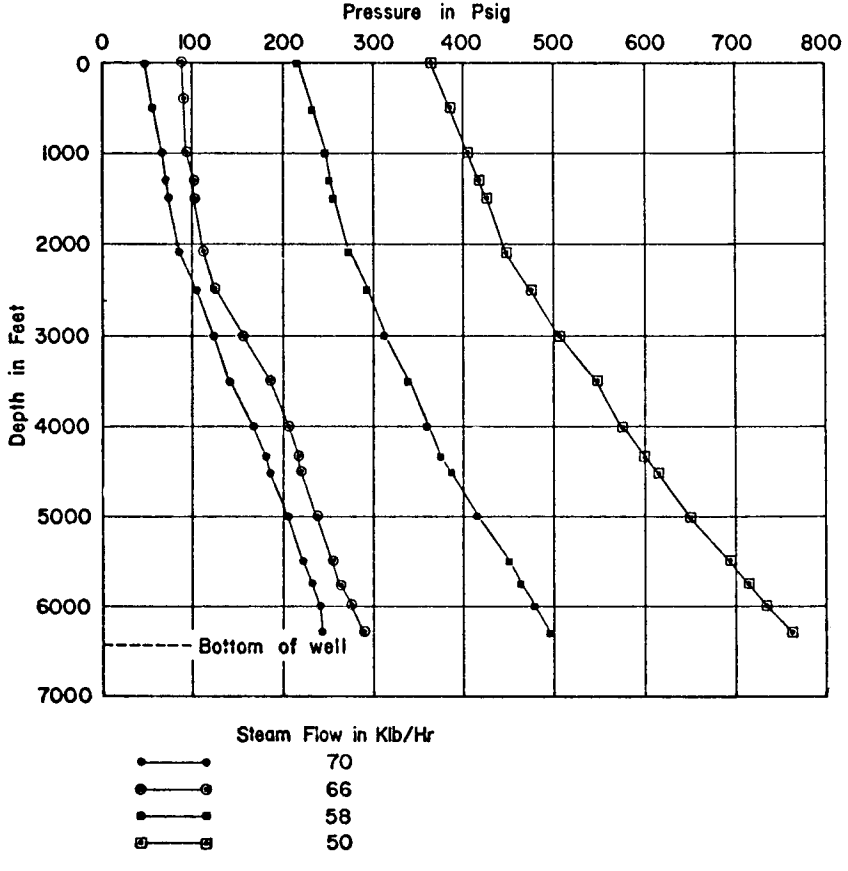

FIGURE 2. PRESSURE PROFILES FOR HGP-A

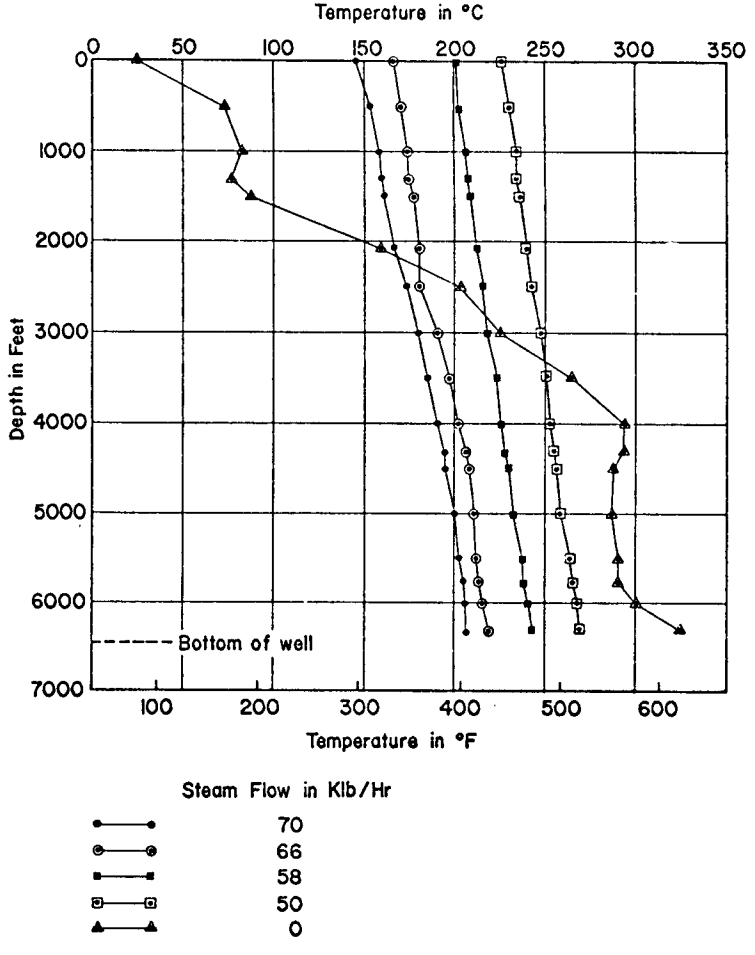

FIGURE 3. TEMPERATURE PROFILES FOR HGP-A

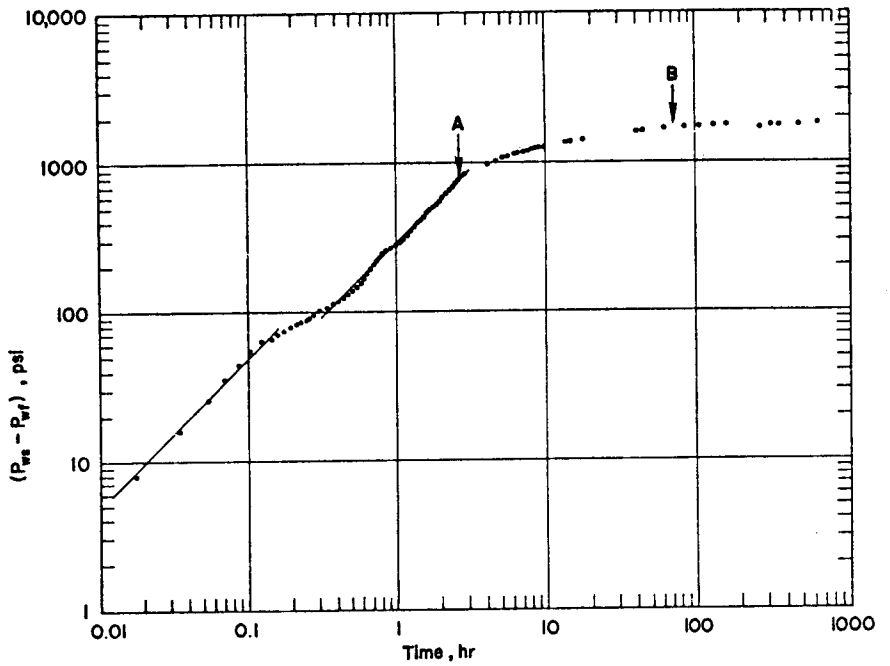

FIGURE 4. LOG-LOG PLOT OF DECEMBER PRESSURE BUILDUP TEST DATA

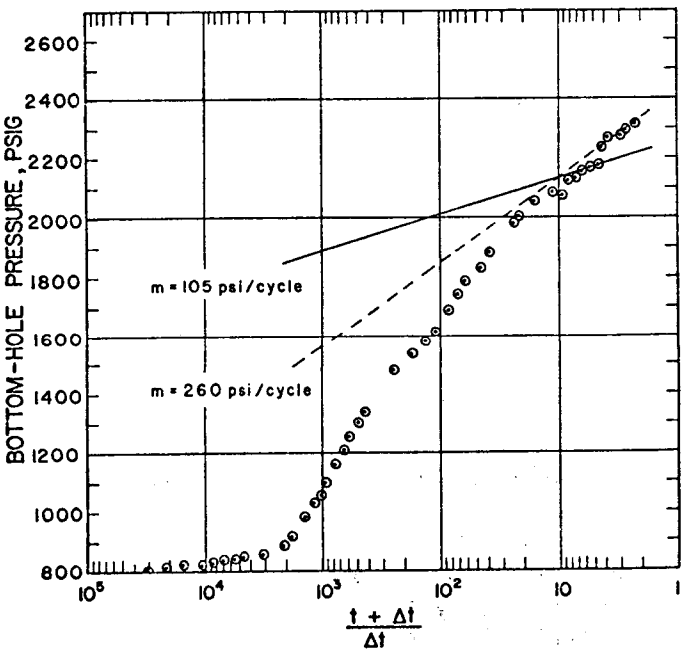

FIGURE 5. JANUARY/FEBRUARY PRESSURE BUILDUP TEST

Table 4 COMPARISON OF PRESSURE DRAWDOWN AND BUILDUP TESTS

	Constant Production Drawdown	December Buildup		January Buildup
		One Layer	Two Layer	Two Layer
Permeability thickness, kh, md-ft	1356	880	1553	1089
Apparent skin factor, s	-0.86	4.3	14.8	4.3
Pressure drop across skin, psi	---	561	1098	575
Flow efficiency	1	0.65	0.38	0.60

There is a substantial problem associated with the deposition of scale, primarily from dissolved silica. As an example, the muffler that was installed uses an annular region filled with cinders as a sound-absorbing agent. However, after only 16 days of flow, the scale deposited was sufficient to cement the cinders together so that removal required extensive chipping of the bound cinders.

A summary of the results of tests thus far is presented in Table 5.

Table 5 SUMMARY OF PRELIMINARY TEST RESULTS AND ANALYSES

Kapoho Geothermal Reservoir

1. Liquid-dominated
2. Tight Formation: Permeability Thickness ∿ 1000 md-ft
3. Very High Temperatures ∿ 350°C
4. High Formation Pressure ∿ 2000 psi
5. Slightly Brackish Water
6. Potentially Large Reservoir
7. High Silica Content

HGP-A Geothermal Well

1. During Flash Borehole Contains Steam and Water at Saturation
2. Flashing Occurs in Formation
3. High Wellhead Pressures ∿ 160 psi at 50 Klb/hr Steam
4. Producing Regions Probably at Bottomhole and 4300 Feet
5. Probably Has Severe Skin Damage
6. Potential Power Output ∿ 3.5 MWe
7. Flows Have Increased with Each Test

WELL INTERFERENCE STUDY OF THE MULTI-LAYERED SALTON SEA GEOTHERMAL RESERVOIR

J. G. Morse
University of California
Lawrence Livermore Laboratory
P. O. Box 808
Livermore, California 94550

A well interference testing program of the Salton Sea Geothermal reservoir is being conducted as part of a resource evaluation study by the Earth Sciences Geothermal Industrial Support Program of the Lawrence Livermore Laboratory. Studies to date indicate the reservoir rock to be composed of layered sequences of shales and sands. Wells involved in the testing program are being used in support of, or are in the vicinity of, the MAGMA-SDG&E Geothermal Loop Experimental Facility (GLEF), located in the Salton Sea Geothermal Field (SSGF). Between these wells, a shale layer has been correlated which appears to divide the reservoir into an upper and lower portion. Other thick sand and shale sequences may provide additional stratification. This report describes work in progress on a well testing program designed to determine the horizontal and vertical transmissivity and storage parameters between wells in the vicinity of the GLEF. These tests are being conducted with the cooperation and support of Magma Power Company and San Diego Gas and Electric Company.

The Salton Sea Geothermal Field

The Salton Sea Geothermal Field is located at the southeastern end of the Salton Sea which is within the physiographic province known as the Salton Basin. This basin which forms the northern part of the Colorado River Delta is a sediment filled structural trough called the Salton Trough.[1] The Salton Trough is part of a transition from the oceanic spreading center associated with the East Pacific rise to a major continental fault system that includes the San Andreas Fault.[2] The sequence of sedimentary rocks in the Salton Trough has been determined to be approximately 6000 m thick and composed primarily of detritus from the Colorado River.[3] A Geologic map of part of the Salton Trough that includes the Salton Sea Geothermal Field is shown in Figure 1.[3] Figure 2 shows locations of wells in the SSGF.[3] The shaded portion shows wells currently used in support of the GLEF.

A recent study, by Tewhey (1977), of drill cuttings and core samples from wells in the vicinity of the GLEF indicate the sequence of sedimentary rocks in the SSGF "can be divided into three catagories: (1) cap rock, (2) unaltered reservoir rocks, and (3) hydrothermally altered reservoir rock".[3] The cap rock extends from the surface to approximately 350 m. The first

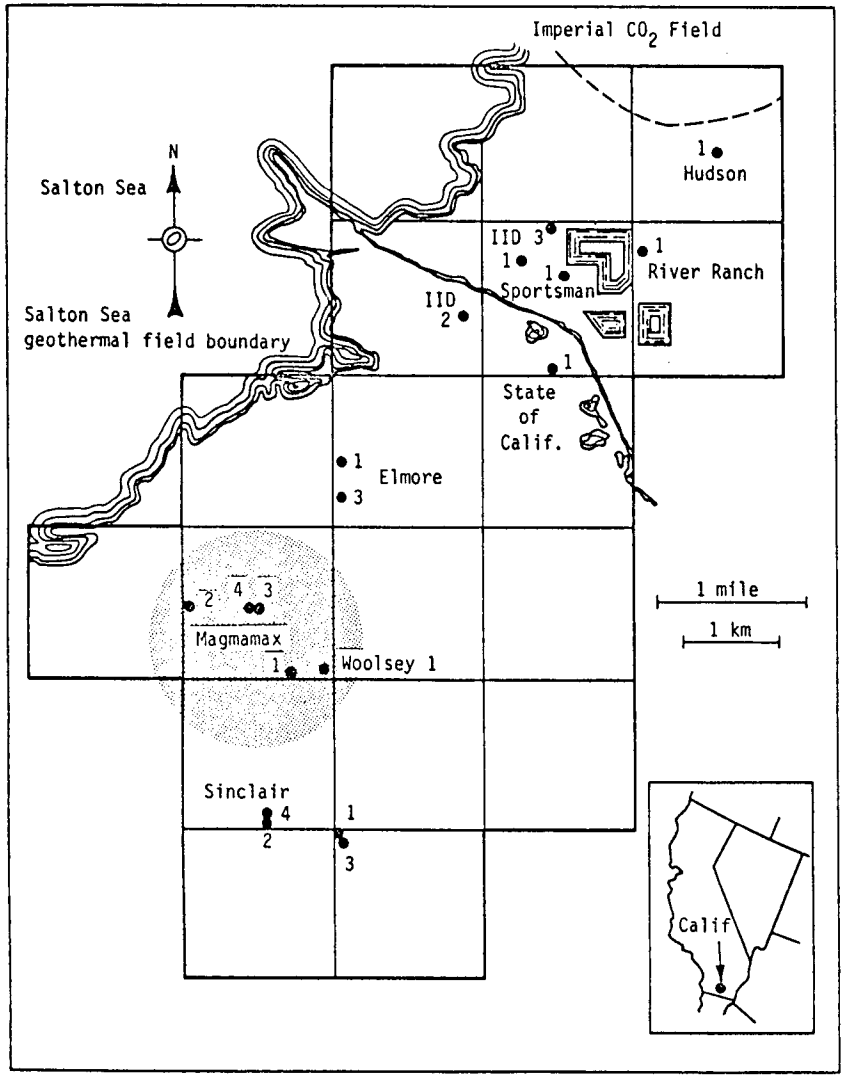

Fig. 2. Well locations in the SSGF. Wells in shaded area are presently used in support of Geothermal Loop Experimental Facility.

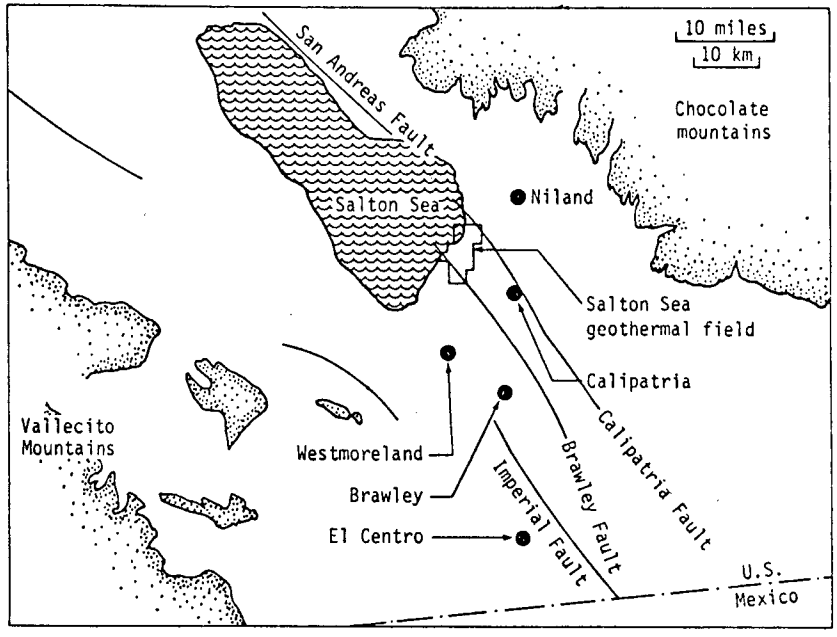

Fig. 1. Location of Salton Sea Geothermal Field and nearby faults in Imperial Valley.[3]

200 m consist of unconsolidated silt, sand and gravel. The rocks from 200 to 350 m are of low permeability consisting of a carbonate-clay matrix which appears to have undergone self-sealing through interaction with the brine.[3] The reservoir rocks consist of layered sequences of well-indurated shales, sandy-shales and sandstones. The transition from unaltered to hydrothermally altered rock is marked by the appearance of epidote.[3] The hydrothermal alteration appears to reduce the permeability and porosity of the reservoir rock. Secondary porosity and permeability appears to be present and renewable in the reservoir due to fracturing associated with natural seismicity and or hydraulic fracturing.

Description of Wells

The wells involved in this study are shown schematically in Figure 3. The location of the bottom of the cap rock, top of the zone of hydrothermal alteration and construction details in each well can be seen in Figure 3. A sequence of alternating sand and shale beds overlying a major shale break is present in all the wells involved in this study. This apparently continuous shale break was first correlated by Towse and Palmer.[4] The approximately 12 m thick shale divides the main reservoir rock sequence into an upper and lower reservoir. There appear to be additional thick sand and shale sequences which might produce further stratification of the reservoir.

The wells involved in this study are completed with perforations either above or below this correlated shale layer (shale break) except Woolsey #1 which is perforated above and below, see Figure 3. The well testing program is designed to take advantage of the wells being perforated in different lithologic horizons so as to measure the horizontal and vertiCle flow properties between wells.

Description of Tests

The initial tests, which are in progress, involve the wells in the immediate vicinity of the MAGMA-SDG&D GLEF. These are wells, Magmamax #1, 3, and 4 (MM 1, 3 and 4) and Woolsey #1 (WW 1). MM 1 and MM 4 are completed above the shale break and perforated in same lithologic horizons. MM 3 is perforated just below the shale break and is within 15 m of MM 4. WW 1 has a portion of its perforated interval in the same horizon as MM 1. Production wells for the GLEF are MM 1 and WW 1. They are operated in either a single or two well production mode. MM 3 is used as the injection well and MM 4 is designed as an observation well. To date interference tests have been conducted between MM 1 and WW 1, MM 3 and MM 4, and MM 4 and MM 1.

The interference test between MM 1 and WW 1 was conducted from June 16, 1977 to July 10, 1977. The reservoir had been shut-in for two months prior to the test. In this test, WW 1 was the production well and MM 1 was the observation well. MM 3 was the injection well for the spent brine and its interaction with MM 4 will be discussed later. Pressure was monitored in MM 1 for two weeks prior to starting interference test to establish a baseline pressure. WW 1 was primed using N_2 and commenced flowing

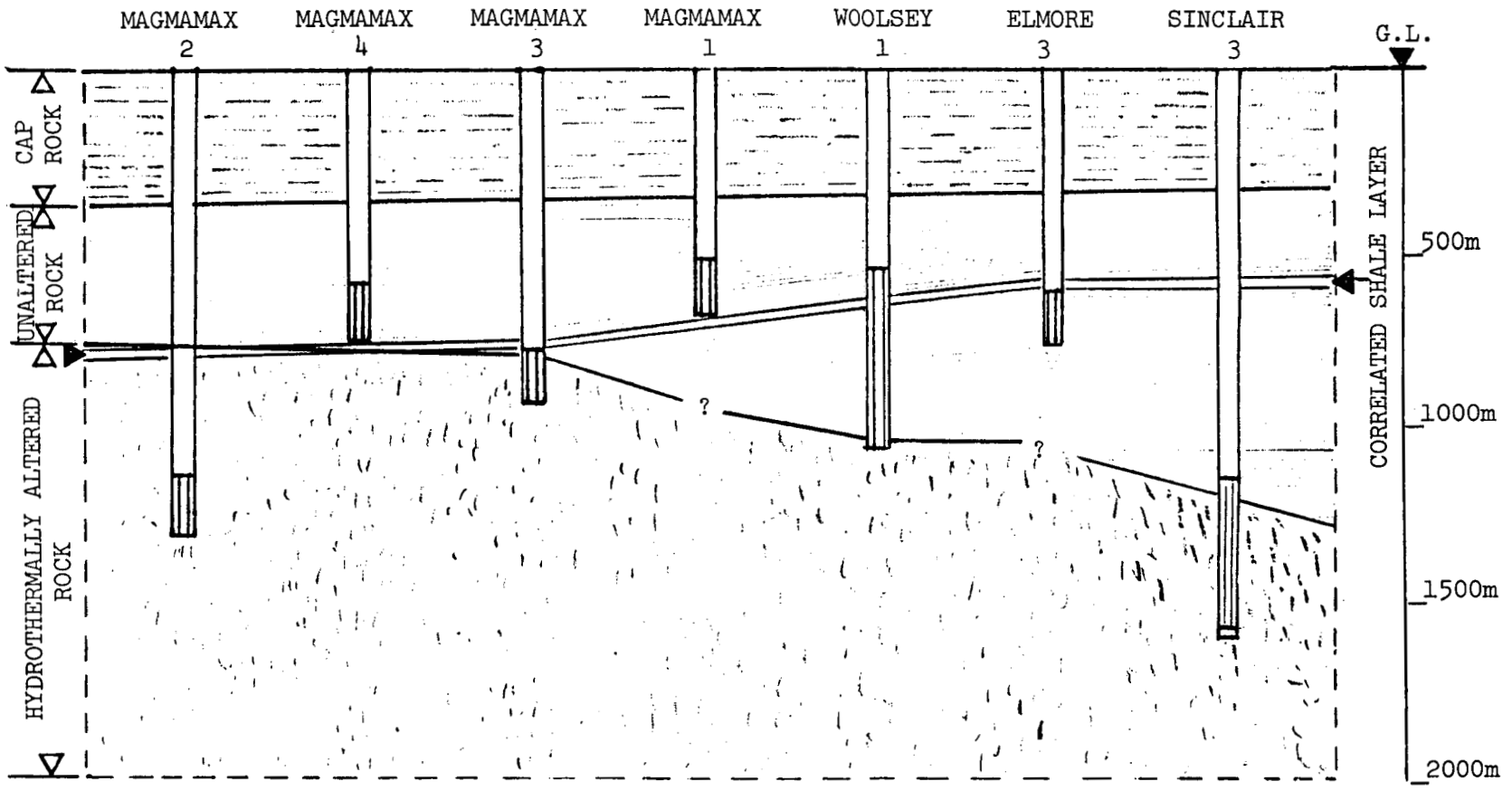

Figure 3: Schematic cross-section of wells involved in well testing program showing completion details within geothermal reservoir. Stripped intervals in wells indicate perforated zones. Note the unaltered rock portion of the reservoir increases in depth as you move away from Magmamax 2 toward Sinclair 3. Distances between wells are not drawn to scale.

on July 2, 1977. Well production was approximately 600-700 GPM. The well was shut-in on July 5. A pressure drawdown was observed in MM 1.

Pressure transient data was measured in MM 1 using a Sperry Sun pressure transmission system (0-1000 psi range). Because of corrosion problems, the pressure transient measurements were made at 30 m below the surface of the static fluid column rather than at reservoir depth. Pressure data recorded for two weeks prior to the test was somewhat noisy with an overall 24-hour pressure variation of 0.3 psi. This ambient noise appears to have been related to the sensitivity of the surface pressure transducer to ambient temperature changes. An overall pressure drop of 1.0 psi was observed during the test period. Analysis of the test data was done using the standard line source solution, log-log, curve matching technique. Interpretation of the data was complicated by a varying production rate and periodic flow reductions during the test to permit a "pigging" operation to be conducted. It was not possible to know exactly the percentage of production from WW 1 which was producing the drawdown in MM 1. An estimated flow rate was used to solve for transmissivity and storage parameters. Results from this test showed the two wells to be in communication and provided an estimate of permeability for the upper reservoir in the 500 md range. To resolve ambiguities present in this test, another test is planned with MM 1 as the producer and WW 1 as the observation well.

The test between MM 3 and MM 4 was conducted from June 16, 1977, thru the end of August. MM 3 was the injection well and MM 4 the observation well. The test was designed to measure the response in MM 4 (perforated above the shale break) to injection in MM 3 (perforated just below shale break). Pressure monitoring during the test was done first with Sperry Sun type equipment and then with a quartz crystal pressure gauge.

Injection pressures during the test averaged approximately 350 psi over static reservoir pressure in MM 3. During the entire period of the test no pressure response was observed in MM 4 which could be related to injection activities at MM 3. Flow rate into the injection well was approximately 600 gpm.

On both the Sperry Sun and quartz crystal pressure gauge, a daily 1.0 to 3.0 psi pressure fluctuation was observed. The diurnal cycle had a high at 03:00 am and a low at 17:30 pm. The phenomena appears to be related to daily heating and cooling of the lubricator. When opened, MM 4 produced a fair amount of CO_2 and seeped fluid at a low rate. When shut-in, the fluid pressure in the lubricator rose within 20 min to approximately 50 psi. Overall response of the well seems to indicate it is partially blocked with sufficient gas and fluid entry to rebuild surface pressure. If there is vertical leakage across the shale break due to injection into MM 3, it is sufficiently small so as not to produce an observable pressure response in partially blocked Magmamax #4 only 15 m away.

The test between MM 4 and MM 1 was conducted for approximately three weeks in September. MM 1 was the production well and MM 4 was the observation well. As in the previous test, no response was observed in MM 4. If a response was present, it was masked by the diurnal pressure noise in MM 4. An additional noise was present in this test due to a leak which developed in the hydraulic line wiper on top of the lubricator.

Additional Testing Plans

Plans are in motion to work over MM 4 so as to improve its performance as an observation well. Recent efforts at the MAGMA-SDG&E GLEF have been directed at installing solids control equipment so as to improve injectability of the spent brine. As a result of these activities, additional tests have not been conducted to date. In the near future, interference tests between MM 1, MM 4, MM 3, and WW 1 will be conducted. Fall-off surveys are also planned for MM 3 using the quartz gauge at reservoir depth. Improved well conditions and equipment should enable these tests to provide less ambiguous results.

Early in 1978, a long term multi-well interference test is planned. Magmamax #2 (MM 2), Elmore #3 (EM 3) and Sinclair #3 (SN 3) will be used as observation wells. The wells will be instrumented with quartz pressure gauges. During the test, MM 1 will be the production well and MM 3 will be the injection well. All three observation wells are perforated below the shale break. EM 3 is perforated in same interval as MM 3. MM 2 and SN 3 are both perforated at greater depth than MM 3. In this configuration, pressure transients recorded in the observation wells should provide a measure of the horizontal and vertical flow characteristics of the lower reservoir.

Upon completion of the well testing program, a formal report of the results will be issued by Lawrence Livermore Laboratory.

REFERENCES

1. T. D. Palmer, J. H. Howard, and D. P. Lande, 1975; Geothermal Development of the Salton Trough, California and Mexico, Lawrence Livermore Laboratory, Report UCRL-51775.

2. R. C. Schroeder, 1976; Reservoir Engineering Report for the Magma-SDG&E Geothermal Experimental Site Near the Salton Sea, California, Lawrence Livermore Laboratory, Report UCRL-52094.

3. J. D. Tewhey, 1977; Geologic Characteristics of a Portion of the Salton Sea Geothermal Field, Lawrence Livermore Laboratory, Report UCRL-52267.

4. D. Towse and T. D. Palmer, 1976; Summary of Geology at the ERDA MAGMA-SDG&E Geothermal Test Site, Lawrence Livermore Laboratory, Report UCID-17008.

PANEL SESSION--RAPPORTEURS' REPORTS

VARIOUS DEFINITIONS OF GEOTHERMAL RESERVES

Moderator: J. H. Howard, Lawrence Berkeley Laboratory, Berkeley, CA

Panelists: Dr. Stephen Lipman, Union Oil Co., P.O. Box 6854, Santa Rosa, CA 95406
Mark N. Silverman, Director Geothermal Loan Guarantee Program, DOE/SAN, 1333 Broadway, Oakland, CA 94612
James G. Leigh, Vice-President Lloyd's Bank of California, 612 S. Flower St., Los Angeles, CA 90017
Dr. L. J. Patrick Muffler, USGS, 345 Middlefield Road, Menlo Park, CA 94025
Mark Mathisen, Planning Department, Pacific Gas & Electric, 77 Beale St., San Francisco, CA 94106

Rapporteurs: George A. Frye, Aminoil USA, Inc., P.O. Box 11279, Santa Rosa, CA 95406
Vasel W. Roberts, Electrical Power Research Institute, P.O. Box 10412, Palo Alto, CA 94303
Alexander N. Graf, Lawrence Berkeley Laboratory,UC-Berkeley, 1 Cyclotron Rd., Berkeley, CA 94720

Introduction: Jack Howard and Werner Schwarz, LBL

To assess the importance of the confidence level of geothermal resources to those involved with the decisions on utilization, it was felt that a panel discussion to review the factors which affect the confidence level would be of general interest. With that objective, the panel members listed above were convened to discuss the problems of confidence level of the various sectors of the geothermal community. To allow for freedom of expression of the panel members, formal prepared presentations were not required. Instead three rapporteurs also representing diverse sectors of the community, industry, non-profit institutions, and government agencies, were requested to prepare summary overviews of the panelists' remarks. The rapporteur reports follow:

George A. Frye

The title of the panel could have alternatively been "What Constitutes Geothermal Reserves?" To answer this question the panelists presented almost a continuum of viewpoints from optimistic liberalism to extreme conservatism.

Dr. L. J. Patrick Muffler from the U.S. Geological Survey presented the Survey's methodology in reserve classification. He discussed the analogy with petroleum and mineral classification and presented Flawn's 1966 definition of reserves as "that quantity of minerals that can be reasonably assumed to exist and which are producible with existing technology and under present economic conditions." To implement this

definition the Survey first identifies a resource base, quantifies the resource within it, and finally applies existing technology and present economic condition constraints to develop a reserve number.

Under this methodology, the concept of reserves in the future is highly speculative even for a quantified resource. Geological Survey Circular 726, Assessment of Geothermal Resources - 1975 is therefore explicitly resources and "in lieu of an objective analysis, subjective decisions were made as to the most likely divisions" (reserves or other categories). As a final comment Dr. Muffler stated "you must have drill holes for reserve calculations."

The second panelist, Stephen C. Lipman of Union Oil Company of California, concurred that Flawn's reserve definition was reasonable for Circular 726 as a national energy planning guide. He cautioned, however, that we should not be overly optimistic in making reserve estimations. For a resource industry standpoint the key phrases in this definition are existing technology and present economic conditions.

The geothermal developers are spending large sums of money to establish the size of the geothermal reserves, which are orders of magnitude larger than the initial plants being planned. Initial designs at East Mesa, Brawley, Heber, Valles Caldera, and Roosevelt Springs vary between 10 and 50 megawatts. The capital requirements for this initial reserves determination must come from the corporation, which will not see any return on its investment for eight to ten years. In contrast, this utility will begin generating income within three years from its initial capital outlay. The rate payer could benefit by having the utility share some of the developer's risk by installing the small initial plants during the reserve determination phase of development.

Union does not list geothermal reserves in their Annual Report to the stockholders until a contract has been consummated with a utility and the required construction permits have been obtained (e.g., Philippines, The Geysers).

Mr. Lipman was questioned on Union's method of reserve determination. He responded that it would take a minimum of three deep wells to perform an interference test. Assuming that these wells were in hydrologic communication with each other, this would provide data of reservoir productibility, injectivity, permeability, and porosity-thickness. Geological and geophysical studies could provide estimates on the size and configuration of the resource. This is the stage of development when a small power plant would be most beneficial in determining the optimum surface and subsurface engineering design for the ultimate field development.

Mark R. Mathisen, Pacific Gas and Electric Company, substituted for Arthur L. Martinez, Public Service Company of New Mexico. Due to Mr. Mathisen's experience he confined his comments to The Geysers and related PG&E's history. PG&E began construction on their first unit of twelve megawatt capacity in 1958. All wells required for this unit were drilled and completed. At that time the company viewed this effort as a research and development project. The unit commenced commercial production in 1960; additional units followed and by 1965 the company had adopted a development attitude toward geothermal resources at The Geysers.

Reflecting on this history, Mr. Mathisen commented that a utility is closely regulated and reviewed for undue risks; a utility does not normally fund research and development. However, in this case risk acceptability was favored by low entry costs. Thus for utility, as with many private enterprises, risk has a size connotation. Risk acceptance is increased by knowledge and at The Geysers PG&E has made commitments to build units of 110 megawatts on about 800 acres of proven area. The number of steam wells per unit varies due to individual well flow capacities. Even at The Geysers reserves determinations contain uncertainty and pose the problem of reservoir guarantee. That is, the company must be on the alert for any reduction in geothermal generating capacity so it can fulfill its supply commitments.

James G. Leigh, Lloyd's Bank of California, spoke as a representative of the banking industry. A banker is not trained to determine the reservoir, but to assess its value. A banker utilizes the asset anology "Can it be sold?" If affirmative, "What is its fair market liquidation value?" A banker's method for this value (and implicitly reserves) is to discount (at loan interest rate) future cash flows from a proven field. A proven field must be running a minimum of six months. In addition, commercial banks will only write loans with firms of established collateral value, i.e., loan is fully guaranteed against balance sheet or the federal government.

As to risk analysis, banks assess more carefully than steam suppliers or utilities, generally one per cent and under. Rates of interest are contingent on risk and federal guarantees command the best rate. Finally, the contract geothermal steam price and terms are crucial to the fair market liquidation value, i.e., take or pay, advance payments.

Mark N. Silverman, Director, Geothermal Loan Guarantee Program, DOE, discussed geothermal reserves from the federal government aspect. While the goal of the DOE is to encourage geothermal exploration, the loan guarantee program requires reasonable assurance that the loan can be repaid. Sufficient data must be available to substantiate claims of applicant. While the definition of sufficient data varies, an application based solely on geothermal surface manifestations, i.e., tuffa mounds, is clearly inadequate. The federal program's risk acceptability appears to be more conservative than the geothermal resource seller, buyer, and federal scientist; it certainly must be more liberal than a commercial bank in order to encourage geothermal development. In actual numbers, approved loan applications have been assessed at greater than 60 per cent success. Mr. Silverman believed that utilities can and will do more, as knowledge is gained, to assume more of the risk caused by uncertainty of reserves that is now assumed by the steam supplier.

Vasel W. Roberts

At a time when geothermal energy producers and users are on the threshold of commercial development of water-dominated geothermal resources, the need for a common basis of communicating ideas and concepts about a relatively complex commodity has never been greater. The Workshop organizers are to be commended for recognizing this need and addressing the perplexing use of the term "geothermal reserve." Since a commonly accepted definition of geothermal reserve has not yet emerged, it is difficult to use the term with any degree of certainty.

The panel discussion revealed some of the reasons for this difficulty, namely, the use of different definitions for different purposes, none of which are mutually exclusive, but may yield significantly different interpretations of the quantity of energy on hand at any given time. Similar problems exist with other terms, such as reservoir, resource and resource base, due in part to the possibility of different depth and temperature datum, coincidence of heat and fluid deposits, and purity and producibility.

Dr. Muffler discussed a generic definition that has application to mineral resources in general. His definition was as follows:

> --Quantities of minerals that can be reasonably assumed to exist and that are producible with existing technology under present economic conditions--

Dr. Muffler also discussed the McKelvey diagram as a convenient method for graphically describing the resource. This definition is excellent from a national and regional point of view, for the purpose of estimating relative importance, developing policy, and placing effort in areas of greatest potential. On the other hand, the definition is not precise, since it relies on "reasonable assumptions" rather than hard data and marketability. It seems to have limited application at the point of negotiation of energy sales or purchase.

Dr. Lipman approached the subject from an entirely different point of view. From the resource companies' point of view the definition is as follows:

> --A geothermal resource becomes a reserve when commitments are made to build power plants to utilize a portion of the resource--

This definition says that a resource is not a reserve until a sales contract exists. This poses some interesting problems in that the prospective buyer of the energy usually would like assurance that a reserve exists prior to the commitment to build power plants.

Indeed, Mr. Mathisen's view was that:

> --A portion of the resource is considered a reserve only after the necessary wells for the power plant have been drilled and flow tested for a specified period of time--

The definitions by Dr. Lipman and Mr. Mathisen tend to be conservative, and underestimate reserves in comparison with Dr. Muffler's definition.

Mr. Leigh's viewpoint as a banker was:

> --A resource becomes a reserve only after its market liquidation value is known with 99 per cent certainty--

Under this definition, the market liquidation value of all leases might be construed to represent reserve, albeit small. Since the value of a lease may increase as exploration and development progresses, the amount of recognized reserve could steadily increase well into the production phase. This definition is only loosely related to the magnitude of the resource, but faces the reality of the need for liquidity by lending institutions.

The fifth definition was given by Mr. Silverman, Director of the Geothermal Loan Guarantee Program for the Department of Energy. His definition uses probability of project success as the criteria as follows:

> --A reserve is considered to exist if a project proposed by an applicant for a loan guarantee has a 60 per cent or higher probability of success--

It is interesting, but perhaps not surprising, that the five panelists, representing the resource, utility, and banking industries, and two federal agencies, expressed five different definitions of geothermal reserve. Each serves a particularly useful purpose, yet none of them seem to qualify as a common denominator. Although these definitions are valid under each set of circumstances and can be very useful, there still seems to be a need for an acceptable industry-wide definition that all can use in communicating with each other.

Mr. Leigh suggested that the resource be accounted in terms of BTU's to which a value could be associated. This is a fundamental approach that is well understood, and is one that most probably could be generally accepted; however, it is important to recognize that the value of a BTU will be dependent on the temperature at which it is delivered and the purity of the fluid in which it is contained. Temperature affects conversion efficiency, and both temperature and purity can affect capital costs and O&M.

Dr. Lipman suggested that utilities should be willing to share more of the initial risks of geothermal development with the resource companies. There are indications in evolving projects that there may be a trend in this direction. Certainly, the risk seems to be higher on first-of-a-kind geothermal resources or power plants, but may be a transient phase in the course of geothermal development. In any case, there is little actuarial geothermal data upon which to base risk assessment; however, as more power plants are constructed, the level of confidence in the resource among utilities should increase.

Alexander N. Graf

The purpose of this panel was to consider the definition of geothermal reserve. Each panelist represented a different viewpoint or entity concerned with the development of geothermal resources. It is quite evident that significant variations in the definition exist.

Dr. Muffler's interest was in defining reserves in terms of an available national energy resource. Dr. Lipman's concern centered on the importance of expediting the development of specific projects, and protecting the interest of stockholders. Mr. Mathisen's position was that of defending the conservative nature of public utilities in their cautious development of new energy sources. Mr. Leigh's concern with the definition of geothermal reserve was limited to the determination of collateral value of producing reserves, which might be used to finance new or further development. Mr. Silverman's interest seemed to focus on expediting development by providing needed guarantees to worthy projects, based on a definition of geothermal reserves utilizing probability of success.

Dr. Muffler, USGS-Menlo Park, began the discussion with three commonly accepted definitions--Resource base, Resources, and Reserves. Reserves were defined as the quantities of minerals that can be reasonably assumed to exist and which are producible with existing technology under present economic conditions. Dr. Muffler reviewed the McKelvey Diagram, and a logic diagram which might jointly be described as follows: The resource base is split into accessible and inaccessible, the accessible resource base (defined by depth) is divided into useful (Resource) and residual, with useful split further as identified and undiscovered. Reserves are defined as accessible, useful, identified, and economic. Dr. Muffler concluded that a reserve is something you really know, and that you can make hard, immediate investment decisions on.

Dr. Lipman, Union Oil Company, felt that Dr. Muffler's definitions are useful for defining national energy strategies, but that the key words in the definition of geothermal reserves should be economically recoverable, and using current technology. From an industry standpoint the use made of reserve determinations are twofold, to convince a utility that there are sufficient reserves to build a plant, and for reservoir management planning. Industry's experience has been that they have been required to 'over prove' by many orders of magnitude the reserves required to safely install an electrical generating plant, resulting in delays and greater capital expenses. The development process might be expedited if the utilities would assume a share of the initial risk. The economics of geothermal energy are different than those of oil and gas because of the extended development/return of investment time period. Dr. Lipman indicated that Union Oil Company carries economic identified resources on its books as reserves only if there is a commitment from a utility to build a plant. The only current Union Oil Company reserves are at The Geysers, and in the Philippines.

Mr. Mathisen, Planning Department-PG&E, stated that PG&E recognizes that its position with regard to geothermal resources development has been conservative. Among the reasons cited for this approach are that PG&E is responsible to the CPUC, concerned about maintaining its high bond rating, and naturally wary about entering financial commitments to new energy sources. PG&E's position in the past has been that only after the wells necessary to service a plant have been drilled and satisfactorily flow tested by the developer, can the resource be elevated to a reserve. PG&E's position has become more flexible due to the positive experiences it has had at The Geysers. Mr. Mathisen believes that faced with the opportunity to develop a new geothermal field PG&E might require less proof of multiple reserves than they did from the developers of The Geysers.

Mr. Leigh, Energy Department-Lloyd's Bank of California, considers a geothermal reservoir an asset. A bank's definition of a reservoir is its fair market liquidation value today (which is the sum of all discounted future net revenues from the field, assuming that it has been operating at least six months), as opposed to definitions involving economic recoverability or current technology. It is the practice in the oil and gas industry to raise capital for the development of a new field by using their producing fields as collateral. A commercial bank is not in the business of providing funds for a new geothermal field

development without additional collateral. A commercial bank's risk ratio must be 1 per cent or less, thus a bank's definition of geothermal reserve is a resource suitable for use as collateral, which is 99 per cent known. Very few geothermal fields can qualify as collateral.

Mr. Silverman, Geothermal Loan Guarantee Program-DOE/SAN, considers each loan guarantee application to determine if the data submitted is sufficient to substantiate the applicant's claims. If the claims are confirmed then an economic analysis is conducted in order to determine that the applicant will be able to repay the loan according to the specified schedule. The definition of reserve will vary depending on the type of application, location, known data, and claims made by the applicant. As a general rule a reserve is considered to exist if the analysis of the applicant's proposal indicates that the probability of success is in excess of 60 per cent.

Each of the entities represented by the panelists plays an essential role in the development of geothermal prospects. A common definition of reserves would be a useful tool for communication among these groups. Developing a definition common to all of them may be an unrealistic goal; however, discussions of this type are very stimulating, and play an important part in defining differences.

Optimal Timing of Geothermal Energy Extraction

Kamal Golabi
Woodward-Clyde Consultants, San Francisco

Charles R. Scherer
University of California, Berkeley

Introduction

This paper is concerned with the optimal time to commence extraction of energy from a hot-water geothermal reservoir. The economic models that we have presented in the past have the common characteristics that the extraction program starts immediately (see [1] and [2]). Based on this assumption, we determined optimal extraction strategies and planning horizons such that the present values of total profits were maximized. In this study we relax the requirement that extraction be undertaken immediately, seeking instead the delay in starting time that along with the other decision variables maximizes the present value of total profits over the economic life of the reservoir. Of course, optimal starting time, economic life of the reservoir, optimal extraction rate, and optimal injection temperature are interrelated, and therefore, we analyze their effect on the overall planning strategy simultaneously.

Physical Assumptions

Our economic model is based on a production-reinjection well doublet (Gringarten-Sauty model [3]) where the aquifer is assumed to be saturated and homogeneous and is bounded top and bottom by impermeable aquicludes. The initial equilibrium temperature of the aquifer is T_o. After τ years from the start of pumping, the temperature declines below T_o, and this temperature is denoted by T_o^t, showing the dependence of the temperature on time. Our economic model can easily accommodate other hydrothermal models. However, the Gringarten-Sauty model allows for expressing T_o^t as a function of energy extraction rate (see Trang et al. [4]), and this functional relationship simplifies our analysis of the economic model.

Hot water is pumped from the aquifer, run through a heat exchanger and reinjected to the aquifer. Low-pressure steam is generated on the other side of the heat exchanger. We will assume that steam can be sold at the cost of the least expensive alternative to produce this steam.

The Economic Model

We will assume that the real value of energy increases with time in an exponential manner. Extraction commences at time u and continues for L years at the rate of Q, and the brine is reinjected in the aquifer at the temperature of T_i. We are interested in maximizing the total discounted profits. In other words, we like to:

$$\underset{u,\,L,\,Q,\,T_i}{\text{Maximize}} \quad \Pi(u, L, Q, T_i) = (1-\eta)\int_{u}^{\tau+u} a\,P_o e^{rt} Q c_f \rho_f (T_o - T_i) e^{-it} dt$$

$$+ (1-\eta)\int_{\tau+u}^{L+u} a\,P_o e^{rt} Q c_f \rho_f (T_o^t - T_i) e^{-it} dt \qquad (1)$$

$$- C(u, L, Q, T_i),$$

subject to:

$$u, L, Q \geq 0$$

$$T_i \geq T_s$$

$$T_o^t - T_i \geq \delta$$

where

P_o = price (value) of energy at time zero,

r = rate of increase of real energy price,

η = royalty for geothermal lease paid as a fraction of revenues,

Q = extraction rate (m^3/hr)

c_f = specific heat of the fluid (cal/gr°C),

ρ_f = fluid density (gr/cm^3),

i = discount rate,

u = starting time (years),

τ = breakthrough time (years),

L = extraction period (years),

T_i = injection temperature (°C),

T_o^t = production temperature as a function of time (°C) for given extraction rate,

T_s = steam temperature (°C).

$C(\ )$ = total cost as a function of decision variables,

and a is a conversion factor to yield revenues in dollars/year.

The cost function includes capital costs for wells and equipment, operating and maintenance costs, rents and salaries, and termination costs. C is, of course, a function of our four decision variables.

The constraints simply imply that the injection temperature (which is the same as the heat exchanger outlet temperature) should remain above the steam temperature, and that the difference between the inlet and outlet temperatures of the heat exchanger should not fall below a certain level, δ (we are ignoring heat losses in surface pipes).

Optimization

Denoting the sum of the first two expressions in (1) as revenues $R(u, L, Q, T_i)$, we show that if total revenues associated with immediate extraction (R) can be computed (as done in [2]), then the analogous revenue when extraction delay is incorporated is just:

$$R(u, L, Q, T_i) = e^{(r-i)u} R \tag{2}$$

Likewise, for costs we show that total costs when delay is considered may be written as:

$$C(u, L, Q, T_i) = C_1 e^{-iu} + C_2 e^{(r-i)u} \tag{3}$$

where

C_1 = total extraction costs less pumping energy costs

and

C_2 = pumping energy costs.

We also show that the optimal injection temperature T_i can be expressed as a function of Q and L. These results enable us to show that for each Q and L, the optimal starting time is either equal to zero or is given by

$$u^* = -\frac{1}{r} \ln\left[\frac{(i-r)B}{iH}\right] \qquad (4)$$

where

$$B = R - C_2$$

and

$$H = C_1 - (\text{annual pre-exploition rent}/i).$$

In other words, depending on the value of the parameters involved, the profit maximizing entrepreneur should either start extraction immediately or wait for a time of u* years (as given by equation 4) before commencing extraction.

An interesting result which greatly facilitates the computation of the optimal vector (Q*, L*, u*) is our result that for each L, either the optimal extraction rate is the Q that maximizes B^1/H^{i-r}, or Q_o, the optimal extraction rate when extraction is immediate, depending on whether the ratio (i-r)B/iH falls between 0 and 1 or not. Using this result, we have developed an algorithm that finds the global maximum efficiently.

Results

The optimization is conducted with a particular set of data which to our best judgment reflects the current value of pertinent costs. The geohydrological data have generally been chosen in mid-range of values associated with known hot-water geothermal resources.

We note that the computer program developed for this study can be readily utilized for decision making under a different set of conditions. Geohydrological and economic data are inputs to the program, and the cost subroutine can be easily modified to accommodate the particular costs involved in the exploitation of each individual field.

In our computations we allowed interest rate i to vary from 4% to 15% and r, the real energy value growth rate, from 1% to 3%.

As expected, optimal profits decrease as i increases and increase as r increases. Also, the optimal starting time increases with r and decreases with i. In other words, when the rate of increase in value of energy is high, the profit maximizing entrepreneur postpones the onset of extraction, while he prefers to start extraction immediately if the value of energy is not expected to rise as fast.

The optimal pumping rate increases with i and decreases with r. Thus, as r is increased, the optimal decision is to extract heat more slowly and leaving more heat for the future when the value is higher. An interesting result is the fact that even when extraction is postponed, the optimal extraction rate is approximately the same as the optimal rate when extraction is immediate.

The economic lives L* are nonincreasing in i and nondecreasing in r (with L* taking predominantly the value of the assumed well life). Thus, when future profits are discounted more heavily, the entrepreneur tends to start extraction sooner and pumps the energy faster over a shorter period of time compared to when the discount rate is not as high.

References

1. Golabi, K., and C.R. Scherer. "Optimal Management of a Geothermal Reservoir." Proceedings of the Second Workshop on Geothermal Energy Reservoir Engineering. Stanford, California, December 1976.

2. Golabi, K., and C.R. Scherer. Optimal Extraction of Geothermal Energy. University of California, Los Angeles, California. ENG-UCLA Report 7715. June 1977.

3. Gringarten, A.C., and J.P. Sauty. "A Theoretical Study of Heat Extraction for Aquifers with Uniform Regional Flow." Journal of Geophysical Research, pp. 4956-4962. December 1975.

4. Tsang, C.F., P. Witherspoon, and A.C. Gringarten. "The Physical Basis for Screening Geothermal Production Wells from the Effects of Reinjection." Lawrence Berkeley Lab, Report LBL 5914. 1976.

PREDICTING THE RATE BY WHICH SUSPENDED SOLIDS PLUG GEOTHERMAL INJECTION WELLS

L. B. Owen, P. W. Kasameyer, R. Netherton, and L. Thorson
University of California
Lawrence Livermore Laboratory
P. O. Box 808
Livermore, California 94550

Standard membrane filtration tests have been used by the oil industry for more than 20 years to evaluate injection well performance. Published analytical models are also available for relating filtration data to injector lifetimes. We have utilized these techniques to evaluate injection at the Salton Sea Geothermal Field, Southern California. Results indicate that direct injection into reservoir zones with primary porosity is not feasible unless 1 μm or larger particulates formed during or after the energy conversion process are removed.

Injection Rationale

Commercialization of geothermal resources in the United States will require injection as the preferred means of waste effluent disposal. Prevention of surface and groundwater pollution is an obvious rationale for waste injection. Reservoir pressure- and temperature-maintenance and subsidence control may also, in many instances, mandate subsurface disposal. When evaluating geothermal injection systems, advantage can be taken of the extensive experience gained by the oil industry during the last 20 years in the design and operation of massive waterflood operations.

Potential injection problems can be grouped with respect to well completion techniques, casing corrosion and waste effluent chemistry (Jordan et al., 1969). This paper deals with evaluation of injection problems at the Salton Sea Geothermal Field (SSGF) caused by suspended solids formed during or after the energy conversion process.

WORK PERFORMED UNDER THE AUSPICES OF THE U.S. DEPARTMENT OF ENERGY, CONTRACT NO. W-7405-ENG-48.

The work was carried out as part of the Lawrence Livermore Laboratory Industrial Support Program which provides technological support for the joint Magma Power-San Diego Gas and Electric Company-DOE 10 mw Geothermal Loop Experimental Facility (GLEF) located in the SSGF (Austin et al., 1977; Quong et al., 1977).

Analytical Method

Barkman and Davidson (1972) developed quasi-steady-state analytical solutions for calculating the effect of suspended solids on a porous medium. The models require injection well geometry, formation characteristics, suspended solids concentration and filter cake permeability as input data. We used the open-hole solution for injector failure by filter cake build-up on the porous formation surface (no invasion) to arrive at a conservative estimate of injector half-life:

$$t_{1/2} = \frac{3\pi\, r_w^2\, h\, (\rho_c/\rho_w)}{i_o w} \left(\frac{k_c}{k_f}\right) \ell n \left(\frac{r_e}{r_w}\right) \quad \text{for} \quad \frac{k_c}{k_f} \leq 0.05$$

where:

i_o	=	injection rate (m^3/sec)
r_w	=	wellbore radius (m)
h	=	injection interval (m)
r_e	=	effective radius (m)
k_f	=	formation permeability (mD)
k_c	=	filter cake permeability (mD)
(ρ_c/ρ_w)	=	density ratio: filter cake/brine
$t_{1/2}$	=	half-life of injector (sec)
w	=	suspended solids concentration (ppm)

For a single well at the SSGF operating at an injection rate of 0.04 m^3/sec (Figure 1), the injection rate-permeability product $(i_o/h)\, k_f$ ranges between 4000 and 100,000 (B/D-FT) mD. To insure injectivity with a half-life greater than one year, the water quality ratio w/k_c must be $<<1$. For a perforated completion, the half-life estimate is reduced by a factor proportional to the perforated area.

Membrane filtration tests were used to measure the ratio w/k_c. A plot of cumulative filter throughput as a function of time approaches a straight line provided a filter cake forms.

$$\frac{w}{k_c} = \frac{2000}{S^2/60} \left[\frac{\left(\frac{\rho_c}{\rho_w}\right) A_c^2 \Delta p_t}{\mu} \right]$$

S= slope of linear portion of filtration curve $(ml/\sqrt{min})$
A= area of filter exposed to brine (cm^2)
ΔP_t= pressure drop across filter (Atm)
μ= brine viscosity (cp)

The intercept of the linear portion of the filtration curve, if negative, indicates plugging without filter invasion, or, if positive, plugging with filter invasion. Examples of both types of filtration curves for effluents from the SSGF are shown in Figure 1.

Membrane Filtration Apparatus

A schematic diagram of the filtration apparatus is shown in Figure 2. 47 mm Nuclepore polycarbonate membrane filters were mounted in Nuclepore stainless steel in-line holders. Temperature drops in the system were minimized by insulating all lines and bypassing most of the flow at the filter holder. All runs were made at a differential pressure of 50 psig and temperatures of $\sim 80°C$. Suspended solids concentrations were measured in accordance with procedures outlined by Doscher and Weber (1957).

A novel brine-tolerant flow metering system was employed. The volume measuring system consisted of a 23 kgm load cell and associated power supply, digital voltmeter and elapsed timer. This system produced accurate average flow rates and total volume throughputs. Linear calibration curves were obtained by transferring known volumes of brine to the storage container and recording load cell output in millivolts.

Results

Filtration tests were performed with three types of brine effluents: One experiment was run adjacent to the injector (Magmamax No. 3) and two experiments were run in conjunction with the LLL test unit located adjacent to the producing well (Magmamax No. 1).

The effect of process chemistry on filtration characteristics is summarized in Table 1. None of the effluents were suitable for direct injection into a porous medium as indicated by relatively high values of w/k_c.

Magmamax No. 3 Wellhead

Tests run at the injection wellhead were carried out during a period when acidified condensate was remixed with brine effluents (∿110°C) from the GLEF at a point upstream of the injection pump. Dilution of brine by acidified condensate significantly reduced scaling in the injection line and improved long-term performance of the injection pump. Suspended solids (lead sulfide) concentrations were also reduced to <50 ppm with respect to nominal solids levels of ∿150 ppm (mostly silica) during injection without condensate recombination. Most of the PbS particles were between 5-10 μm in diameter.

LLL Test Unit

Filtration characteristics of acidified and unmodified effluents from the LLL four-stage flash system were also determined. The flash system is a model of the GLEF and is being used to assess scale control, by chemical modification (primarily acidification), and corrosion. During acidification runs, hydrochloric acid was injected into the brine input line of the second-stage separator (190-210°C). Filtered solids were composed of iron-rich amorphous silica. The concentration of particulates in brine prior to filtration was 14 ppm for acidified effluent and 150 ppm for unmodified effluent. The order of magnitude decrease in suspended solids in acidified brine demonstrates the effect of reduced pH on silica precipitation kinetics. The diameter of deposited solids varied from collodial to about 10 μm. Low permeability filter cakes formed because dissolved silica effectively sealed interstices between deposited solids.

Discussion

Data from membrane filtration tests indicated that silica solids, ranging in size from<1μm to 10μm, are present in SSGF effluents. These solids form low permeability filter cakes (0.4 to 10^{-5} mD). The analytical model was used to compute the half-life of the Magmamax No. 3 injection well. Our measured values of water quality ratio lead to a short predicted lifetime for injection into porous formations in Magmamax No. 3 ($t_{1/2}$ < 0.01 years). However, brine has been successfully injected into Magmamax No. 3 on an intermittent basis from March of 1976, to the present, far longer than expected for a porous medium. This contridiction is resolved by results of a spinner survey reported by Nugent and Vick (1977) which indicated plugging of all but four feet of the 458-foot slotted liner during the initial eight months of intermittent injection. Subsequently, the well was worked over and injection resumed. One week later, all

porous zones were plugged again as predicted by the model. The four-foot interval, which is interpreted as a fracture zone, continues to accept fluid at rates up to 800 gal/min.

The analytical model was also used to evaluate injection data presented by Mathias (1975) for East Mesa well 5-1. The observed half-life of 0.0002 years is in good agreement with our calculated half-life of less than 0.002 years (assuming w = 92 ppm, k_f = 69 mD, h $\leq$ 301 m, open hole completion, and $k_c \leq 1$ mD.).

Brine Treatment Requirements for Injection

Removal of solids from brine prior to injection may require some form of final filtration. Knowledge of effective pore size of the formation is required for establishment of minimum filtration requirements. Since core samples of reservoir rocks from Magmamax No. 3 were not available, absolute filtration requirements were estimated on the basis of filter tests and calculations of mean reservoir pore diameter.

Formation pore size can be estimated to be less than 20 μm since a 20 μm filter does not plug, but the formation does. The Carman-Kozeny equation can be used to estimate mean pore diameter for given values of porosity and permeability (Champlin et al., 1977). Using values of average porosity 20% (Tewhey, 1977) and average permeability 500 mD (Morse, 1977) estimated mean pore diameter are about 11 μm. The largest particle that can pass through pores is conservatively estimated to be 10% of the average pore diameter (Barkman and Davidson, 1972) suggesting that absolute filtration to 1 μm or less will be required to insure injectivity in porous zones.

Formation damage may occur even after absolute filtration. Harrar et al. (1977) found that solids continue to precipitate from SSGF effluents held at 90°C at rates controlled by brine pH or degree of dilution with water prior to incubation. The effect of delayed precipitation away from the well is difficult to forecast, and successful injection may require hold-up time prior to filtration. Chemical reactions between formation rock and filtered effluents must be understood. To that end, cores flushing experiments with filtered brine will be continued at the SSGF.

Conclusions

Membrane filter tests are useful in evaluating injectivity of geothermal effluents. Techniques are available for estimating injector half-life utilizing filtration data. Injection of brine with suspended solids is not feasible in reservoir zones with primary porosity. However, long-term injection of brine and suspended solids can apparently be achieved in fracture zones.

Table 1. Filtration Characteristics of SSGF Effluents (80°C)

Process Chemistry	Filter Pore Size (μm)	Slope (ml/$\sqrt{min}$)	w/k_c (ppm/mD)	w (ppm)	Solids
	0.4	1010	448	24	
Acidified Condensate Recombination	0.4	190	12,655	27	
	1.0	210	10,360	32	5-10 μm PbS
Brine pH ∿5.5	5.0	169	15,996	46	
	10.0	95	50,621	10	
	0.4	32	123,464	150	
Unmodified Brine pH 5.8	2.0	540	434	150	<1-10 μm Amorphous SiO_2
	5.0	147	5,851	150	
	10.0	44	65,303	150	
	1.0	50	50,629	14	
Acidified Brine pH ≤4.6	5.0	12	878,972	14	<1-10 μm Amorphous SiO_2
	10.0	21	287,011	14	

FILTRATION CURVE WITHOUT INVASION

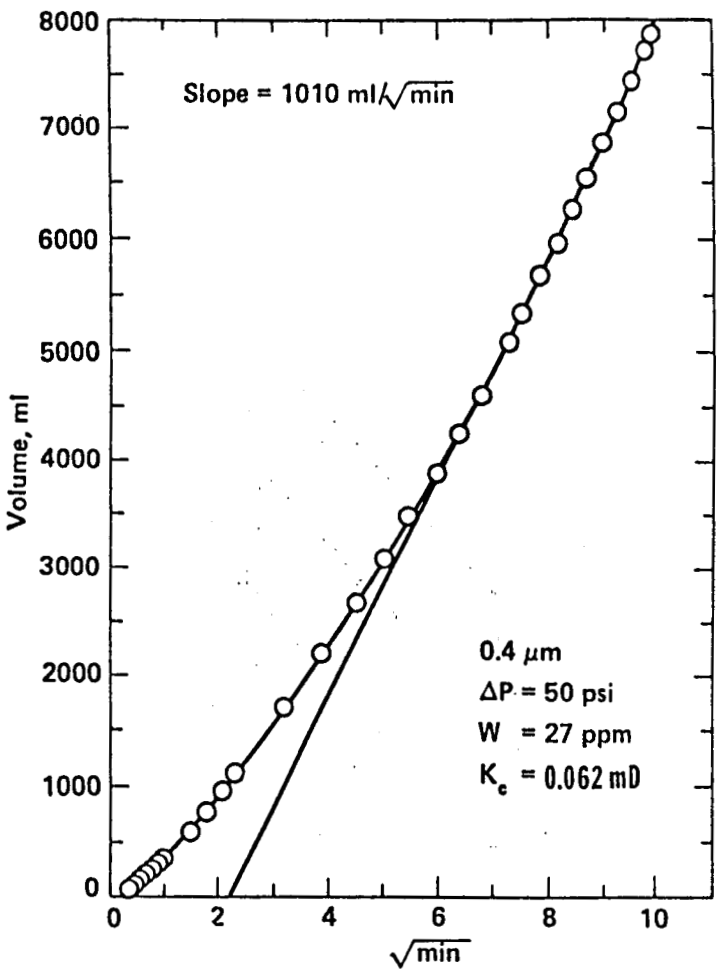

FILTRATION CURVE WITH INVASION

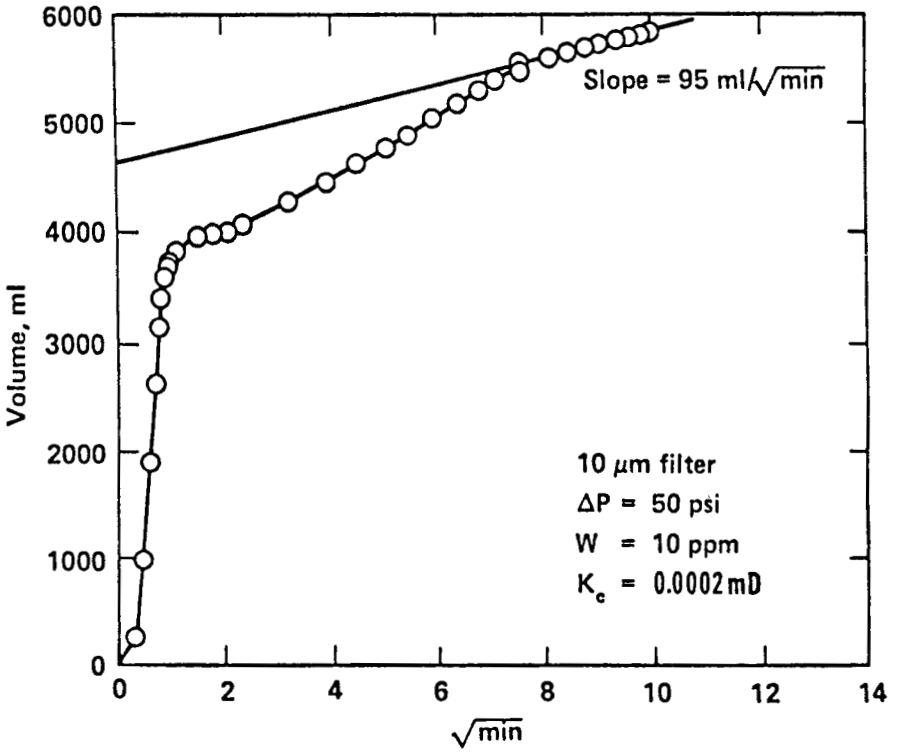

Figure 1. Filtration curves for Magmamax #1 brine, measured at the injection wellhead.

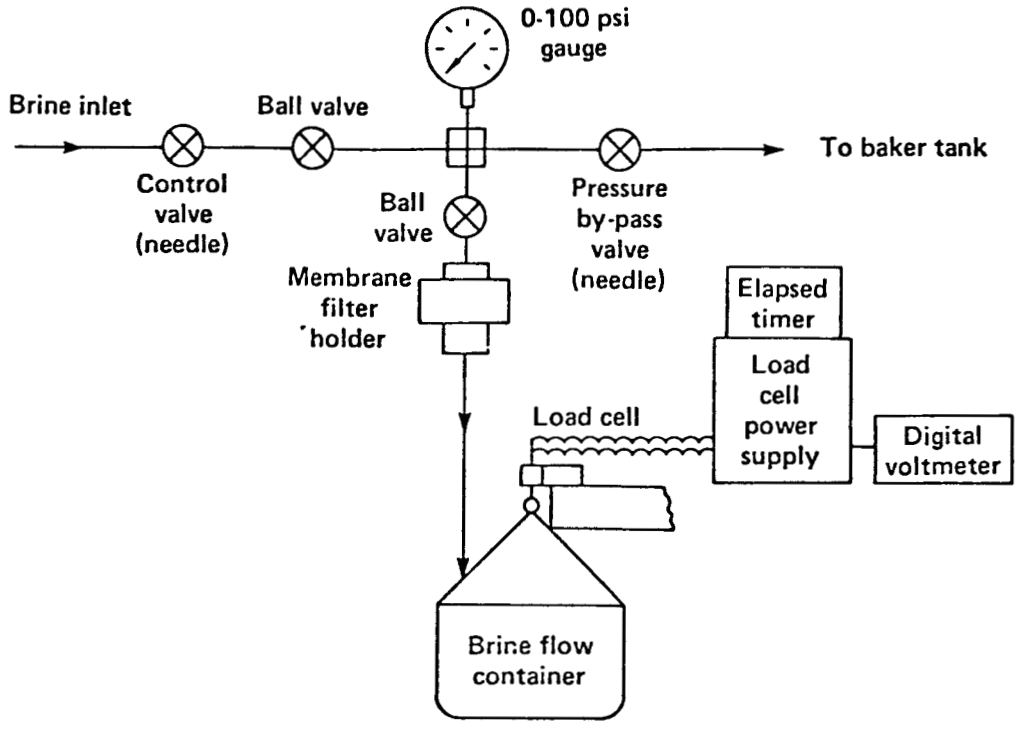

Figure 2. Membrane filtration apparatus.

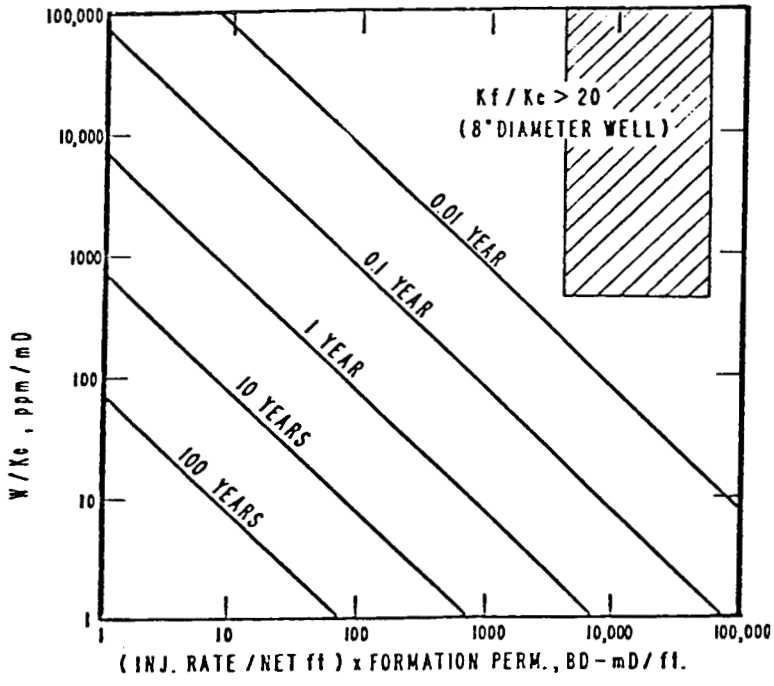

Figure 3. Calculated injection half-lives for porous formations (after Barkman and Davidson, 1972). The shaded area indicates the range of values assumed for Magmamax #3. (k_f=100-300 mD, i_0=0.04 m^3/sec., h=100-500 feet, and the measured water quality ratios are 450-100,000 ppm/mD.)

References

Austin, A. L., Lundberg, A. W., Owen, L. B., and Tardiff, G. E., (1977), the LLL Geothermal Energy Program Status Report January 1976-January 1977: Lawrence Livermore Laboratory Report UCRL-50046-76.

Barkman, J. H., and Davidson, D. H., (1972), Measuring Water Quality and Predicting Well Impairment: Jour. Petroleum Technology, p. 865-873.

Champlin, J. B. F., Thomas, R. D., and Brownlow, A. D., (1967), Laboratory Testing and Evaluation of Porous Permeable Rock for Nuclear Waste disposal: U.S. Bureau of Mines Report of Investigations No. 6926.

Doscher, T. M., and Weber, L. (1957), The Use of the Membrane Filter in Determining Quality of Water for Subsurface Injection: Drilling and Production Practice, (API), p. 169-179.

Harrar, J. E., Otto, C. H., Jr., Hill, J. H., Morris, C. J., Lim R., and Deutscher, S. B., (1977) Determination of the Rate of Formation of Solids from Hypersaline Geothermal Brine: Lawrence Livermore Laboratory Report UCID-17596.

Johnston, K. H., and Castagno, J. L., (1964), Evaluation by Filter Methods of the Quality of Waters Injected in Waterfloods: U.S. Bureau of Mines Report of Investigations No. 6426, 14 pgs.

Jordan, C. A., Edmondson, T. A., and Jeffries-Harris, M. J., (1969), The Bay Marchand Pressure Maintenance Project-Unique Challenges of an Offshore Sea-Water Injection System: Jour. Petroleum Technology, p. 389-396.

Mathias, K. E., 1975, The Mesa Geothermal Field - A Preliminary Evaluation of Five Geothermal Wells: Second U.N. Symposium on the Development and Utilization of Geothermal Resources, V. 3, p. 1741-1747.

Morse, J. G., (1977), Well Interference Study of the Multi-layered Salton Sea Geothermal Reservoir: Third Annual Workshop on Geothermal Reservoir Engineering, Stanford University.

Nugent, J. M., and Vick, L. R., (1977) Well Operations - Salton Sea Geothermal Field: Geothermal Resources Council, Transactions, V. 1, p. 233-234.

Quong, R., Bishop, H. K., and Hill, J. H., (1977), Scale and Solids Deposition in the SDG&E/U.S. ERDA Geothermal Loop Experimental Facility at Niland, California: Geothermal Resources Council, Transactions, V. 1, p. 249-250.

Tewhey, J. D., (1977), Geologic Characteristics of a Portion of the Salton Sea Geothermal Field: Lawrence Livermore Laboratory Report UCRL-52267.

The Effect of Radially Varying Transmissivity on the Transient Pressure Phenomenon

Leonard D. Mlodinow and Chin Fu Tsang
Lawrence Berkeley Laboratory
University of California
Berkeley, California 94720

1. Introduction

During reinjection of cooled geothermal fluid into a reservoir, chemical precipitation and other processes may occur changing the permeability of the aquifer. In general, the permeability becomes a function both of time and space. This will, of course, affect the injection well. Some attempts† have been made to analytically predict the pressure response. The present paper describes our calculations which yield analytic expressions, in terms of a single integral, for a wide class of physically reasonable permeability functions. Results are presented for a few typical examples.

2. Governing Equations

Consider an aquifer consisting of a horizontal slab of thickness, h, penetrated normally by a line source supplying a flow Q. The aquifer medium is taken to be isotropic. In our simplified model we neglect gravity, consider the system to be isothermal, and consider only a single fluid phase. The governing equation is then given by

$$\beta_o \mu \phi \frac{\partial p}{\partial t} = \nabla \cdot K \nabla p \qquad (1)$$

if we assume that $\beta \nabla p \cdot \nabla p << \frac{1}{K} \nabla \cdot K \nabla p$. Here $\beta_o \equiv$ compressibility, $\mu \equiv$ viscosity. $\phi \equiv$ porosity, are taken constant*, and $K \equiv$ permeability, $p \equiv$ pressure.

Given a permeability function of space and time, (1) yields the pressure distribution that results. The present work solved equation (1) for a large class of physically reasonable permeability function. In particular, we look for a family of constant K surfaces in space-time which may be physically reasonable. Let r_o be the distance from the line source to the fluid front. Since the volume of fluid pumped into aquifer equals the volume of aquifer occupied, we see that the fluid front propagates to

$$r_o(t) = Ct^{1/2}$$

where C is a constant. Thus if r is the distance of any point in the

* The same analysis can be easily adapted to the case where μ is not a constant, but that K/μ is in the form of the permeability functions described below.

† For example, A. Sklar, Lawrence Livermore Laboratory Annual Report (1977) unpublished.

aquifer to the source, then points with $r^2/t < C^2$ will have permeability K_∞ and if $r^2/t > C^2$ they will have permeability K_o. Points with the same value of the ratio r^2/t will have the same permeability. We shall solve equation (*1*) first for permeabilities of the form,

$$K(\underset{\sim}{r},t) = K_o\, \beta(r^2/t) \qquad (2)$$

where r is the cylindrical radial coordinate, and β is an arbitrary function. We shall then extend the class of solutions to those of the more general permeability function

$$K(\underset{\sim}{r},t) = K_o\, \alpha(t)\, \beta\left[r \Big/ \int_o^t \alpha(t')dt'\right] \qquad (3)$$

where α is an arbitrary positive function of t.

3. Solution

To make equation (*1*) dimensionless, units are chosen so that $\beta_o\phi = 1$, $\mu = 1$, and *limit* $K(\underset{\sim}{r},t) \equiv K_o = 1$ then dimensionless quantities are:
$r \to o$

$$m' = \frac{m(gm)}{c} \quad ; \quad r = \frac{r(cm)}{b} \quad ; \quad t' = \frac{t(sec)}{a}$$

where typically $a = \beta_o\mu\phi \sim 10^{-13}$sec; $b = \sqrt{K_o} \sim 10^{-5}$ cm; $c = \mu ab \sim 10^{-20}$gm.

Thus (*1*) becomes

$$\frac{\partial p}{\partial t} = \underset{\sim}{\nabla} \cdot \beta\, \underset{\sim}{\nabla}\, p \qquad (4)$$

If we look at the solutions where p is a function of r only, $p(\underset{\sim}{x},t) = \bar{p}(r,t)$. Then

$$\frac{\partial \bar{p}}{\partial t} = \beta \frac{\partial^2 \bar{p}}{\partial r^2} + \left[\frac{\beta}{r} + \frac{\partial \beta}{\partial r}\right]\frac{\partial \bar{p}}{\partial r} \qquad (5)$$

Next we change variables $\begin{matrix} r \\ t \end{matrix} \longrightarrow \begin{matrix} z \equiv r^2/t \\ w \equiv t \end{matrix}$, and apply the separation of variables,

$$\bar{p}(r,t) = P(z,w) = \phi(w)\chi(z)$$

On substitution, we find $\phi(w) = 1$ and χ satisfies

$$\frac{\partial^2 \chi}{\partial z^2} + \left[\frac{1}{z} + \frac{\partial\, \ell n\beta}{\partial z} + \frac{1}{4\beta(z)}\right]\frac{\partial \chi}{\partial z} = 0 \qquad (6)$$

which is really a first order differential equation for $\partial\chi/\partial z$.

It remains only to integrate the equation and impose the remaining boundary conditions, which are

$$p(r,o) = p_o \qquad p(\infty,t) = p_o$$

$$\lim_{r\to o} 2\pi rhK(\underset{\sim}{r},t)\frac{\partial p}{\partial r} = -Q$$

$$\lim_{t\to\infty} 2\pi rhK(\underset{\sim}{r},t)\frac{\partial p}{\partial r} = -Q$$

In terms of the variable z, these boundary conditions correspond to

$$\chi(\infty) = p_o \qquad \lim_{z\to o} z\frac{\partial \chi}{\partial z} = \frac{-Q}{4\pi h}$$

Thus the solution of (6) after putting in units is,

$$p(\underset{\sim}{x},t) = p_o + \frac{\mu Q}{4\pi hK_o} e^{(1/4)I(0)} \int_{\frac{\beta_o\mu\phi}{K_o}\frac{r^2}{t}}^{\infty} \frac{e^{-(1/4)\,I(z')}}{z'\beta(z')}\,dz' \qquad (7)$$

where $$I(z) \equiv \int^z \frac{dz'}{\beta(z')} .$$

Finally, we obtain the solutions for the more general permeability (3) from those solutions already obtained. The method depends on a property of the differential equation

$$\frac{\partial f}{\partial t} = K(r,t)\frac{\partial^2 f}{\partial r^2} + \left[\frac{K}{r} + \frac{\partial K}{\partial r}\right]\frac{\partial f}{\partial r} \qquad (8)$$

and does not depend on the specific form of K other than its being a function of r and t only (e.g., the same method could be used to generate new solutions if [8] is initially solved for other forms of K).

To get the new solutions assume that (8) has been solved for f, with a given K. Then consider the transformed function

$$f_\alpha(r,t) \equiv f\left[r, \int_o^t \alpha(t')\,dt'\right]$$

where α is an arbitrary positive function. f_α does not satisfy (8) since

$$\frac{\partial f_\alpha}{\partial t} = \alpha(t)\frac{\partial f}{\partial t}$$

Rather f_α satisfies,

$$\frac{\partial f_\alpha}{\partial t} = K_\alpha(r,t)\frac{\partial^2 f_\alpha}{\partial r^2} + \left[\frac{K_\alpha}{r} + \frac{\partial K_\alpha}{\partial r}\right]\frac{\partial f}{\partial r}$$

where $$K_\alpha(r,t) \equiv \alpha(t)\,K\left[r, \int_o^t \alpha(t')dt'\right]$$

Furthermore, the boundary conditions on f_α and f are the same so that if p is the pressure response due to K, then to find the pressure at the

point (r,t) when the permeability is K_α, we just evaluate p at the point (r,τ) where

$$\tau = \int_0^t \alpha(t')dt' \ .$$

4. Results

We have calculated the pressure distributions resulting from the following permeability functions

$$K_0 = K_0$$

$$K_1 = K_0\left[1 - \frac{\rho}{z+\varepsilon}\right], \ \rho = 10^{-7} \ \varepsilon = 4\rho/3$$

$$K_2 = K_0\left[1 - \frac{\rho}{z+\varepsilon} + \frac{1}{3}\frac{\rho^2}{(z+\varepsilon)^2}\right], \ \rho = 10^{-6} \ \varepsilon = 2\rho/3$$

$$K_3 = K_0 \exp\left[-\rho/(z+\varepsilon)\right] \ , \ \rho = 10^{-6} \ \varepsilon = 4\rho/3$$

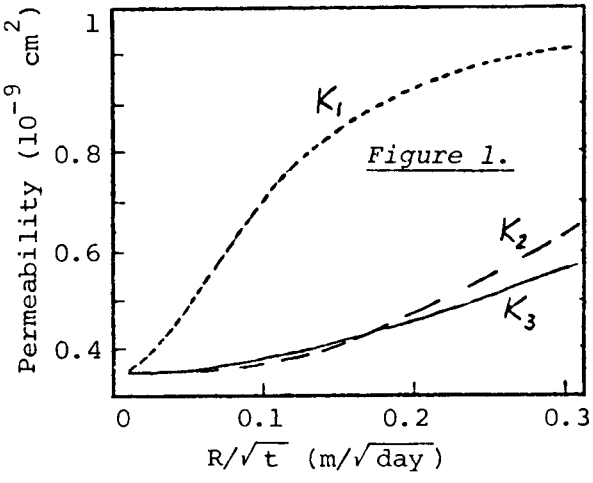

Figure 1.

For comparison permeabilities K_1 - K_3 are graphed v s. $r/\sqrt{t}$ in Figure 1*.

The constant permeability K_0 leads to the Theis Solution which is graphed in Figure 2. Figures 3-5 give graphs of K_1 - K_3 and the corresponding calculated pressure distributions.

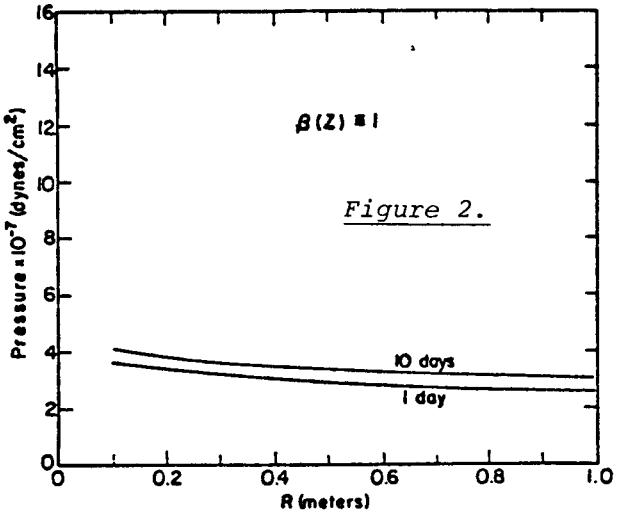

Figure 2.

5. Summary

We have obtained an analytical solution for the pressure response in a reservoir with permeability of the form $K = K(r^2/t)$. It has been found that these solutions may be used to generate additional solutions for

$$K = \alpha(t)K\left[r^2 \Big/ \int_0^t \alpha(t')dt'\right]$$

---

* In this Figure, the parameters in K_3 are $\rho = 1.85 \times 10^{-6}$ and $\varepsilon = (4/3)\rho$. Hence, at z=o all the permeability functions K_1 to K_4 have the value $0.25\,K_0$.

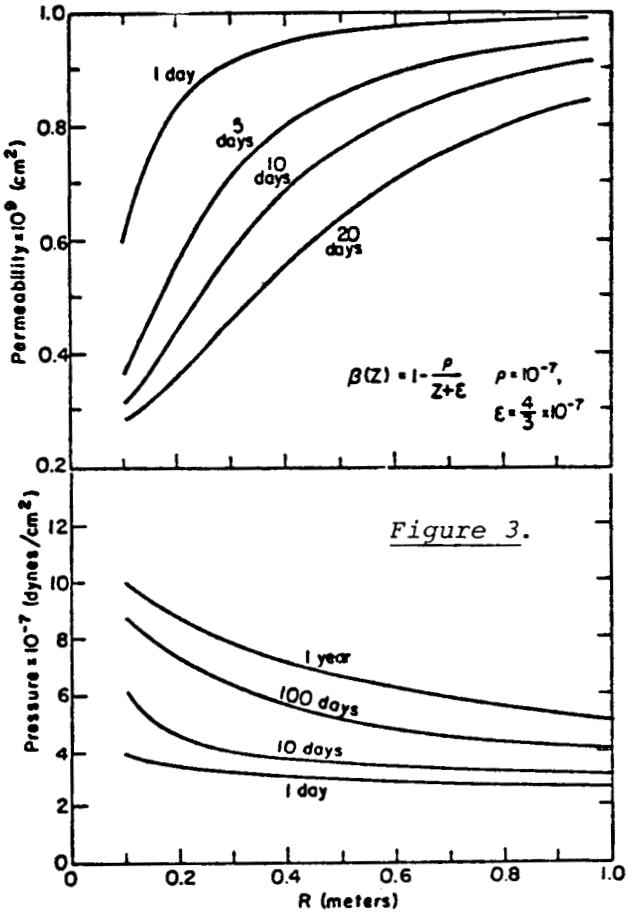

Figure 3.

Several function forms for $K(r^2/t)$ have been studied and the resulting pressure distributions calculated.

A general method for generating the pressure response $\bar{p}$ for a permeability

$$\bar{K}(r,t) = \alpha(t) K\left[r, \int_0^t \alpha(t')dt\right]$$

was developed, once the solution $p(r,t)$ is previously found (analytically or numerically) for a permeability function $K(r,t)$. The solution for $\bar{K}(r,t)$ is

$$\bar{p}(r,t) = p\left[r, \int_0^t \alpha(t')dt\right]$$

The only restriction on α is that it be positive.

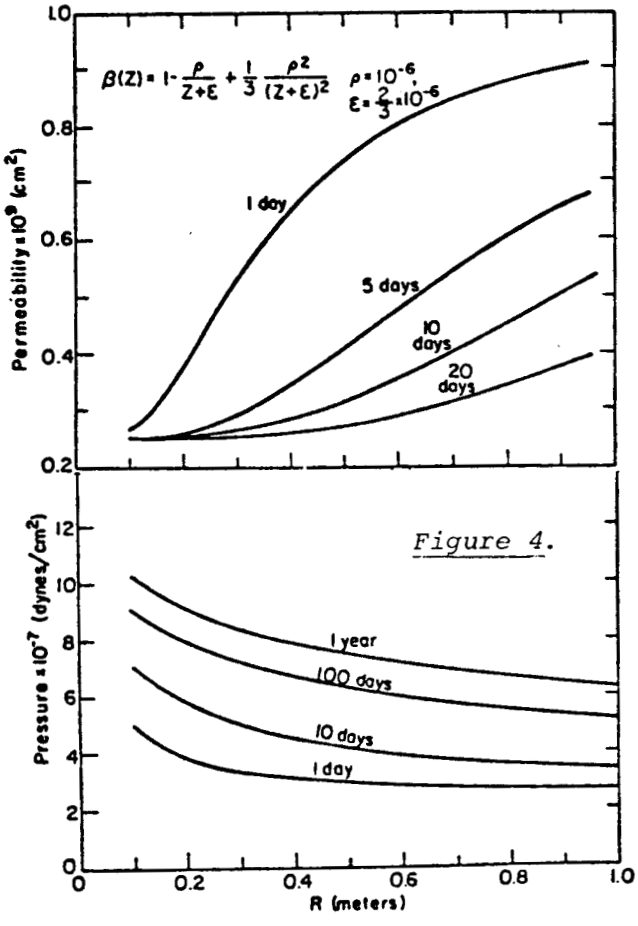

Figure 4.

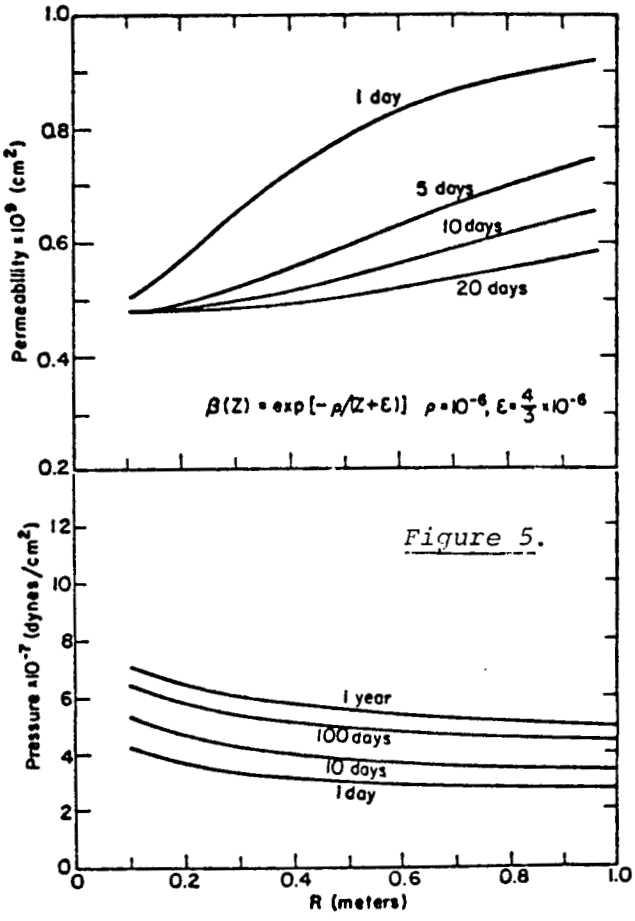

Figure 5.

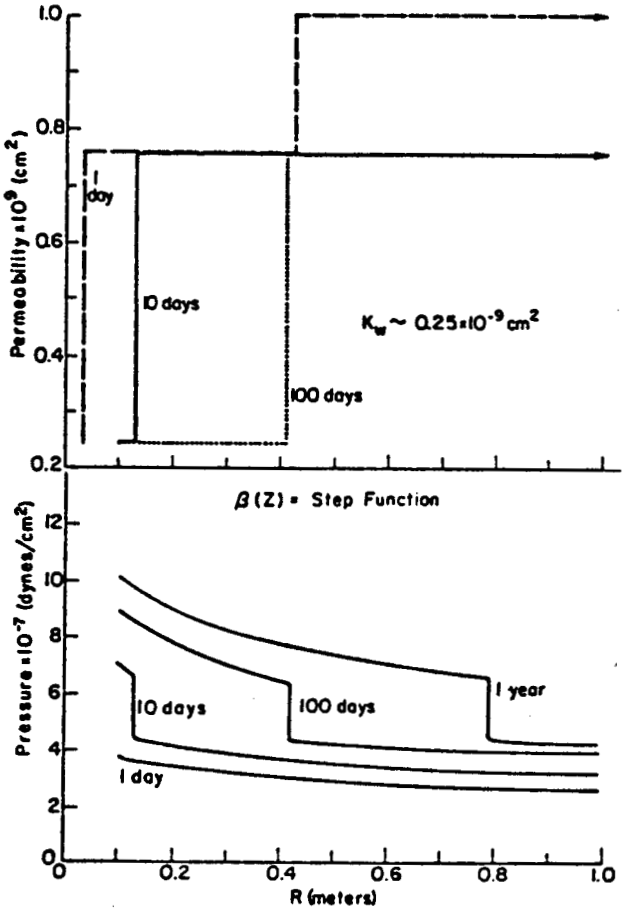
1.0
0.8
0.6
0.4
0.2
Permeability x10⁹ (cm²)
1 day
10 days
100 days
K_w ~ 0.25x10⁻⁹ cm²
β(Z) = Step Function
12
10
8
6
4
2
0
Pressure x10⁻⁷ (dynes/cm²)
10 days
100 days
1 year
1 day
0
0.2
0.4
0.6
0.8
1.0
R (meters)

Figure 6.

SALTON SEA GEOTHERMAL RESERVOIR SIMULATIONS*

T. D. Riney, J. W. Pritchett and S. K. Garg
Systems, Science and Software
P. O. Box 1620, La Jolla, California 92038

The Salton Sea Geothermal Field (SSGF) is a high-salinity, high-temperature resource. The San Diego Gas & Electric Company has constructed a nominal 10 MWe Geothermal Loop Experimental Facility (GLEF) which will use brine produced from Magma Power Company's Woolsey No. 1 (W1) and Magmamax No. 1 (M1) wells; the Magmamax No. 2 (M2) and No. 3 (M3) wells will be used for reinjection. Intermittant brine production/injection has been performed since May 1976, but no associated fluid flow data have been published. The Lawrence Livermore Laboratory (LLL), however, has correlated the data available from surface measurements and logs from various wells in the SSGF. We have used this limited data base and the MUSHRM simulator to synthesize a preproduction reservoir model for a portion of the SSGF which contains the GLEF site. The simulator is then applied to the model to examine reservoir performance under different assumptions to improve our understanding of the system and its potential for exploitation.

DATA BASE AND MODELING APPROACH

The main sequence reservoir rock in the SSGF is bedded sandstone with shale lenses and layers, overlain with a relatively impermeable shale bed (caprock), and is believed by the LLL investigators to be separated into "upper" and "lower" reservoirs by a relatively thick and continuous shale layer [Towse, 1975; Schroeder, 1976]. From studies of cores, cuttings and logs from wells drilled in the SSGF, Towse [1975] determined the approximate depths to the top of the upper reservoir and to the major shale break separating the upper and lower reservoirs. Since the geologic layers dip in a northwesterly direction essentially parallel to the Brawley Fault Zone, we selected the region covered by the finite difference mesh in Figure 1 for our study. A cross-section is constructed by projecting the data onto a vertical plane parallel to the surface trace of the Brawley Fault Zone (Figure 2). The interfaces between the geologic layers are taken to be planes dipping to the northwest which approximate the points depicted. The temperature-depth profiles measured in the geothermal wells [Palmer, 1975] have been projected to construct the approximate temperature contours shown in Figure 2. The GLEF production wells (W1, M1) are perforated almost entirely within the upper reservoir whereas the injection wells (M2, M3) are perforated mostly within the lower reservoir.

Whether or not the interfacial shale barrier prevents significant fluid exchange between the two reservoirs will have a profound effect on

*Work performed under NSF Grant No. AER75-14492 A01.

their response to imposed production/injection conditions. In the absence of vertical permeability data, two limiting cases were analyzed.

1. Production from upper reservoir without injection, i.e., shale barrier prevents fluid injected into lower reservoir from entering upper reservoir.
2. Production and injection occur in upper reservoir, i.e., vertical fractures channel injected fluid into upper reservoir.

Schroeder [1976] analyzed the sparse data available from drillstem test records from M1 and W1 and concluded that the horizontal permeability of the reservoir sands in the upper reservoir shale/sand sequence exceeds 500 md. The sands comprise over 50 percent of the sequence and their porosity exceeds 0.3. For the upper reservoir sequence we assume the following properties: rock horizontal permeability = 500 md; grain density of rock = 2.65 g/cm^3; initial porosity of rock = 0.20; rock thermal conductivity = 2.1×10^5 ergs/sec-cm-°C; rock specific heat = 10^7 ergs/g-°C; brine salinity(s) = 0.25; irreducible liquid saturation = 0.3 and irreducible vapor saturation = 0.05. The latter two parameters define the relative permeabilities, in the case of two-phase flow, using the Corey formulation.

The 2D areal version of S^3's MUSHRM reservoir simulator is capable of treating the dipping and thickening upper reservoir if we consider the component of gravity along the direction of dip and vary the rock properties to offset variations in thickness. The Brawley and Red Hill faults are assumed to prevent any fluid flow across the side boundaries (Figure 1). The fluids produced by wells on opposite sides of the Brawley fault appear to have a different origin, but there is no definite evidence that the Red Hill fault is a sealing fault.

PREPRODUCTION MODEL

Figure 2 shows that the temperature at the mid-plane of the upper reservoir is much less at the southeastern end (left, y = 0) than at the northwestern end (right, y = L). Using the S^3 brine equation-of-state (s = 0.25) and the temperature-depth profiles at the two ends, the corresponding mid-plane hydrostatic pressures are computed to be P(0) = 38.02 bars and P(L) = 85.07 bars. By considering the temperature variation and dip angle along the length of the reservoir (Figure 2), it is found that if there were no preproduction flow, the value of P(L) would need to be 88.24 bars. The lengthwise pressure drive, ΔP = 3.17 bars, apparently causes an influx of $\sim$ 50°C groundwater from the southeast end (y = 0) which would cool the upper reservoir if hot brine infusion from the lower reservoir were completely precluded by the shale barrier. A vertical permeability of 0.01 to 0.1 md would suffice for steady state convective transport across the shale barrier to swamp heat conduction, a value too small to affect reservoir response performance.

These boundary conditions and reservoir properties were incorporated into MUSHRM and a series of calculations performed until a satisfactory match with the mid-plane preproduction temperatures in the upper reservoir was obtained. A 1D version was first applied to the dipping and thickening

upper reservoir with the provision that for each zone there is infusion of 275°C brine (s = 0.25) at the rate required to obtain the corresponding projected mid-plane preproduction temperature. The total rates of 50°C groundwater (s = 0.25) influx and convective brine infusion are calculated to be $\dot{M}_0$ = 26.7 kg/sec and $\dot{M}_c$ 294.8 kg/sec, respectively. These totals and the lengthwise variation of the influx rate were maintained, but the temperature of the brine and the lateral distribution of the influx rate were allowed to vary in a subsequent series of 2D areal calculations. A symmetric distribution with maximum at the center was found to best fit the lateral variation of the mid-plane temperatures measured in the wells. Having selected the lateral distribution influx rate, the calculation was then rerun with the temperature of the brine source reduced to 251°C in order to better match the mid-plane temperatures. The desired mid-plane temperatures for the well locations are satisfactorily matched by the steady-state temperature contours calculated with the preproduction model (Figure 3). The velocity plot, Figure 4, shows that the infusion of hot brine from the lower reservoir pushes a large part of the incoming cold groundwater to the edges of the upper reservoir, producing the lower temperatures there.

RESERVOIR RESPONSE CALCULATIONS

We make the conservative assumption that the infusion of hot brine from the lower reservoir remains at its preproduction value ($\dot{M}_c$ = 294.8 kg/sec) during exploitation of the upper reservoir. The hydrostatic pressure at the downstream end of the reservoir is maintained (P(L) = 85.07 bars); the production/injection rates are held constant during the course of a given calculation. When injection occurs, the injected brine is taken to be 50°C and to comprise 80 percent of the mass produced ($\dot{M}_I$ = 0.8 $\dot{M}_p$).

A production rate of $\dot{M}_p$ = 100 kg/sec is assumed appropriate for a net 10 MWe at the GLEF site. For convenience, this equivalence is used for higher rates, e.g., nominal 50 MWe means $\dot{M}_p$ = 500 kg/sec. Since the temperature of the produced brine declines with time, these nominal values of electrical power production become less meaningful.

A series of preliminary calculations using an approximate equation-of-state was performed to examine the sensitivity of results to the boundary condition assumed at the upstream (southeast) end of the reservoir. Above nominal 50 MWe (production only) to 250 MWe (with injection), the assumption of constant hydrostatic pressure requires increasing groundwater influx above the preproduction value. Constant groundwater flow ($\dot{M}_0$ = 26.7 kg/sec) was selected as being a more realistic boundary condition since the available groundwater is limited primarily to leakage from irrigation canals supplied by the Colorado River.

Essentially steady-state pressure and velocity fields are soon established wherein the mass flow rate out of the downstream end of the reservoir ($\dot{M}_L$) plus the excess rate of production over injection must balance the mass rate of fluid entering the reservoir from the upstream

groundwater and convective mass sources: $\dot{M}_L + (\dot{M}_P - \dot{M}_I) = \dot{M}_0 + \dot{M}_c =$ 321.5 kg/sec. The following table gives the values of $\dot{M}_L$ for imposed production/injection rates of interest. For $\dot{M}_L < 0$, fluid is entering the downstream end of the upper reservoir and the time (t_r) required for this replacement fluid mass to equal the total preproduction fluid mass in the upper reservoir (3.05×10^{12} kg) is also given. Power production in excess of nominal 50 MWe (production only) to 250 MWe (with injection) requires a tremendous replenishment of hot brine from the downstream end.

Production Rates		Production Only ($\dot{M}_I = 0$)		With Injection ($\dot{M}_I = 0.8\ \dot{M}_P$)	
Nominal MWe	$\dot{M}_P$ (kg/sec)	$\dot{M}_L$ (kg/sec)	t_r (yrs)	$\dot{M}_L$ (kg/sec)	t_r (yrs)
0	0	322	---	322	---
10	100	222	---	302	---
50	500	-179	542	222	---
250	2500	-2179	44	-179	542
325	3250	-2929	33	-329	295

Two nominal 50 MWe simulations treated the four-zone production/injection pattern shown in Figure 1. All production wells are located within the two computational zones containing W1 and M1, and all injection wells are in the zones containing M3 and M2. Figure 5 shows the time history of the bottomhole temperature of the brine produced from each of the two production zones. Results for both assumptions regarding the effectiveness of the shale barrier are presented. The proximity of the production zones to the injection zones causes a rapid decline of the temperature of the produced fluid when the injected fluid is assumed to enter the upper reservoir. Without injection, there is a reversal of the flow at the downstream boundary as anticipated by the table.

From the preproduction model it is apparent that the preferred production region of the upper reservoir is near its center; the injection zones should be either along the two edges of the reservoir or downstream to minimize potential cooling of the produced brine. Figure 6 depicts an improved (and symmetric) production/injection pattern used for a nominal 50 MWe simulation. Both production and injection areas are five times those used above and the intensity of exploitation (well spacing) is more realistic. Figure 7 shows the time history of the bottomhole temperature of the produced brine averaged over all the calculational zones in the production area for the case where it is assumed that the injected fluid enters the upper reservoir. The maximum and minimum brine temperature decline of only 2°C over the 30-40 year period is in sharp contrast to the result obtained with the simple four-zone pattern with injection. Flow at the downstream end of the reservoir remains outward, in agreement with the table; no assumption on the availability of hot brine recharge is required (with injection).

Two additional simulations examined the response of the upper reservoir to nominal 250 MWe power production using a preferred production/injection pattern (Figure 6). Compared to the nominal 50 MWe simulations, the intensity of exploitation is one-third that employed when using the simple four-zone pattern and five-thirds that employed when using the improved pattern. Figure 8 shows the time history of the maximum, minimum and averaged bottom hole temperature of produced fluid for the case where all of the injected fluid is assumed to enter the upper reservoir. A 20°C decline of the averaged temperature is predicted over a 30-40 year period. There is a reversal of the flow at the downstream end required for this large scale exploitation of the upper reservoir even with injection. The case where no injected fluid is assumed to enter the upper reservoir results in an average temperature decline of only 3°C over a 30-40 year period. Attainment of this reservoir response, however, requires tremendouw replenishment of hot brine at the northwest end.

CONCLUDING REMARKS

Because of the limited data base, the simulations presented necessarily invoked a variety of hypotheses concerning geology, temperature distribution, groundwater flow, convective flow, etc. and will likely require revision to include new information as the SSGF resource moves from the exploration and assessment stage of development to the exploitation and utilization stage. Only the upper reservoir of a portion of the SSGF was treated. This portion of the resource appears capable of supplying brine for a net 50 MWe demonstration plant with very little temperature decline over a 30 to 40 year design life. Uncertainties regarding boundary conditions and the effectiveness of the shale barrier between the upper and lower reservoir prevent an evaluation of the ability of the upper SSGF to sustain a 250 MWe plant. The capacity of the lower reservoir should also be considered in such an evaluation.

REFERENCES

Palmer, T. D. [1975], "Characteristics of Geothermal Wells Located in the Salton Sea Geothermal Field, Imperial County, California," Lawrence Livermore Laboratory Report, UCRL-51976.

Schroeder, R. C. [1976], "Reservoir Engineering Report for the Magma-SDG&E Geothermal Experimental Site Near the Salton Sea, California," Lawrence Livermore Laboratory Report, UCRL-5094.

Towse, D. F. [1975], "An Estimate of the Geothermal Energy Resource in the Salton Trough, California and Mexico," Lawrence Livermore Laboratory Report, UCRL-51851.

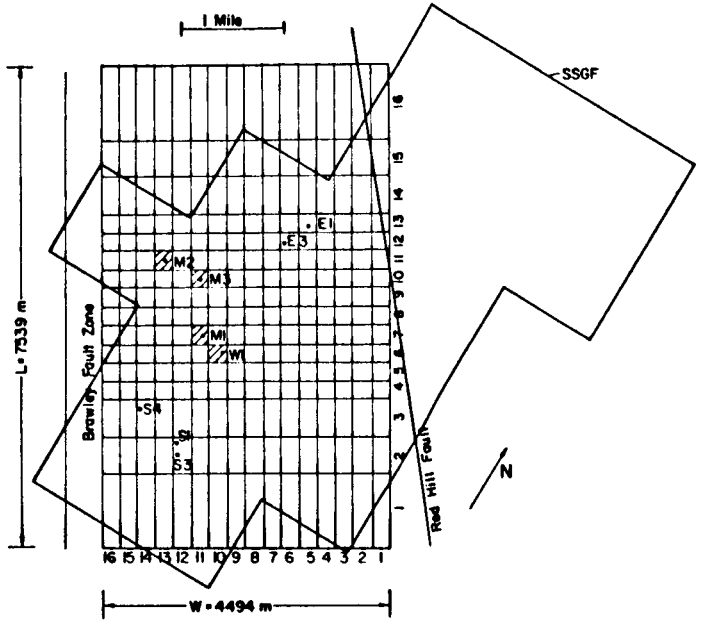

Figure 1. Portion of the SSGF chosen for simulation. Development wells within the region are also shown.

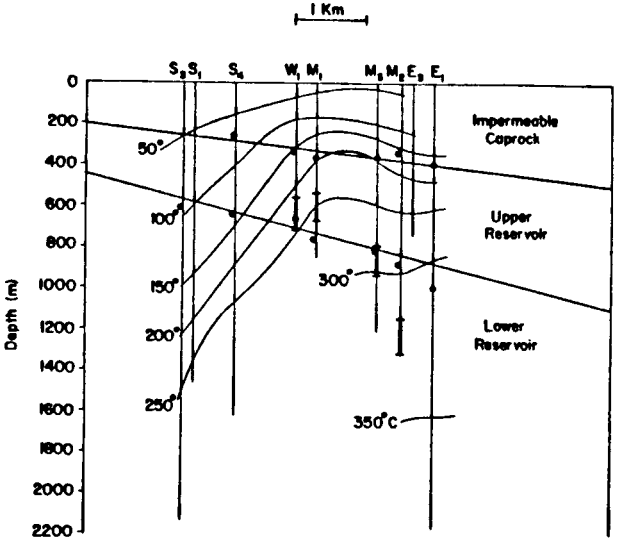

Figure 2. Vertical section and projected data from development wells. Points due to Towse [1975].

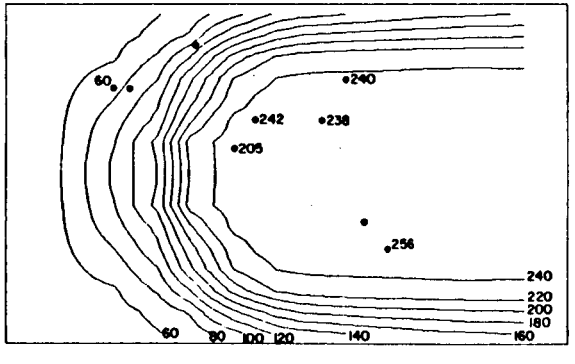

Figure 3. Preproduction model temperature contours (°C) compared with mid-plane temperatures measured at well locations.

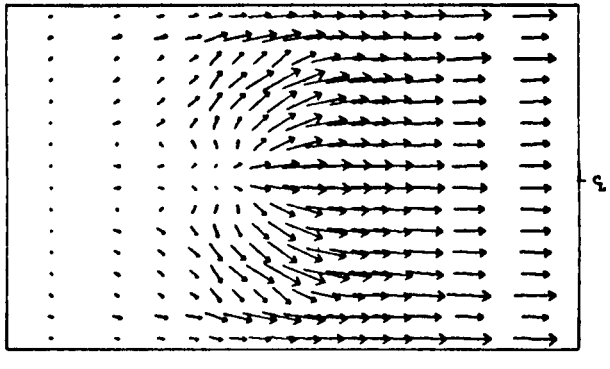

Figure 4. Preproduction model velocity field in upper reservoir (longest vector is 0.91×10^{-4} cm/sec.

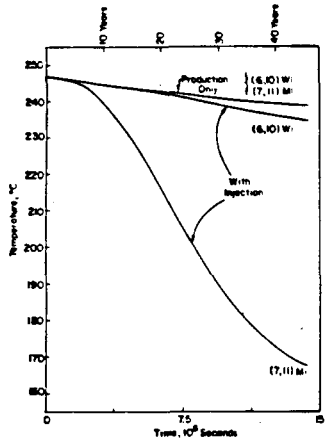

Figure 5. Wellbottom temperature of brine produced from upper reservoir (nominal 50 MWe, simple four zone pattern).

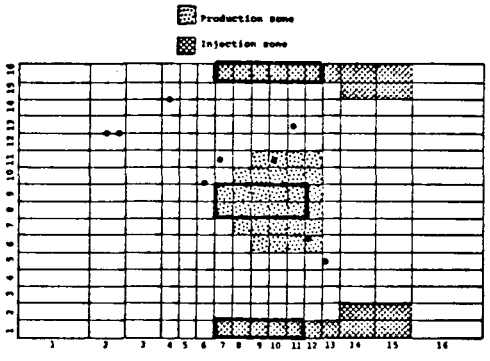

Figure 6. Improved production/injection patterns for exploitation of upper reservoir: nominal 50 MWe (heavily outlined areas) and nominal 250 MWe (total areas shown).

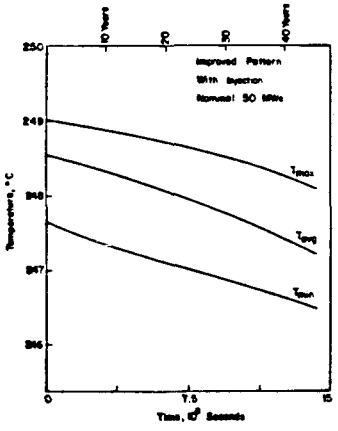

Figure 7. Wellbottom temperature range of brine produced from upper reservoir (nominal 50 MWe, improved pattern with injection).

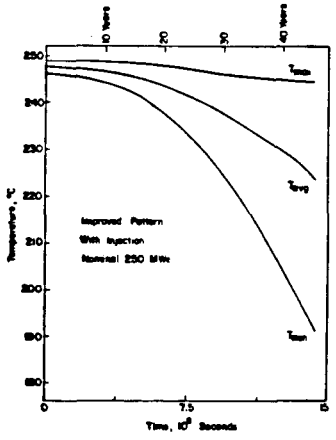

Figure 8. Wellbottom temperatures of brine produced from upper reservoir (nominal 250 MWe, improved pattern with injection).

PROGRESS REPORT ON MULTIPHASE GEOTHERMAL MODELING

James W. Mercer and Charles R. Faust
United States Geological Survey
Reston, Va.

Work over the past year has concentrated on three areas: 1) to implement a concept of vertical equilibrium in geothermal modeling, 2) to improve the matrix equation solution technique for both two- and three-dimensional models, and 3) to apply a vertical equilibrium, areal model to the Wairakei, New Zealand geothermal field.

At the last Stanford meeting, a concept of vertical equilibrium as applied in the petroleum industry was outlined (for example, Coats and others, 1967). That is, vertically averaged liquid saturations are related to pressure at some reference level by employing pseudo capillary pressure and pseudo relative permeability curves. For the geothermal problem, many thermodynamic properties are strongly dependent functions of pressure and enthalpy, and an analogous approach would require many pseudo functions. Instead, the concept of vertical equilibrium is used to vertically integrate the thermodynamic properties and relate them to vertically averaged pressure and enthalpy. This results in a quasi three-dimensional model that allows a finite-difference block to become two-phase as soon as the pressure at the top of the block drops below the saturation pressure. The normal procedure for determining thermodynamic properties on the basis of pressures and enthalpies at specified reference levels in the grid block (usually the center) can lead to significant errors for thick blocks. The implementation of this vertically averaging approach has been verified by comparing a vertical equilibrium, areal model with a three-dimensional model.

To improve the matrix equation solution technique in the two-dimensional (vertical equilibrium) model a sequential solution formulation outlined in Coats and others (1974) is used. Solving the enthalpy equation first, the Newton-Raphson iteration is used on only the accumulation terms in two symmetric matrix equations that are each N x N (N being the number of nodes). By imbedding the sequential solution in the linearized Newton-Raphson equations, decomposition of the two matrices is required only on the first "sequential" iteration. Subsequent sequential iterations require only the formulation of a new righthand side and back substitution. Each additional Newton-Raphson iteration requires the formulation of an updated lefthand side, one decomposition, and several back substitutions.

The work involved in solving the matrix equation includes the initial decomposition plus 3-5 back substitutions depending on the convergence criterion. Usually, the computation time for all back substitutions is less than the computation time for the one decomposition. The symmetric matrix equations are solved using Gauss-Doolittle decomposition that takes advantage

of D4 ordering (Price and Coats, 1974). In this ordering the finite-difference blocks are numbered in alternating diagonals. This numbering schemes results in a matrix with the upper half already in upper triangular form, so that only the lower half needs to be decomposed.

To summarize, the current model for areal problems incorporates the concept of vertical equilibrium, includes gravity terms, and the equations are solved using Newton-Raphson iteration on the accumulation terms. The resulting matrix equations are solved sequentially using D4 ordering and Gauss-Doolittle decomposition.

For the three-dimensional problems slice successive over-relaxation (SSOR) is imbedded in the Newton-Raphson iteration. For a description of SSOR see Wattenbarger and Thurnau (1976) or for the more general case of block successive over-relaxation (BSOR) see Woo and Emanuel (1976). This method is similar to line successive over-relaxation (LSOR) in two dimensions for coupled equations, except that rather than solving each row implicitly, each vertical cross-section of the grid is solved implicitly. This results in a matrix equation for each slide in which the matrix contains five non-zero diagonals. Thus, of the seven non-zero diagonals in the total three-dimensional matrix equation, only two are treated explicitly. Each of these matrix equations are solved using the Gauss-Doolittle method with normal ordering. Since SSOR is imbedded in the Newton-Raphson iteration, only linearized equations are solved. Therefore, the matrix decomposition for each slide is required only on the first SSOR iteration of each Newton-Raphson iteration. On subsequent SSOR iterations only back substitution is necessary. In addition, since the SSOR is imbedded in the Newton-Raphson iteration, the convergence is obtained in only a few iterations.

The vertical equilibrium (areal) model was applied to the Wairakei, New Zealand geothermal field. It is commonly believed that the Wairakei field was completely single phase (water) prior to exploitation; however, our recent steady-state modeling indicates that large regions in the reservoir probably had a small steam cap prior to exploitation. Furthermore, transient simulations indicate that leakage into the reservoir is significant; that is, the Wairakei reservoir is not a closed system. The most difficult part of history matching at Wairakei is adjusting permeabilities in order to remove enough mass from storage (as opposed to leakage) and reproduce the observed pressure decline trends.

REFERENCES

Coats, K.H., George, W.D., Chu, C., and Marcum, B.E., 1974, Three dimensional simulation of steamflooding: Soc. of Petroleum Engineers Jour., December 1974, p. 573-592.

Coats, K.H., Nielson, R.L., Terhune, M.H., and Weber, A.G., 1967, Simulation of three-dimensional, two-phase flow in oil and gas reservoirs: Soc. of Petroleum Engineers Jour., December 1967, p. 377-388.

Price, H.S., and Coats, K.H., 1974, Direct methods in reservoir simulation: Soc. of Petroleum Engineers Jour., June 1974, p. 295-308.

Wattenbarger, R.A., and Thurnau, D.H., 1976. Application of SSOR to three-dimensional reservoir problems, in Numerical simulation of reservoir performance, Society of Petroleum Engineers of AIME, 4th Symposium, Los Angeles, Calif., Feb. 19-20, 1976, Proc.: Soc. Petroleum Engineers, Paper SPE-5728.

Woo, P.T., and Emanuel, A.S., 1976, A block successive over-relaxation method for coupled equations, in Society of Petroleum Engineers of AIME, 51st Ann. Fall Mtg., New Orleans, Louisiana, Oct. 3-6, 1976, Proc.: Soc. Petroleum Engineers, Paper SPE-6106.

SIMULATION OF SATURATED-UNSATURATED DEFORMABLE POROUS MEDIA

Nader M. Safai and George F. Pinder
Water Resources Program
Department of Civil Engineering
Princeton University, Princeton, N. J. 08540

A multiphase consolidation theory is presented which considers a three-dimensional deformation field coupled with a three-dimensional hydrologic flow field. The governing system of equations describes the components of displacement, the fluid pressures and the saturations. The system of equations governing saturated-unsaturated consolidation is obtained as a subset of the above equations. A mixed stress-displacement formulation of the governing equations is introduced, and it facilitates handling of load type boundary conditions while solutions in terms of displacements are still possible. Finite element Galerkin theory is used for spatial approximations, and a weighted implicit finite difference time-stepping scheme is employed to approximate the time derivative terms. Due to the nonlinear nature of the problem, an iterative solution scheme is necessary within each time step.

The model predicts the commonly ignored horizontal displacements in a variably saturated system undergoing simultaneous desaturation and deformation, while using a completely interconnected coupling of the stress and pressure fields within the medium. The model is applied to obtain vertical and horizontal displacements, pressure (head) and saturation values due to pumpage in a phreatic aquifer.

Introduction

Vertical and horizontal ground motions due to changes in pore pressure have been observed in several areas around the world (e.g., at Wairakei, New Zealand, 4.5m vertical and 0.8m horizontal and at Long Beach, California, 8.8m vertical and 3.6m horizontal). In analyzing soil consolidation, research efforts have traditionally focused on the saturated zone. However, unsaturated flow plays an important role in a large number of engineering problems and is the first step in analyzing the multiphase geothermal system.

Narasimhan and Witherspoon, 1977[10], have considered the problem. Their model uses Terzaghi's theory for determining consolidation. Thus, it ignores the lateral soil movement.

In the present work, an iterative Galerkin type finite element method is used to solve the equations of transient flow in saturated-unsaturated deformable porous media in regions having complex geometry. Flow and deformation can take place in both the vertical and horizontal planes, or in a three-dimensional system displaying radial symmetry.

Governing Equations

The system of nonlinear partial differential equations governing saturated-unsaturated flow in a deforming porous medium are[10]:

$$\mu \frac{\partial}{\partial x_i}\left(\frac{\partial u_j}{\partial x_i}\right) + (\lambda+\mu)\frac{\partial}{\partial x_j}\left(\frac{\partial u_i}{\partial x_i}\right) - (S_w P_w)\delta_{ij} = 0 \tag{1a}$$

$$\frac{\partial}{\partial x_i}\left[\frac{K_{ij}K_{rw}}{\gamma_w}\left(\frac{\partial P_w}{\partial x_j} + \rho_w F_j\right)\right] = \frac{\partial}{\partial t}\left(\frac{\partial u_i}{\partial x_i}\right) + nS_w\beta_w\frac{\partial P_w}{\partial t} \tag{1b}$$

$$(i,j = 1,2,3)$$

To solve Equations (1) additional information on the relationship between relative hydraulic conductivity and pressure head and degree of saturation and pressure head is required. These functions are usually determined experimentally for each soil type encountered. Two typical curves, one for a coarse soil and one for a fine soil, are presented in Figures 1 and 2. The following mathematical functions are used to characterize the hydraulic properties of the two soil materials.

$$K_{rw} = \left\{1 + \left(a'|h_w|\right)^{b'}\right\}^{-r'} \tag{2a}$$

$$S_w = \frac{\theta'_r}{\theta'_s} + \left(1 - \frac{\theta'_r}{\theta'_s}\right)\left\{1 + \left(\beta'|h_w|\right)^{\gamma'}\right\}^{-r'} \tag{2b}$$

where values for the various coefficients entering Equations (2) are given in Table 1.

The system of equations (1) in terms of the stress tensor and displacement vector becomes [12, chapters 5 and 7]:

$$\frac{\partial t'_{ij}}{\partial x_i} - \frac{\partial}{\partial x_i}\left(S_w P_w\right) = 0 \tag{3a}$$

$$\frac{\partial}{\partial x_i}\left[\frac{K_{ij}K_{rw}}{\gamma_w}\left(\frac{\partial P_w}{\partial x_j} + \rho_w F_j\right)\right] = \frac{\partial}{\partial t}\left(\frac{\partial u_i}{\partial x_i}\right) + n\beta_w S_w\frac{\partial P_w}{\partial t} \tag{3b}$$

$$(i,j = 1,2,3)$$

This system of equations is employed in our analysis.

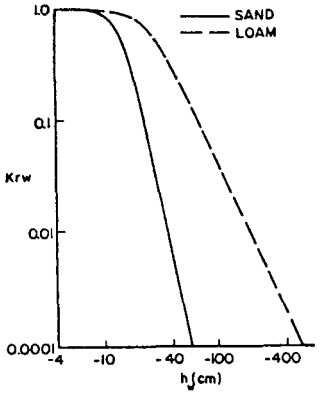

FIGURE 1: RELATIVE HYDRAULIC CONDUCTIVITY VERSUS THE HEAD FOR TWO SOIL MATERIALS. AFTER VAN GENUCHTEN ET AL., 1976 [8].

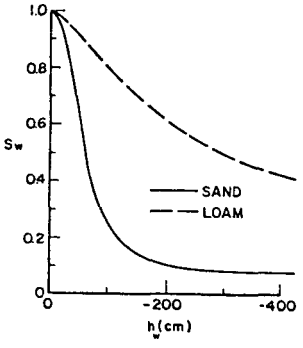

FIGURE 2: DEGREE OF FLUID SATURATION VERSUS THE PRESSURE HEAD FOR TWO SOIL MATERIALS. AFTER VAN GENUCHTEN ET AL., 1976 [8].

VARIABLE	SAND	LOAM	UNITS
θ_r'	0.031	0.10	dimensionless
θ_s'	0.45	0.50	dimensionless
β'	0.0174	0.00481	cm^{-1}
γ'	2.5	1.5	dimensionless
a'	0.0667	0.04	cm^{-1}
b'	5.0	3.5	dimensionless
r'	1.0	0.64	dimensionless

TABLE 1: PHYSICAL DATA OF SAND AND LOAM.

Subsidence Due to Pumpage from a Phreatic Aquifer

The saturated-unsaturated consolidation equations have been applied to the system whose r-z cross section is shown in Figure 3. The finite element solution predicts the vertical and horizontal displacements, excess pore pressure and change in water saturation arising during the pumping process. The bottom impervious layer is assumed fixed and no vertical movement can take place. The wall of the well is also restrained from any lateral movement, and there is seepage into the well. At sufficiently large distance away from the pumping area, the pressure head is not disturbed. Here and at the top surface the soil is free to move both vertically and laterally.

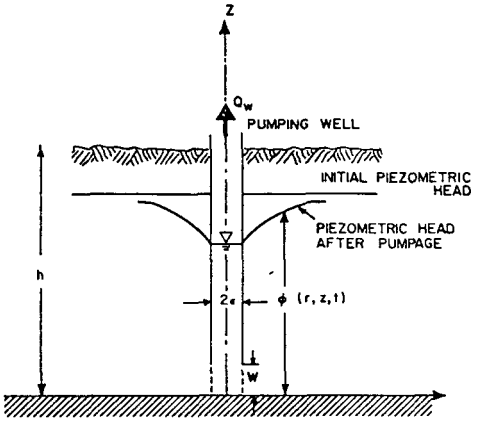

FIGURE 3: A FULLY PENETRATING SCREENED WELL IN AN UNCONFINED AQUIFER. THE SECTION OF THE WELL WHERE SEEPAGE INTO THE WELL CAN TAKE PLACE IS DESIGNATED BY W.

In the numerical solution the spatial domain is divided into isoparametric quadrilateral elements. The time domain is discretized using unequal time intervals and a weighted implicit finite difference iterative scheme [12, chapter 4]. The time step size is calculated according to:

$$\Delta t^{(k)} = K \times \Delta t^{(k-1)}$$

and the elapsed time is given by:

$$t^{(k)} = t^{(k-1)} + \Delta t^{(k)}$$

where K takes values of 0.8, 1.0 and 1.25 depending on the number of iterations required for convergence at the preceding time step. If the required number of iterations is greater than nine, $k = -1$, and we reset our calculations at an earlier time, i.e.:

$$t^{(k)} = t^{(k-1)} - \Delta t^{(k)}$$

and choose a smaller size time step.

A few of the selected results are presented in Figures 4 - 10.

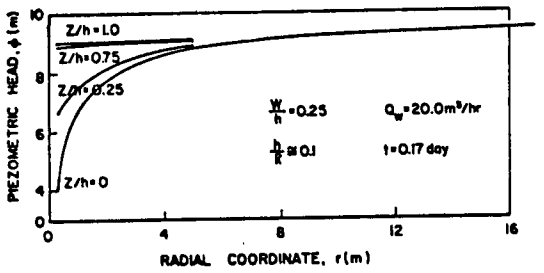

FIGURE 4: HORIZONTAL DISTRIBUTION OF HEAD AT DIFFERENT VERTICAL POSITIONS.

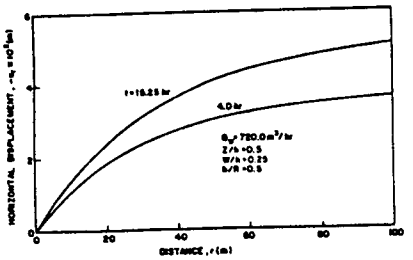

FIGURE 5: HORIZONTAL VARIATIONS OF HORIZONTAL DISPLACEMENT AT THE GIVEN TIME.

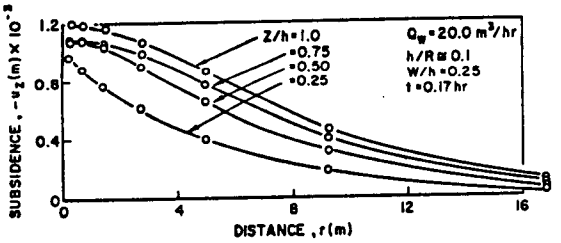

FIGURE 6: HORIZONTAL VARIATION OF SUBSIDENCE FOR DIFFERENT VERTICAL LOCATIONS.

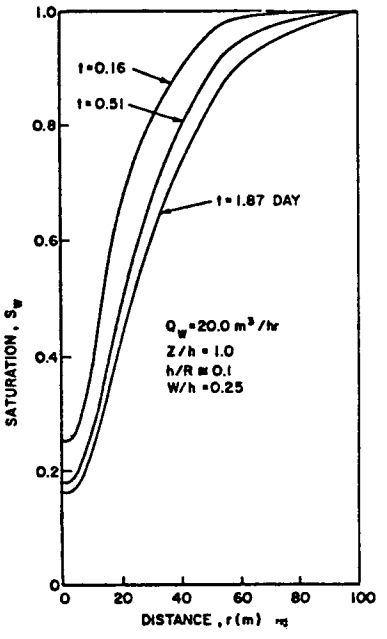

FIGURE 7: HORIZONTAL DISTRIBUTION OF SATURATION FOR THE GIVEN TIMES.

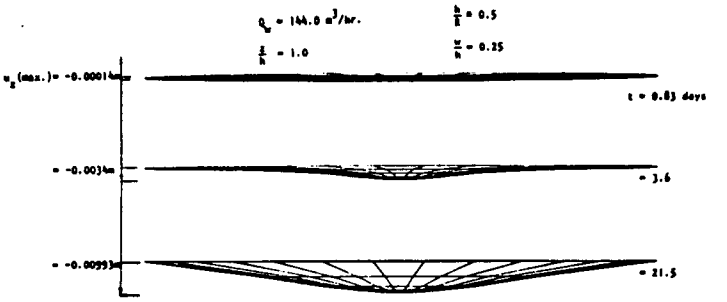

FIGURE 8: THE LAND SURFACE LOWERING AS VIEWED BY AN OBSERVER POSITIONED ON THE SURFACE (ZERO ELEVATION).

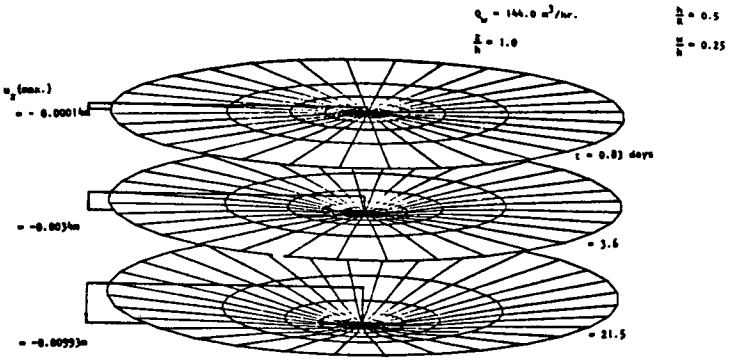

FIGURE 9: THE CONE OF DEPRESSION AS VIEWED FROM ABOVE THE SURFACE FOR SELECTED DIFFERENT TIMES.

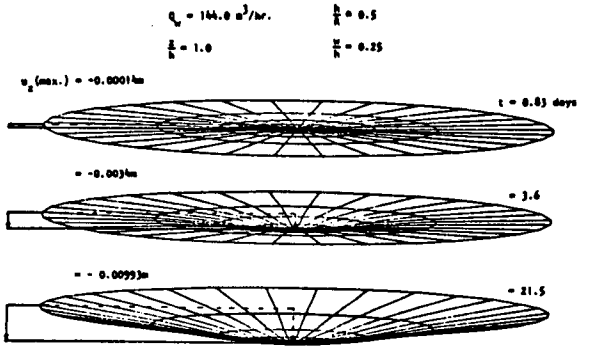

FIGURE 10: THE CONE OF DEPRESSION AS VIEWED BY AN OBSERVER LOCATED BELOW THE SURFACE LEVEL AT DIFFERENT TIMES.

Summary and Results

A mathematical model was developed and used to simulate the deformation field in a desaturating porous medium in which the air phase is assumed to be continuous in the unsaturated zone and to remain at atmospheric pressure. The mathematical model is not applicable to liquid which contains dissolved gas (air bubbles) at different pressures. When the soil is extremely dry and relative hydraulic conductivity, as well as saturation, becomes highly nonlinear the approximating equations may become very difficult to solve. Therefore, the model is best suited to soils of moderate to high saturations.

Acknowledgements

This work was supported by the United States National Science Foundation, NSF-RANN, grant number NSF-AER74-01765, and the University of California, through subcontract P. O. 3143202 under Energy Research and Development Administration contract no. W-7405-ENG.48.

Nomenclature

u_i	displacement vector
P_w	pressure of water
S_w	water saturation
K_{rw}	relative hydraulic conductivity of water
K_{ij}	hydraulic conductivity tensor
β_w	compressibility of water
γ_w	specific weight of water
ρ_w	density of water
λ	Lamé constant
μ	Lamé constant
δ_{ij}	Kronecker delta
x_i	coordinate variables
t	time variable
n	porosity
F_i	body force
h_w	pressure head
θ'_r	residual moisture content
θ'_s	moisture content at saturation
t'_{ij}	effective stress tensor
h	vertical depth
Q_w	volumetric rate of pumping
ϵ	radius of the pumping well
$\phi(r,z,t)$	piezometric head
W	z-coordinate of the seepage zone
R	lateral extent of the aquifer

References

1. VanGenuchten, M. Th., Pinder, G. F., and Saukin, W. P., "Use of Simulation for Characterizing Transport in Soils Adjacent to Land Disposal Sites," Water Resources Program, Princeton University, Princeton, N.J., 1976.
2. Biot, M. A., "General Theory of 3-Dimensional Consolidation," J. Appl. Phys., Vol. 12, pp. 155-164, Feb. 1941.
3. Eringen, A. C., "Mechanics of Continua," Wiley and Sons, 1969.
4. Malvern, L. E., "Introduction to the Mechanics of a Continuous Medium," Prentice-Hall, Inc., 1969.
5. Pinder, G. F., and Gray, W. G., "Finite Element Simulation in Surface and Subsurface Hydrology," Academic Press, N.Y., 1977.
6. Bear, J., "Hydraulics of Groundwater in Aquifers," American Elsevier Pub. Co., Inc., N.Y., 1972.
7. Safai, N. M., and Pinder, G. F., "Multiphase Flow Consolidation, Theory and Application," Water Resources Program, Princeton University, Princeton, N.J., Nov. 1977.
8. Pinder, G. F., Van Genuchten, M. Th., and Saukin, W. P., "Modelling of Leachate and Soil Interactions in an Aquifer," Water Resources Program, Princeton University, Princeton, N.J., 1976.
9. Narasimhan, T. N., and Witherspoon, P. A., "Numerical Model for Land Subsidence in Shallow Groundwater Systems," Int. Symp. on Land Subsidence, Anaheim, California, 1976.
10. Narasimhan, T. N., and Witherspoon, P. A., "Numerical Model for Saturated-Unsaturated Flow in Deformable Porous Media," WRR, Vol. 13, No. 3, June 1977.
11. Terzaghi, K., "Principles of Soil Mechanics," Eng. News Record, 1925.
12. Safai, N. M., "Simulation of Saturated and Unsaturated Deformable Porous Media," Ph.D. thesis, Princeton University, Princeton, N.J., 1977.
13. Freeze, R. A., "Three-Dimensional Transient Saturated-Unsaturated Flow in a Groundwater Basin," Water Resources Research, 7, pp. 347-366, 1971.

BENCH-SCALE EXPERIMENTS IN THE STANFORD GEOTHERMAL PROGRAM

R. N. Horne, J. Counsil, C. H. Hsieh, H. J. Ramey, Jr., and P. Kruger
Stanford Geothermal Program
Stanford University
Stanford, Ca. 94305

The emphasis of the smaller scale laboratory of the Stanford Geothermal Program is on improving the understanding of the physics of flow through porous materials in a geothermal environment. Three major investigations are in progress: (1) examination of the phenomenon of vapor pressure lowering in porous media, (2) determination of the temperature dependence of absolute and relative permeabilities of steam and water in sandstones under high confining pressures, and (3) observation of steady and unsteady, single- and two-phase flows of water or brine through permeable cores. In addition, development continues on the dielectric constant liquid content detector--a device which would prove extremely useful in these and subsequent experiments.

Vapor Pressure Lowering

Due to the presence of solid boundaries, the saturated vapor pressure of water in a consolidated sandstone core may be lowered by as much as 15 psia at temperatures between 200°F and 290°F. See Fig. 1 (from Chicoine, Strobel, and Ramey[1]). As a result, the water boils at a higher temperature. It is anticipated that vapor pressure lowering is due to capillarity and/or adsorption-desorption phenomena at low water saturation (below the irreducible water saturation).

Initial theoretical analysis of the experimental data of Calhoun, Lewis and Newman[2] produces strong evidence that the phenomenon is due to adsorption/desorption rather than capillary effects. Three facts are indicative of this:

(1) If the pore size implies a radius of curvature 10 Å in the experimental porous medium, which is about the minimum radius for which capillarity may be considered (for water), then vapor pressure lowering due to capillarity would result in a vapor pressure 0.61 times the "flat surface" value. In fact, the observed value is much lower (~0.03).

The relative orders of the effects of capillarity and adsorption can be estimated from the equation:

Capillarity: $\ln \frac{p}{p_o} = -\frac{2rV}{RT}\frac{1}{R_m}$ (from Leverett[3]) (can be obtained from thermodynamics)

where p/p_o is the saturated vapor pressure relative to that on a flat surface, γ is the surface tension, V is the molar volume, R is Boltzman's constant, T temperature, and R_m the mean radius.

Adsorption: $$\frac{P}{x(p_o-p)} = \frac{1}{x_m c} + \frac{c-1}{x_m c} + \frac{P}{P_o}$$ (the BET eq., Brunauer, Emmett & Teller[4])

for $0.05 < \frac{P}{P_o} < 0.35$

where x is the value of fluid adsorbed at pressure P and x_m is the volume of fluid required for monolayer adsorption. c is the ratio of activation energy for rock/water and water/water interactions.

(2) It can be seen from these equations that the adsorption effect is a function of surface area and not necessarily of permeability and porosity. Calhoun's[2] data show this surface area dependence.

(3) In Calhoun's[2] experimental data there is no noticeable hysteresis in the vapor pressure/saturation curve during a drainage/imbibition cycle. Such hysteresis would be anticipated if capillarity were significant, as the water/vapor interface would have a different shape during filling and emptying a pore.

The objectives of the program are to reevaluate the results of Chicoine, et al.[1], using steady rather than time-varying experiments. This should represent the phenomenon of vapor pressure lowering better because it is not a transient effect. It is also intended that the range of temperatures for the experiment be increased.

Permeability to Water and Brines--Effects of Temperature

Experimental studies of fluid flow through porous media have shown that temperature and the confining pressure affect both relative and absolute permeabilities. Several workers in the past have demonstrated that relative permeability is a temperature-dependent property of rocks (e.g., Weinbrandt[5]), but results published on absolute permeabilities show a lack of consistency.

Under the sponsorship of the Stanford Geothermal Program, Cassé[6] sought to clarify these results by investigating the combined effects of mechanical and thermal stresses. In his work, water, nitrogen, and mineral oil were used to find absolute permeabilities of three consolidated sandstone samples for confining pressures ranging from 450 to 4000 psia and temperatures ranging from room temperature to 325°F. Results from these experiments showed that the temperature effects on permeability depended on the nature of the saturating fluid. For water-saturated cores, permeability reductions of up to 65% were observed over the temperature range studied.

Because of the lack of absolute permeability variation with temperature for both nitrogen and mineral oil, Cassé[6] concluded that the temperature effect is not caused by changes in physical properties of the fluids, such as viscosity or density, or by thermally-induced mechanical stresses. Instead, the unique results obtained for water suggest that a temperature-dependent rock-fluid interaction was the dominant factor responsible for permeability reductions for water.

In order to verify the results of these and other previous studies, and to investigate the causes for the observed behavior, Aruna[7], also under SGP sponsorship, extended the work of Cassé to clay-free systems, and to unconsolidated sands under the theory that the main effect was water-silica development (Aruna, et al.[8]). Figure 2 shows Aruna's results for permeability variation with temperature for water flowing through a consolidated sandstone core. Additional tests using octanol-saturated cores did not show temperature effect of permeability. From these results, Aruna concluded that the permeability reduction for water flowing through sandstone cores is due to attractive forces between silica and water molecules at elevated temperatures. Further evidence for this conclusion was derived from a series of tests using a water-saturated limestone core which did not show permeability change with temperature, and tests with clean, unconsolidated sands and water which did show a large effect.

The work now continues with similar apparatus. The new objectives are to evaluate the relative permeabilities of steam and water or brine at different temperatures under high confining pressure. It should also be possible to evaluate the immobile water saturation in an all-water system, and the irreducible water saturation in a two-phase system, by using traced water (e.g., brine). It will also be interesting to determine whether steam absolute permeabilities are temperature dependent in sandstones, as other gases tested to date were not.

Two-Phase Flow of Water and Brine

A third bench-scale apparatus has been developed to investigate the flow of water and brine through porous materials.

Relative permeability/saturation relationships are needed to forecast the mass and energy recovery from geothermal reservoirs. Steam and water relative permeability/saturation data have not been presented in the literature. Since brine geothermal fields are common, answers to the following questions are needed: (1) where does salt deposit in the reservoir when boiling occurs? (2) does salt deposition affect the rock permeability?

In an earlier study, temperature profiles were measured by Arihara[9] during steam injection into a cold water saturated core. Injection rates were low enough that a steam front and hot water region was calculated from the experimental data and found to be only slightly higher than that calculated for hot water injection. It was believed

that the difference might have resulted from a small error in estimating the position of the steam front. It was recommended that future steam injection studies be designed to achieve stagnation of the steam front, and steady state in the hot water zone.

Relative permeabilities of steam and water were determined by Chen[10] (see Fig. 3); however, results indicated an irreducible water saturation larger than 60%, a figure which requires further investigation. This work continues to provide quantitative information that can be used to evaluate the performance of two-phase flow computer simulation programs, which is an important objective of the study. At present, emphasis is being placed upon:

(1) studying the pressure, temperature, and salt deposition characteristics of high temperature depletion and approximate steady flow processes for a variety of brine concentrations, and

(2) improving the materials and design features of high temperature flow equipment in order to obtain detailed data on relative permeabilities.

The Capacitance Probe

This device is being developed further for use in both the vapor-pressure lowering and relative permeability/brine experiments. The probe has been used previously in the Stanford Geothermal Program by Chen[10] as a means of determining the water saturation. The probe (see Fig. 4) is positioned inside a glass tube cemented into the center of a synthetic core, and its capacitance may be calibrated to give a measure of the fluid saturation. The two-phase flow apparatus will now be used to calibrate the probe signal with liquid water saturation as a function of frequency. An optimum frequency can then be selected to linearize the correlation between capacitance and water saturation as closely as possible.

References

1. Chicoine, S.D., Strobel, C.J., and Ramey, H.J., Jr.: "Vapor pressure lowering in two-phase geothermal systems," paper SPE 6767 presented at the 52nd Annual Fall Meeting of SPE, Denver, Oct. 1977.

2. Calhoun, J.C., Jr., Lewis, M., Jr., and Newman, R.C.: "Experiments on the capillary properties of porous solids," Trans. AIME, 186 (1949), 189-96.

3. Leverett, M.C., "Capillary behavior in porous solids," Trans. AIME, 142 (1941), 152-69.

4. Brunauer, S., Emmett, P.H., and Teller, E.: "Adsorption of gases in multimolecular layers," J. Am. Chem. Soc., 60 (1938), 309-19.

5. Weinbrandt, R.M.: "The effect of temperature on relative permeability," Ph.D. Dissertation, Stanford University, 1972.

6. Cassé, F.J.: "The effect of temperature and continuing pressure on single-phase flow in consolidated rocks," SGP-TR-3, 1974.

7. Aruna, M.: "The effects of temperature and pressure on absolute permeability of sandstones," SGP-TR-13, 1976.

8. Aruna, M., Arihara, N., and Ramey, H.J., Jr.: "The effect of temperature and stress on the absolute permeability of sandstones and limestones," presented at the American Nuclear Society Meeting, April 12-14, 1977, Colorado School of Mines, Golden, Colorado.

9. Arihara, N.: "A study of nonisothermal single- and two-phase flow through consolidated sandstones," SGP-TR-2, 1974.

10. Chen, H.K.: "Measurement of water content in porous media under geothermal fluid flow conditions," SGP-TR-15, 1976.

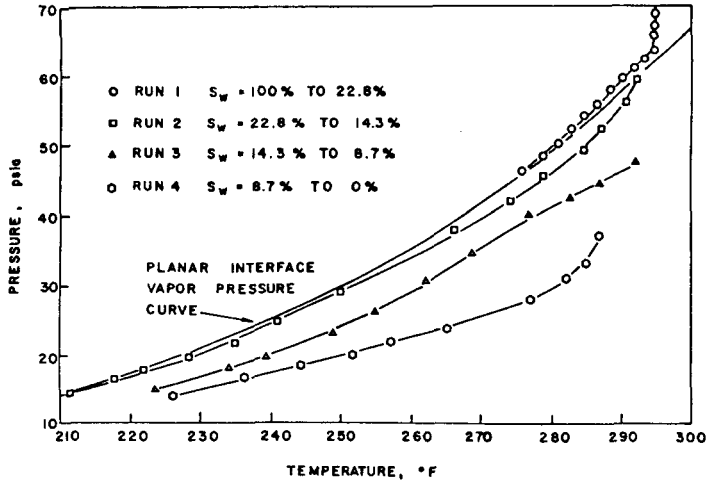

Fig. 1 - Pressure vs. temperature for the two-phase zone. (K=80 md, ϕ = 0.18)

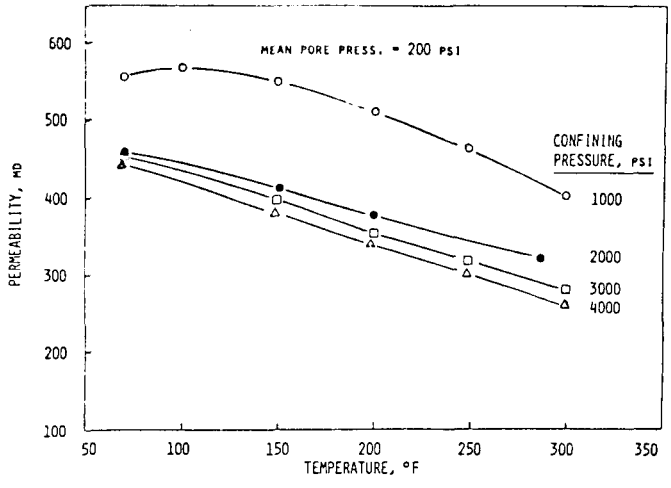

Fig. 2. Water Permeability vs. Temperature, Massillon Sandstone Core No. 2

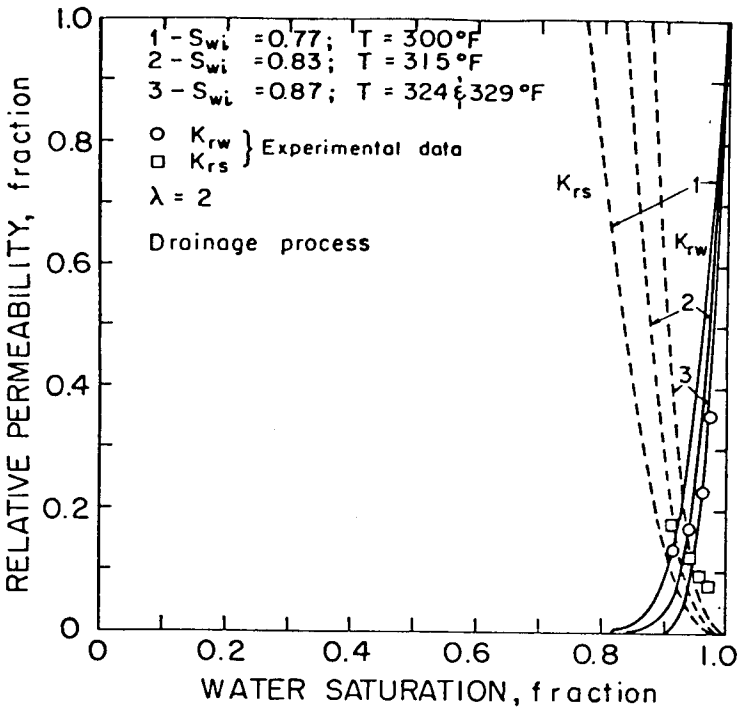

FIGURE 3. RELATIVE PERMEABILITY TO STEAM AND WATER VS. WATER SATURATION FOR A SYNTHETIC CONSOLIDATED SANDSTONE CORE

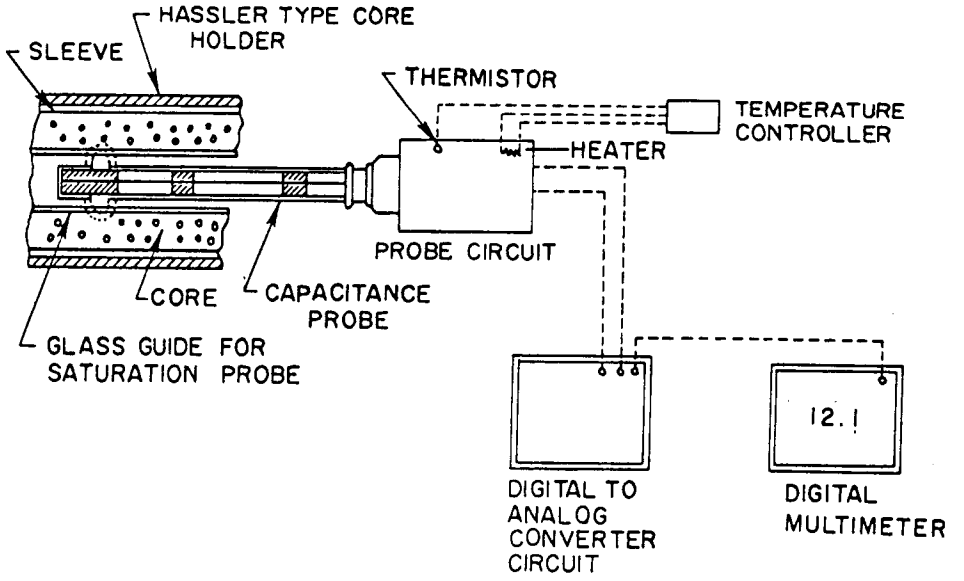

FIGURE 4 SCHEMATIC DIAGRAM FOR IN SITU MEASUREMENT OF WATER SATURATION IN STEAM-WATER FLOW IN SYNTHETIC CONSOLIDATED SANDSTONE CORE

MEASUREMENT OF STEAM-WATER FLOWS FOR THE TOTAL FLOW TURBINE

Russell James
Department of Scientific and Industrial Research
Taupo-Wairakei, New Zealand

Hot water geothermal fields discharge steam-water mixtures, which have proved difficult to measure compared with the dry steam from fields like The Geysers and Larderello.

With the development of the lip pressure method, however (James 1962), an accurate method was derived which could measure the flow when a geothermal well discharges to the atmosphere at sonic velocity. Fortunately most discharges from wells do in fact attain such velocities, and as long as the enthalpy of the mixture is known, the flow can be determined. Where the enthalpy is unknown some other measurement has also to be made in order to solve the two factors of flow and enthalpy. By discharging the whole mixture into a silencer, the water portion can be estimated by means of a weir, and this provides the second measurement (described in James 1966) required to solve both unknowns.

The relationship at the location of sonic flow has been empirically determined as follows:

$$\frac{G\, h_0^{1.102}}{P_c^{0.96}} = 11\ 400 \qquad (1)$$

where G is the mass-velocity in lb/ft^2s
h_0 is enthalpy in Btu/lb
P_c is critical discharge pressure (lip pressure) in psia.

To convert units of G into units of W lb/h

$$W = G \left(\frac{\pi}{4}\right) \left(\frac{d}{12}\right)^2 60^2$$

where d is the inside diameter of the discharge pipe in inches.

The Total Flow Turbine

This approach entails the discharge of the whole unseparated steam-water mixture from the geothermal well through nozzles onto the wheel of a specially designed impulse turbine and thence into a separating condenser. A development program to solve the various problems involved is underway at the Lawrence Livermo: Laboratory, University of California. With the more conventional approach of separating the steam from the water and passing it into a steam turbine, flows can

be measured by means of orfice plate meters as described by the ASME (1959), although there is some difficulty with the hot water flow as this is exactly at the boiling point and flash steam can appear in the line and falsify the flow estimate. Worse still, even a small quantity of carryover steam from the separator can wildly distort the readings and result in large errors (James 1975). Such steam carryover is by no means uncommon; in fact, there is some indication that effective separation depends to an extent on small steam loss into the water phase due to vortexing within the vessel. The measurement problem can be overcome by external cooling of the water line or increasing the pressure head by raising the level of the water within the separator.

How then can we measure the flow of a steam-water mixture to a total flow turbine? This can be accomplished by means of the nozzle which discharges onto the wheel, so long as the mixture enthalpy is known. As the LLL program is specifically directed to exploiting the large geothermal resources of the Salton Sea, the enthalpies of the wells there appear to be fairly stable and draw on hot water with temperatures of about 300°C (A.L. Austin and others 1977).

A convergent-divergent nozzle is the means by which the heat and pressure energy of the fluid is converted to kinetic energy for directing onto the turbine blades. Study of such nozzles for the flow of superheated and saturated steam has been well documented in the literature and in textbooks on fluid flow and thermodynamics (Streeter 1966).

Sonic velocity is attained at the throat of such nozzles and the ratio between the throat pressure and the up-stream manifold pressure has been experimentally determined for steam. For superheated steam, the ratio is about 0.55 and for saturated (moist) steam is about 0.58 (Potter 1958). Unpublished tests by the author on steam-water flows through steam nozzles gave the same ratio of 0.59 as for saturated steam. This is confirmed by the tests undertaken by LLL in their report on the program status (1977).

Hence, it is clear that so long as the mixture enthalpy is known, together with the nozzle throat pressure, then the formula for the lip pressure given as equation (1) may be employed to determine the flow, with P_c taken as the throat pressure and d being the throat diameter. However, it would be unnecessary to attach a pressure tapping directly to the throat of the nozzle, as the manifold pressure just up-stream of the throat would be rather precisely controlled by a turbine governor valve and using the ratio of 0.58, the pressure at the throat where critical flow occurs (sonic velocity) can be estimated.

Let suffix 0 represent up-stream stagnation conditions within the manifold and suffix t represent throat conditions where sonic flow occurs.

From equation (1),

$$\frac{G_t \; h_0^{1.102}}{P_t^{0.96}} = 11\ 400$$

and $P_t = 0.58 \; P_0$

while $\dot{W} = G_t \left(\frac{\pi}{4}\right)\left(\frac{d_t}{12}\right)^2 \; 3600 = 19.6 \; d_t^{\,2} \; G_t$

so $G_t = 11\,400 \; \frac{P_t^{\,0.96}}{h_o^{\,1.102}} = 11\,400 \; \frac{0.58^{0.96} \; P_o^{\,0.96}}{h_o^{\,1.102}}$

$= 6758 \; \frac{P_o^{\,0.96}}{h_o^{\,1.102}}$

$$W = 19.6 \; d_t^{\,2} \; \frac{6758 \; P_o^{\,0.96}}{h_o^{\,1.102}} = 132\,450 \; \frac{d_t^{\,2} \; P_o^{\,0.96}}{h_o^{\,1.102}} \qquad (2)$$

As it is more usual to give flow through nozzles in lb/s

$$w \text{ lb/s} = 36.8 \; \frac{d_t^{\,2} \; P_o^{\,0.96}}{h_o^{\,1.102}} \qquad (3)$$

Illustrative Example

Taking the LLL report (1977) on a nozzle test from their Table 3-2, we have P_o = 367 psia, h_o - 526 Btu/lb

Nozzle throat diameter calculated from the throat area of $6.87 \; (10)^{-4}$ ft^2 · given on their Figure 3-16. d_t = 0.35 inches diameter.

From equation (3) above:

$$W = 36.8 \; \frac{d_t^{\,2} \; P_o^{\,0.96}}{h_o^{\,1.102}}$$

$$= 36.8 \; \frac{(0.35)^2 \; (367)^{0.96}}{526^{1.102}} = 1.31 \text{ lb/s}$$

This equals the flow-rate given for their test conditions, so agreement looks very good.

Saturated Water Flow Through Nozzles

In observing steam-water flow through nozzles we assume that there is steam present within the up-stream manifold with a volume exceeding that of the associated water. In the example above, for instance, the LLL test gave a

manifold dryness fraction of 14% quality and such steam is necessary to give a ratio of 0.58 for $\frac{P^t}{P_o}$ and for sonic conditions to prevail at the throat.

Where an all-water state occurs in the manifold, even if it is exactly at the boiling point for the liquid pressure, the throat pressure has been found from tests at Wairakei to be greater than 0.9 P_o. It appears that the time duration is so short when the fluid passes from the manifold to the throat that none is available for bubble formation. Hence, only an all-water condition exists at the throat. This invalidates the conditions for sonic flow and thus the relationship of equation (3) does not hold. It is also difficult to sustain stable flow as the flash front within the nozzle constantly "hunts" from the throat to some distance downstream within the convergent part, leading to pulsations of pressure and presumably cyclic flow variation. This might create problems when applied to a turbine as resonance effects might follow.

Therefore it may be necessary to execute some degree of throttling upstream of the nozzle manifold in order to permit some steam to exist within this chamber and thereby stabilize the flow; perhaps this will allow sonic flow at the nozzle throat. If this proves correct, measurement of the discharge may again be possible as for genuine steam-water flow described above.

Field Test Conditions

This example was based on values taken from a laboratory test using clean water and negligible non-condensible gas. Future tests in the Salton Sea geothermal field will involve steam-water mixtures where the water contains up to 30% wt of dissolved solids, while the steam phase may contain substantial quantities of gas, mainly carbon dioxide (perhaps up to 10% wt). Correction factors will have to be estimated to allow for these significant departures from the steam-water employed in laboratory experiments. Grens (1975) has calculated the effect of intense brines on dryness fraction and enthalpies of such mixtures. Also the quantity of gas can be used to compute the partial gas pressure at the nozzle throat which, together with the vapor pressure of the steam, combines to give the total throat pressure.

Obviously some field tests will be required to ascertain the effectiveness of these "corrections" on true flow-rates.

CONCLUSIONS

With the hoped-for commercial success of the total energy turbine in the near future, it will be necessary to have a means of measuring the steam-water flow into the machine. As long as the enthalpy of the flowing fluid is known, there should be no intrinsic difficulty in obtaining this, as the nozzles themselves act as metering devices due to the phenomena of sonic velocity at the throat. High gas concentrations in the steam phase, together with high chemical content in the water phase, require the use of "corrections" which will have to be determined from field tests to confirm theory. Clean steam-water mixtures appear to present no difficulties.

REFERENCES

ASME, 1959 — Fluid meters - their theory and application. American Soc. Mech. Engrs., New York, U.S.A.

Austin, A.L. 1977 — The LLL Geothermal energy program status report, Jan. 1976-Jan. 1977. Lawrence Livermore Laboratory, University of California.

James. R. 1962 — Steam-water critical flow through pipes. Proc. Inst. Mech. Engrs., 176 (26):741.

James, R. 1966 — Measurement of steam-water mixtures discharging at the speed of sound to the atmosphere. New Zealand Engineering, 21 (10):437.

James. R. 1975 — Possible serious effects of the presence of steam on hot-water flow measurements utilizing an orfice meter. Sec. U.N. Symp. on the Develp. and Use of Geothermal Resources, San Francisco, University of California.

Potter, P.J. 1959 — Power plant theory and design. The Ronald Press, New York, U.S.A.

Streeter, V.L. 1966 — Fluid mechanics. McGraw-Hill Book Co., New York, U.S.

INTERPRETATION OF BOREHOLD TIDES AND OTHER ELASTOMECHANICAL OSCILLATORY PHENOMENA IN GEOTHERMAL SYSTEMS

Gunnar Bodvarsson
School of Oceanography
Oregon State University
Corvallis, Oregon 97331

Introduction

Ultralow to low-frequency oscillatory phenomena of elastomechanical nature have been observed in a number of geothermal areas. These include pressure and water level oscillations in the tidal frequency range 10^{-6} to 10^{-4} Hz (White, 1968), flow oscillations at around 10^{-3} Hz (Bodvarsson and Bjornsson, 1976) and ground noise in the range 10^{-1} to 10 Hz (Douze and Sorrel, 1972). The presence of such oscillations conveys certain information on the underlying geothermal systems which is of both theoretical and practical interest. In the following, we will very briefly discuss a few aspects relating to the interpretation of oscillatory field data with the main emphasis on borehole tides.

Oscillations of Tidal Origin

Pressure oscillations in the tidal frequency range, which may be observed either directly by pressure transducers emplaced in closed subsurface fluid spaces, or, as water level oscillations in boreholes, result from the straining of the surrounding formations by forces of tidal origin. The water level oscillations represent a breathing of the formations through the borehole. The volume amplitude of the oscillating fluid must therefore give clues as to the local strain amplitude and the formation volume in direct contact with the borehole. To obtain quantitative cause-effect relations, we have to consider the diffusion of low frequency pressure fields in natural formations.

Concentrating on the case of fluid-saturated Darcy-type porous media, the simplified linear pressure diffusion theory given by Bodvarsson (1970) can be applied to obtain useful relations. The oscillatory pressure field is then derived as a solution to a standard linear scalar diffusion equation. Applying the theory to the simple but practically relevant model shown in Figure 1, we consider a spherical volume V of radius R of a homogeneous and isotropic Darcy-type medium saturated by a fluid of density ρ and which is embedded in a formation of negligible permeability. The capacitivity or storage coefficient of the wet medium is s and its hydraulic conductivity $c = k/\nu$ where k is the permeability of the medium and ν the kinematic viscosity of the fluid. The skin depth d of a harmonic oscillatory pressure field with an angular frequency ω is then obtained by (Bodvarsson, 1970)

$$d = (2c/\rho s\omega)^{\frac{1}{2}} \qquad (1)$$

A borehole of cross-section $\underline{a}$ has been drilled into the center of the porous formation and for convenience we assume that it is connected with V through a small spherical cavity of radius r. The borehole is cased all the way to the cavity and there is a free water surface at an elevation h. Moreover, we assume that tidal forces of angular frequency ω produce a homogeneous and isotropic strain of amplitude b in V. The formation matrix coefficient ε characterizes the relation between the imposed strain and the porosity (Bodvarsson, 1970).

Omitting details of derivation, we obtain by solving the pressure diffusion equation with appropriate boundary conditions at the inner and outer boundaries of the porous formation, the following relation for the amplitude of the water level

$$h = h_s T(1 + T)^{-1} \tag{2}$$

where h_s is the static amplitude (Bodvarsson, 1970)

$$h_s = -\varepsilon b/\rho g s, \tag{3}$$

g is the acceleration of gravity and T is the tidal factor

$$T = \rho g s V_d F/a \tag{4}$$

which is characterized by two quantities, the skin volume

$$V_d = \pi r^2 d \tag{5}$$

and the complex dimensionless reflection factor F which depends primarily on the ratio R/d.

The permeability of common Darcy-type reservoir formations is frequently of the order of 10^{-2} to 1 darcy and the skin depth at tidal frequencies is then 50 to 500 meters (Bodvarsson, 1970). Moreover, reasonable values for the cavity radius r are of the order of one meter. Cases where $r/d \gg 1$ and $d/r \gg 1$ are therefore of particular practical interest. An elementary derivation shows that in this case the coupling between the borehole and the formation is resistive and the tidal factor can then be approximated by

$$T = -i\rho g s \pi r d^2/2a = -ig\pi rc/\omega a \tag{6}$$

This expression which can be assumed for a number of Darcy-type porous reservoirs furnishes the main clues as to the problem of interpreting borehole tides in such cases.

In all practical cases, the density ρ and cross-section a are well known. The capacitivity can generally be estimated with sufficient accuracy on the basis of core samples. Moreover, although boreholes rarely open into spherical cavities, most practical cases involving irregular cavities of small dimension compared with the skin depth d can be approximated by spherical cavities with an equivalent radius r which can be estimated within reasonable limits. The skin depth d is therefore the principal unknown on the right of equation (6).

Moreover, the static amplitude h_s given by equation (3) can in principle often be determined experimentally by closing the borehole with packers at appropriate levels and placing instrumentation to record the tidal pressure amplitude in the enclosed space. Provided that such observation can be made, we can conclude that the skin depth is the principal unknown on the right of equation (2). Hence, observing the tidal water level amplitude h, we can obtain data on the skin depth d and thereby because of (6) information on the hydraulic conductivity c. These two quantities, d and c, are therefore the principal targets of most interpretive efforts involving borehole tides.

Local Enhancement of the Tidal Dilatation

Elementary considerations indicate that the local tidal dilatation is generally modified by variations in the subsurface elastic parameters. The effect is most obvious at very abrupt inhomogeneities such as in the case of open subsurface spaces. Consider, for example, an open very flat penny-shaped cavity of radius r and width w. The cavity is placed in homogeneous solid rock at a depth which is substantially greater than the diameter 2r and such that its axis is parallel to the direction of maximum principal tidal strain. A simple argument (Bodvarsson, 1977) indicates that the cavity will breathe in response to the tidal stresses and that the dilatation amplitude of the open space is enhanced by a factor of approximately r/w relative to the undisturbed dilatation at a distance from the cavity. In specific cases, the local dilatation amplification can thus attain very large values. Moreover, there is also a substantial enhancement of the tidal stresses along the edge of the cavity. This is a typical notch effect.

Analog effects, but generally of a more complex nature, are obtained in the cases of other types of inhomogeneities (Bodvarsson, 1977). Inclusions of porous fluid-saturated material in solid rock will also breathe in response to the solid earth tides, and there will be notch type stress concentrations in particular locations. The theory of these phenomena is somewhat complex, in particular, when the dimensions of the inclusions exceed the hydraulic skin depth at tidal frequencies of the porous material.

The case of fracture zones with a permeable fluid-saturated gouge is of particular interest. We assume that the fluid can breathe freely through the surface of the gouge. Although very little is known about the fluid

conductivity characteristics of gouge materials, we can on the basis of rather simple theoretical modeling (Bodvarsson, 1977) infer that the tidal fluid pressure amplitude within the gouge may in some cases, at least, vary along the fracture zone as indicated in Figure 2. There is an upper zone, the depth of which is of the order of the hydraulic skin depth in the gouge, where the breathing through the open surface causes a reduction of the tidal pressure amplitude. Further below is a zone of an enhanced pressure amplitude. This is a notch type effect caused by the reduced pressure amplitude in the surface zone. Deeper in the fracture zone, where the effect of the open surface is negligible, the pressure amplitude attains the local static value given by equation (3).

The above considerations indicate that data on the local tidal pressure amplitude, as measured in closed boreholes, can be of some value as an exploration tool. Some characteristics of the local geological structure and material properties can be reflected in the observational data.

Hydroelastic Oscillations

Helmholtz type borehole-cavity oscillations. Small amplitude temperature oscillations of frequency around 10^{-3} Hz have been observed in a thermal borehole in Southwestern Iceland. The hole flows about 0.5 kg/s at 43°C. Bodvarsson and Bjornsson (1976) have discussed this phenomenon and have concluded that it may be caused by weak flow oscillations due to a hydroelastic Helmholtz type borehole-cavity resonance excited by pressure fluctuations of turbulent origin.

Fracture oscillations and geothermal ground noise. When properly excited, fluid filled fracture spaces can perform hydroelastic oscillations and radiate very low frequency seismic signals. A simple approximate theory of such oscillations has been given by Bodvarsson (1978). The frequency f of the basic oscillation mode of a very thin fracture space of constant width w, vertical dimension L, and which is open to the surface as shown in Figure 3, can be estimated by the following relation

$$f = (\mu w/\rho L^3)^{\frac{1}{2}} \qquad (7)$$

where μ is the shear modulus of the rock and ρ is the density of the fluid.

The above result indicates that fracture spaces of width 10^{-3} m and vertical dimension of 10 to 100 m have basic frequencies in the range 0.2 to 5.0 Hz. This is the frequency range of seismic ground noise which has been observed in many geothermal areas (Douze and Sorrels, 1972). The observed seismic signals may thus result from hydroelastic oscillations of thin fracture spaces. As in the above case of Helmholtz type oscillations, the excitation may again be provided by pressure fluctuations of turbulent nature in the convecting geothermal fluid.

Provided the above interpretations are correct, the observed frequencies give some clues as to the dimensions of the oscillating spaces.

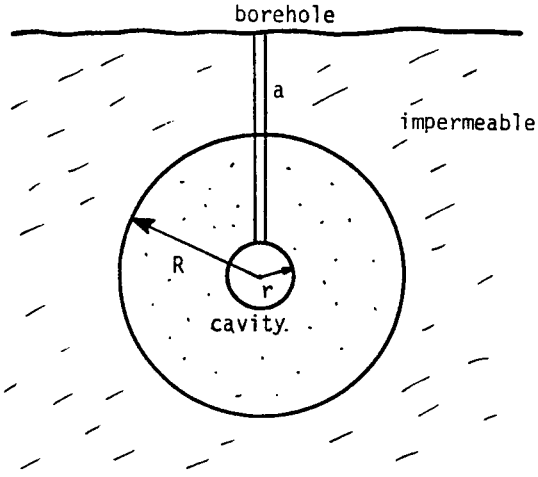

Figure 1. Spherical volume of a porous Darcy type material.

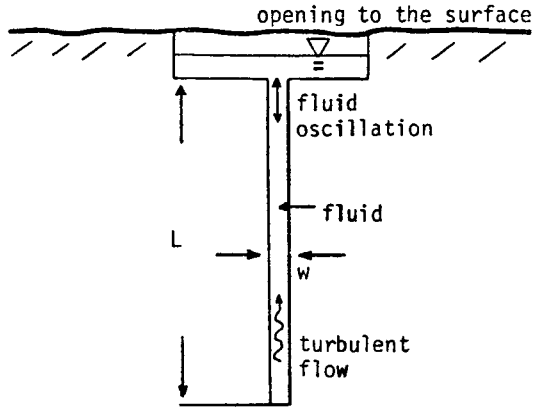

Figure 3. Open vertical fracture.

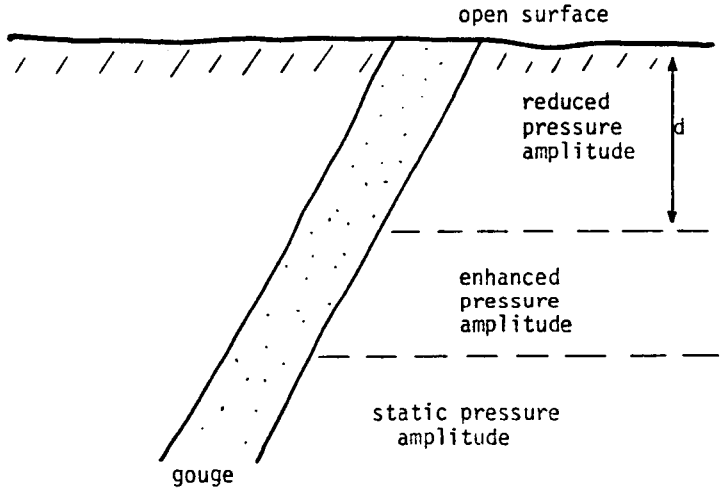

Figure 2. Fracture zone containing a permeable gouge.

References

Bodvarsson, G., Confined fluids as strain meters, J. Geophys. Res., 75, 2711-2718, 1970.

Bodvarsson, G. and A. Bjornsson, Hydroelastic cavity resonators, Jokull, 26, 1976.

Bodvarsson, G., Interpretation of borehole tides, to be published, 1977.

Bodvarsson, G., Hydroelastic fracture oscillations, in preparation, 1978.

Douze, E.J. and G.G. Sorrels, Geothermal Noise Surveys, Geophysics, 37, 813-824, 1972.

White, D.E., Hydrology, activity, and heat flow of the Steamboat Springs thermal system, Washoe County, Nevada, Geol. Surv. Prof. Pap. 458-C, United States Government Printing Office, Washington, D.C., 109 pp., 1968.

A FAULT-ZONE CONTROLLED MODEL OF THE MESA ANOMALY[†]

K. P. Goyal and D. R. Kassoy[*]
University of Colorado
Boulder, Colorado 80309

1. Introduction

Recent studies of liquid-dominated systems like Wairakei (Grindley, 1965), Broadlands (Grindley, 1970), Cerro Prieto (Mercado, 1969), Long Valley (Rinehart and Ross, 1964, Bailey, et al. 1976), Ahuachapan (Ward and Jacob, 1971) suggest that geothermal anomalies are intimately associated with specific patterns of faulting.

In the Imperial Valley, California, there are several geothermal anomalies which are close to or intersected by active faults (Elders, et al. (1972)). The basic field data for these systems are described by Babcock, Combs and Biehler in Rex (1971), Helgeson (1968), Meidav and Furgerson (1972), Goforth, et al. (1972), Douze and Sorrells (1972), Combs and Swanberg (1977), Combs and Hadley (1975, 1977), Loeltz, et al. (1975), Dutcher, et al. (1972), Elders, et al. (1972), Swanberg (1974, 1976), Elders and Bird (1974), Coplen, et al. (1975) and Coplen (1976). Some of the information is surveyed in Kruger and Otte (1973) and in a series of Bureau of Reclamation Reports (1974). Black (1975) and Bailey (1977) have summarized a large spectrum of the available geological, geophysical, geochemical, hydrological and heat flux data for the purpose of synthesizing a composite conceptual model of the Mesa system. In addition they used primary bore hole logging data to provide additional input.

One may infer from these studies that the East Mesa anomaly is intersected by a seismically active fault which acts as a conduit of heated water from depth. The fault appears to extend through the sediments and into the basement rock beneath. It is almost certainly closed off in the first 0.6-0.7 km by shaley deposits, and no surface expression exists.

The fault itself is hypothesized to be a vertically oriented region of heavily fractured material of finite width. The vertical extent of the fault, and the second horizontal dimension are large compared to the width. The fault has probably been active for an extensive period because the region exhibits tectonic activity (Elders, et al. (1972)). The continual microearthquake activity (Combs

[†]Research supported by NSF(RANN) and ERDA Geothermal Programs.

[*]Current mailing address: Department of Applied Mechanics and Engineering Sciences, University of California, San Diego, La Jolla, California 92093.

and Hadley (1977)) suggests that there are mechanical processes available for fracturing of the rock. This is necessary to counteract the mineral deposition associated with a rising, cooling column of saline geothermal fluid which tends to close up the system by reducing the permeability (Ellis (1975)).

It is surmised that water, derived basically from the Colorado River (Coplen, 1976), percolates gradually into sediments and/or fractured basement rock over an area considerably larger than the anomaly itself. Heated at depth by an unknown source the liquid can rise in the high permeability fractured fault zone convecting energy toward the surface. The artesian over-pressure, between 50 psi and 120 psi, associated with the convection process leads to aquifer charging whenever the fault intersects a horizontal layer of relatively large permeability. Extensive fracture systems are presumed to provide the basic permeability in the aquifers. The deposition of calcite and silica over extended periods has probably closed up the intergranular spaces in the sandy sediments.

Heat flux measured near the surface of the clay cap, enhanced by the upflow of hot liquid water beneath, is as much as 7.9 HFU compared to a background level of 1.5 HFU. Temperatures to 200°C at 2.4 km have been measured in Mesa 6-1 and Combs (1977) has suggested a sediment-basement interface temperature between 325°C and 365°C at 4.15km.

Semi-quantitative estimates of heat and mass transfer can be obtained by considering key parameters. The Rayleigh number (R) is a measure of convective effects in the system. Here R is defined by

$$R = \frac{gk\alpha\ell_R\Delta T}{\nu^2} Pr_m$$

where g is the gravity constant, k is a characteristic permeability, α is a characteristic thermal expansion coefficient for water, ℓ_R is the reservoir depth, ΔT is the characteristic temperature difference through the reservoir, ν is the characteristic kinematic viscosity of water and Pr_m is the Prandtl number for water based on the thermal conductivity of the saturated porous medium. For typical high temperature thermodynamic values, a permeability $k = 10^{-9}$ cm^2 and minimal reservoir values ℓ_R = 1.5 km and $\Delta T = 50°C$, then $R \approx 940$. Of course sensitivity to the value of k, which is a bit speculative, is noted. If Combs' (1977) prediction of depth to the basement interface is correct, then ℓ_R = 3 km and $\Delta T \approx 200°C$. This gives R = 6000. Even if the value of k is reduced considerably it is clear that Rayleigh numbers of 500 should be viable (Kassoy and Zebib (1975)).

Natural convection theory (Kassoy and Zebib (1975)) can be used to show that the vertical convection velocity in the fault zone is characterized by

$$v_V = g\, k\alpha\Delta T/\nu$$

For the first set of values used above $v_V \approx 1$ cm/day. Assuming an average temperature of about 175°C in the convection-active section of the fault, one finds that 1.75×10^7 cal/s km^2 is convected upward. This is about 3 orders of magnitude larger than the purely conductive flux.* If 10% of this energy is lost to the claycap and conducted to the surface where Combs (in Rex (1971)) measured 4.88×10^6 cal/s crossing about 110 km^2, then the horizontal area of the fault zone is about 2.9 km^2. Since thermal activity of the Mesa extends along the primary fault for about 16 kms., a fault (fracture-zone) width $h \approx 180$m is suggested. One should recognize that this is an order of magnitude estimate. Given the variable nature of the input a range $100\text{m} \leq h \leq 300\text{m}$ might be appropriate. If k were far smaller than 10^{-9} cm^2 the fault zone area estimate would be far larger, and thus not representative of the relatively localized anomalous properties at the Mesa field.

Convection theory (Kassoy and Zebib (1975)) can also be used to show that the artesian over-pressure magnitude is given by

$$\Delta P_A = \rho g \ell_R\, \alpha\, \Delta T$$

where ρ is the characteristic liquid density. ΔP_A is of the magnitude of 10 bars for the parameters given above. Coplen (1976) has noted that shut-in-pressures for Mesa 6-2 have ranged from 3.5 to 8.2 bars, which indicates that there is reasonable agreement between field data and theoretical assessment for the selected parameter values.

2. Modelling

The conceptual model of the system is based on a fracture zone (the fault) of finite width h' which extends downward nearly vertically through a clay-rich region (the cap) of thickness ℓ_c', through the interbedded sediments of the reservoir for a distance ℓ_R' and finally into the basement rock for a length ℓ_B'. It is postulated that the fault is charged at depth by liquid which has been heated in an extensive basement fracture system. The rate of charge cannot be speculated *a priori* without a global analysis of the convection process. Liquid rises in the reservoir section of the fault. The presence of clays in the cap suppresses vertical transport there. Water pushed out of the fault by artesian overpressure is assumed to flow horizontally in the reservoir aquifer. Vertical transport should be less important in-the-large because of the presence of shaley-layers associated with interbedding.

For mathematical purposes the fracture zone is idealized as a vertical slab of porous media. The adjacent reservoir aquifer is

*The value is based on the temperature difference between well-bores 5-1 and 6-2 in the convective zone.

represented as a porous medium of lateral halfwidth y_R' with horizontal permeability only. Finally the overlying clay cap is assumed to be impermeable.

Spatially uniform temperature boundary conditions are imposed on the cold cap surface and at the hot bottom boundary of the reservoir. On the lateral boundary far from the fault ($y_R' >> \ell_R' >> h'$) the temperature distribution is controlled by vertical conduction, the pressure distribution is hydrostatic and mass flux is permitted to conserve matter.

A quasi-analytic theory is developed for high Rayleigh number convection of a liquid in a rigid porous medium. In this approximation liquid rises up the fault and spreads into the near-region of the reservoir adiabatically. The cooling effect of the cap in the reservoir is confined to a thin layer adjacent to the interface. The layer grows with distance from the fault. In the far field of the aquifer the full depth of the reservoir is cooled by the surface. Predicted temperature distributions with depth in the near field are quite like that for Mesa borehole 8-1, and qualitatively similar to those in 6-1 and 6-2. Far field profiles can be related to those in 5-1 and 31-1. Although the flow field is purely horizontal in the aquifer one finds steep temperature gradients in the cap and reduced variations at depth. The heat flux calculated at the cap top compares favorably with Mesa field data.

REFERENCES

Bailey, T. (1977) CUMER-77-4, Mechanical Engineering Department, University of Colorado, Boulder.

Black, H. (1975) CUMER 75-4, Mechanical Engineering Department, University of Colorado, Boulder.

Bureau of Reclamation (1974) Geothermal Resource Investigation, East Mesa Test Site, Imperial Valley, California.

Combs, J. (1977), Trans. Geothermal Resources Council 1, 45.

Combs, J. and Hadley, D. (1975) EOS, Trans. Am. Geophys. Union 54, 1213.

Combs, J. and Hadley, D. (1977) Geophysics 42, 17.

Combs, J. and Swanberg, C. (1977) (to appear).

Coplen, T. B. (1976) Cooperative Geochemical Resource Assessment at the Mesa-Geothermal System, I.G.P.P., University of California, Riverside.

Coplen, T. B., Kolesar, P., and Taylor, R. C., Kendall, C. and Mooser, C. (1975) Investigations of the Dunes Geothermal Anomaly, Imperial Valley California. Part IV, I.G.P.P., University of California, Riverside.

Douze, E. J. and Sorrels, G. G. (1972) Geophysics 37, 813.

Dutcher, L. C., Hardt, W. F., Moyle, W. R. (1972) USGS Circular 649.

Elders, W. A., Rex, R. W. and Meidav, T. (1972) Science 178, 15.

Elders, W. A. and Bird, D. K. (1974) Investigations of the Dunes Geothermal Anomaly, Imperial Valley, California: Part II, I.G.P.P. University of California, Riverside.

Ellis, A. J. (1975), American Scientist 63, 510.

Goforth, T. T., Douze, E. J. and Sorrells, G. G. (1972) Geophys. Prosp. 20, 76.

Grindley, G. W. (1965), New Zealand Geol. Sur. Bull. 75, 131.

Grindley, G. W. (1970), Geothermics 2, 248.

Helgeson, H. C. (1968), Am. J. Sci. 266, 129.

Kassoy, D. R. and Zebib, A. (1975) Phys. of Fluids 18, 375.

Kruger, P. and Otte, C. (1973) Geothermal Energy, Stanford University Press, Stanford, California.

Loeltz, O. J., Ireland, B., Robison, J. H. and Olmsted, F. H. (1975) USGS Prof. Paper 486-K.

Meidav, T. and Furgerson, R. (1972) Geothermics 1, 47.

Mercado, S. (1969) EOS, Trans. Am. Geophys, Union 50, 59.

Rex, R. W. (1971) Cooperative geological-geophysical-geochemical investigations at geothermal resources in the Imperial Valley area of California, University of California, Riverside.

Rinehart, C. D. and Ross, D. C. (1964), U.S.G.S. Prof. Paper #385, 1.

Swanberg, C. (1974) Proc. Conf. on Res. for the Develop. of Geothermal Energy Resources, Pasadena, California, 85.

Swanberg, C. (1976) Proc. 2nd U.N. Symposium on the Development and Use of Geothermal Resources, San Francisco, 2, 1217.

Ward, P. L. and Jacobs, K. H. (1971) Science 173, 328.

A MODEL OF THE SERRAZZANO ZONE

Oleh Weres
Lawrence Berkeley Laboratory
University of California
Berkeley, California

Lithology

For hydrogeological purposes, the rocks of the Lardarello Basin may be divided into three main complexes:[1]

i) A weakly metamorphic basement complex of quartzites, phyllites, and schists. Although deep exploratory drilling has found occasional fractures and isolated pockets of permeable rock, it is believed that the basement complex is largely impermeable and contributes little to steam production.

ii) A so-called "evaporite" complex of anhydrite, limestones, dolostones, and radiolarites. These rocks are absent in some areas and up to a kilometer thick in others. The limestones and dolostones are known to be highly porous and permeable. The lower-lying anhydrite is believed to be highly porous and permeable where it has been tectonically sheared and brecciated. Because a major regional thrust fault passes through this complex, the tectonically sheared and brecciated zones are believed to be extensive. Overall, this complex is believed to be the main reservoir of liquid water and source of steam in the geothermal system.

iii) A largely sedimentary caprock sequence consisting of unmetamorphosed and weakly metamorphosed shales, marls, feldspathic sandstones, and ophiolitic rocks. Although there are significant volumes of permeable and porous limestones and sandstones in this complex, the preponderance of argillaceous rock types makes it effectively impermeable as a whole. It serves as a caprock for the geothermal system.

Structure

Most wells in the Lardarello Basin produce from an interval at or near the bottom margin of the caprock. Where the evaporites are absent, the producing interval is the thrust fault zone at the contact of basement and caprock. This fault zone is not the ultimate source of steam, but only a conduit which conducts it from permeable complex rocks elsewhere to the wellbores.

The elevation of first commercial steam throughout the Basin is shown in Figure 1. It is apparent that the Castelnuovo-Lardarello, Serrazzano, Lago, and Lagoni Rossi productive areas are centered near distinct highs in the reservoir top. (They account for nine tenths of the Basin's steam production). At Castelnuovo-Lardarello and Serrazzano the permeable complex rocks are thin or absent and the highs are simply highs in the basement.

Reservoir Statics and Dynamics

There is a clear analogy to the well-known structural trap reservoirs of petroleum geology. Steam can be trapped under an anticlinal caprock like petroleum.

There appears to be reasonably continuous permeability and flow at the reservoir top throughout the Basin. Isotopically demonstrated flow of water from surrounding aquifers into the reservoir [3] indicates hydraulic continuity with them as well. This suggests that prior to exploitation there must have been hydrostatic equilibrium between reservoir and aquifers. The (simplified) condition for such equilibrium is that

$$h_{aq} - h_{res} = 10 \times [P_{sat}(T_{res}) - 1]$$

where h_{aq} is the isopiestic level of the surrounding aquifers (in meters), h_{res} is the elevation of the steam-water interface under the trap, and $P_{sat}(T_{res})$ is the steam saturation pressure at reservoir temperature. Analysis of water level and temperature survey data from the few "wet" wells in the Serrazzano zone should provide a good test for this equation.

A detailed analysis of various published data has led to an estimate of 275°C for the initial reservoir temperature. As h_{aq} averages about 100 meters around the periphery of the Basin, an initial h_{res} of about -500 meters is indicated.[4] This is deep enough to allow for fair-sized initial steam zones in the major areas.

Early wells never reached 500 meters subsea and never encountered water. The fact that most modern deep wells have also not encountered water is probably due to a lowering of the water table by steam production.

Hydrogen and oxygen isotope studies[3] show clear evidence of massive incursions of recently meteoric groundwaters from the southeast at Castelnuovo and Sasso. Smaller incursions are suggested from the southwest between Lagoni Rossi and Lago, and from the west at Serrazzano.

It is likely that the incursion of surrounding cooler groundwaters is due to the lowering of reservoir pressure caused by steam production. A hydrological balance calculated for the entire basin suggests that the rate of recharge is about one-third that of steam production[5].

Toward a Numerical Model of the Serrazzano Zone

LBL's part in the U. S. DOE/ENEL cooperative program is to numerically model the reservoir dynamics of the Serrazzano and Castelnuovo zones. The author is presently well along in the development of a geologically accurate computer-generated mesh for use in modelling Serrazzano.

Figure 2 shows a recent version of this mesh. The input data for the mesh generator is essentially a set of digitized geological cross-sections. The two cross-sections labeled in Figure 2 are shown as such in Figure 3.

The three lithological layers distinguished in the cross-sections are the three complexes defined and discussed above. Where there is a significant thickness of "the evaporites," the mesh elements all lie completely within this complex. Where the basement and caprock are in direct contact, the mesh elements are taken to lie along the contact surface and to be about 120 meters thick. 120 meters was chosen because it is about twice the root mean square distance for heat diffusion through rock over 25 years. (This roughly corresponds to the history of full-scale steam production at Serrazzano.) The underlying physical model is that of steam flowing through a thin fault zone and extracting heat from the surrounding impermeable rock by conduction.

The points plotted within the evaporite stratum and at the caprock-basement contact correspond to the individual elements of the mesh. The points within the basement or caprock and not on the contact do not correspond to mesh elements. Their function is to define the bounding planes of the adjacent mesh elements. In all cases, the bounding and interface planes are the plane bisectors of the line segments between the corresponding pairs of points. This prescription for choosing interface planes is believed to be optimal for our purposes. The only input data required are the coordinates of the various points. The mesh shown has 227 elements and 448 bounding points. The calculation found 2404 boundary and interface planes between them.

Water Reserves and Boundary Conditions

The mesh in Figure 2 is geologically accurate in its depiction of the reservoir, and the volume and elevation of each element is known. This allows us to estimate initial heat and water reserves within the region modelled.

Figure 4 shows just those elements whose content is about one-half or more "evaporitic" rock. The total volume of these elements is about $4.2\,km^3$ Of this, about $3.1\,km^3$ is below about-450 to-500 meters and was probably initially water saturated. How much water this represents depends on the average porosity which is unknown. If we make a moderately optimistic estimate of 10%, this is $0.31\,km^3$. Assuming an initial temperature of 275°C gives an estimated initial mass of about 2.3×10^8 metric tons. This amount of steam would suffice to run the 32MW Serrazzano power plant for about one hundred years. The magnitude is completely consistent with cumulative steam production of about 0.9×10^8 tonnes to date.

Clearly, the extent of mass flow in and out of the region studied will also effect the validity of such estimates. It appears that the Serrazzano zone is the most isolated subarea within the Basin in this regard. (This is one reason why Serrazzano was chosen for study. The other is that relatively complete historical production data is available.) However, as is evident from the concentration of the "evaporites" at the very edges of the mesh, it cannot be perfectly isolated. The very thick evaporite stratum in the southeast corner of the mesh (also see Section C) is continuous with the diapiric evaporite outcrop between Monterotondo and Sosso. This is known to be a major recharge area.[3] Although the recharge water does not appear to have reached the Serrazzano zone yet, it is possible that it has already displaced significant volumes of "old" water toward Serrazzano. There may also be some influx of water and/or steam from west-southwest where the mesh

is truncated due to lack of stratigraphic data. The large volume of evaporites in the south-southwest octant is about midway between Serrazzano on one side and Lagoni Rossi and Lago on the other. It is very likely that some of the steam generated here flows south toward the latter two zones.

Heat Reserves

We will assume a volumetric heat capacity of 2460 kJ/m^3 °C for the reservoir rock and an initial temperature of 275°C. 8 bar seems to be a reasonable estimate for ultimate abandonment pressure, and this corresponds to an abandonment temperature of 170°C. We again take $\phi = 0.1$ for the "evaporites" and $\phi \approx 0$ for the other rock types.

This leads us to estimate the total quantity of useful heat within just the "evaporite" elements of the mesh to be about 9.8×10^{19} kj. This quantity of heat is enough to convert 3.6×10^8 metric tonnes of water initially at 25°C to steam of 2800 kj/kg enthalpy. Water initially at 275°C would require less heat. If we assume an initial "preheated" water supply of 2.3×10^8 tonnes, we find that an equal volume of cold recharge water is needed to cool the evaporites down to 170°C. Another 2.0×10^8 tonnes would be required to cool the nonevaporite portions of the mesh down to 170°C, for a grand total steam production of 6.6×10^8 tonnes. This is enough for 9,400 MW-years of electrical generation.

It seems clear that water reserves will prove to be the limiting factor at Serrazzano. A long term program of water injection appears to be called for if anything like the above figure is to be reached.

Acknowledgements

I would like to thank Ron Schroeder and Romano Celati for stimulating discussions and correspondence which contributed much to the development and refinement of this model. In particular, Ron Schroeder directed my attention to the "trap" nature of the Serrazzano structure. I wish to thank the ENEL geothermal staff as a whole for kindly allowing us access to their voluminous unpublished data which made this work possible.

Mr. Chris Weaver generated the excellent graphics which make my mesh output comprehensible. Ms. Chris Doughty assisted me with the tedious work of digitizing the geological input data.

References

1) R. Cataldi, G. Stefani and M. Tongiorgi. pp.235-274 in Tongiorgi, ed., Nuclear Geology on Geothermal Areas. Pisa, 1963

2) Lardarello and Monte Amiata: Electric Power by Endogenous Steam. ENEL Compartimento di Firenze, and Direzione Studi e Richerche - Roma. No date.

3) R. Celati, P. Noto, C. Panichi, P. Squarci and L. Taffi. Geothermics, 2 174(1973).

4) O. Weres, K. Tsao, B. Wood. Report LBL-5231. Lawrence Berkeley Laboratory, July 1977.

5) C. Petracco and P. Squarci, pp.521-529 in the Proceedings of the Second United Nations Symposium on the Development and Use of Geothermal Resources. San Francisco, 1975.

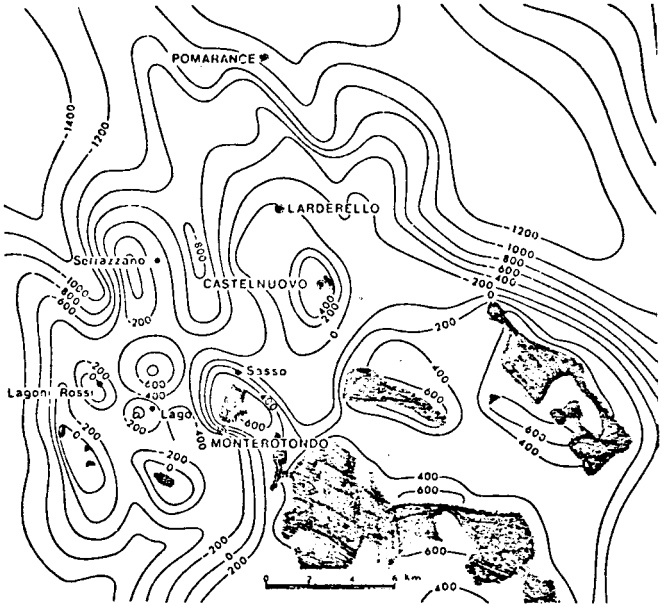

Figure 1. Elevation of reservoir top throughout Lardarello Basin in meters. Shaded areas indicate "evaporite" outcrops. From Reference 2.

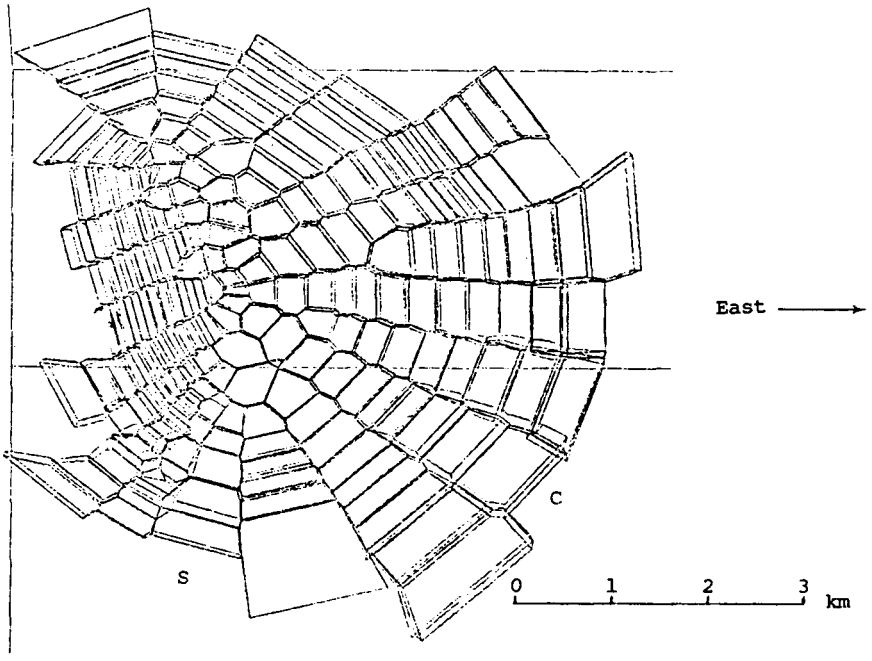

Figure 2. A computer-generated mesh for modelling the Serrazzano zone reservoir.

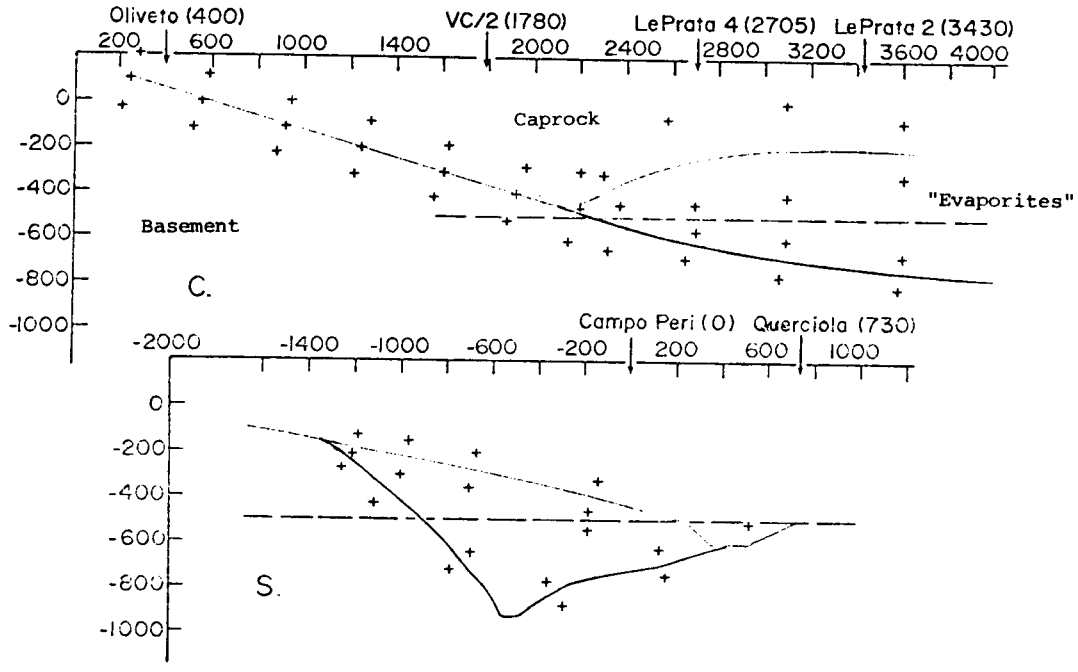

Figure 3. Typical geological cross-sections of Serrazzano zone. The points are input for the mesh generator code.

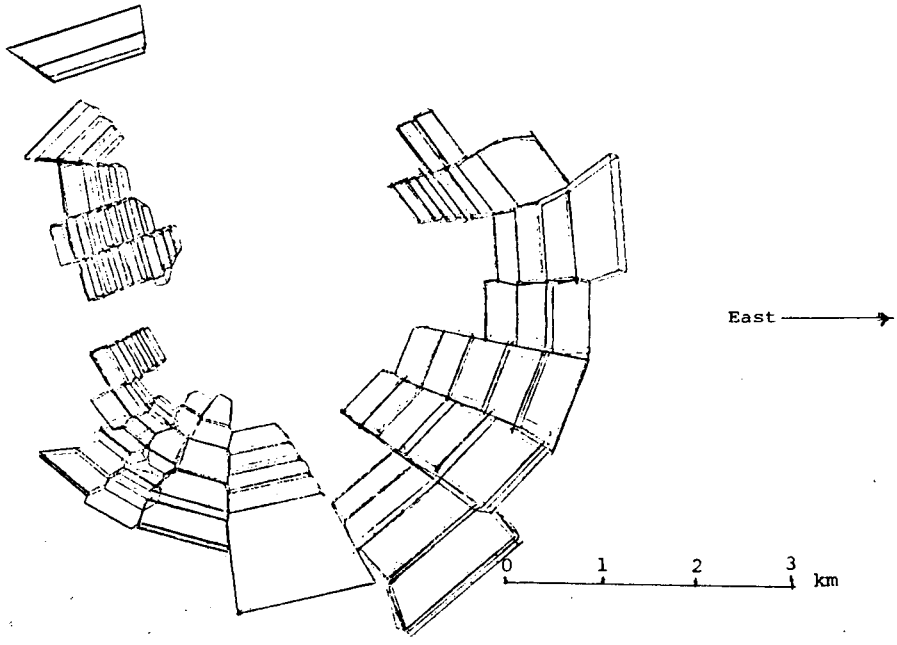

Figure 4. Same as Figure 2, but showing "evaporite" mesh elements only.

SUBJECT INDEX

AUTHOR INDEX